



Rulach, Robert John (2023) *Identification of dose constraints and evaluation of optimal planning technique for radical thoracic re-irradiation for non-small cell lung cancer*. PhD thesis.

<https://theses.gla.ac.uk/84009/>

Copyright and moral rights for this work are retained by the author

A copy can be downloaded for personal non-commercial research or study, without prior permission or charge

This work cannot be reproduced or quoted extensively from without first obtaining permission from the author

The content must not be changed in any way or sold commercially in any format or medium without the formal permission of the author

When referring to this work, full bibliographic details including the author, title, awarding institution and date of the thesis must be given

Enlighten: Theses

<https://theses.gla.ac.uk/>
research-enlighten@glasgow.ac.uk

Identification of dose constraints and evaluation of optimal planning technique for radical thoracic re-irradiation for non-small cell lung cancer

Robert John Rulach

BSc, MBChB, MCRP, FRCR

This thesis is submitted in fulfilment of the requirements for the Degree of
Doctor of Philosophy

Institute of Cancer Sciences

College of Medical, Veterinary and Life Sciences

University of Glasgow

May 2023

Abstract

Background

There are approximately 48,000 new diagnoses of lung cancer in the United Kingdom. It is one of the most lethal cancers, with a 10% chance of survival at 10 years. A third of patients receive radiotherapy a part of the primary treatment for lung cancer. However, there is an approximately 30% local recurrence rate after radical radiotherapy for non-small cell lung cancer, and there is a 14% risk at 10 years of developing a second lung cancer. There are no treatment guidelines for patients who are diagnosed with intra-thoracic relapsed disease. Radical thoracic re-irradiation for non-small cell lung cancer has been performed in selected patients from the 1970s with promising efficacy. However, re-irradiation is associated with increased risk of toxicity compared to *de novo* radiotherapy. Re-irradiation is being delivered more frequently due to the advances in radiotherapy technology and better detection of recurrent disease, despite the lack of evidence in how to deliver re-irradiation safely, or any recent prospective studies that demonstrate efficacy.

Aim of thesis

The aim of this thesis is to investigate how to optimise the safety of radical thoracic re-irradiation, in preparation for a future prospective clinical trial.

Methods

- (i) An international Delphi consensus process with thoracic oncologists was performed to identify current practice in thoracic re-irradiation, patient selection, develop dose constraints and radiotherapy planning strategies.
- (ii) A retrospective review of 39 patients who underwent re-irradiation in the Beatson West of Scotland cancer centre was conducted. Clinical outcomes and cumulative dosimetric information were analysed. Image and dose registration strategies were developed to account for

the previous dose delivered from initial radiotherapy with the re-irradiation dose.

- (iii) A literature review was performed to collect information (including toxicity, cumulative dose, interval between treatments and use of chemotherapy) about thoracic re-irradiation. This was divided into five datasets for the organs at risk in the chest (spinal cord, oesophagus, lungs, proximal bronchial tree, and aorta) and logistic regression modelling was performed to determine cumulative dose constraints.
- (iv) A literature review was performed to collect information (including cumulative dose, local control, and overall survival rates) from thoracic re-irradiation for non-small cell lung cancer. Logistic regression modelling was performed to determine the dose required for 50% rates of 2-year local control and overall survival.
- (v) A radiotherapy planning study using the 39 Beatson patients was conducted using volumetric arc therapy (VMAT) and multi-criteria optimisation (MCO). Patients were re-planned to the cumulative dose constraints and the models developed in sections (iii) and (iv) were applied to assess if the re-planned re-irradiation was safer.
- (vi) Patients who had completed a course of radical lung radiotherapy were recruited into a qualitative interview study to explore patients' perspectives on re-irradiation. The interviews were transcribed and underwent thematic analysis.

Results

- (i) Fifteen lung oncologists participated in the Delphi process. Patients being considered for radical re-irradiation should be PS 0-2, and radical resection should be discussed. Staging with PET-CT and brain imaging was endorsed. Consensus dose constraints based on clinician expertise were agreed upon for the oesophagus, spinal cord, brachial plexus and aorta. There was no consensus for lung and proximal bronchial tree doses.

- (ii) Clinical outcomes and cumulative dose of 39 patients from the Beatson were analysed and divided into patients with local recurrence and second primary lung cancers. The 2-year OS rate was 38.5% in the local recurrence group, and 69.2% in the SPLC group. Sixteen patients (41%) experienced grade 3 toxicities and one patient (2.6%) had fatal haemoptysis. A reproducible process to accumulate dose was developed, which identified that using the whole lung for image registration was the optimal strategy.
- (iii) The literature search identified 55 studies with the cumulative dose and toxicity required for modelling. Dose/toxicity models were developed using logistic regression for the spinal cord, oesophagus, the mean lung dose, the lung V20Gy, the proximal bronchial tree and aorta. There was insufficient data to model the heart, chest wall and brachial plexus dose. For the spinal cord, oesophagus, proximal bronchial tree and aorta, the maximum likelihood 5% risk of grade 3 toxicity was seen at 77.2Gy, 94.3Gy, 157.5Gy and 142.5Gy respectively (all doses in equivalent dose in 2-Gray fractions, median values used if other variables were included in the model). The mean lung dose and V20Gy associated with 20% grade 3 toxicity were 19.3Gy and 28.4% respectively. These models were validated on the Beatson data, and dose constraints developed.
- (iv) The literature search identified 21 studies with 2-year local control or overall survival data and cumulative dose to the tumour. Dose/outcome models were developed using logistic regression modelling. The modelling predicted a 50% 2-year local control rate at 67.8Gy using a median planning target volume of 112cc. The predicted dose to the tumour for a 50% 2-year overall survival rate was 76.5Gy. A sub-study to assess if 13 locally recurrent patients from the Beatson cohort could have dose escalation identified six patients where their re-irradiation dose could potentially be increased.
- (v) The planning study identified 15 patients from the 39 patients in the Beatson cohort that breached the re-irradiation dose constraints. These patients mostly had locally recurrent disease. Seven patients

were replanned using VMAT and MCO and met the dose constraints. The remaining eight patients required alternate strategies (such as a change in dose fractionation or modification of the planning target volume) to meet the constraints. Six patients were able to be safely replanned with these alternate strategies. The combination of VMAT and MCO was superior to VMAT alone when planning re-irradiation for sparing the serial organs at risk in the chest.

- (vi) Eight patients participated in a qualitative interview exploring their perspectives on radical re-irradiation. Thematic analysis identified two main themes from the interviews: fear and control. The key finding was that all patients would consider re-irradiation. A common reason given was they were not afraid of it having experienced radiotherapy before. Each patient had a very different attitude to risk, with some patients stating that they would accept high risk treatment if the outcomes were better, whereas others preferred to prioritise avoiding toxicity.

Conclusions

The research detailed in this thesis contributes to the delivery of safe re-irradiation in several ways. The consensus statements provided guidance for the selection and staging of patients to be considered for radical re-irradiation, ensuring that only suitable patients proceed with high-risk treatment. The dose constraints developed from the dose/toxicity can be used to limit severe re-irradiation toxicity and allows patients to be better counselled prior to treatment. The dose/outcome study identified that recurrent disease required higher doses for disease control, and that dose escalation may be possible in selected patients. The planning study identified that the optimal planning technique is VMAT with MCO. The qualitative study demonstrated that patients may consider re-irradiation and require individual counselling regarding their acceptance of risk. This research provides insights to the inclusion criteria, dose constraints, radiotherapy planning technique and the patient and public involvement necessary for a prospective clinical study of re-irradiation.

Table of Contents

Abstract.....	2
List of Tables	12
List of Figures.....	16
Acknowledgements	18
Author’s Declaration.....	19
Abbreviations	20
1 Introduction	22
1.1 Overview	22
1.2 Lung cancer	22
1.2.1 Epidemiology.....	22
1.2.2 Histology.....	23
1.2.3 Diagnosis and staging.....	23
1.2.4 Treatment of NSCLC	23
1.3 Role of radiotherapy in lung cancer.....	25
1.3.1 Radical radiotherapy in non-small cell lung cancer	26
1.3.2 Trials testing novel radiotherapy schedules and dose.....	26
1.3.3 Trials testing systemic therapies with radical radiotherapy	28
1.4 The radiobiology of ionising radiation as treatment for cancer	31
1.4.1 The effect of ionising radiation on cells.....	31
1.4.2 The linear-quadratic model	33
1.4.3 Fraction sensitivity.....	33
1.4.4 Tumour control probability models	36
1.4.5 Normal tissue complication probability models	37
1.5 Radiotherapy planning and delivery for lung cancer	40
1.5.1 Radiotherapy technique.....	40
1.5.2 Image guided radiotherapy	43
1.5.3 Developments in dose prediction.....	44
1.5.4 Modality	45
1.6 Recurrent disease	46
1.6.1 Epidemiology of intra-thoracic disease recurrence.....	46
1.7 Re-irradiation as a treatment of recurrent disease.....	48
1.7.1 The classification of intra-thoracic tumour recurrence.....	48
1.7.2 Review of published data of efficacy of radical re-irradiation	49
1.7.3 Review of published data of safety of radical re-irradiation.....	54
1.8 Aim of this thesis.....	61
2 Aims and objectives	62
2.1 Clinician consensus	62

2.2	Beatson re-irradiation cohort	62
2.3	Dose/toxicity modelling.....	63
2.4	Tumour control modelling	63
2.5	Planning study	64
2.6	Patient survey	64
3	Clinician consensus	65
3.1	Introduction.....	65
3.2	Methods.....	66
3.2.1	Participant selection	66
3.2.2	Ethics and consent	66
3.2.3	Survey process	66
3.3	Results	68
3.3.1	Participants and response rates	68
3.3.2	Definition of re-irradiation	68
3.3.3	Patient suitability for re-irradiation in terms of disease stage and fitness 71	
3.3.4	Re-irradiation investigations	72
3.3.5	Acceptable risks of toxicity.....	72
3.3.6	Radiotherapy planning technique and delivery.....	73
3.3.7	Follow-up after re-irradiation.....	74
3.4	Discussion	81
3.4.1	Methodology	81
3.4.2	Lack of definition	83
3.4.3	Suitability for re-irradiation.....	84
3.4.4	Radiotherapy planning	85
3.4.5	Conclusion and summary.....	88
4	Beatson re-irradiation cohort.....	89
4.1	Introduction.....	89
4.2	Method.....	91
4.2.1	Ethics and Caldicott guardian review	91
4.2.2	Patient identification and clinical information.....	91
4.2.3	Radiotherapy scan processing.....	91
4.2.4	Generation of EQD2 using Velocity	92
4.2.5	Deformable dose registration	92
4.2.6	Statistical analysis	93
4.3	Results	93
4.3.1	Patient characteristics	93
4.3.2	Region of interest selection	94
4.3.3	Re-irradiation toxicity.....	96

4.3.4	Cumulative doses	99
4.3.5	Survival	100
4.4	Discussion	102
4.4.1	Outcomes in the context of other studies.....	103
4.4.2	Investigation of uncertainty from the clinician consensus.....	104
4.4.3	Cumulative doses and constraints	107
4.4.4	Strengths and limitations	109
4.5	Summary.....	110
5	Re-irradiation normal tissue analysis.....	112
5.1	Introduction.....	112
5.1.1	Current re-irradiation dose constraints.....	113
5.1.2	Aims of modelling	114
5.2	Methods.....	115
5.2.1	Overview	115
5.2.2	Datasets used in modelling and model validation.....	115
5.2.3	Data collection and format	116
5.2.4	Method of deriving cumulative doses	117
5.2.5	Choice of endpoints.....	118
5.2.6	Selection of α/B ratio	119
5.2.7	Modelling process	119
5.3	Results	124
5.3.1	Structure of reports	124
5.3.2	Data collection	124
5.3.3	Models for cord	126
5.3.4	Models for oesophagus	142
5.3.5	Models for lung	160
5.3.6	Models for proximal bronchial tree	187
5.3.7	Models for aorta.....	198
5.3.8	Thoracic organs at risk not modelled	208
5.4	Discussion	211
5.4.1	Main findings.....	211
5.4.2	Data issues affecting all models	215
5.4.3	Issues related to modelling technique	218
5.4.4	Conclusions.....	221
6	Re-irradiation tumour control models.....	222
6.1	Introduction.....	222
6.1.1	Aims of tumour control modelling.....	223
6.2	Methods.....	224
6.2.1	Datasets used in modelling and model validation.....	224

6.2.2	Data collection and dose combinations.....	224
6.2.3	Selection of α/β ratio for tumour	224
6.2.4	Choice of endpoints.....	225
6.2.5	Modelling process	225
6.2.6	Dose escalation feasibility.....	229
6.3	Results	231
6.3.1	Data collection	231
6.3.2	Dose/2-year local control model	237
6.3.3	Dose/overall survival model.....	246
6.3.4	Feasibility of dose escalation	252
6.4	Discussion	259
6.4.1	Main findings.....	259
6.4.2	Local control models	259
6.4.3	Overall survival	263
6.4.4	Feasibility study.....	265
6.4.5	Data limitations	266
6.4.6	Conclusions.....	269
7	Re-irradiation planning	270
7.1	Introduction.....	270
7.2	Methods.....	272
7.2.1	Ethics and data collection	272
7.2.2	Identification of patients that passed or failed the cumulative dose constraints	272
7.2.3	Re-irradiation re-plan	274
7.2.4	Cumulative dose verification.....	278
7.2.5	Outcome risk calculation	278
7.2.6	Statistical analysis	280
7.3	Results	280
7.3.1	Desirable dose constraints and cumulative doses delivered in the Beatson cohort	280
7.3.2	Re-planning cohort.....	282
7.3.3	Unable to meet essential constraints group	291
7.3.4	Verification	296
7.3.5	Changes in risk compared to delivered dose.....	299
7.3.6	Changes in tumour control.....	309
7.4	Discussion	312
7.4.1	Identification of high-risk patients	312
7.4.2	High risk re-irradiation planning.....	314
7.4.3	Re-planning failures	317

7.4.4	Dose verification	319
7.4.5	Risk prediction.....	319
7.4.6	Conclusions.....	321
8	Patient perspectives on re-irradiation	322
8.1	Introduction.....	322
8.1.1	What are patients' perspectives of re-irradiation?	322
8.1.2	Relationship of symptoms from initial radiotherapy and willingness for re-treatment	323
8.1.3	Alternative treatments.....	323
8.1.4	Patient perspectives on risk and benefit	324
8.1.5	Patient perspectives on surveillance scans	324
8.1.6	Summary.....	325
8.2	Aims	326
8.2.1	Primary objective	326
8.2.2	Secondary Objectives.....	326
8.3	Methods.....	327
8.3.1	Design	327
8.3.2	Ethics approval	327
8.3.3	Participants	327
8.3.4	Recruitment and study process	328
8.3.5	Interview topics	328
8.3.6	Analysis	330
8.4	Results	331
8.4.1	Recruitment.....	331
8.4.2	Fear	332
8.4.3	Control.....	334
8.5	Discussion	339
8.6	Conclusion.....	345
9	Final Discussion	346
9.1	Definition of radical thoracic re-irradiation	346
9.2	Rationale for radical re-irradiation	348
9.2.1	The biology of tumour radioresistance	348
9.2.2	A rationale for why re-irradiation may be effective.....	351
9.2.3	Re-irradiation compared to alternative treatments.....	352
9.3	Prediction and management of the risks of toxicity.....	355
9.3.1	Re-irradiation dose/toxicity models	355
9.3.2	Risk-based planning.....	356
9.4	Future studies	358
9.4.1	Studies in progress	358

9.4.2	Potential pre-clinical studies.....	360
9.4.3	Potential clinical studies.....	361
9.5	Conclusion.....	366
	List of References.....	368

List of Tables

Table 1.1 Summary of re-irradiation studies and efficacy.....	51
Table 1.2 Summary of the safety of re-irradiation studies.....	58
Table 3.1 Consensus statements regarding the clinical stage of suitable re-irradiation patients.	75
Table 3.2 Consensus statements regarding the fitness of suitable re-irradiation patients.	76
Table 3.3 Consensus statements regarding investigations for suitable re-irradiation patients.	77
Table 3.4 Clinician suggested acceptable toxicity rates.....	78
Table 3.5 Consensus statements regarding radiotherapy planning technique....	79
Table 3.6 Consensus statements regarding cumulative dose constraints.	80
Table 3.7 A comparison of putative cumulative dose constraints.....	87
Table 4.1 Demographics of the second primary lung cancer and locally recurrent groups.....	94
Table 4.2 Doses of OARs predicted by ROI-PTV subtracted from ROI-WL	96
Table 4.3 Grade and number of observed re-irradiation toxic events.....	97
Table 4.4 Re-irradiation toxicity divided by grade 3 toxicity encountered at initial radiotherapy	98
Table 4.5 Cumulative mean doses to thoracic organs at risk	99
Table 4.6 Comparison of suggested dose constraints and delivered dose.....	109
Table 5.1 Overview of studies used to form re-irradiation dose constraints	114
Table 5.2 Outline of outcome and predictor variables in modelling.....	118
Table 5.3 List of studies used to form cord dataset.....	128
Table 5.4 List of studies used to form cord dataset.....	130
Table 5.5 Summary of whole cord dataset.....	131
Table 5.6 Results of χ^2 tests when whole dataset split using median values ...	131
Table 5.7 Relative risk table for the whole dataset.....	131
Table 5.8 Summary of complete dataset univariable and multivariable modelling	132
Table 5.9 Summary of multivariable model dose predictions.....	133
Table 5.10 Development of cord dose constraints using bootstrapping.	135
Table 5.11 Testing complete and individual model constraints on individual data	136
Table 5.12 List of studies used to form the oesophageal dataset.	143
Table 5.13 List of studies used to form the oesophageal dataset.	145
Table 5.14 Summary of the oesophageal dataset.	147
Table 5.15 Type of Grade 3 or above toxicity.	147
Table 5.16 Results of χ^2 and Fisher's exact tests when oesophageal dataset split by median values.....	148
Table 5.17 Relative risk table for the oesophageal dataset.....	148
Table 5.18 Results from univariable and multivariable modelling.	149
Table 5.19 Summary of multivariable model dose predictions with and without chemotherapy.	150
Table 5.20 Development of oesophageal dose constraints using bootstrapping.	154
Table 5.21 Testing multivariable model constraints on individual data.....	156
Table 5.22 List of studies used to form the lung dataset.	162
Table 5.23 List of studies used to form the lung dataset.	163
Table 5.24 Summary of lung dataset.....	165
Table 5.25 Results of χ^2 and Fisher's exact tests when lung dataset split by median values.	165

Table 5.26 Summary of lung dataset univariable and multivariable modelling.	166
Table 5.27 Leave one out cross validation values for univariable and multivariable chemotherapy models.	167
Table 5.28 Relative risk table for the cumulative mean lung dose dataset.	168
Table 5.29 Relative risk table for the grouped cumulative V5 dataset.	171
Table 5.30 Relative risk table for the grouped cumulative V20 dataset.	173
Table 5.31 Development of lung dose constraints using block bootstrapping.	175
Table 5.32 Summary of Hosmer Lemeshow and Pearson correlation tests for lung models.	175
Table 5.33 Testing lung dose constraints on external Beatson cohort.	180
Table 5.34 Testing cumV20 constraints on individual dataset.	180
Table 5.35 List of studies used to form the proximal bronchial tree dataset.	188
Table 5.36 List of studies used to form the proximal bronchial tree dataset.	189
Table 5.37 Summary of proximal bronchial tree dataset.	190
Table 5.38 Results of Fisher's exact tests when the dataset is divided using median values.	190
Table 5.39 Relative risk table for the complete proximal bronchial tree dataset.	191
Table 5.40 Results from univariable and multivariable modelling (using the imputed data).	191
Table 5.41 Development of proximal bronchial tree constraints using block bootstrapping.	193
Table 5.42 Testing proximal bronchial tree dose constraints on complete dataset.	195
Table 5.43 Testing proximal bronchial tree dose constraints on individual dataset.	195
Table 5.44 Testing proximal bronchial tree dose constraints on external Beatson cohort.	195
Table 5.45 List of studies used to form the aorta dataset.	199
Table 5.46 List of studies used to form the aorta dataset.	200
Table 5.47 Summary of complete aorta dataset.	201
Table 5.48 Results of Fisher's exact tests when the complete dataset is divided using median values.	201
Table 5.49 Relative risk table for the aorta dataset by dose.	202
Table 5.50 Summary of complete aorta dataset univariable modelling.	202
Table 5.51 Development of aorta constraints using block bootstrapping.	204
Table 5.52 Testing aorta dose constraints on complete dataset.	206
Table 5.53 Testing aorta dose constraints on individual dataset.	206
Table 5.54 Summary of the brachial plexus dataset.	209
Table 5.55 Summary of the chest wall dataset.	210
Table 5.56 Summary of the heart dataset.	211
Table 5.57 Comparison of expert dose constraints and modelling dose constraints.	214
Table 5.58 Existing dose constraint toxicity rate predictions using models.	215
Table 6.1 Outline of the outcome and predictor variables.	225
Table 6.2 List of studies used in the local control and overall survival dataset.	232
Table 6.3 Further details of studies used in the local control and overall survival dataset.	235
Table 6.4 Summary of the local control dataset.	237
Table 6.5 Results of χ^2 tests when local control dataset split using median values.	238

Table 6.6 Univariable and multivariable modelling of the local control dataset.	239
Table 6.7 Predicted 2 year local control rate by increasing retreatment dose.	240
Table 6.8 Univariable and multivariable modelling of the local control dataset.	242
Table 6.9 Testing maximum-likelihood PTV cut-off for 50% 2-year local control.	246
Table 6.10 Testing maximum-likelihood RT dose cut-off for 50% 2 year local control.	246
Table 6.11 Summary of the overall survival dataset.	247
Table 6.12 Results of x2 tests when overall survival dataset split using median values.	248
Table 6.13 Univariable and multivariable modelling of the overall survival dataset.	249
Table 6.14 Testing maximum likelihood retreatment dose on the overall survival dataset.	252
Table 6.15 Location and PTV size of the locally recurrent Beatson re-irradiation cases.	253
Table 6.16 Predicted 2-year overall survival and local control rates using delivered dose.	253
Table 6.17 Maximum retreatment doses and predicted 2 year local control and overall survival rates.	254
Table 6.18 Comparison of the mean predicted toxicity risk between the delivered dose and maximum retreatment dose groups.	255
Table 6.19 Comparison of predicted toxicity between the delivered dose and maximum retreatment dose.	255
Table 6.20 Summary of dose and predicted risk to the cord, oesophagus, proximal bronchial tree and aorta from the delivered treatment.	257
Table 6.21 Summary of dose and predicted risk to the cord, oesophagus, proximal bronchial tree and aorta from the maximum retreatment dose.	258
Table 7.1 Dose constraints split into desirable, moderate and essential criteria.	273
Table 7.2 Rate of observed toxicity in relation to desirable constraints breached.	282
Table 7.3 Patient and tumour details for the patients that failed the desirable dose constraints.	283
Table 7.4 Mean delivered and replanned OAR doses.	284
Table 7.5 Differences between delivered and replanned OAR doses.	284
Table 7.6 Delivered and replanned PTV doses.	285
Table 7.7 Differences between the delivered and replanned PTV doses.	286
Table 7.8 Mean delivered and replanned OAR doses.	287
Table 7.9 Differences between the delivered and replanned OAR doses.	287
Table 7.10 Mean delivered and replanned PTV doses to moderate constraints.	288
Table 7.11 Differences between the delivered and replanned PTV doses using moderate constraints.	289
Table 7.12 Mean delivered and replanned OAR doses.	290
Table 7.13 Differences between the delivered and replanned OAR doses.	290
Table 7.14 Mean delivered and replanned PTV doses.	291
Table 7.15 Differences between the delivered and replanned PTV doses.	291
Table 7.16 Characteristics of re-plans unable to meet essential dose constraints.	292
Table 7.17 Original and Delphi PTV volumes.	294

Table 7.18 Original and cropped PTV volumes.	295
Table 7.19 Initial and adaptive PTV volumes.	295
Table 7.20 Summary of verification of cumulative EQD2 doses using the re-plans.	296
Table 7.21 Proximal bronchial tree cumulative dose from the delivered and replanned treatments that exceeded the dose constraints.	297
Table 7.22 Comparison of delivered and replanned dose to organs at risk.	300
Table 7.23 Change in predicted efficacy and toxicity between the delivered dose and the replanned treatments.	311
Table 8.1 Demographics of trial participants.....	331
Table 8.2 Toxicity experienced by participants.....	331
Table 8.3 Outline of themes and sub-themes	332
Table 9.1 Re-irradiation studies currently in recruitment.....	359

List of Figures

Figure 3.1 Outcomes from each round of questionnaires.....	69
Figure 4.1 Direction vectors with a limited region of interest.....	95
Figure 4.2 Direction vectors with a whole organ region of interest.....	95
Figure 4.3 Subgroup analysis of the hazard ratio for toxicity.....	98
Figure 4.4 Kaplan-Meier plot of overall survival for the whole group.....	100
Figure 4.5 Kaplan-Meier plot of overall survival split by second primary and locally recurrent lung cancers.....	101
Figure 4.6 Sub-group analysis of hazard ratios for death.....	102
Figure 5.1 Diagram outlining sources of data used in modelling.....	116
Figure 5.2 Flow chart detailing the process to select a dose constraint.....	122
Figure 5.3 PRISMA diagram.....	125
Figure 5.4 Plot of the cord multivariable model.....	134
Figure 5.5 Predicted vs observed spinal cord grade 3 toxicity rate by decile using the multivariable model.....	136
Figure 5.6 Plot of the oesophageal multivariable model without concurrent chemotherapy.....	151
Figure 5.7 Plot of the oesophageal multivariable model with concurrent chemotherapy.....	152
Figure 5.8 Plot of the oesophageal multivariable models with and without concurrent chemotherapy.....	153
Figure 5.9 Plot of the actual and predicted oesophageal multivariable model toxicity rates.....	155
Figure 5.10 Plot of cumulative mean lung dose multivariable model.....	169
Figure 5.11 Plot of cumulative mean lung dose univariable model.....	170
Figure 5.12 Plot of cumulative V5 univariable model.....	172
Figure 5.13 Plot of cumulative V20 univariable model.....	174
Figure 5.14 Plot of the actual and predicted cumulative mean lung dose multivariable model toxicity rates.....	176
Figure 5.15 Plot of the actual and predicted cumulative mean lung dose univariable model toxicity rates.....	177
Figure 5.16 Plot of the actual and predicted cumV5Gy model toxicity rates.....	178
Figure 5.17 Plot of the actual and predicted cumV20Gy model toxicity rates.....	179
Figure 5.18 Plot of the proximal bronchial tree multivariable model.....	192
Figure 5.19 Plot of the actual and predicted imputed PBRT model toxicity rates.....	194
Figure 5.20 Plot of cumulative aorta EQD2 Dmax univariable model.....	203
Figure 5.21 Plot of the actual and predicted aorta model toxicity rates.....	205
Figure 6.1 PRISMA diagram.....	231
Figure 6.2 Plot of the local control multivariable model (estimated PTV and re-treatment dose).....	241
Figure 6.3 Plot of the local control multivariable model (PTV and assumed concurrent chemotherapy).....	243
Figure 6.4 Predicted and observed 2 year local control rate by decile of model prediction.....	244
Figure 6.5 Predicted and observed 2 year local control rate by decile of model prediction.....	245
Figure 6.6 Plot of the 2 year overall survival univariable model by retreatment dose.....	250
Figure 6.7 Predicted and observed 2 year overall survival rate by study using the unadjusted model.....	251

Figure 7.1 Re-irradiation planning process.....	277
Figure 7.2 Replanning process for plans that failed essential constraints.	279
Figure 7.3 Beatson cohort and compliance with desirable dose constraints.....	281
Figure 7.4 Number of breached desirable organ at risk constraints.	281
Figure 7.5 Outline of replanning using alternative strategies.....	293
Figure 7.6 Patient 27 initial 3-field radiotherapy plan.....	298
Figure 7.7 Patient 27 re-irradiation re-plan.	298
Figure 7.8 Patient 27 cumulative dose plan in EQD2 Gy.	299
Figure 7.9 Change in cumulative dose to spinal cord between delivered and re-irradiation replan.	301
Figure 7.10 Change in cumulative risk to spinal cord between delivered and re-irradiation replans.	301
Figure 7.11 Change in cumulative lung V20Gy between delivered and re-irradiation replans.	302
Figure 7.12 Change in cumulative risk for grade 3 lung toxicity between delivered and re-irradiation replans.	303
Figure 7.13 Change in cumulative mean lung dose between delivered and re-irradiation replans.	304
Figure 7.14 Change in cumulative risk for grade 3 lung toxicity between delivered and re-irradiation replans.	304
Figure 7.15 Change in cumulative dose to the proximal bronchial tree between delivered and re-irradiation replans.	305
Figure 7.16 Change in cumulative risk for grade 3 proximal bronchial tree toxicity between delivered and re-irradiation replans.....	306
Figure 7.17 Change in cumulative dose to the oesophagus between delivered and re-irradiation replans.....	307
Figure 7.18 Change in cumulative risk for grade 3 oesophageal toxicity between delivered and re-irradiation replans.	307
Figure 7.19 Change in cumulative dose to the aorta between delivered and re-irradiation replans.	308
Figure 7.20 Change in cumulative risk for grade 3 or above aortic toxicity between delivered and re-irradiation replans.....	309
Figure 7.21 Predicted 2-year local control rate between the delivered plans and the re-plans.	310
Figure 7.22 Predicted 2-year overall survival rate between the delivered plans and the re-plans.....	311
Figure 8.1 Study schema	329

Acknowledgements

I would like to thank the following people whose patience and assistance made this research possible. I am extremely grateful to my supervisors, Dr Stephen Harrow and Prof Anthony Chalmers. This project was Stephen's idea, and his provision of wisdom, constant guidance, and good humour kept it on track. Anthony's advice and support with applications and funding, and relentless optimism in the face of minor setbacks like a global pandemic have been instrumental in bringing this work to completion.

I am deeply indebted to The Beatson Cancer Charity, The University of Glasgow and Cancer Research UK for their generous financial support of this project.

Dr John Fenwick and Prof Katie Robb have been invaluable sources of assistance for the modelling and qualitative research chapters respectively. Their advice and insights have been essential, and I have learned so much from our discussions. Dr Craig Dick, Dr Kevin Franks, Prof Gerry Hanna, Dr Louise Murray, Dr David Palma and Dr Claire Paterson were all kind enough to give their time and expertise at the outset and throughout this project. Thank you all for helping me plot a course through the occasionally choppy re-irradiation waters.

I am also grateful to the Physics team at the Beatson, especially Suzy Currie, Richard Ferguson, Martin Glegg, Peter Houston and Susan Morris for teaching me how to plan re-treatments (and letting me use all the buttons that clinicians shouldn't really press) and the Lung team for helping me realise some of the clinical nuances of re-irradiation that I would never have thought about.

Special thanks also to the trial team and the patients who participated in the interview study, and the clinicians who shared their expertise in the Delphi process.

To my Mum and Dad, thank you for giving me all the tools that I needed to get here, and for your love and support over the years.

And finally, to Kat and Olive. Thank you for putting up with me, when things have been hard going, and for providing the light over the last four years.

Author's Declaration

I declare that the work presented here is my own, unless otherwise acknowledged. This thesis has not been submitted for consideration of another degree at the University of Glasgow or any other institution.

Abbreviations

2D	Two-dimensional
3D	Three-dimensional
4D-V/Q PET-CT	Four-dimensional ventilation/perfusion positron emission tomography-computed tomography
AAA	Analytical anisotropic algorithm
AIC	Akaike's information criterion
AJCC	American Joint Committee on Cancer
ALK	Anaplastic lymphoma kinase
AUC	Area under the receiver operator curve
BED	Biological effective dose
BRAF	B-raf proto-oncogene
CALGB	Cancer and Leukaemia Group B
CBCT	Cone beam computed tomography
CCI	Charlson comorbidity index
CFRT	Conventionally fractionated radiotherapy
cGAS-STING	cyclic GMP-AMP synthase-stimulator of interferon genes
CHART	Continuous Hyperfractionated Accelerated Radiotherapy
CI	Confidence interval
COPD	Chronic obstructive pulmonary disease
CT	Computed tomography
CTCAE	Common terminology criteria for adverse events
cum-(prefix)	cumulative
CXR	Chest radiograph
DCR	Disease control rate
DDR	DNA damage response
Dmax	Maximum dose
DNA	Deoxyribonucleic acid
DSB	Double strand breaks
DVF	Deformation vector field
DVH	Dose volume histogram
Dx ³ cc	Dose to x cubic centimetres e.g. D1 ³ cc
ECOG-PS	Eastern Cooperative Oncology Group Performance Status
EGFR	Epidermal growth factor receptor
EQD2	Equivalent dose in 2 Gray fractions
EUD	Equivalent Uniform Dose
FLASH	Ultra-high dose radiotherapy
FSU	Functional sub-units
GARD	Genomic adjusted radiation dose
Gy	Gray
HR	Hazard ratio
ICRU	The International Commission on Radiation Units and Measurements

IGRT	Image guided radiotherapy
ILLRR	Isolated local or loco-regional recurrence
IMRT	Intensity modulated radiotherapy
kV	Kilovoltage
LBTE	Linear Boltzmann Transport Equations
LKB	Lyman-Kutcher-Burman
LQ	Linear-quadratic
MCO	Multi-criteria optimisation
MLC	Multi-leaf collimator
MLD	Mean lung dose
MRI	Magnetic resonance imaging
MV	Megavoltage
NHS	National Health Service
NSCLC	Non-small cell lung cancer
NTRK	Neurotrophic tyrosine receptor kinase
OS	Overall survival
PBrT	Proximal bronchial tree
PCI	Prophylactic cranial irradiation
PD-1	Programmed cell death protein 1
PD-L1	Programmed death-ligand 1
PET-CT	18-Fluorodeoxyglucose-positron emission tomography-computed tomography
PFT	Pulmonary function test
PRISMA	Preferred Reporting Items for Systematic Reviews and Meta-Analyses
PTV	Planning target volume
QUANTEC	Quantitative Analyses of Normal Tissue Effects in the Clinic
ROI	Region of interest
ROS1	ROS proto-oncogene 1
RSI	Radiosensitivity index
RTOG	Radiation therapy oncology group
RTV	Reported target volumes
SABR	Stereotactic ablative body radiotherapy
SARP	Small Animal Radiotherapy Platform
SARS-CoV-2	Severe acute respiratory syndrome coronavirus 2
SCLC	Small cell lung cancer
SNP	Single nucleotide polymorphism
SPLC	Second primary lung cancer
SSB	Single strand breaks
TKI	Tyrosine kinase inhibitors
TME	Tumour micro-environment
TNM	Tumour-Node-Metastasis
Vx Gy	Volume of a tissue receiving at least x Gray

1 Introduction

1.1 Overview

Second courses of radical radiotherapy for lung cancer have been given to selected patients since the 1970s, with long-term disease control in some. This is not standard practice due to concerns regarding the safety and efficacy of repeated radiation, and the lack of data to support treatment decisions. Radical re-irradiation is an attractive treatment as it offers patients with recurrent disease a second chance of disease control. This thesis investigates how re-irradiation can be delivered safely, by developing practice guidelines, safe dose limits, evaluating planning techniques and patient opinions on re-irradiation.

This introduction summarises the impact of lung cancer as a disease, the current treatment paradigm and why new treatments are required. This is followed by a short history of the clinical trial evidence for radiotherapy for non-small cell lung cancer (NSCLC), the effects of ionising radiation on tumour and normal tissue, and an overview of the recent advances in radiotherapy technology. This is required to provide context as the delivery and effects of the first course of radiation has an impact on the second course and illustrate how the technology to facilitate re-irradiation was developed.

The final section of the introduction outlines the possible treatments for recurrent disease, reviews the literature of re-irradiation for lung cancer and why re-irradiation is worthy of further investigation.

1.2 Lung cancer

1.2.1 Epidemiology

Lung cancer is the commonest cause of cancer death in the UK, with over 48,000 people diagnosed each year, and 35,000 deaths. The 5 year survival from lung cancer is 16.2%¹. In addition to the untold amount of human suffering, lung cancer has the highest economic cost of any tumour type, costing the EU €18.8 billion (15% of all cancer costs) in 2009 and is responsible for 23% of the total lost productivity from all cancers². In the UK, the demographics of lung cancer

are changing, with the incidence rising in women by 15% and decreasing in men by 8% from 2007 to 2017, and this shift is mirrored globally^{1,3}. Half of patients diagnosed with lung cancer are 75 years of age or above, and incidence and mortality are higher in socio-economic classes IV and V^{1,4,5}.

The predominant risk factor for lung cancer is tobacco smoke. This has been shown to increase the risk of lung cancer and all-cause mortality in several studies⁶⁻⁸. Other factors are air pollution, occupational exposures to asbestos, silica dust, polycyclic aromatic hydrocarbons and chromium compounds, chronic inflammation of the lung and genetic predisposition⁹.

1.2.2 Histology

Lung cancer can be divided into two broad categories pathologically: NSCLC, (85%) and small cell lung cancer (SCLC, 15%). The main histologies represented by NSCLC are squamous cell cancers, adenocarcinomas and large cell carcinoma. Considerable heterogeneity is seen in the behaviour and response to treatment of NSCLC, with the discovery of driver mutations and the interaction with the immune system leading to new targeted therapies and immunotherapies. There has been less progress in the management of SCLC, the main development being the addition of immunotherapy to platinum-based chemotherapy¹⁰.

1.2.3 Diagnosis and staging

Diagnosis and staging of lung cancer typically involve a series of investigations that may include chest radiographs (CXR), computed tomography (CT) of the thorax, abdomen and pelvis, 18-fluorodeoxyglucose-positron emission tomography-computed tomography (PET-CT), magnetic resonance imaging (MRI) brain and a biopsy, either bronchoscopically, thorascopically or percutaneously. Staging of lung cancer is according to the tumour-node-metastasis (TNM) system from the American Joint Committee on Cancer (AJCC)¹¹.

1.2.4 Treatment of NSCLC

Treatment of lung cancer is dependent on the stage at diagnosis and the pathology of the tumour. In NSCLC, stage I and II tumours can be treated with radical surgery, or in patients who are unfit or decline thoracic surgery, radical

radiotherapy^{12,13}. There are several approaches for stage III tumours depending on the operability of the disease. For patients with operable disease, options include radical surgery followed by adjuvant treatment, neo-adjuvant chemotherapy (+/-immunotherapy) and surgery, or chemo-radiotherapy followed by surgery. Adjuvant chemotherapy, immunotherapy or targeted treatment (depending on molecular markers) post-operatively may be offered for patients of Eastern Cooperative Oncology Group Performance Status (ECOG-PS) of 0 or 1, with positive lymph nodes¹⁴. Post-operative radiotherapy may be offered in selected patients with positive resection margins; a recent study concluded that there is no survival benefit to irradiating completely resected disease¹⁵. Patients with inoperable disease can be treated with definitive chemo-radiotherapy with adjuvant immunotherapy or sequential chemotherapy and radical radiotherapy. There is considerable variation in practice in this area¹⁶.

Patients with stage IV disease are treated palliatively, except for patients with a solitary brain metastasis and a radically treatable lung primary, where radical treatment can be given to both sites. There is an increasing number of treatment options for patients with metastatic disease, dependent on the mutational status and expression of programmed death-ligand 1 (PD-L1) of the tumour. Prior to 2009, platinum doublet chemotherapy was the standard of care, and remains so for patients with no oncogenic mutations and are unsuitable for immunotherapy¹⁷. Historically, the median overall survival (OS) from chemotherapy is 8 months¹⁸. Between 2009 and 2015, tyrosine-kinase inhibitors in patients with oncogenic mutations (such as gefitinib and erlotinib for epidermal growth factor receptor (EGFR) mutation positive tumours, or crizotinib for anaplastic lymphoma kinase (ALK) rearranged tumours) demonstrated superior efficacy to chemotherapy and were approved for treatment in the UK¹⁹⁻²¹. Since then, further targeted therapies for mutations in ROS proto-oncogene 1 (ROS1), B-raf proto-oncogene (BRAF), and neurotrophic tyrosine receptor kinase (NTRK) are now available. Immunotherapy with PD-1 or PD-L1 blockade has been used for NSCLC, initially in the second line setting after chemotherapy, then subsequently in the first line setting for patients with PD-L1 $\geq 50\%$ as monotherapy, or in combination with chemotherapy regardless of PD-L1 status²²⁻²⁴. These trials have demonstrated longer median OS compared to chemotherapy alone. When compared to chemotherapy alone, there is less

toxicity with immunotherapy monotherapy and similar amounts of toxicity with the chemotherapy-PD-L1 combination.

In summary, lung cancer is a common and lethal cancer with poor outcomes, often affecting older patients with comorbidities associated with tobacco smoke. Radiotherapy is a curative option in the primary treatment of both NSCLC and SCLC. It can be used as the sole modality or in combination with chemotherapy or immunotherapy.

1.3 Role of radiotherapy in lung cancer

Roentgen discovered x-rays in 1895 and one year later, there were reports of radiation being used to treat benign and malignant diseases²⁵. Lung cancer was considered a rare disease in the 19th and early 20th centuries, likely due to the absence of tobacco smoking and very limited techniques to diagnose thoracic malignancies^{26,27}. However, the incidence of lung cancer increased dramatically as tobacco consumption became commonplace. Radiotherapy also had extremely poor outcomes in part because the x-ray energies generated by cathode ray tubes were too low to give tumoricidal doses to deep tissues (such as in the lung) without causing significant skin toxicity. This is reflected in the outcomes from the use of kV (kilovoltage) radiotherapy as the sole modality of treatment with a 5 year survival of 2.7%²⁸. Therefore, the role of radiotherapy in lung cancer between 1930 and 1950 was generally used as neo-adjuvant or adjuvant treatment after surgery or to palliate symptoms²⁹.

The development of the megavoltage (MV) linear accelerator allowed greater skin-sparing. Results from 8MV and 240kV radiotherapy for lung cancer were reported in the late 1950s. This showed an improvement in 1 year survival for squamous cell lung cancer (38% for 8MV and 24.2% for 240kV). In addition, there were fewer radiation reactions in the MV group³⁰. A randomised trial compared radiotherapy (4500 rads given over 4 weeks using 8MV beams) against surgical management. This study reported a statistically significant survival benefit with surgery. However this study generated interest in how to improve radiotherapy for those unable to have an operation³¹.

1.3.1 Radical radiotherapy in non-small cell lung cancer

The first major trial to test the different doses and schedules in a defined population was the landmark Radiation Therapy Oncology Group (RTOG) trial 73-01, published in 1982. This study enrolled unresectable NSCLC patients with stage III disease and randomised them into 4 groups: 4000 rad in a split course, 4000 rad, 5000 rad and 6000 rad in daily 200 rad doses. It demonstrated a greater response rate (71%) and reduced intra-thoracic recurrence (30%) in the 6000 rad group, significantly better than the other groups³². This study established 60 Gy (equivalent to 6000 rad) as the standard of care dose for NSCLC. The two main questions that defined subsequent radiotherapy trials in lung cancer were (i) what is the optimal schedule and dose to increase tumour control and (ii) what is the best systemic treatment to give with radiotherapy to improve outcomes?

1.3.2 Trials testing novel radiotherapy schedules and dose

Three key studies in the 1990s explored different radiotherapy schedules. The phase I/II RTOG 83-11 trial explored hyperfractionation and dose escalation. Patients with stage II - IV NSCLC were given 1.2 Gy twice daily four hours apart, to increasing prescription doses (60 Gy, 64.8 Gy, 69.6 Gy, 74.4 Gy and 79.2 Gy). Toxicity was deemed acceptable with a grade 3 or worse rate between 5.7% and 10.5% across all arms. There was no OS difference between the dose groups on intention to treat analysis, however in a subgroup analysis of patients with PS 0-1 and stage III disease, 69.6 Gy had superior 2 year OS rate compared to 60 Gy (35% vs 13% respectively)³³.

One study that did demonstrate a survival advantage was the CHART (Continuous Hyperfractionated Accelerated Radiotherapy) trial. This phase III study randomised patients with stage I - III NSCLC to either standard radiotherapy with 60 Gy in 2 Gy fractions or 54 Gy in 1.5 Gy fractions given three times a day over 12 days with no interruptions (CHART). The majority of the patients had stage III disease (61%). Patients in the CHART arm had a 24% reduction in the risk of death (hazard ratio (HR) for death 0.76, $p=0.004$, 95% confidence interval (CI) 0.63-0.92). This translated to an improvement in 2-year OS from 20% to 29%. This was at the cost of increased early dysphagia³⁴. The barriers to universal

adoption of this approach were the logistical challenges of delivering the treatment and how to incorporate chemotherapy into this regime³⁵.

Dose escalation and hypofractionation were evaluated in the phase I/II RTOG 83-12 trial, where patients with stage III disease received 75 Gy in 28 treatments, given once daily over 5.5 weeks. The 2-year OS was 24% with a 5% rate of severe late toxicity. Despite the high dose to the tumour, the local failure rate was 33%³⁶. This early trial of hypofractionation demonstrated tolerability of high dose radiotherapy.

Both CHART and subsequent research, in part on head and neck cancers, demonstrate that extending overall treatment time beyond 4 weeks is detrimental to overall disease control, due to accelerated repopulation of the tumour³⁷. Therefore, subsequent studies used hypofractionation to reduce the duration of the radiation course with the additional benefits of a convenient once daily schedule and the ability to include chemotherapy. Early studies of hypofractionation used 55 Gy in 20 fractions and this was widely adopted in the UK without a randomised controlled trial^{38,39}.

As radiotherapy technology improved in the 2000s, hypofractionation became possible with manageable toxicity due to the advances in radiotherapy planning and delivery, with a move from 2-dimensional (2D) planning to 3 dimensional (3D) CT planning, and image guided radiotherapy (IGRT). This increased the precision of treatment, allowing for greater sparing of normal tissue. These developments were applied not only to stage III NSCLC, but also in stage I and II, with the use of stereotactic ablative body radiotherapy (SABR).

SABR involves the use of high dose per fraction radiotherapy (≥ 5 Gy per fraction) over shorter courses (1 - 2 weeks). The use of SABR for patients with inoperable early-stage NSCLC had an 88% 3-year cause-specific survival, a 6% local failure rate, and little acute toxicity⁴⁰. These impressive outcomes were replicated in several other studies⁴¹⁻⁴⁵. A subsequent randomised trial compared conventional fractionation and SABR in early-stage NSCLC. The two-year cumulative incidence of local failure was 10% in the SABR arm, compared to 26% in the conventional fractionation arm (HR 0.32, 95% CI 0.13-0.77, p-value = 0.008). Median OS was 5

years in the SABR group and 3 years in the standard arm (HR 0.53, 95% CI 0.30-0.94, p-value = 0.027)⁴⁶.

The trials of the last 50 years have tested several different radiotherapy regimes. The standard of care for stage I-II NSCLC is SABR. For stage III tumours or stage I-II patients unsuitable for SABR, CHART, 55Gy in 20 fractions or 60-66Gy in 30-33 fractions are in common use in the UK⁴⁷. Dose escalation beyond this has not demonstrated a survival benefit, therefore research proceeded to enhance the effect of radiotherapy with systemic treatment.

1.3.3 Trials testing systemic therapies with radical radiotherapy

At the same time as RTOG 83-11 was recruiting patients in the mid-1980s, the Cancer and Leukaemia Group B (CALGB) 8433 studied the addition of induction chemotherapy with cisplatin and vinblastine with stage III NSCLC. This phase III study randomised patients between two months of induction chemotherapy followed by radical radiotherapy (60 Gy in 2 Gy fractions) or radical radiotherapy alone. The combination group had a superior median OS of 13.6 months compared to 9.6 months for radiotherapy alone group (p-value 0.012), and 2-year OS rates of 26% vs 13% respectively⁴⁸.

The results of RTOG 83-11 and CALGB 8433 made it difficult to determine what was the optimal treatment for patients with stage III NSCLC. To resolve this question, RTOG 88-08 compared induction chemotherapy followed by radical radiotherapy (60Gy in 2 Gy fractions), high dose hyperfractionated radiotherapy (69.6 Gy in two daily 1.2 Gy fractions) and radical radiotherapy alone (60Gy in 2 Gy fractions). The sequential chemotherapy/radical radiotherapy arm had significantly longer median OS 13.8 months compared to 12.3 and 11.4 months in the hyperfractionated and standard radiotherapy arms (p-value 0.002) with acceptable toxicity⁴⁹. However, the 5-year survival remained low at 5-8% for all groups⁵⁰.

Subsequent trials focused on investigating chemotherapy concurrently with radiotherapy. RTOG 88-04 was a phase II study in stage II or III NSCLC using conventionally fractionated radiotherapy (61.2 Gy in 1.8 Gy fractions once daily) with two cycles of cisplatin and vinblastine pre-radiotherapy and then

concurrently with the radiation. The grade 4 or worse acute toxicity rate was 31% and the median OS was 13.9 months⁵¹.

RTOG 09-15 was a phase II study using hyperfractionated radiotherapy (69.6 Gy in 1.2 Gy fractions twice daily) and concurrent cisplatin-vinblastine. The acute grade 4 or worse toxicity rate was 45%, and this resulted in only 53% completing treatment on protocol. Despite the high burden of toxicity of the intensified treatment, the 2-year OS rate was 28% and 31% had local recurrence at 18 months⁵².

Further analysis of the data from these trials showed that regardless of which strategy was used (induction chemotherapy and standard radiotherapy, concurrent chemotherapy and standard radiotherapy or concurrent chemotherapy and hyperfractionated radiotherapy), the in-field failure rate was high (58%, 71% and 55% respectively)⁵³.

Two large phase III randomised controlled trials compared sequential and concurrent chemoradiotherapy. In a Japanese study, there was longer median OS in a group of stage III patients treated with concurrent chemotherapy compared with sequential (16.5 months to 13.3 months, p-value 0.04) with a 2 year OS rate of 34.8% in the concurrent arm⁵⁴. The RTOG 94-10 randomised PS 0-1 patients with unresectable stage III NSCLC to either cisplatin/vinblastine and standard radical radiotherapy (60 Gy in 2 Gy fractions) sequentially, cisplatin/vinblastine and standard radical radiotherapy concurrently, or cisplatin/etoposide and hyperfractionated radiotherapy (69.6Gy in 1.2 Gy fractions twice daily). Patients treated with once daily concurrent chemoradiotherapy had a significantly longer median OS compared to the other groups (17 months compared to 14.6 months for the sequential arm and 15.6 months for the hyperfractionated arm, p-value 0.046)⁵⁵. The 5-year survival for the concurrent arm was 16%. A third trial compared sequential against concurrent chemotherapy with hypofractionated radiotherapy (55 Gy in 20 fractions). This confirmed the safety of the hypofractionated regime, but due to poor recruitment, the trial closed early, resulting in inadequate power to assess for any difference in OS⁵⁶. A subsequent meta-analysis of 19 trials demonstrated a reduction in the risk of death with concurrent chemoradiotherapy compared to radical radiotherapy alone (HR 0.71, 95% CI 0.64 to 0.80). Concurrent chemoradiotherapy compared to sequential

treatment also had a reduced risk of death (HR 0.74, 95% CI 0.62 to 0.89) on meta-analysis of 6 trials⁵⁷. This established concurrent chemoradiotherapy as the standard of care in fit patients with irresectable stage III NSCLC.

More recently, the use of biological agents and immunotherapy in conjunction with concurrent chemoradiotherapy. The RTOG 06-17 trial is a controversial phase III study with a 2x2 factorial design. It compared standard concurrent chemoradiotherapy (60 Gy in 2 Gy fractions) with or without cetuximab (an anti-EGFR antibody) against high dose concurrent chemoradiotherapy (74 Gy in 2 Gy fractions), again, with or without cetuximab. The standard dose arms had longer OS compared to the high dose arms (28.7 months vs 20.3 months, two-sided p-value 0.008) and cetuximab had no effect on survival⁵⁸. This was unexpected as there was a growing body of evidence that the higher the delivered dose, the greater the chances of tumour control⁵⁹. In addition, the local relapse rate was worse in the high dose arm compared to the standard arm, although not statistically significant (45.7% vs 38.2%, p-value=0.07)⁶⁰. One theory for why the high dose arm performed worse is due to increased cardiac doses in the high dose arm resulting in undetected early cardiac deaths⁶¹. Other possibilities are related to the longer overall treatment time in the high dose arms and less adherence to dose constraints due to variance in the radiotherapy quality assurance⁶².

The PACIFIC trial recruited a similar group of patients as RTOG 06-17 (unresectable stage III NSCLC) but used standard dose concurrent chemoradiotherapy followed by immunotherapy. Chemotherapy and radiotherapy in pre-clinical studies demonstrated increased expression of PD-L1 on tumour cells^{63,64}. Immunotherapy with PD-1 and PD-L1 inhibitors had proven efficacy in metastatic NSCLC. It was hypothesised that chemoradiotherapy would therefore sensitise the tumour to PD-L1 inhibitors. This practice-changing trial demonstrated that the addition of adjuvant durvalumab (a PD-L1 inhibitor) started within 42 days of completing concurrent chemoradiotherapy improved median OS when compared to adjuvant placebo (47.5 months vs 29.1 months, HR = 0.71, 95% CI: 0.57-0.88, p-value <0.01)^{65,66}. This is now the standard of care for fit stage III NSCLC patients, although despite this, local failure remains at 36.6%⁶⁷.

Radiation treatment for NSCLC has evolved over the last 70 years from high dose palliation with poor overall survival outcomes, to a treatment that now has a chance of 5-year survival for a large group of patients. This was achieved through a series of trials, which firstly established a safe radical radiotherapy dose of 60 Gy in 30 fractions (median OS of 9 - 12 months) for all stages of NSCLC. For stage I and II NSCLC, SABR has excellent outcomes with 80-90% local control rates. For stage III NSCLC, the use of sequential chemotherapy improved OS by 3 months, and the use concurrent chemoradiotherapy improved this further to approximately 17 months initially. Further improvements in pre-treatment staging with PET-CT and radiotherapy treatment increased OS to 28 months as seen in RTOG 06-17. The addition of adjuvant PD-L1 inhibitors increased this further to 47.5 months. However, local control remains troublesome with RTOG 06-17 and PACIFIC reporting rates of local only failure between 36-46%. There is strong evidence relating local control to overall survival, and dose escalation has not provided the predicted benefits, resulting in a large number of patients who have localised recurrence after initial radiotherapy.⁶⁸

1.4 The radiobiology of ionising radiation as treatment for cancer

The previous section summarised the clinical trial evidence of radiation as a curative treatment for lung cancer. The triallists tested higher radiotherapy doses in attempt to reduce the amount of treatment failures, but this approach caused significant toxicity. The next section details the effect of radiation on tumours and normal tissue, and the methods that have been developed to model efficacy and toxicity.

1.4.1 The effect of ionising radiation on cells

When ionising radiation reaches cells, a series of physical, chemical and biological events occur. The physical events involve the interaction between charged particles and the organic matter of the cell. This interaction creates ionisation events in the cell and the formation of free radicals, which are highly reactive species. The free radicals undergo a chain of chemical reactions, before they are either scavenged by intra-cellular mechanisms or damage cellular

structures. The physical and chemical reactions take place within a millisecond of irradiation.

The critical structure for cell survival and ability to proliferate is the nucleus of the cell, due to the presence of DNA⁶⁹. The biological consequences of these reactions revolve around the cellular response to DNA-damage and can take minutes to many years to take effect. Ionising radiation damages DNA by the creation of single strand or double strand DNA breaks (SSBs or DSBs). One Gray of radiation will create approximately 1000 SSBs and 30-40 DSBs. DSBs are the most lethal type of damage as they interfere most with the cells ability to undergo mitosis successfully. Cells have evolved a complex system called the DNA damage response (DDR) to identify and repair SSBs, DSBs and other changes to the DNA that may affect genomic fidelity. The three main outcomes from the DDR are checkpoint activation, DNA repair, or cell death. Whether a cell survives ionising radiation depends on several factors including the extent and location of damage and how well that damage is repaired. Tumour cells often have impaired DDR mechanisms and may be in a proliferative phase of the cell cycle, therefore may be more susceptible to radiation induced injury compared to normal tissue.

Cells can die in several different ways after radiation. The main ways are apoptosis, autophagy, necrosis, senescence and mitotic catastrophe. These processes can happen over a long period of time. This makes it difficult to accurately measure the amount of cell death as changes in the DNA take time to manifest themselves. Therefore, a different method, called clonogenic survival is used, which determines the ability of an irradiated cell to firstly survive and subsequently undergo multiple rounds of proliferation. The clinical outcomes of any radiotherapy treatment are dependent on the survival of normal tissue cells (which predict normal tissue toxicity), and the death of tumour cells (tumour control). These two competing aims are described in the therapeutic index. The ideal situation for radiotherapy would be to treat only the tumour and have no dose to normal tissue. However, this is impossible to achieve, as radiation has to travel through normal tissue to reach the tumour, and an adequate margin needs to be included around the tumour to ensure that all of the cancer cells are treated. Moreover, most cancer cells invade normal tissue, making tumour and normal cells inseparable. Therefore, for a given radiation treatment, a fraction

of normal tissue cells and a fraction of tumour cells will die. The biological effect of the loss of normal tissue may lead to toxicity, and the biological effect of the death of tumour cells is eradication of the cancer. A radiation treatment will be useful if the biological effect on the tumour is significant, without causing severe toxicity. The prediction of the biological effects of radiation on normal tissue and tumours is important to identify if a treatment will be beneficial for patients.

1.4.2 The linear-quadratic model

Several models can be used to predict the survival of irradiated cells. One model is the linear-quadratic (LQ) model. In simple terms, it is a mathematical expression that fits observed survival curves from clinical experiments. It is in common use as it has been proven to be accurate over 1-6Gy per fraction (the fraction sizes commonly used clinically). The expression is:

$$SF = \exp(-\alpha D - \beta D^2)$$

where D = total dose, SF = surviving fraction.

The first order term ($\exp(-\alpha D)$) describes the linear contribution to cell death, and the second order term ($\exp(\beta D^2)$) relates to the quadratic component of cell death. It is postulated that that these two mathematical terms represent different types of DNA damage. The linear part of the equation describes where a single electron damages two adjacent chromosomes, leading to serious damage to the DNA in the form of dicentric or centric-ring chromosomes which make mitosis impossible. The quadratic part of the equation describes where two independent single electron tracks damage to neighbouring chromosomes, leading to lethal damage. However, there remains uncertainty on the exact mechanism that this model describes. Additionally, the LQ model becomes inaccurate at fraction sizes beyond 6Gy, as the radiation damage relationship becomes more linear, represented by the linear-quadratic-cubic model.

1.4.3 Fraction sensitivity

From the start of the use of radiation as a cancer treatment, splitting the dose of radiotherapy into smaller fractions causes less normal tissue toxicity with

similar effect on the tumour⁷⁰. Fraction sensitivity is an intrinsic characteristic of a cell's response to radiation and is described by the α/β ratio. This describes the point of the LQ curve where the contribution of the linear and quadratic parts of the equation are equal. Each tissue has a different α/β ratio and is often different for the specific outcome that is being assessed. The ratios for human tissue have been determined experimentally. For example, late toxicity from radiation is associated with low α/β ratios, and early toxicity is associated with high α/β ratios⁷¹. Tumours were thought to all have high α/β ratios, however, recent clinical data demonstrates that for breast and prostate tumours, the α/β ratio is lower than what had been assumed, leading to the adoption of hypofractionated regimes^{72,73}.

The LQ model incorporates fractionation by adding the terms total effect (E) in n number of fractions, and D = total dose, and d = dose per fraction:

$$SF_d = \exp(-\alpha d - \beta d^2)$$

$$E = -\log_e(SF_d)^n$$

$$E = -n \log_e(SF_d)$$

$$E = -n(-\alpha d - \beta d^2)$$

$$E = \alpha n d + \beta n d^2$$

Adding $nd=D$

$$E = \alpha D + \beta d D$$

This equation gives the total expected effect of a course of radiotherapy. It is useful in clinical practice to re-arrange this formula to compare different dose fractionation schedules, by calculating the equivalent dose. As the α/β value is a measure of fraction sensitivity, first this equation is rearranged to include this term:

$$E = \alpha D + \beta d D$$

$$E = \alpha D \left(1 + \frac{\beta d}{\alpha}\right)$$

$$E = \alpha D \left(1 + \frac{d}{\alpha/\beta}\right)$$

E and α are constant and the equation can be reformulated like this, for two equivalent dose fractionation schedules:

$$\alpha D_1 \left(1 + \frac{d_1}{\alpha/\beta}\right) = \alpha D_2 \left(1 + \frac{d_2}{\alpha/\beta}\right)$$

$$D_1 \left(1 + \frac{d_1}{\alpha/\beta}\right) = D_2 \left(1 + \frac{d_2}{\alpha/\beta}\right)$$

$$\frac{D_1}{D_2} = \frac{\left(1 + \frac{d_2}{\alpha/\beta}\right)}{\left(1 + \frac{d_1}{\alpha/\beta}\right)}$$

Expressing 1 with α/β as the denominator (i.e., $\alpha/\beta / \alpha/\beta$), and then dividing the right-hand side of the equation gives:

$$\frac{D_1}{D_2} = \frac{\left(\frac{\alpha}{\beta} + d_2\right)}{\left(\frac{\alpha}{\beta} + d_1\right)}$$

To convert between different dose and fractionation schedules, the concept of EQD2 (equivalent dose in 2 Gray fractions) has been used widely, as the 2 Gy per fraction is a frequently used dose in clinical practice, and the units from this equation are in Gy, which make the results easier to understand in a clinical context. Taking D_1 as EQD2 and d_1 as the 2 Gy dose per fraction:

$$EQD2 = D_2 \frac{(d_2 + \alpha/\beta)}{(2 + \alpha/\beta)}$$

An alternative method is to calculate the biological effective dose (BED), which is a theoretical dose that gives the total effect of radiation if it was given continuously i.e., E/α :

$$E = \alpha D \left(1 + \frac{d}{\alpha/\beta}\right)$$

$$BED = \frac{E}{\alpha} = nd \left(1 + \frac{d}{\alpha/\beta}\right)$$

BED produces values in $Gy_{\alpha/\beta}$ which makes it difficult to apply in clinical situations, therefore the ICRU recommends using EQD2 for dose conversions. The utility of the LQ model (and of its derivatives EQD2 and BED) allow the biological effects of different dose and fractionations to be compared in a single term, for both tumour control and normal tissue.

1.4.4 Tumour control probability models

The dose required to maximise the probability of killing all proliferating tumour cells is important, as too low a dose will result in sub-optimal control rates, and too high a dose will cause unnecessary normal tissue death with resulting toxicity.

Historically, doses for tumour control have been determined by the maximum dose the normal tissues can tolerate, with the assumption that the higher the dose, the better chance of tumour control. However, tumour response to the same delivered dose is often heterogenous. There are many possible reasons why the responses of tumours are not uniform, such as different phases of the cell cycle, tumour hypoxia and the intrinsic radiosensitivity of a cell.

The LQ model can be used for tumour control probability (TCP) modelling with corrections for repopulation and sub-lethal repair. This approach has been used for modelling outcomes from SABR, and comparing 3D-conformal radiotherapy,

CHART and SABR in early-stage lung cancer^{74,75}. The SABR modelling study developed tumour control models from clinical trial data. They demonstrate that high rates of local control are achieved with a dose of 50Gy in 5 fractions, and that higher doses may not add extra efficacy⁷⁵.

1.4.5 Normal tissue complication probability models

The ability to predict the normal tissue effects from a dose of radiation is critical at reducing the toxicity from treatment. These NTCP models are different to TCP models, in terms of how normal tissues respond to radiation, the measurement of outcomes and how the dose to normal tissue can be calculated.

Normal tissue responds differently to radiation damage compared to tumour cells. Toxicity can be divided into early side effects (within three months of radiation) and late side effects (beyond three months). Early side effects affect cells which are highly proliferative such as bone marrow, skin or cells lining mucosal barriers. These cells have a rapid turnover as part of their physiological function. Radiation depletes the available cells for cell division, leading to acute toxicity such as mucositis, or pancytopenia. However, cellular repopulation occurs either by migration of stem cells or the division of surviving stem cells in the irradiated area, and the tissue regains its function. Consequential late side effects occur when the radiation damage that resulted in the early side effects is so severe that the tissue is unable to repair, leading to long term toxicity. Late side effects can affect any type of tissue, can occur many years after radiation, and are often irreversible. It is a complex interaction between the immune system, the tissue vasculature, and the tissue parenchyma, triggered by the loss of functional cells.

In addition to the proliferation rate of cells, the architecture of an organ is important in how radiation damage can manifest itself as clinical toxicity. Tissue organisation can be classified as parallel or serial. Parallel organs are able to withstand high doses to a small part of their structure and still function (e.g., lung). The failure of the organ is therefore largely dependent on the total volume of tissue irradiated. Serial organs require all parts of the structure to function, therefore if a part of the organ had a high dose and failed, the whole

structure would fail (e.g., spinal cord, bowel). Therefore, the highest dose received by any part of the structure is predictive of toxicity. Some organs have elements of both, and this can be characterised by the relative seriality index.

Due to how normal tissue is organised and responds to radiation, there is a range of clinical presentations of toxicity. To accurately capture this, grading systems for toxicity are more detailed. Several toxicity grading scores exist such as the CTCAE (common terminology criteria for adverse events) or RTOG scales. These scales rank toxicity between zero to five, with zero having no toxicity, and five being severe toxicity leading to death.

Another difference between NTCP and TCP models is the homogeneity of the radiation dose. Most non-SABR radiation doses to the tumour are calculated to be within 95 - 107% of the prescription dose so can be considered generally homogenous⁷⁶. In order to reduce the dose to normal tissue, there is often dose fall-off across an organ. For example, in thoracic radiotherapy, the dose across the lungs varies widely, with some parts having the prescription dose, and other having virtually no dose. NTCP models therefore must accommodate this added complexity.

There are two general approaches to NTCP modelling: mechanistic models and phenomenological models. Mechanistic models, such as the LQ model, express mathematically the biological events that occur in irradiated cells.

Phenomenological models attempt to describe dose and outcome data in mathematical terms that are not connected to the biological processes of irradiated tissue. The first widely used model is the Lyman model which was initially used to describe the probability of cardiac toxicity as a function of the total dose and the partial volume uniformly irradiated (i.e. a third of the organ received a given dose)⁷⁷. However, normal tissues had a range of doses across the organ, rather than one part of the organ receiving a given dose. To resolve this problem of dose heterogeneity across an organ, the Lyman-Kutcher-Burman (LKB) model was developed. This took the maximum dose and dose-volume histogram (DVH) of an organ and converted it to the effective volume. This can be used to predict the probability of toxicity by interpolating between the existing known toxicity rates from partial organ uniform irradiation⁷⁸.

The Lyman and LKB models were developed as tools to select the optimal radiotherapy plan. The models predict the risk of toxicity and allow clinicians to choose the most suitable plan. Radiotherapy planning systems improved from forward planning (where a dose distribution was calculated by placing the beams first, then predicting the dose) to inverse planning (where a set of objectives are provided to the planning system and a beam arrangement is calculated to deliver the pre-specified dose targets). A further development from inverse planning (where the dose determines the target) is the concept of an equivalent uniform dose (EUD) planning. The EUD is derived from the LQ model for a given target with corrections for inhomogeneities and can be used in inverse planning optimisation^{79,80}. An EUD based model uses the calculated probability of complication for a given plan as a target, rather than physical dose constraints.

These models are limited as the primary variable in the calculation is the dose received by the normal tissue. This is an important factor which is modifiable by the clinician. However, there are many different variables that could influence toxicity. For example, patients with lung cancer often have chronic obstructive pulmonary disease (COPD), the severity of which could make them more likely to develop toxicity after radiotherapy⁸¹. The addition of genetic information to a LKB model of radiation pneumonitis demonstrated superior predictive ability than the LKB model alone⁸². Therefore, the ideal NTCP model should account for additional non-dose variables. Data driven models have the flexibility to accommodate both dose and other variables and have the benefit of relative ease of use.

There are several different data driven modelling techniques, including logistic regression and machine learning models. Logistic regression is a common statistical method of predicting a binary outcome (i.e., toxicity or no toxicity) from independent predictor variables. The logistic regression formula is:

$$P = \frac{e^{a+bX}}{1 + e^{a+bX}}$$

where P is the probability of an event occurring, a is a constant, and b is a coefficient of predictor variable X . The formula can be expanded to accommodate any number of variables:

$$P = \frac{e^{a+b_1X_1+b_2X_2+b_3X_3\dots b_nX_n}}{1 + e^{a+b_1X_1+b_2X_2+b_3X_3\dots b_nX_n}}$$

when n is the number of variables included in the model. This model produces a sigmoid graph like the previously discussed models. The main drawback to data driven modelling is the quantity and quality of the data, with large amounts of accurate predictor variable data needed, consistent outcome detection, and enough outcome events for statistical validity.

The practical applications of these models are seen first in the work of Emami *et al.* who describes the dose and expected toxicity with partial volume uniform irradiation of the organs of the body⁸³. As the dose to normal tissues became more heterogenous as radiotherapy moved from 2D to 3D planning, these dose constraints became outdated. The Quantitative Analyses of Normal Tissue Effects in the Clinic (QUANTEC) series of papers in 2010 used data from 3D dosimetry. They form the basis of the current dose constraints used in clinical practice for conventionally fractionated treatments⁸⁴. For SABR, dose constraints have been developed as part of the high dose per fraction, Hypofractionated Treatment Effects in the Clinic (HyTEC) initiative⁸⁵. These dose constraints are essential to reduce the risk of toxicity from radiation treatments.

1.5 Radiotherapy planning and delivery for lung cancer

Ionising radiation has been used as a treatment for cancer for over 100 years. Radiotherapy has adopted vast scientific and technological developments over that time to improve treatments. The advances in technology have directly led to more conformal radiotherapy delivery, more precise treatments using image guidance, better methods to predict dose deposition, and the use of different types of ionising radiation. The cumulative benefits of this slew of innovation improve tumour control and minimise toxicity.

1.5.1 Radiotherapy technique

Radiotherapy for deep seated tumours was limited in the first part of the 20th century due to the low energy of the photons produced by radioactive sources and kV x-ray tubes, as this would cause unacceptably large dose deposition to subcutaneous tissue. The linear accelerator, developed at Stanford University in

the 1940s, allowed the widespread clinical use of high energy photons and made the treatment of deep seated tumours such as lung cancers possible⁸⁶.

Planning radiotherapy in the 1970s and 80s used 2D plain x-rays and a range of beam modifying devices such as wedges, to shape the beam to the planning target volume. This is an example of forward planning, as the dose delivered to the target is calculated by the beam arrangement. If any changes were required to the plan, the beams would have to be re-arranged and the dose recalculated.

Planning using plain x-rays required larger margins to be added when treating a tumour due to the difficulty in predicting the tumour location. CT scans provide better visualisation of the tumour. This technique of 3D-radiotherapy planning allows for the margins to be smaller, thereby treating less normal tissue. A comparative study of 2D and 3D planning for lung cancer demonstrated significant normal tissue sparing and similar tumour doses with 3D planning compared to 2D⁸⁷. Two key technological advances in the 1990s - intensity modulated radiotherapy (IMRT) with the multi-leaf collimator (MLC) and improved computing power enabled increased sophistication of radiotherapy delivery.

The MLC is a beam shaping device that uses leaves that sit on automated tracks to block parts of the beam. This creates a shaped beam that better resembles the planning target volume (PTV). The PTV is created by a series of steps, to ensure with a high degree of confidence that the tumour, at the time of treatment is in that volume. The initial step is delineating the gross tumour volume (GTV), which is the tumour on the CT scan (or other imaging). This GTV is grown by a margin (which depends on the type of tumour) to account for the microscopic disease that is surrounding the tumour but is not visible on the scan. This is known as the clinical target volume (CTV). The CTV is finally grown to form the PTV, to accommodate for the factors that can change over the multiple treatments that form a course of radiotherapy, such as the patient's organ motion, changes in how the patient is positioned on the treatment couch and machine variability. Utilising the variety of shapes that the MLC can make, and the different angles that a gantry can be placed to deliver multiple beams, with different intensities converging on the PTV enabled the development of IMRT. This resulted in better dose conformity to the tumour.

Due to the non-uniform field sizes the MLC would make to approximate the PTV size, forward planning IMRT treatments would be difficult due to the number of calculations involved⁸⁸. Therefore, inverse planning is used, where a dose is specified to be given to the PTV, or the maximum dose to an OAR, and a planning algorithm calculates iteratively the optimal leaf-sequence and intensity to achieve the planning objectives. IMRT was compared to 3D-conformal radiotherapy for lung cancer, and significant improvements were seen in the dose to the lung using IMRT, provided the IMRT used greater than 3 fields⁸⁹.

IMRT resulted in longer treatment times because of the increased number of beams compared to 3D-CRT. A version of IMRT was subsequently developed called volumetric modulated arc therapy (VMAT). This is where the gantry speed, dose rate and MLC shape vary continuously through a treatment. The time taken for this treatment was less than for standard treatments. VMAT IMRT also delivered a lower volume of lung receiving at least 20 Gray (lung V20 Gy) and mean lung dose (MLD), with an increase in lung V5 Gy^{90,91}.

Inverse optimisation can be viewed as a cost/benefit function, where for each possible beam arrangement, it will benefit the dose to the PTV, but have a cost on the dose to the OARs. Inverse planning iteratively works through many potential plans to determine an optimal solution, where the PTV dose is met, and the OAR dose is minimised. However, when plan objectives are not met, planners will adjust the priorities of the plan variables, and re-optimize. This is time consuming and may not lead to the best plan solution. Where there are multiple OARs competing against each other, inverse planning may present sub-optimal solutions, as it is difficult to specify which OAR is of greater importance. Multi-criteria optimisation (MCO) is a development of inverse planning, where several plans are created for each OAR, and then the planner can modify the dose to each OAR to find the global optimal solution for the whole plan⁹².

Craft *et al.* describe the algorithm that underpins MCO planning⁹³:

$$\text{minimise } \{F_i(x)\}, i = 1 \dots N, \quad x \in X$$

where F_i is the i^{th} objective function, x is a vector of decision variables, and X is a convex constraint set in the decision variable space. This function takes a

series of variables (in the case of radiotherapy planning, the PTV and OAR doses), and will create a series of plans to approximate the Pareto surface. The Pareto surface is a mathematical solution to the practical situation where one objective cannot be improved without degradation of another. As there is no mathematical way to improve on a Pareto-optimal solution, it is the decision of the planner to choose a plan along this space.

To illustrate the use of MCO, consider a radiotherapy plan where the oesophageal and the spinal cord both receive a high dose. MCO will generate a series of plans to approximate the Pareto surface. If the radiotherapy plan is Pareto-optimal, an increase in the dose to oesophagus will cause a corresponding decrease in cord dose. At this point, the radiotherapy planner is required to make a clinical decision on how to distribute the dose to each OAR, accounting for patient factors and likely toxicity.

MCO planning is computationally demanding as it involves calculating several plans - in the Varian MCO module, it calculates 3 plans for each variable and a balanced plan. In clinical practice, a study comparing MCO against non-MCO IMRT, the use of MCO reduced planning time and produced MCO plans that were preferred by clinicians⁹⁴.

1.5.2 Image guided radiotherapy

Image guidance in radiotherapy can be divided into two categories: the use of imaging in radiotherapy simulation and the use of imaging in treatment delivery. Both have adopted new technology to better target tumours.

In radiotherapy simulation, CT is commonly used instead of plain films, due to the better visualisation of the tumour, and it also provides the Hounsfield units required for radiotherapy planning⁸⁶. In order to account for tumour movement in the breathing cycle, 4D-CTs are used to allow the creation of an internal target volume (ITV). This allows delineation of the tumour throughout the breathing cycles, allowing a smaller CTV to PTV margin⁹⁵. Some lung tumours are better visualised using PET-CT, and this can be fused to the simulation CT scan. There are unresolved issues regarding respiratory motion in PET-CT capture and the risk of false positive FDG avidity which means that the routine use of PET-CT

fused images for radiotherapy planning remains non-standard⁹⁶. The use of MRI in radiotherapy planning is established for other tumour types (brain and pelvic cancers) but it is not in standard use for lung cancer, unless the tumour is abutting the superior sulcus or chest wall involvement is suspected⁹⁷.

Image guidance in treatment delivery has undergone a similar transformation. The addition of kV imagers to linear accelerators have allowed for on-board imaging of the patient in the treatment position. However, plain radiographs use bony anatomy as a surrogate marker for the tumour position, which may not be accurate. The use of cone beam CTs on the treatment machine allows the matching of the radiation dose to the tumour, reducing the chance of geographical misses whilst also confirming the position of OARs⁹⁸. CBCTs were evaluated in the setting of frameless SABR for lung cancer and demonstrated that reduced PTV margins were achievable in the majority of patients⁹⁹.

1.5.3 Developments in dose prediction

The dose deposited to tissue from a beam depends on several factors, such as the size of the field, the focus to skin distance and the electron density of the material the radiation is travelling through. The prediction of where dose is deposited is essential to maximise the chance of tumour control and minimise normal tissue toxicity. With the advances in computer power, dose calculation has become more and more accurate. Lu has summarised the developments in a review article, which is summarised here¹⁰⁰.

For 2D planning, the dose deposition was estimated from observed measurements from phantoms and adapted to meet the specific characteristics of the treatment field. This was called correction-based calculations. This technique was accurate for where the tissue density was homogenous, but was inaccurate for inhomogeneous media e.g., lung and failed to predict lateral scatter.

Model-based dose calculation algorithms became commercially available in the 1980s and are based on Monte Carlo modelling. This models the process of where a single incident photon interacts with tissue, creating secondary electrons and a deflected photon. Both will continue to have subsequent interactions leading to

dose deposition. The Monte Carlo model tracks each photon and electron path and determines the dose deposited. This requires a large amount of computing power and is impractical to use clinically, yet it is considered the most accurate way of determining dose¹⁰¹.

Due to the time and computing power required for Monte Carlo calculations, alternative faster methods have been developed to closer match the Monte Carlo predictions. The most recent versions of these are the analytical anisotropic algorithm (AAA) which was superseded by an algorithm was developed called Acuros XB. This method has been shown to give excellent correlation with Monte Carlo models and superior dose prediction than other models^{102,103}.

1.5.4 Modality

Photons have been historically used for treatment. Initially limited due to beam low energies to treating superficial tumours, technological advances led to the development of Cobalt⁶⁰ treatment units, and the linear accelerator in the 1950s. The photon energies of these machines were 1.33MV and between 4-25MV respectively. As the beam energy determines the depth a beam can penetrate tissue, the delivery of radiotherapy to deep tumours was now possible²⁵.

The increased penetration of photon beams meant that the photons would continue to deliver dose beyond the PTV. The excess tissue irradiated from the exit dose however could cause additional toxicity, especially where critical OARs are distal to the tumour. Particle therapy such as protons and carbon ions have dosimetric benefits due to the way they deposit their dose along the Bragg peak. This leads to a sharp dose fall-off beyond the PTV and sparing of the distal tissues. This is of critical importance to tumours located at the base of skull or retinoblastomas where avoiding dose to the central nervous system is needed to deliver a tumoricidal dose⁸⁶.

Proton therapy and carbon ion radiotherapy has been used for lung cancer for both stage I and stage III tumours. Particle therapy has longer overall survival compared to conventional radiotherapy (but not SABR) for early stage lung cancers on meta-analysis of 30 studies¹⁰⁴. However, when proton treatment was compared to photon radiotherapy in a randomised clinical trial for unresectable

stage III patients, there was no improvement in toxicity or better tumour control in the patients who received protons¹⁰⁵. There are several possible reasons for these negative results. There was only a significant difference in the lung V5-V10Gy metrics, but not in the lung V20Gy, implying that sparing the low dose areas of the lung does not impact on the pneumonitis rate. In addition, the target volume size of the proton treatments was larger, due to the uncertainty of dose deposition with protons compared to photons, which may have impacted on the perceived reduction in normal tissue dose¹⁰⁶.

For lung cancer radiotherapy, particle therapy remains experimental and may have benefits in certain circumstances. Photon radiotherapy in the form of SABR for early-stage tumours, and conventionally fractionated treatments for stage III cancers, is the treatment modality in common use. The technical development of radiotherapy for lung cancer has changed enormously with improvements in the accuracy of treatment (IGRT), dose planning and calculation and the capabilities of linear accelerators to deliver highly conformal treatments.

1.6 Recurrent disease

1.6.1 Epidemiology of intra-thoracic disease recurrence

Radiotherapy is an established treatment in the radical management of lung cancer. With the exception of SABR, rates of local recurrence are high. In patients with stage III disease, the 1-year local recurrence rate was 24.8% in the high dose arm in RTOG 0617, and the addition of immunotherapy in the PACIFIC regime reduced this to 14%^{58,107}. In patients with stage I or II NSCLC, conventional fractionation is associated with a local failure rate of 26% at 2 years⁴⁶.

However, the rate of recurrence after radiation in routine clinical practice is unknown in the UK. This is due to several reasons: the UK national lung cancer audit does not collect this information; follow-up CT surveillance is not rigorously performed, and diagnosis of recurrent disease is difficult on imaging. Recently published guidelines recommend CT surveillance post-radical radiotherapy every 6 months in patients that are fit for further treatment¹⁰⁸. It is not clear if these guidelines have been implemented widely in the UK. CT

diagnosis of recurrent disease is often made on serial imaging, as post-radiation fibrosis can mask the identification of recurrent disease. In the absence of national data, a recent study by Evison *et al.* analysing outcome data from 9 National Health Service (NHS) trusts (898 patients) described a 30% local recurrence rate and an 8% nodal recurrence rate after curative intent radiotherapy, consistent with the trial data¹⁰⁹.

To estimate the potential number of patients who have local recurrences each year, the national lung cancer audit (NLCA) can be used. The NLCA in 2017 identified 2,680 patients with PS 0-2 stage I - III NSCLC lung cancer who had radical radiotherapy¹¹⁰. Using a local recurrence rate of 10% for SABR and 30% for other radiotherapy regimes, 632 patients will likely have local only recurrence within 2 years of completing treatment. Some patients will be unfit for further treatment, although this is difficult to estimate.

If the definition of recurrence is broadened to include metachronous or second primary lung cancer (SPLC), the rate of recurrence is 14.2% at 10 years¹¹¹. Therefore, the annual number of patients developing SPLC using the NLCA data is estimated at 37.

A total of 669 patients annually are estimated to have local recurrence or SPLC. The treatment at relapse received by these patients is not documented in the NLCA data. However, from the Evison *et al.* cohort, 6.4% of patients with either thoracic or distant recurrent disease had radical treatment (surgery, radiotherapy, or ablation therapy), 36% had palliative systemic therapy, and 58% had best supportive care. If only local recurrences are considered, 78.3% of patients are not receiving radical treatment. For patients with SPLC, 60% had either radical surgery or radiotherapy, 8% had systemic therapy, and 32% had best supportive care¹⁰⁹.

1.7 Re-irradiation as a treatment of recurrent disease

Possible treatments in the event of local recurrence have little evidence to support them. Re-irradiation has been used with increasing frequency over the past decade¹¹². However, there remain several unanswered questions about re-irradiation that need to be resolved. Firstly, if a tumour has recurred after irradiation, then it has demonstrated a degree of radioresistance. It is unclear why repeating the same form of treatment would be effective. Secondly, most radical radiotherapy treatments deliver doses close to the normal tissue tolerance, therefore re-irradiation may exceed these limits and cause severe toxicity. Thirdly, there is a lack of prospective trials or guidelines in this area to give clinicians any high-quality evidence to support decision making.

1.7.1 The classification of intra-thoracic tumour recurrence

Intra-thoracic recurrence of lung cancer after primary radiotherapy can be classified into several groups: local tumour relapse (relapse in the same lobe as the primary tumour) or a SPLC. The former group can be subdivided further into tumour recurrence in the same lobe, but at less than 50% isodose (an “out-of-field” local relapse), or within the 50% isodose line of the radiotherapy plan (an “in-field” relapse). When considering nodal involvement, the following situations may arise: relapse in both the tumour and the nodes, relapse in previously irradiated nodes, or relapse in unirradiated nodes. The definition of SPLC is a tumour arising in the thorax that is either: of a different histology to the primary tumour or; a tumour of the same histology but in a different lobe than the initial primary and no evidence of nodal involvement or systemic metastases or; a tumour of the same histology but temporarily separated with at least a 4-year interval between cancers and no evidence of systemic metastases¹¹³. These subdivisions highlight the range of possible clinical scenarios that can be classed as recurrent disease. Furthermore, these relapse patterns may represent different tumour biology.

The above relapse patterns could be re-grouped into recurrence around a high dose of radiotherapy (in-field local or nodal recurrences) and recurrence in areas of low or no dose (SPLC, out-of-field local or nodal recurrences). SPLCs arising in areas of no dose could be assumed to respond to treatment like *de novo* disease.

Relapse in areas of high dose is often considered to be “radioresistant” disease. There has been extensive pre-clinical research into mechanisms of radioresistance. However, there is retrospective clinical evidence that suggests that some tumours retain radiosensitivity.

1.7.2 Review of published data of efficacy of radical re-irradiation

Re-irradiation efficacy is difficult to predict, as the published data are mainly retrospective studies with a heterogeneous patient population. The main issues about the accuracy of the outcomes of re-irradiation for lung cancer are the methodology of the studies, the heterogeneity of the patients, and the variance in treatment.

Most studies are retrospective with small numbers. The lack of comparator arms in the studies make it difficult to determine whether re-irradiation has a survival benefit. The accuracy of retrospective data depends on how robustly data is recorded, and if adequate follow-up is performed and analysed appropriately. Limitations in retrospective trial design also include the period the data was collected over. As re-irradiation is a relatively uncommon treatment, some studies report outcomes of patients treated over 10 years apart. This may lead to some patients being treated with different techniques, which may influence the efficacy. The choice of efficacy measure is also important. Overall survival is a good measure but may be affected by treatments given after re-irradiation. Using local control as an alternate efficacy measure may be difficult, as fibrosis can often be mistaken for recurrence. A repeat biopsy may be required, but many patients in these studies would not have had this.

Patient heterogeneity in the studies is also a complicating factor. Re-irradiation has been performed in patients with metastatic disease, second cancers of a different histology and local recurrence. Some patients may be treated without a histological confirmation of relapse. Patients included in the study may have a range of comorbidities which may influence survival. In addition, the degree of dosimetric overlap may be significant due to radioresistance but is rarely recorded.

Finally, the choice of treatment varies in the retrospective studies. Re-irradiation has been used with a range of radiotherapy techniques, including conventionally fractionated radiotherapy (CFRT) but also with SABR, protons and carbon ions, with a range of doses. Some patients have had surgery, and some have with concurrent chemotherapy or have additional treatment after re-irradiation. These factors may all affect the accuracy of the overall survival of the patient. The lack of a standardised criteria for patient selection and treatment means that there is clinician bias in the group of patients these studies represent. This may affect the type of patients included and the radiotherapy received. Clinicians' re-irradiation experience also would influence the study outcomes, with some oncologists more aggressive and willing to accept high risk treatment than others.

Despite the variability of the study cohorts, it is possible to divide the studies into patients treated with SABR re-irradiation, and those treated with conventionally fractionated radiotherapy (CFRT). There have been multiple literature reviews and a selection of these studies are summarised in Table 1.1. Longer time to recurrence and smaller PTV size have been associated with better survival¹¹⁴⁻¹¹⁶. There are many confounding factors about fractionation/treatment choice, (e.g. SABR is only feasible in smaller tumours) which determine and influence survival after re-irradiation, other than the fractionation, therefore these data should be interpreted with caution.

Patients re-irradiated with two courses of CFRT have a 2-year OS rate between 11 - 64%, based on 335 patients. Re-irradiation with SABR (either following SABR or CFRT) has been more widely studied. Based on 11 studies and 397 patients, the 2-year OS (from the time of re-irradiation) and local control rates (LCR) are 37-79% (median 47%) and 37-90% (median 71%) respectively¹¹⁷. In comparison, primary SABR has a 2-year OS and LCR of 82.9% and 90% respectively¹¹⁸.

In summary, some patients have long term disease control after radical re-irradiation, although the data is not robust.

Table 1.1 Summary of re-irradiation studies and efficacy Conv/Conv: Conventionally fractionated treatment followed by conventionally fractionated re-irradiation, Conv/SABR: Conventionally fractionated treatment followed by stereotactic ablative body radiotherapy re-irradiation, EQD2: Equivalent dose in 2-Gray fractions, fr: fractions, NR: Not recorded, NSCLC: Non-small cell lung cancer, PTV: Planning target volume, RBE: relative biological effectiveness, Re-RT: re-irradiation, SABR/SABR: stereotactic ablative body radiotherapy followed by stereotactic ablative body radiotherapy re-irradiation, SCLC: small cell lung cancer.

Type of re-RT and study	n	Study type	Inclusion group	Histology	Median initial dose/fractionation	Median Re-RT dose/fractionation	Median OS (months)	1-year OS (%)	2-year OS (%)
Conv/conv									
Okamoto 2002 ¹¹⁹	18	Retrospective	100% locally recurrent	NR	60Gy in 30fr	50Gy in 25fr	15	77	51
Wu 2003 ¹²⁰	23	Phase I/II	100% locally recurrent, 100% in-field	70% NSCLC, 30% SCLC	66Gy in 33fr	51Gy in 25fr	14	59	21
Tada 2005 ¹²¹	14	Retrospective	100% locally recurrent, 100% in-field	100% NSCLC	50-69.6Gy conventionally fractionated	50Gy in 25fr	7.1	26	11
McAvoy 2013 ¹²²	33	Retrospective	64% infield failure	100% NSCLC	63Gy in 33fr	66Gy in 32fr (RBE Protons)	11.1	47	33
Tetar/Griffoen 2015 ^{114,123}	30	Retrospective	60% local recurrence	83% NSCLC, 17% SCLC	59.9Gy in 25fr	60Gy in 30fr	13.5	55	23
Sumita 2016 ¹²⁴	21	Retrospective	100% in-field recurrence	67% NSCLC, 33% SCLC	60Gy ₁₀ (EQD2)	60Gy ₁₀ (EQD2)	31.4	76	64

Chao 2016 ¹²⁵	57	Single arm prospective study	100% in-field or 'near' initial field	100% NSCLC	NR	66.6Gy in 33fr (RBE Protons)	14.9	59	43
Ho 2017 ¹²⁶	27	Retrospective	89% in-field, 11% out of field	81% NSCLC	60Gy ₁₀ (EQD2)	66Gy ₁₀ (EQD2)	18	54	NR
Schlamp 2019 ¹²⁷	62	Retrospective	100% local relapses	84% NSCLC, 16% SCLC, (40% mets)	60Gy in 30fr	38.5Gy in 19fr	9.3	NR	NR
Yang 2020 ¹²⁸	50	Retrospective	All local recurrence within 50% isodose line	8% SCLC, 92% NSCLC	60Gy ₁₀ (EQD2)	51.1Gy ₁₀ (EQD2)	25.1	NR	NR
Conv/SABR									
Trovo 2014 ¹²⁹	17	Retrospective	100% infield local recurrence	100% NSCLC	50-60Gy in 20-30fr	30Gy in 5 or 6fr	19	59	29
Kilburn 2014 ¹³⁰	33	Retrospective	100% locally recurrent, (Conv/SABR 73%, SABR/SABR 22%)	75% NSCLC, 12% SCLC, 13% other	60Gy in 30fr	50Gy in 10fr	21	76	45
Patel 2015 ¹³¹	26	Retrospective	100% locally recurrent, 93% infield,	88% NSCLC	61.2Gy in 32fr	30Gy in 5fr	14	52.3	37

			(Conv/SABR 88%)						
Horne 2018 ¹³²	39	Retrospective	Locally recurrent subset	100% NSCLC	84Gy ₁₀ (BED)	106Gy ₁₀ (BED)	16.2	NR	NR
Sumodhee 2019 ¹³³	46	Retrospective	100% locally recurrent, 63% in-field recurrences	100% NSCLC	66Gy in 33fr	60Gy in 4fr	21.8	NR	NR
SABR/SABR									
Valakh 2013 ¹³⁴	9	Retrospective	All locally recurrent	89% NSCLC	60Gy in 3fr	60Gy in 4fr	NR	NR	68.6
Hearn 2014 ¹³⁵	10	Retrospective	100% local relapses in field	100% NSCLC	50Gy in 5fr	50Gy in 5fr	NR	estimated 50%	NR
Kennedy 2019 ¹³⁶	21	Retrospective	100% locally recurrent (within 25% isodose or 1cm from PTV)	100% NSCLC	54Gy in 3fr	50Gy in 5fr	39	NR	68

1.7.3 Review of published data of safety of radical re-irradiation

1.7.3.1 Pre-clinical research of re-treatment of normal tissue

The published normal tissue dose constraints (QUANTEC and HyTEC) mainly report on maximum doses after a single course of radiation. As discussed above, for acute responding tissues, function is recovered by repopulation of stem cells, or by migration of new stem cells into the irradiated area. The late responding tissue response is more complicated depending on several different biological processes. A key question when considering a second course of radiotherapy is how much recovery the normal tissue makes, as this will define the amount of additional dose that can be given to that structure. Added complicating factors are the amount of time required for a given amount of recovery to occur, and how close the initial dose was to tissue tolerance. The re-irradiation tolerances of the spinal cord, lung, heart and skin have been studied in pre-clinical models.

The re-irradiation tolerance of the spinal cord has been studied in both pre-clinical models and clinical practice, making it one of the best studied organs regarding re-treatment. In rat models, two types of repair mechanism was observed - Elkind repair which takes place within 24 hours, and slow repair which is due to stem cell repopulation¹³⁷. The time for the slow repair to commence varies depending on which area of spinal cord was irradiated - lumbar cord takes approximately 4 weeks after irradiation, cervical cord 8 weeks¹³⁸. The extent of recovery was quantified using studies using rhesus monkeys, chosen because their radiation response is similar to humans. Rhesus monkeys were irradiated in 2.2Gy fractions to an initial dose of 44Gy, then re-irradiated at 1, 2 and 3 years. The recorded toxicity was clinical signs of myelopathy. The most conservative dose-toxicity model identified a recovery of 61% of the initial organ tolerance after 1 year. The authors suggested for humans there was 50% recovery after 1 year, 60% after 2 years and up to 70% recovery after 3 years^{139,140}.

Pre-clinical research on lung re-irradiation is based on murine studies. Terry *et al.* delivered a single dose of 6, 8 or 10 Gy whole thorax radiotherapy on mice, then repeated the single dose at 1, 2, 3, 4, and 6 months¹⁴¹. The clinical measure of

toxicity was increased breathing rate. For the groups who received 6 or 8 Gy single fractions, there was complete recovery by 2 months, but after 6 months there was a trend for decreasing re-irradiation tolerance. This was thought to be due to acute recovery, followed by chronic fibrosis limiting the re-treatment tolerance. The study did not continue for longer than 6 months therefore it is unclear whether this effect continued.

The skin and subcutaneous tissues tolerance to re-irradiation were assessed in a mouse study, where mice were given 40 or 50 Gy in 10 fractions followed by re-irradiation with different doses 6 months after. The measured endpoints were acute skin reactions and leg fibrosis, both graded on a 6-point scale. There was little difference in acute reactions to re-irradiation, whereas dose reductions of 21% and 38% were required to prevent late fibrosis in the mice who had been pre-treated with 40 Gy and 50Gy respectively¹⁴².

Cardiac re-irradiation was investigated in a rodent study, where single initial doses between 17.5 and 35Gy were delivered to the whole heart followed by re-treatment at 6 months¹⁴³. The outcome measure was *ex vivo* cardiac output at time of sacrifice. The main findings were that cardiac function progressively declined over the 14-month period of follow up even in rats that did not have re-irradiation, and that there is some measure of short-term repair over the first 6 months after which there is a chronic decline. This resulted in cardiac tolerance to re-irradiation was reduced by 57% compared to the initial tolerance dose. In addition, the size of the initial dose was inversely proportional to the re-irradiation tolerance, a feature seen in both the lung and spinal cord studies.

The animal models clearly show that some tissues develop some acute re-irradiation tolerance which is followed by late fibrosis (lung, heart and skin), whereas the spinal cord appears to have improved tolerance the longer the interval is between radiation. They also demonstrate that the lower the initial dose, the higher the re-irradiation tolerance. However, there are several issues with the use of pre-clinical models for re-irradiation toxicity, when attempting to correlate these findings to clinical practice.

There are several organs in the thorax that there is no pre-clinical re-irradiation data for (oesophagus, great vessels, brachial plexus and proximal bronchial tree). This may be due to the difficulty in assigning toxicity endpoints for animals. The pre-clinical studies had various endpoints which are difficult to correlate with the range of toxicity humans can develop. The radiation techniques used to irradiate the heart and the lung involved the whole organ. Modern radiotherapy techniques would very rarely deliver a uniform dose to the whole heart or lung. Moreover, heart and lung function are closely interlinked, therefore there may be undetected effects when irradiating one in isolation. In addition, the heart and lung studies used a single dose of radiation, making the findings difficult to extrapolate to fractionation courses of radiotherapy with large dose homogeneities across organs at risk. In addition, humans often have comorbidities that would make it difficult to extrapolate accurate dose constraints from animal studies.

1.7.3.2 Clinical research on re-irradiation toxicity

The risk of toxicity from re-irradiation is a major concern. The studies have several areas of possible inaccuracy. As before, the methodology of studies, the method of toxicity recording, and the outcome measures are all sources of inaccuracy.

Retrospective reviews record toxicity in variable ways and may miss important information, especially if the toxicity is graded retrospectively. In addition, there are a range of toxicity scoring systems which mean that comparing them between studies may be prone to error. Finally, the attribution of toxicity to radiotherapy is often difficult. For example, where a patient has a central relapse re-irradiated and dies from haemoptysis, this may be due to re-irradiation toxicity, but also it may be due to the tumour eroding into the trachea.

The way the studies plan their re-irradiation is also important. Some centres may use institutional dose constraints or have some experience in re-irradiation to guide replanning. Other centres may use different constraints or approaches. Therefore, the most useful information from the retrospective studies is the cumulative doses received by an OAR and the resulting toxicity, rather than the prescription dose. However, for several studies, this data is not given, perhaps due

to the difficulties in obtaining the original radiotherapy treatment plans or summing the doses.

Table 1.2 summarises the reported toxicity rates from a selection of studies for locally recurrent disease, split by CFRT and SABR re-treatment. A review of both CFRT and SABR re-irradiation described \geq Grade 3 pneumonitis rates of 0-21% (median 7%) and \geq grade 3 oesophagitis rates of 0-9% (median 2%)¹⁴⁴. A recent meta-analysis of patients treated only with SABR re-irradiation combines data from 595 patients in 20 observational studies¹¹⁶. This study concluded that there was a 1.5% rate of death from SABR re-irradiation, with a 6.3% rate of grade 3 or above pneumonitis. The rate of other grade three or above toxicities were <1.5%.

Location of the tumour and concurrent chemotherapy with re-irradiation are associated with higher grade toxicity. A Dutch group demonstrated a high rate of grade 5 toxicity (20%) in patients with central disease^{123,145}. Proton re-irradiation may reduce toxicity, as *in silico* studies have demonstrated a dosimetric benefit to the OAR dose¹⁴⁶. A US group reported a high toxicity rate (\geq Grade 3 toxicity of 42%) in a cohort of patients re-irradiated with protons. There was a statistically significant association of central disease and concurrent chemotherapy with toxicity¹²⁵. This highlights the uncertainty of dose delivery with proton re-irradiation. Potential areas of imprecision are related to the radiotherapy technique (pencil beam vs passive scattering) and motion management.

In summary, re-irradiation toxicity is related to several factors such as cumulative dose received to a given OAR, location of the recurrent tumour, use of concurrent chemotherapy, re-irradiation fractionation, tolerance of the initial course of radiation, and patient co-morbidities.

Table 1.2 Summary of the safety of re-irradiation studies BED: biologically effective dose, Central: central location of recurrence, Chemo: concurrent chemotherapy, CFRT: conventionally fractionated radiotherapy, Conv/Conv: Conventionally fractionated treatment followed by conventionally fractionated re-irradiation, Conv/SABR: Conventionally fractionated treatment followed by stereotactic ablative body radiotherapy re-irradiation, EQD2: Equivalent dose in 2-Gray fractions, fr: fractions, LR: local recurrence, NR: Not recorded, NSCLC: Non-small cell lung cancer, PTV: Planning target volume, RBE: relative biological effectiveness, Re-RT: re-irradiation, SABR/SABR: stereotactic ablative body radiotherapy followed by stereotactic ablative body radiotherapy re-irradiation, SCLC: small cell lung cancer. Toxicities – Haemop: haemoptysis, Lfib: lung fibrosis, Oes: oesophagitis, Pneu: pneumonitis, Resp: unspecified respiratory toxicity, TOF: tracheo-oesophageal fistula, Trach: tracheal necrosis

Type of re-RT and study	n	Study type	Inclusion group	Median initial dose/ fractionation	Median re-RT dose/ fractionation	Central (%)	Chemo (%)	G3/4 tox (%) and type		Grade 5 tox (%) and type	
Conv/conv											
Okamoto 2002 ¹¹⁹	34	Retrospective	100% LR	60Gy in 30fr	50Gy in 25fr	NR	NR	20.5	Pneu	0	
								5.8	Oes		
Wu 2003 ¹²⁰	23	Phase I/II	100% LR, 100% in-field	66Gy in 33fr	51Gy in 25fr	NR	0	8.7	Lfibrosis	0	
Tada 2005 ¹²¹	14	Retrospective	100% LR, 100% in-field	50-69.6Gy CFRT	50Gy in 25fr	NR	7	7	Pneu	0	
McAvoy 2013 ¹²²	33	Retrospective	64% infield failure	63Gy in 33fr	66Gy in 32fr (RBE Protons)	85	24	15.2	Pneu	0	
								9	Oes		
								6.6	Trach		
Tetar/Griffoen 2015 ^{114,123}	30	Retrospective	60% LR	59.9Gy in 25fr	60Gy in 30fr	97	NR	3.3	Oes	20	Haemop
								9.9	Other		
Sumita 2016 ¹²⁴	21	Retrospective	100% in-field recurrence	60Gy ₁₀ (EQD2)	60Gy ₁₀ (EQD2)	71	76	4.7	Pneu	0	
	57			NR		64	68	31.5	NR	3.5	Pneu

Chao 2016 ¹²⁵		Single arm prospective study	100% in-field or 'near' initial field		66.6Gy in 33fr (RBE Protons)						1.8	Haemop
											1.8	TOF
											3.6	Other
Ho 2017 ¹²⁶	27	Retrospective	89% in-field, 11% out of field	60Gy ₁₀ (EQD2)	66Gy ₁₀ (EQD2)	81	48	7	Pneu	0		
Ren 2018 ¹⁴⁷	67	Retrospective	80% LR, 49.3% infield	56Gy ₁₀ (EQD2)	54Gy ₁₀ (EQD2)	70	9	26.9	Pneu	0		
Schlampp 2019 ¹²⁷	62	Retrospective	100% LR	60Gy in 30fr	38.5Gy in 19fr	NR	0	4.6	Pneu	1.6	Pneu	
								1.6	TOF			
Badiyan 2019 ¹⁴⁸	79	Prospective registry	68% initial RT conv, 32% initial RT	60.2Gy ₁₀ (68%)/ 83.3Gy ₁₀ (32%) (EQD2)	60Gy ₁₀ (EQD2)	NR	30	3.8	Pneu	2.5	Haemop	
								3.8	Other			
Yang 2020 ¹²⁸	50	Retrospective	100% LR	60Gy ₁₀ (EQD2)	51.1Gy ₁₀ (EQD2)	86	18	12	NR	14	Resp	
Conv/SABR												
Lui 2012 ¹⁴⁹	72	Retrospective	Mixed group of LR and second primaries	63Gy in 32fr	50Gy in 4fr	50%	0	19.4	Pneu	1.3	Pneu	
Trovo 2014 ¹²⁹	17	Retrospective	100% infield	50-60Gy in 20-30fr	30Gy in 5 or 6fr	100	0	23	Pneu	5.5	Pneu	
										5.5	Haemop	

			local recurrence								
Kilburn 2014 ¹³⁰	33	Retrospective	100% LR, (Conv/SABR 73%, SABR/SABR 22%)	60Gy in 30fr	50Gy in 10fr	51.5	42.4	3	Pneu	3	Aortic rupture
Patel 2015 ¹³¹	26	Retrospective	100% LR, 93% infield, (Conv/SABR 88%)	61.2 in 32fr	30Gy in 5fr	41.4	0	0		0	
Horne 2018 ¹³²	39	Retrospective	LR subset	84Gy ₁₀ (BED)	106Gy ₁₀ (BED)	NR	0	10.3	Pneu	0	
Sumodhee 2019 ¹³³	46	Retrospective	100% LR, 63% infield recurrence	66Gy in 33fr	60Gy in 4fr	52.2	0	2.2	NR	2.2	Pneu
										2.2	Haemop
SABR/SABR											
Peulen 2011 ¹⁴⁵	29	Retrospective	100% infield LR	109Gy ₁₀ (EQD2)	109Gy ₁₀ (EQD2)	37.9	0	34.5	Resp	10	Haemop
								10.3	Other		
Valakh 2013 ¹³⁴	9	Retrospective	100% LR	60Gy in 3fr	60Gy in 4fr	0	0	22	Resp	0	
								11	Chest wall		
Hearn 2014 ¹³⁵	10	Retrospective	100% LR infield	50Gy in 5fr	50Gy in 5fr	20	0	0		0	
Kennedy 2019 ¹³⁶	21	Retrospective	100% LR	54Gy in 3fr	50Gy in 5fr	28.5	0	0		0	

1.8 Aim of this thesis

Lung cancer treated by radiotherapy has a high local recurrence rate of 30% and a 14% risk of second lung primaries after 10 years. There is a lack of suitable treatments for the estimated 700 patients in the UK who are in this clinical situation. Radical re-irradiation is associated with a 23-75% 2-year overall survival from the current literature, although there are several possible sources of inaccuracies, and there are no comparative trials. Radical re-irradiation is also associated with high toxicity rates, depending on the technique used, the location of the tumour, and the dose delivered. The lack of cumulative dose constraints, guidelines with how to replan patients and lack of advice about patient selection also contribute to increased toxicity. This thesis aims to investigate the safety of radical re-irradiation, in preparation of developing a prospective study.

2 Aims and objectives

The aim of this thesis is to investigate the safety of radical re-irradiation to guide a future prospective clinical trial. This was performed in six sub-projects.

2.1 Clinician consensus

The aim of the clinician consensus is to identify the current practice of re-irradiation and determine areas of uncertainty. The objectives are:

- (i) Identify international radiation oncologists with expertise in re-irradiation to participate in an expert survey
- (ii) Develop consensus statements on the selection and evaluation of patients for re-irradiation
- (iii) Identify the current re-irradiation dose constraints in use internationally and develop consensus over their use
- (iv) Develop consensus statements on appropriate planning techniques and follow-up for re-irradiation

2.2 Beatson re-irradiation cohort

The aim of the review of Beatson re-irradiation patients is to verify the findings of previous re-irradiation studies using a complete dataset of cumulative doses and clinical outcomes. This formed the basis of the planning study and validation data for the dose/toxicity models. The objectives are:

- (i) Identify a cohort of patients who have received two courses of radical dose radiation to the chest for NSCLC in the Beatson
- (ii) Develop a dose-registration process to determine the cumulative doses received by OARs
- (iii) Determine clinical information, toxicity and outcome data from electronic patient records

2.3 Dose/toxicity modelling

The aim of dose/toxicity modelling is to develop models to enable the prediction of the toxicity of a re-irradiation treatment. The objectives are:

- (i) Synthesise a database from published studies of the cumulative dose delivered to thoracic organs at risk, the interval between treatments and the amount of dose given in the first treatment with associated toxicity.
- (ii) Create dose toxicity models using logistic regression and predict the 5% toxicity rate for each OAR (20% toxicity rate for lung toxicity).
- (iii) Construct and validate the models using a cohort created from re-irradiation data from patients already treated at the Beatson.

2.4 Tumour control modelling

The aim of the tumour control modelling is to develop models to enable prediction of the local control and overall survival of a re-irradiation treatment.

The objectives are:

- (i) Synthesise a database from published studies of the dose delivered to a PTV of recurrent disease, the interval and the PTV size with the local control rate and overall survival rate.
- (ii) Create efficacy models using logistic regression and predict the re-irradiation doses required for 30% and 50% 2-year local control and overall survival rates
- (iii) Assess how much the dose to the PTV can be escalated by and the predicted survival and local control rates without breaching re-irradiation dose constraints

2.5 Planning study

The aim of the planning study is to investigate the safest radiotherapy planning technique to meet the re-irradiation dose constraints. The objectives are:

- (i) Develop a workstream for dose accumulation of two courses of radiotherapy
- (ii) Apply the re-irradiation dose constraints to the Beatson re-irradiation cohort to identify a group of patients that do not meet the dose constraints
- (iii) Replan the group who failed the dose constraints using VMAT and MCO and re-analyse if dose constraints can be met
- (iv) Replan the group who failed the dose constraints with alternate strategies (e.g. change dose/fractionation, alter PTV)
- (v) Using the dose/toxicity and efficacy models, predict the change in the risk of side effects and outcomes with the replanned re-irradiations.

2.6 Patient survey

The aim of the patient survey is to explore patients' attitudes to re-irradiation and whether it would be a treatment they would consider. The objectives are:

- (i) Produce a protocol and gain approval for a qualitative interview study
- (ii) Conduct and transcribe interviews with patients
- (iii) Perform thematic analysis on the transcriptions

Due to the different techniques required for each mini-project, each chapter will have an introduction to the pertinent concepts and describe the methods, results and a discussion. The findings will be summarised in a final discussion section.

3 Clinician consensus

3.1 Introduction

Radical thoracic re-irradiation has been performed on selected patients using a variety of different techniques. The current literature (reviewed in Chapter 1) demonstrate that some patients have durable disease control after re-irradiation, but there are significant toxicity risks¹⁴⁴. The number of re-irradiation treatments is increasing. Data from the University of Michigan show the number of re-irradiation physics requests doubling from 2017 to 2018¹¹². This may be due to several reasons: the advances in precision radiotherapy technology, greater use of surveillance scanning to detect recurrence, better survival after initial treatments, and clinician confidence in re-irradiation.

There is limited clinical guidance on the practice of re-irradiation. The radiotherapy planning process used in the University of Michigan was published and describes suggested institutional OAR dose constraints, dose accumulation and workflow. However, for lung re-irradiation, there are no specific guidelines. A UK clinician survey about re-irradiation demonstrated clear support for further research, which indicates the lack of information in this setting¹⁵⁰. Areas of uncertainty are patient suitability in terms of both clinical stage and fitness, investigations prior to re-irradiation, dose constraints, radiotherapy planning technique and follow-up.

There are several areas of uncertainty about the delivery of re-irradiation. Firstly, no clear definition of re-irradiation exists. Does thoracic re-irradiation refer only to areas where there is an overlap of a significant dose, or should it be considered as any second treatment in the thorax. If it is the former, what would constitute a significant dose? Re-irradiation has been delivered for patients with local recurrence, second primaries or in metastatic disease. The amount of overlap between the first and second treatment may be important in the outcome from re-irradiation or the toxicity, therefore defining a minimum threshold or a way to categorise re-irradiation may be useful. As part of this definition, the clinical scenarios where thoracic re-irradiation can be considered will aid radiation oncologists in appropriate patient selection.

Secondly, should there be a minimum interval between primary radiotherapy and re-irradiation to allow for tissue recovery. Thirdly, what are the minimum lung function parameters that can be considered acceptable for re-irradiation. Finally, what are the necessary pre-treatment investigations and is there an absolute need for biopsy prior to treatment. A biopsy may confirm recurrent disease, but also risk significant side-effects. Information to support clinical practice is limited due to the low patient numbers and the retrospective nature of the current literature. Therefore, an expert survey is a useful method of pooling experience to provide clinical guidance.

The aims of this Delphi consensus process are to develop patient and treatment recommendations including patient suitability, cumulative dose constraints, planning technique and follow up. This work will also identify areas of uncertainty and where further research is required. This process is limited specifically to NSCLC, but the recommendations may be applicable to other thoracic tumours.

3.2 Methods

3.2.1 Participant selection

Thoracic radiation oncologists who have published articles about re-irradiation were invited by e-mail to participate in this study. If they were unable to participate, they could nominate another person who had an interest in re-irradiation. Clinicians were selected from North America, Europe, Asia and Australia to capture a wide range of opinions and practice.

3.2.2 Ethics and consent

Ethics approval was waived by the University of Glasgow Ethics Committee and the West of Scotland Research Ethics Committee. All participants consented to the Delphi process.

3.2.3 Survey process

The Delphi consensus method was chosen to develop recommendations as it allows unbiased anonymised responses, over a large geographic distance¹⁵¹. The

process is divided into rounds of questionnaires. The first round consists of open ended questions to allow the expression of a wide range of opinions. The second round uses the answers given in the first round as the basis of the statements created by the study organisers, which the participants review and vote on using a five-point Likert scale (strongly agree, agree, neutral, disagree, strongly disagree). If $\geq 75\%$ of the responses were strongly agree or agree, then the statement had reached consensus and no further changes were made to it. Where participants did not agree with a statement, they were able to provide feedback on how to improve the statement. In the subsequent rounds, the statements which did not reach consensus were modified by the study organisers and re-presented to the participants to vote on again until it became clear that no consensus can be made in a specific area. The study organisers were blinded from linking the answers to a participant to reduce bias. In addition, the study organisers did not answer the questionnaires. The study was conducted using an online survey website (webropol.com).

The first round consisted of 36 open questions, relating to 6 subject areas: the definition of re-irradiation, patient suitability for re-irradiation in terms of disease stage and fitness, re-irradiation investigations, acceptable risks of toxicity, radiotherapy planning technique and delivery including cumulative dose constraints, and follow-up after re-irradiation. Where a range of values were given (e.g. for minimum lung function) the median value was used in the related statement.

The second round consisted of the 57 statements, with the participants voting on them using the Likert scale. Feedback on each statement and sharing of additional pertinent papers was encouraged. The third round consisted of 19 modified statements, including two new statements regarding if a biopsy was an absolute requirement prior to re-irradiation. Questions regarding the acceptable risks of toxicity were removed based on the feedback from the participants. As clinicians, they felt unable to comment on what an acceptable risk is, as it is likely that it would vary from patient to patient and therefore would not be suitable for a consensus statement.

The fourth and final round consisted of one question regarding the definition of re-irradiation. This was required as consensus was not reached on the definition of re-irradiation. Two separate definitions were presented to the participants with the option to choose one, both or neither. Explanations of how the previous comments had been incorporated were given, and further space to offer feedback was given.

3.3 Results

3.3.1 Participants and response rates

Twenty-one radiation oncologists were invited by e-mail and 15 consented to participate in the study. The respondents were from the following countries: United Kingdom (3), United States (3), Australia (3), Canada (2), the Netherlands (2), Switzerland (1) and Singapore (1). The 15 participants have a total of 44 publications regarding re-irradiation, and a median of 12 years of experience in thoracic oncology (range 7 - 34 years). The first round opened on September 23, 2019 and the final survey was completed on March 2, 2020. The first to third rounds had a 100% response rate, and the fourth round had a 93.3% response.

Of the 57 statements in the second round survey, 26 reached consensus (45.6%). Fourteen statements were also removed regarding acceptable toxicity based on the comments from the group. The third round consisted of 19 modified statements, and consensus was reached on seven (36.8%) of them. The final round featured one question and consensus was not reached. This process is summarised in Figure 3.1.

3.3.2 Definition of re-irradiation

After three rounds of voting, consensus was not reached on a definition of re-irradiation. The round 2 statement came closest to reaching consensus with 67% agreement was “any dose of radical radiation for lung cancer, after initial radical radiotherapy to the thorax or surrounding tissues for any tumour histology, provided there is an overlap of previous dose in either the planning target volume (PTV) or the organs at risk (OARs)”. The main objection to this definition was the use of “any overlap” would refer to the potentially large low dose regions, which may have very little contribution to toxicity. This was

considered by the study organisers at the time of writing the survey and therefore had included a second definition addressing this in the round 2 survey.

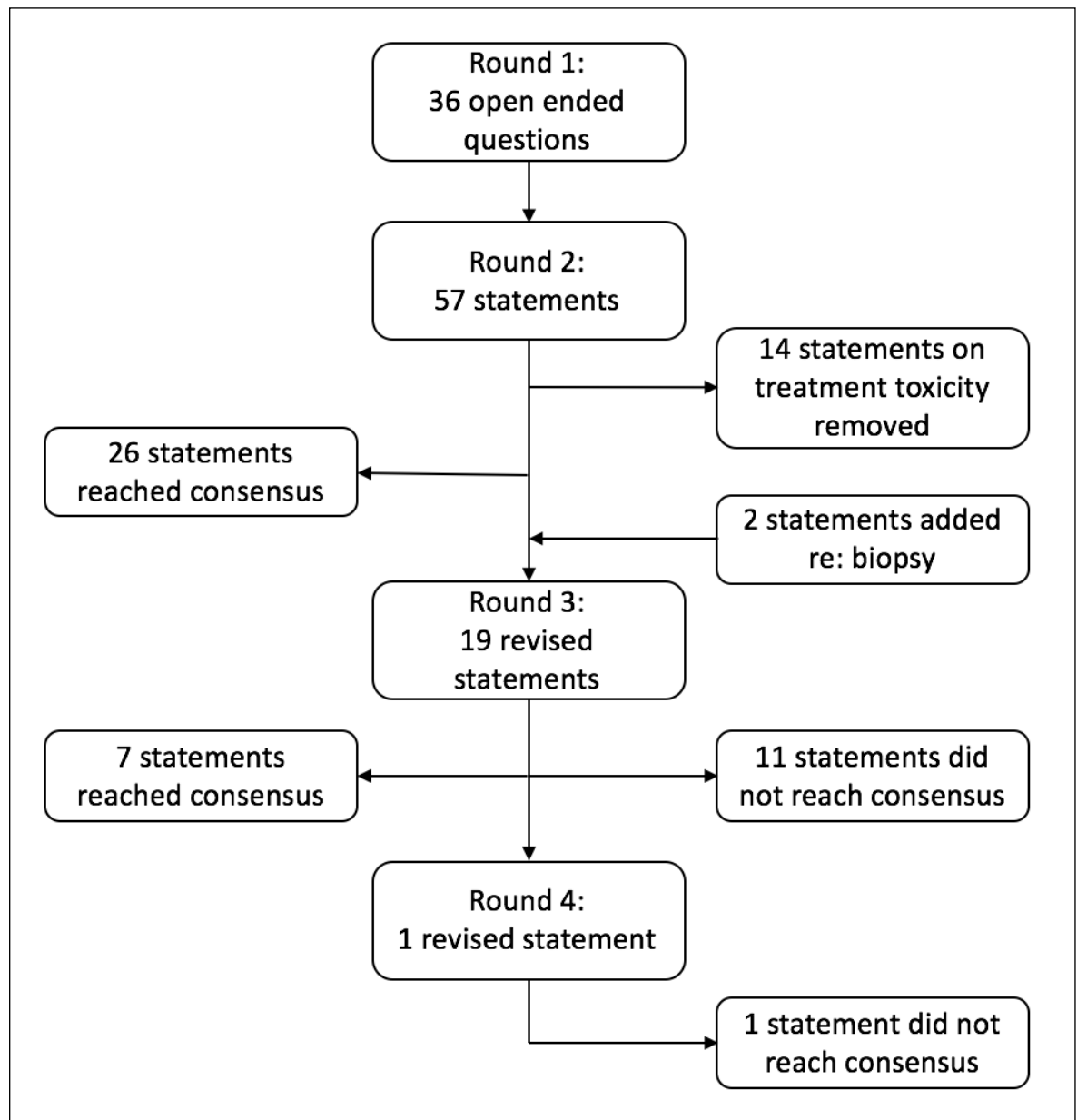


Figure 3.1 Outcomes from each round of questionnaires

The alternate round 2 definition was "Any dose of radical radiation for lung cancer, after initial radical radiotherapy to the thorax or surrounding tissues for any tumour histology, provided there is overlap of the initial treatment at the 50% isodose line of the re-treatment in either the PTV or the OARs". This achieved 33% agreement with several comments suggesting that setting an arbitrary isodose cut-off lacked evidence, and that severe toxicity can be encountered in OARs with less than 50% overlap.

The participants also described a situation where there is no overlap but should be considered re-irradiation, due to the increased dose to the volume of the lung. If a patient had radical radiotherapy to a tumour at the lung apex, and then to another tumour at the lung base, there may be no dosimetric or geometric overlap, but the volume of lung treated may be significant, and may have implications for toxicity. The feedback from the group gave two possible alternate definitions: (i) “a second course of radiation wherein contribution from a previous course of radiation leads to a cumulative dose that is higher than the prescription for the second course, or exceeds standard dose constraints when considered without repair” or (ii) create two definitions where re-irradiation is an overlap of accumulated doses greater than that seen in a single course of radical radiotherapy, and where repeat radiotherapy is two radiotherapy course with dose exposure in the same organ without the need for overlap.

As there were more comments regarding overlap, the former definition was amended and recirculated to the group in round 3. It achieved 60% agreement, and the feedback re-iterated the issues regarding suggesting re-irradiation should have overlap between the tumours, the growing complexity of the definition, and enthusiasm for using the first definition of ‘any overlap’. One comment suggested that even if it includes more patients, it will act as a caution to the clinician to consider re-irradiation risks. Therefore, in the fourth round, the definition was split into type I and type II re-irradiations, where type I re-irradiations were for local recurrences (i.e. high expected overlap in the PTV and/or OARs, and type II re-irradiations were for second primary lung cancers where the overlap would be low or none. In addition, to clarify local recurrence a definition was also added from the RTOG 0236 study which described local recurrence as either within 1cm of the PTV or the 25% isodose line.

The participants did not reach consensus on these final definitions with 43% agreement. The main reasons given for disagreement was that “a tumour in a different part of the lung is not re-irradiation”, splitting the definitions by indication was unnecessary, and the lack of evidence to support splitting the definition into two groups.

3.3.3 Patient suitability for re-irradiation in terms of disease stage and fitness

The statements which achieved consensus for patient suitability and patient fitness and the round in which that was reached are given in Table 3.1 and Table 3.2. Consensus was achieved for re-irradiation of second primaries, local recurrence with <50% overlap with serial OARs in the chest and untreated nodal recurrence. Consensus was not met for re-irradiation in patients who have relapse in the previously irradiated primary and nodes, or in oligometastatic or widely metastatic disease.

Suitable patients for re-irradiation should have a PS of 0-2, no interstitial lung disease and caution should be used where patients had grade 3 toxicity in their first course of radiotherapy.

Consensus on minimum pulmonary function tests (PFT) values could not be reached. From the answers in the first round, a DLCO and a FEV1 > 30-40% was suggested. However, a statement regarding this did not reach consensus (66%). The participants commented that the likelihood of toxicity relates to the volume of disease at re-irradiation and the location, therefore setting arbitrary limits could exclude patients who may benefit. Related to this, one clinician used the change in PFTs from pre-radiotherapy to pre-re-irradiation as a guide to suitability of treatment. An amended statement reached consensus placing emphasis on clinician judgement.

The minimum interval between treatments did not meet consensus. Most participants (73.3%) agreed that a minimum interval should at least 6 months, with 6.7% suggesting that the minimum interval be over 12 months. However, 20% did not support any minimum interval. The respondents gave the rationale for a longer interval based on data suggesting longer overall survival where the interval is longer than 12 months, implying less aggressive disease. In contrast, the rationale given for having no minimum interval is the clinical scenario where a second primary is diagnosed with minimal overlap with the previous radiotherapy. The respondents felt it unreasonable to delay that treatment given the risk of toxicity was low.

Statements about alternate treatments to re-irradiation demonstrated a preference for surgery in resectable patients, and immunotherapy or targeted therapy for patients with a high likelihood of response.

3.3.4 Re-irradiation investigations

The statements that reached consensus regarding investigations prior to re-irradiation are detailed in Table 3.3. Consensus was achieved with >93% agreement that patients need clinical staging with PET-CT, CT/MR head, and CT-chest with contrast. Another suggestion in the comments was the use of MRI in apical tumours, but as consensus was reached in round 2, there was no possibility to add this to the statement.

In the second round, a third of respondents suggested that pathological confirmation of the tumour was essential, with the other 66% suggesting that it was acceptable to treat without it. This was further explored in round three, with agreement around a pragmatic approach where a biopsy must be considered by the MDT, allowing re-irradiation for patients where the risk of biopsy would be unacceptably high.

3.3.5 Acceptable risks of toxicity

The aim of this section was to identify the toxicity rates that clinicians would deem acceptable at re-irradiation. Median acceptable toxicity rates were taken from the first round of answers and divided into low grade (grade 1-2) and high grade (grade 3-5) toxicity. Table 3.4 summarises the rate and grade of toxicity and the amount of clinician agreement. This section was ultimately excluded from further analysis as the comments in the feedback highlighted that the patient ultimately decides what risk is acceptable to them, and that the risk of toxicity can only be considered against the risk of symptoms from untreated disease.

Despite not exploring this in further rounds, there was general agreement to accept high rates of reversible acute grade 1-2 toxicity in terms of pneumonitis, oesophagitis and skin erythema. Most clinicians accepted a rate of between 5-

10% grade 3-4 toxicity, and consensus was agreed to keep grade 5 toxicity below 5%.

3.3.6 Radiotherapy planning technique and delivery

Statements that reached consensus regarding radiotherapy planning and cumulative dose constraints are outlined in Table 3.5 and Table 3.6 respectively. There was no recognised method to summate the doses from two courses of treatment and some comments raised concerns about the quality assurance of deformable image registration. The delineation of the tumour may be helped using PET-CT given the possibility of lung fibrosis from the first course of radiation. In addition, the respondents agreed that compromising PTV dose to prioritise OAR dose is important. There were several comments accepting compromise of the expansion margins from GTV to CTV and from CTV to PTV, using margin reduction as a strategy to reduce high grade toxicity. Related to this, the respondents agreed that highly conformal planning techniques should be used, ideally stereotactic radiotherapy if tumour size and position allows. There was agreement to limit the use of SABR in ultracentral disease, but central disease was acceptable to be treated, although one participant felt that any central re-treatment was high risk and would not be recommended. There was strong consensus on the use of daily CBCT for any re-irradiation to ensure that the dose delivery is as close to the planned dose as possible.

The initial cumulative dose constraints presented in round two were derived from the median answers from round one. The most common approach was to use EQD2 rather than BED to sum doses from two treatments from round one. The respondents noted the lack of evidence for the dose constraints, even in *de novo* radiotherapy. Two approaches were described; the first assumed a certain percentage of recovery of radiation tolerance after a given period, the second noted that the amount of recovery was impossible to determine for most OARs therefore it was safest to assume no recovery. The latter principle was presented to the participants in round three in this statement: “For cumulative dose constraints, the amount of normal tissue recovery has limited evidence and therefore the safest approach is to assume no tissue recovery”. This met with 60% agreement. The main issues raised were firstly some tissue recovery is known to happen and rather than ignore it, more efforts should be made to

quantify it. Secondly, even if this is the safest approach, it may result in patients being excluded from high risk re-irradiation, where they may benefit from treatment.

Despite the lack of agreement on a standard approach, cumulative dose constraints were agreed for the spinal cord, the aorta and pulmonary artery, the brachial plexus and the oesophagus. The proximal bronchial tree did not reach consensus, with 67% agreeing with a cumulative EQD2 dose between 80 and 105Gy₃. The reasons given for disagreement were lack of evidence, and whether the tumour was invading the PBrT, as the risk of haemorrhage would then be higher, and a higher risk may be warranted.

Agreement was not reached for the lung constraints suggested in round two (V5<65%, V20<35% and MLD<20Gy) with 53% approval. Several respondents commented that these values were too restrictive, especially the V5 value. A key point was also raised that when suggesting these constraints, they must not be considered absolute limits and can be exceeded depending on the clinical situation. This statement was reworded for round three to highlight the lack of evidence, therefore lung dose constraints could not be stated. This statement reached 80% agreement.

3.3.7 Follow-up after re-irradiation

There was 87% agreement for surveillance CTs every three to six months after re-irradiation for the first two years in patients who are fit for further treatment, followed by 6-12 monthly scanning thereafter. The comments reflected that this had little evidence supporting it but would be the only way to determine if re-irradiation has been effective.

Table 3.1 Consensus statements regarding the clinical stage of suitable re-irradiation patients. SA/A: Strongly agree/agree, N: Neutral, D/SD: Disagree/Strongly Disagree, R2: Round 2.

	Consensus agreed	SA/A	N	D/SD	Round agreed	Median
1.1	Radical re-irradiation can be considered for suspected new lung primaries with minimal overlap with previous radiotherapy fields.	93%	7%	0%	R2	SA
1.2	Radical re-irradiation can be considered for lung tumours which develop new nodal disease after an initial course of radiotherapy only to the primary tumour (therefore minimal overlap).	100%	0%	0%	R2	SA
1.3	Radical re-irradiation can be considered where a lung tumour relapses locally (or develops a suspected second primary tumour with >50% overlap with the original primary tumour), but low overlap with serial structures in the thorax.	93%	0%	7%	R2	SA
1.4	Alternative treatments (e.g. systemic therapy) are preferred to radical re-irradiation to the primary lung cancer where the lung tumours have relapsed both locally and with widespread metastatic disease.	93%	7%	0%	R2	A

Table 3.2 Consensus statements regarding the fitness of suitable re-irradiation patients. SA/A: Strongly agree/agree, N: Neutral, D/SD: Disagree/Strongly Disagree, R2: Round 2, R3: Round 3.

	Consensus agreed	SA/A	N	D/SD	Round agreed	Median
2.1	In general, patients should have an ECOG performance status (PS) of 0 - 2 to be considered for radical dose re-irradiation, with exceptions being made for selected PS 3 patients (e.g. SABR re-irradiation, or PS 3 due to non-respiratory issues).	93%	0%	7%	R2	SA
2.2	Re-irradiation should be avoided in patients with interstitial lung disease.	86%	7%	7%	R2	SA
2.3	Re-irradiation should be performed cautiously with patients who developed grade 3 or higher toxicity with their initial radiation treatment.	86%	7%	7%	R2	A
2.4	Surgery should be considered in all appropriate patients being assessed for re-irradiation.	93%	0%	7%	R2	A
2.5	In locally advanced recurrent lung cancer, where there is an increased likelihood of response to immunotherapy (e.g. PD-L1 >50%), immunotherapy may be preferable to high-risk radical re-irradiation.	80%	0%	20%	R2	A
2.6	In locally advanced recurrent lung cancer, where there is an actionable mutation (e.g. EGFR mutation, ALK fusion), targeted treatment may be preferable to high-risk radical re-irradiation.	79%	7%	14%	R2	A
2.7	For conventionally fractionated re-irradiation, the clinician must consider re-treatment to have a positive risk/benefit ratio considering the current pulmonary function tests and the likely exposure of the lung to re-irradiation, with no minimum PFTs values applicable.	86.6%	6.7%	6.7%	R3	A
2.8	For re-irradiation with SABR, no minimum PFTs apply.	87%	0%	13%	R2	A

Table 3.3 Consensus statements regarding investigations for suitable re-irradiation patients. SA/A: Strongly agree/agree, N: Neutral, D/SD: Disagree/Strongly Disagree, R2: Round 2, R3: Round 3.

	Consensus agreed	SA/A	N	D/SD	Round agreed	Median
3.1	Investigations prior to commencing radical re-irradiation are: Whole body PET-CT, CT chest + contrast, and CT/MRI brain.	>93%	-	-	R2	Essential
3.2	Consideration for biopsy must be made in a tumour board/multi-disciplinary team meeting before considering radical re-irradiation.	86.6%	6.7%	6.7%	R3	SA
3.3	Re-irradiation can be considered where the tumour board/multi-disciplinary team agrees that there is a high likelihood of cancer, but despite best efforts, histological confirmation of cancer is not possible.	86.6%	6.7%	6.7%	R3	SA

Table 3.4 Clinician suggested acceptable toxicity rates. SA/A: Strongly agree/agree, N: Neutral, D/SD: Disagree/Strongly Disagree.

Toxicity	Grade	Toxicity rate (%)	SA/A (%)	N (%)	D/SD (%)
Pneumonitis	G1-2	50	73	14	13
Oesophagitis	G1-2	70	93	0	7
Skin erythema	G1-2	50	74	13	13
Brachial plexopathy	G1-2	10	53	27	20
Pericarditis	G1-2	10	67	20	13
Pneumonitis	G3-4	10	53	20	27
Oesophagitis	G3-4	10	53	20	27
Skin toxicity	G3-4	5	60	20	20
Brachial plexopathy	G3-4	5	59	27	14
Pericarditis	G3-4	10	53	40	7
Bronchial fibrosis	G3-4	5	67	20	13
Haemoptysis	G3-4	5	60	13	27
Cord myelitis	G3-4	5	46	20	34
Any cause	G5	5	80	7	13

Table 3.5 Consensus statements regarding radiotherapy planning technique. SA/A: Strongly agree/agree, N: Neutral, D/SD: Disagree/Strongly Disagree, R2: Round 2, R3: Round 3.

	Consensus agreed	SA/A	N	D/SD		Median
4.1	When combining initial and re-irradiation plans, either rigid or deformable dose registration are acceptable methods (although there are considerable uncertainties in either process and further investigation is warranted).	80%	6%	14%	R2	SA
4.2	18-FDG-PET-CT is recommended to aid tumour volume delineation.	86%	7%	7%	R2	SA
4.3	When contouring for conventionally fractionated radical re-irradiation, an acceptable minimum expansion from CTV to PTV is 5mm (or follow institutional guidelines where available).	86%	7%	7%	R2	A
4.4	PTV coverage can be compromised to achieve acceptable OAR doses.	80%	6%	14%	R2	SA
4.5	Radical re-irradiation should be performed using highly conformal radiotherapy techniques (e.g. VMAT, Tomotherapy, Cyberknife).	100%	0%	0%	R3	SA
4.6	SABR is the preferred re-irradiation technique where the tumour is not ultra-central, the tumour volume is small and there is minimal overlap with OARs.	80%	13.3%	6.7%	R2	SA
4.7	Protons may have a role for re-irradiation and requires further evaluation in the context of a clinical trial.	80%	20%	0%	R3	A
4.8	Acceptable doses for conventionally fractionated radical thoracic re-irradiation are 60Gy in 30 fractions or 55 Gray in 20 fractions once daily for non-small cell lung cancer.	93%	0%	7%	R2	A
4.9	Any dose and fractionation that can safely deliver a BED >100Gy to the tumour is acceptable for radical re-irradiation with SABR.	86.7%	0%	13.3%	R3	A
4.10	Daily cone beam CT is recommended for treatment verification for conventionally fractionated re-irradiation.	100%	0%	0%	R2	SA
4.11	Daily cone beam CT is recommended for treatment verification for SABR re-irradiation.	100%	0	0	R2	SA

Table 3.6 Consensus statements regarding cumulative dose constraints. SA/A: Strongly agree/agree, N: Neutral, D/SD: Disagree/Strongly Disagree, R2: Round 2, R3: Round 3.

	Consensus agreed	SA/A	N	D/SD		Median
5.1	There is insufficient evidence to suggest volumetric cumulative dose constraints for the lung due to the changes in anatomy and function of the lung after an initial course of radiotherapy.	80%	13.3%	6.7%	R3	A
5.2	For radical re-irradiation, the desirable cumulative maximum point dose constraint to the oesophagus is an EQD2 of 75Gy, although up to 100Gy is acceptable (using an $\alpha/\beta = 3$), with the volume of the oesophagus getting 55 Gray should be less than 35% ($V_{55Gy} < 35\%$). ¹²	86%	7%	7%	R2	A
5.3	For radical re-irradiation, the desirable cumulative maximum point dose constraint to the spinal cord is an EQD2 of 60Gy (using $\alpha/\beta = 2$), with a maximum EQD2 of 67.5Gy (provided that the initial irradiation dose to the cord did not exceed 50Gy). ¹³	80%	13%	7%	R2	A
5.4	For radical re-irradiation, the desirable cumulative maximum dose (D_{max}) constraint to the brachial plexus is an EQD2 of 80Gy ($\alpha/\beta = 2$) and an acceptable cumulative D_{max} is 95Gy (if the interval between treatments is greater than 2 years). ¹⁴	80%	0	20%	R2	A
5.5	For radical re-irradiation, the desirable cumulative maximum dose (D_{max}) constraint to the aorta is an EQD2 of 115Gy ($\alpha/\beta = 3$). The desirable cumulative D_{max} to the pulmonary artery is an EQD2 of 110Gy. ^{15,16}	80%	0%	20%	R2	A
5.6	There is a lack of information to guide re-irradiation dose constraints for the skin and the heart, therefore the use of other guidelines (e.g. QUANTEC or SABR guidelines) and to keep the dose to these organs as low as reasonably achievable are recommended.	100%	0	0	R2	A

3.4 Discussion

This Delphi process has produced expert consensus statements suggesting suitable patients for re-irradiation, appropriate staging investigations, preferred radiotherapy technique and cumulative dose constraints. It identified areas where there is a lack of evidence (minimum PFTs, cumulative lung and PBrT doses, definition of re-irradiation). It has also demonstrated that re-irradiation can be applied to a range of different situations, with different risks and benefits, and therefore a single set of guidelines will not account for all the clinical possibilities.

3.4.1 Methodology

These guidelines were developed using a Delphi consensus method. This technique was first used in the 1950s by the RAND corporation who used a panel of experts to determine the number of nuclear bombs required to reduce the United States' capacity to make munitions¹⁵². It has since been used in many other settings including healthcare where expert opinion is sought. This method was chosen as it was suitable to gather international opinion on a range of issues. The anonymised nature of the study and the feedback allowed each participant an equal voice, with less opportunity to be biased by other members of the group¹⁵³.

In the Delphi technique, participant selection is key as they will be the source of the consensus statements. This study invited radiation oncologists with publications (or nominated by clinicians with publications) in thoracic re-irradiation. This is appropriate, as they have experience of the practice of re-irradiation. However, it would be impractical to invite all the clinicians who had published on lung re-irradiation or clinicians with extensive experience of re-irradiation but no publications therefore some opinions may have been excluded at study recruitment. Therefore, there is inherently a selection bias to the opinions of academic clinicians. The influence of this may reflect on the treatment modality preferred (e.g. use of tomotherapy, which is rarely available) and the likely fitness of patients referred in to a superspecialised oncology centre, as opposed to an unselected patient cohort. In addition, no physicists or imaging specialists were invited, whose input would have been

valuable when considering re-irradiation planning and technique. The views of patients were also not represented which resulted in the acceptable risks of re-irradiation section having to be curtailed. This study had 15 participants which is in keeping with most other publications¹⁵⁴. However, it may have benefitted from increased numbers from different backgrounds¹⁵⁵. As such, there is a risk of groupthink, with only clinicians providing the source material for statements and then subsequently agreeing to them. A range of different perspectives would be useful, especially pertaining to the physics and treatment delivery aspect of the consensus statements.

The nature of the process involved multiple rounds of surveys and reviewing the previous answers which is time consuming. The drop-out rate of this study was low, with only one unanswered questionnaire out of a total of 60 surveys sent out over a six-month period. However, 57.9% (33 out of 57 round two statements) met consensus, leaving several key areas with no agreement including the definition of re-irradiation.

Further iterations of the statements could have continued, but would have risked participant drop out, especially as the severe acute respiratory syndrome coronavirus 2 (SARS-CoV-2) became a global pandemic at the start of the fourth round. In addition, there is little to be gained from further questionnaires if there are no new suggestions around an issue, although this study did not use any pre-specified stopping rules. Other studies have used an hierarchical stopping criteria, although many also use a subjective approach¹⁵⁶. In many of the areas where consensus was not met, a lack of evidence was a limiting factor. For the areas where consensus was not met, a face-to-face meeting could have taken place to discuss unresolved issues. However, this would have made any outcomes potentially biased as anonymisation would have been lost.

The process of editing statements in response to comments is a source of bias¹⁵³. The study organisers, who are also clinicians familiar with lung re-irradiation, are likely to have opinions on the topic. Even though they did not take part in the survey, the processing of the statements can lead to their viewpoints being over-represented and amplified in subsequent rounds. It would be difficult to minimise this effect as a researcher with no knowledge of radiotherapy may not be able to interpret the comments. Another area that could be improved is the

lack of experience of the researcher in performing a Delphi process. In the literature, there are several different ways to plan and perform this technique, and a more experienced investigator may have been able to gain consensus over some issues.

3.4.2 Lack of definition

Re-irradiation can be used in a range of different scenarios, and with limited data on outcomes. This made the development of a single definition difficult. There are some interesting points which came from the discussion of definition. There was 71% agreement to divide re-irradiation by broad indication (for local recurrence or second primaries). However, the purpose of dichotomising a group of patients is if there is a difference in outcomes. In addition, this division also excludes re-irradiation in the metastatic setting. There is sparse evidence of a difference between second primaries and local recurrences. Empirically, local recurrence would be thought to have a poorer prognosis due to the increased likelihood of radioresistance, but little data exists to support this.

Discussion about the definition in round two centred on the degree of overlap (if any) that would be significant. Several published studies have defined re-irradiation as overlap of isodose levels of between 25-50%, although this is an arbitrary cut-off and often used also as the definition of local recurrence^{128,136}. An alternate definition designated re-irradiation “if $>0.5\text{cm}^3$ of the thoracic region received a radiotherapy dose higher than the maximum dose delivered in either of the two radiotherapy plans”¹¹⁵. This definition implies that any degree of overlap, even low dose scatter, in the PTV would be considered re-irradiation.

The above definitions would not consider the total volume of lung irradiated from two spatially distant lung primaries (i.e. no overlap) as significant. The term repeat radiotherapy has been used in this context¹¹⁵. If the total volume of lung irradiated is less than the dose constraint in a *de novo* treatment, then it could be argued that it should not be considered re-irradiation. However, there is a high rate of pneumonitis from re-irradiation in published series. One possible reason may be the mechanism of re-irradiation lung injury is different compared to radiation-naïve lungs and therefore caution should be used.

Further data is required to determine if the differences in outcomes that would warrant defining re-irradiation by indication, and at what threshold the total volume of irradiated lung causes retreatment toxicity.

3.4.3 Suitability for re-irradiation

Patient suitability for any given treatment can be based on inclusion criteria from landmark clinical trials. None of the respondents suggested any trial-based data to aid patient selection. The main prospective study of re-irradiation is the 2003 study by Wu *et al.*, which accepted patients with loco-regional relapse and a Karnofsky PS of ≥ 70 , aged 18-80, minimum interval between radiotherapy 6 months, and a FEV1 of >1 litre¹²⁰. This study was published in 2003 and therefore may have been considered outdated by the participants, especially as this was before the widespread use of SABR.

Minimum PFT levels did not reach agreement, although a majority supported a minimum FEV1 and DLCO of 30-40%. This lack of consensus is due to difficulty in predicting radiotherapy induced lung injury (RILI). RILI is multifactorial and predictive models are inaccurate¹⁵⁷. Therefore, the clinicians experience and judgement may be of more value than strict limits. After a course of radiotherapy, the PFTs generally decline, although in some studies they can improve¹⁵⁸. A meta-analysis suggested the main dosimetric factors that are related to reduction in PFTs are dose to the lungs (V5, V20 and MLD) and mean heart dose. Patient and tumour characteristics were less commonly significant¹⁵⁸. There is little data available to suggest how re-irradiating lung affects PFTs.

One consideration is that radiotherapy in previously irradiated lung may cause less damage as it is deposited in already damaged non-functioning lung. Alternatively, the lung may be in a pro-inflammatory state post-radiotherapy, and a further radical dose may cause significant symptoms. The high rate of pneumonitis post-re-irradiation supports the latter suggestion, although the quality of evidence is poor.

The minimum interval between re-irradiation treatments did not meet a consensus. 71% felt that a minimum of 6 months was acceptable, with

explanations for no minimum period (in the event of no overlap), and for longer than 12 months (more likely to have improved survival). Normal tissue recovery in animal studies varies by organ. Spinal cord has demonstrated a recovery of tolerance which starts at 6 months, whereas lung and heart have lower re-irradiation tolerance after 6 months^{139,141,143}. The lack of a clear definition of re-irradiation, or clear clinical scenario, is one reason why consensus for this statement was not met, as the range of different situations that a broad definition covers has implications for real world practice.

The participants considered patients who developed grade 3 toxicity with initial radiotherapy at higher risk of severe consequential late side effects. This recommendation is supported by pre-clinical data of re-irradiation of the rat spinal cord that shows that the higher the level of initial injury, the less further radiation dose was tolerated¹⁵⁹. The practical application of this may be omitting dose entirely from organs which developed grade 3 toxicity with initial treatment where possible.

3.4.4 Radiotherapy planning

Cumulative dose constraints over two courses of treatment have been approached in two methods in the literature. One method is to adopt an ‘discount’ based scheme where a given percentage of dose is subtracted after a period of recovery time. The other is to assume no recovery and have a fixed cumulative value.

Over the time the Delphi surveys were in progress, three other groups published cumulative dose guidelines. Paradis *et al.* used a ‘discount based scheme’, while Troost *et al.*, Hunter *et al.*, and the American Radium Society used a fixed cumulative value^{112,146,160,161}. The discount based scheme is accurate for well researched OARs like the spinal cord and brachial plexus, where the amount of recovery is well known from pre-clinical and clinical models. However, for less researched OARs, there is little evidence to suggest the amount of recovery if any, which is potential source of inaccuracy. A discount based scheme is also more complicated to apply. Fixed cumulative values are simpler to apply clinically, and easier to use for dose/toxicity modelling, as it is a single variable (rather than interval between treatments and dose, as would be with discount

based constraints). A fixed cumulative value does not represent the radiobiology of tissue recovery. A mixed method, using discount modelling for OARs with well-known recovery characteristics (e.g. spinal cord), and fixed cumulative doses for others may also be reasonable. A table comparing the cumulative dose constraints from the Delphi process and the other published constraints are presented in Table 3.7.

Where possible, the recommended radiotherapy technique is SABR, with 80% agreement. SABR is a highly conformal treatment, delivered with daily image guidance. This approach spares normal tissue toxicity, although it is limited by the size of the tumours that can be treated (usually tumours less than 5cm in diameter with no nodal involvement). In addition, the radiobiological effects of SABR are different, and may circumvent the mechanisms of radioresistance developed after initial radiotherapy¹⁶². Retrospective studies have demonstrated clinical efficacy of SABR re-irradiation with a two year local control rate of 37 to 90%¹¹⁷.

The respondents agreed that proton re-irradiation required further investigation. Protons, with their rapid dose fall-off distal to the PTV may reduce the dose to tissues distal to the PTV. A planning study comparing photons to protons in re-irradiation demonstrated lower OAR doses with protons¹⁴⁶. However, it is unclear from this study the location of the tumours which were replanned and the robustness of the proton planning. The respondents reflected on the negative study comparing protons and photons in stage III NSCLC and the lack of accessibility of protons as reasons why protons were currently not recommended¹⁰⁵.

Table 3.7 A comparison of putative cumulative dose constraints EQD2: Equi-effective dose in 2-Gray fractions. ALARA: as low as reasonably achievable. PBrT: Proximal bronchial tree. *Consensus not reached. [§]Dose constraints converted from α/β ratio of 2.5 to the stated α/β ratios in the table to allow ease of comparison, dose constraints derived using a 6-12 month interval, with OARs being treated to tolerance in the first treatment. [^]Dose constraints α/β ratios not quoted in the American Radium Society abstract.

	α/β	Delphi	Paradis et al., 2019 [§]	Troost et al., 2020	American radium Society, 2020 [^]	Hunter et al., 2021
Spinal cord	2	Dmax 60Gy	D0.1cc<61.6Gy	Dmax<65Gy	Dmax <57Gy	Dmax<67.5Gy
Brachial plexus	2	Dmax 80-95Gy	D0.1cc<86.9Gy	Dmax<85Gy	Dmax <85Gy	Dmax<80Gy (if <24m), Dmax<95Gy (if >24m)
Skin/Chest wall	2.5	ALARA	D0.1cc<116Gy	n/a	n/a	n/a
Heart	2.5	ALARA	D0.1cc<86.1Gy	Dmean<70Gy	Mean: ALARA, V40 <50%	no evidence provided in article
Lung	3	Individualised	Individualised	.	V20<40%	V20<30-35%
Lung	3	Individualised	Individualised	Dmean<22Gy	.	n/a
PBrT	3	Dmax <80-105Gy*	D0.1cc<85.8Gy	Dmax<110Gy	Dmax <110Gy	Dmax<105Gy
Oesophagus	3	Dmax 75-100Gy	D0.1cc<87.5Gy	Dmax<100Gy	Dmax <100-110, V60<40%	Dmax<110Gy
Great vessels	3	Dmax 110 – 115Gy	D0.1cc<116.5Gy	Dmax<110Gy	Dmax <120Gy	Dmax<110Gy (Pulmonary artery) D1cc<120Gy (Aorta)

3.4.5 Conclusion and summary

This Delphi process has generated expert consensus on patient selection for re-irradiation, pre-radiotherapy investigations, radiation technique and cumulative dose constraints. It is the first set of recommendations for lung re-irradiation from an international group of thoracic oncology specialists. The evidence for the statements is mostly opinion and experience based, with little prospective trial data available. However, this study does give clinicians with little experience of re-irradiation some general guidance on how to perform this treatment as safely as possible. The definition of re-irradiation, cumulative dose constraints and optimal dose registration strategies did not meet consensus and are worthy of further investigation.

4 Beatson re-irradiation cohort

4.1 Introduction

Many of the published studies regarding lung re-irradiation are retrospective reviews. They often lack detailed cumulative dose and toxicity data for the re-irradiation treatments delivered. This may be because the initial and subsequent radiation courses were performed in different hospitals with no access to both plans and there is no established protocol to co-register the doses. Dose accumulation, which is a complicated process, is necessary to ascertain the cumulative dose an OAR would have received accurately. The studies also group several different tumour histologies together (e.g., SCLC, NSCLC and metastases) and used different doses (some patients were treated with lower palliative doses) therefore interpretation of the expected overall survival for NSCLC is difficult. The studies also describe re-irradiation depending on variable levels of overlap with the PTV, which make it unclear how much of the original tumour has been treated.

Image registration and dose summation of the initial radiotherapy treatment and the re-irradiation plan is prone to error, has significant uncertainties and lacks a 'ground truth'. The image registration can be either rigid or deformable. Rigid registration is matching the initial and re-irradiation image without changing the shape of the initial tissues to match the re-irradiation images. Deformable image registration (DIR) produces a transformation matrix than can morph the initial image into a similar shape to the re-irradiation image. DIR therefore may provide a better estimate than rigid registration where the tissues have changed significantly and in a predictable way.

The transformation matrix formed in DIR can be applied to the dose map of the initial course of radiation and at re-irradiation. There are two considerations when applying DIR applied to dose: volume-conservation or dose-conservation. Volume conservation uses the transformation matrix to deform the dose accordingly. However, this does not account for the changes in dose deposition caused by the change in density of tissues. Dose conservation methods add an extra layer of analysis where the dose is assumed to be a constant is a given volume and can account for the changes in density. Volume-conservation

methods are accurate where the anatomy has not changed significantly, but dose conservation techniques may be more appropriate in areas where there has been significant changes¹⁶³. The choice of image registration technique and dose summation is a source of error between studies and inherent to any future study of re-irradiation.

The Delphi consensus study demonstrated that thoracic re-irradiation can be delivered in many different clinical scenarios. There was strong agreement to treat second primary lung cancers (SPLC) and locally recurrent disease, but there was reluctance to categorise these as different types of re-irradiation. The local recurrence rate after initial radiotherapy is approximately 30% and the rate of SPLC is 14% at 10 years^{111,164}. There are limited data to suggest there is a difference in outcomes between the two groups in terms of toxicity and efficacy. However, in principle SPLC should have better outcomes in terms of toxicity and efficacy as there is less likely to be significant overlap, and the tumour will not have developed any radioresistant changes.

The consensus study also highlighted areas of uncertainty in terms of minimum interval between radiation courses. A minority of clinicians (20%) felt that a minimum interval of 12 months was warranted before re-irradiation with 71% preferring an interval of 6 months. The clinicians also had concerns re-irradiating patients who had grade ≥ 3 toxicity with the initial radiotherapy, although there is little clinical data to support this. Finally, the clinicians suggested dose constraints based on experience and a small number of studies, but it is unclear if these novel constraints are feasible in a real-world setting.

A retrospective analysis of patients who received two courses of curative intent radiotherapy was performed in the Beatson, a tertiary level oncology centre. The aims are to verify the toxicity and efficacy of radical re-irradiation in NSCLC in relation to the published literature, assess the differences in outcomes between SPLC and local recurrences, and investigate the areas of controversy from the consensus study. As part of this, a method to calculate the cumulative doses received by OARs over two courses of radiation will be developed.

4.2 Method

4.2.1 Ethics and Caldicott guardian review

Approval was granted by the NHS Greater Glasgow and Clyde Caldicott Guardian for use of patient radiotherapy and clinical data for the purposes of this project.

4.2.2 Patient identification and clinical information

The Beatson radiotherapy database was searched to identify any patients who had two radical courses of radiation for lung cancer between 01/01/2014 and 02/11/2020. Patients' clinical information and dates of death was obtained from electronic medical records. Toxicity was obtained from clinical letters, or date of hospitalisation and graded using CTCAE v5. Early toxicity is defined as either during treatment or within 90 days after the completion of a course of radiation, late toxicity is any toxicity after 90 days. Where there was uncertainty regarding causality, e.g., chest infections, they were included as radiotherapy related toxicity. A stricter exploratory measurement of toxicity entitled "Likely re-irradiation toxicity" included early chest infections and clinician assessed likely radiotherapy toxicity. The Charlson Comorbidity Index (CCI) was used to score each patient¹⁶⁵. There was no formal surveillance CT scanning protocol after re-irradiation, therefore local tumour control data was unable to be ascertained. The date from the first fraction of re-irradiation to death was used to calculate the overall survival. Data were censored on 15th September 2021.

4.2.3 Radiotherapy scan processing

The radiotherapy CT scans and associated delivered plans were duplicated and renamed zzCT1 and zzCT2 respectively for the initial and re-irradiation treatments. The gross tumour volume, the clinical target volume and the planning target volume were unchanged from the original structure sets. The following organs at risk were contoured on both zzCT1 and zzCT2: aorta, pulmonary artery, brachial plexus, chest wall, heart and substructures (left anterior descending artery, base of heart), oesophagus, trachea, proximal bronchial tree (PBrT), spinal cord, and whole lung. The RTOG and heart atlases were used to ensure standardisation of the contouring^{166,167}.

The dose of some of the plans were calculated using older dose algorithms (e.g., AAA). Therefore, to get as accurate as possible dose information, the same plan parameters were used, and the doses of all plans were recalculated using AcurosXB. Rigid registration was performed on zzCT1 and zzCT2, and the initial PTV structure from zzCT1 was copied on to zzCT2. If there was any overlap of the zzCT1 PTV and zzCT2 PTV, the patient was deemed to have had an 'in-field' local recurrence. If there was no overlap, then the recurrence was classed as a second primary. One limitation of this process is that the original PTV and the OARs would have changed due to the effect of the initial course of radiation, therefore this can only be considered an estimate.

4.2.4 Generation of EQD2 using Velocity

The re-calculated and contoured CT scans, dose maps, and structure sets were imported into VelocityAI (Version 3.2, Varian Medical Systems, Palo Alto, California, US). This program performs image registrations and biological dose calculation. The doses from zzCT1 and zzCT2 were converted to EQD2 in a voxel-by-voxel process. Four separate dose maps were created for each scan using the following α/β ratios (OARs in parentheses) 2 (spinal cord and brachial plexus), 2.5 (heart and chest wall), 3 (lung, oesophagus, proximal bronchial tree and great vessels) and 10Gy (tumour).

4.2.5 Deformable dose registration

The EQD2 dose maps of zzCT1 and zzCT2 for each α/β value were combined using a predesigned process in VelocityAI. The first step in the process was to image register the CT scans from zzCT1 and zzCT2. Taking the latest scan as the template, zzCT1 underwent rigid and then multi-pass deformable registration to deform the images to match zzCT2. The voxel transformations from this process were then applied to the zzCT1 EQD2 dose map, therefore matching the previous dose to the new anatomy for the second treatment. The EQD2 dose maps from the transformed zzCT1 and zzCT2 are then summated on a voxel-by-voxel basis. The cumulative EQD2 for each structure was taken from the appropriate dose map (e.g., spinal cord cumulative EQD2 was taken from the α/β 2Gy dose map). The dose data was collected into a database and linked to the toxicity experienced.

To determine the optimal consistent method of selecting a region of interest (ROI), deformable image registration was performed setting the ROI as the whole lung fields and a 2cm area in all directions around the PTV. The warp maps were visually assessed and doses to different OARs were calculated using the different ROI settings to evaluate which ROI produced the most plausible deformation and what the range of uncertainty was from the predicted doses.

4.2.6 Statistical analysis

Patient demographics and dose data were calculated using descriptive statistics and compared using either a Chi-squared test for categorical variables, a Fisher's exact test where the expected outcomes were less than 5, or t-test for continuous variables. Toxicity outcomes were calculated as rates. Overall survival was calculated using the Kaplan-Meier method. The median follow-up time was calculated by the reverse Kaplan-Meier method. For all analyses, a p-value of <0.05 was used for significance.

4.3 Results

4.3.1 Patient characteristics

The search identified 39 patients who had completed two radical courses of radiotherapy for NSCLC, 26 for SPLC and 13 for LR. All patients had a PS of 0-2, with a statistically significant larger proportion of PS 2 patients in the SPLC group. There were several statistically significant differences between the two groups. Patients with SPLC had a higher proportion of stage I disease at re-irradiation ($p=0.038$). The SPLC group had a smaller PTV volume ($p=0.009$), and a greater proportion had re-irradiation with SABR ($p=0.013$). This is reflected in the higher mean re-irradiation prescribed EQD2 dose given to the SPLC group (72.3Gy_{10} compared to 58.8Gy_{10} in the LR group, $p=0.006$). Table 4.1 summarises the demographics of the group.

Table 4.1 Demographics of the second primary lung cancer and locally recurrent groups
 CCI: Charlson Comorbidity Index, EQD2: equivalent dose in 2 Gray fractions, Gy: Gray, LR: local recurrence, PS: performance status, PTV: planning target volume, re-RT: re-irradiation, SABR: stereotactic ablative body radiotherapy, SPLC: second primary lung cancer

		Whole group	SPLC	LR	p-value
n		39	26	13	-
Mean age at re-RT (range)		71.3 (47.8 - 86.0)	70.5 (52.9 - 84.1)	72.7 (47.8 - 86.0)	0.5
Sex	male	19	10	9	0.14
	female	20	16	4	
PS at re-RT	0	3	1	2	0.045*
	1	24	14	10	
	2	12	11	1	
CCI score	<6	18	14	4	0.307
	≥6	21	12	9	
Stage at re-RT	1	23	19	4	0.038*
	2	10	4	6	
	3	6	3	3	
Mean Interval between two treatments (months, range)		17.24 (2.2 - 62.9)	14.5 (2.2 - 62.2)	22.8 (8.2 - 51.3)	0.085
Location of tumour at re-RT	Peripheral	22	17	5	0.209
	Central	17	9	8	
Mean PTV overlap (% , range)		13.8 (0 - 97.5)	0	41.6 (0.8 - 97.5)	<0.001*
Mean PTV size (cm ³ , range)		116.8 (8.4 - 417.5)	84.2 (8.4 - 365.9)	189.9 (52.8 - 417.5)	0.009*
Type of Re-RT	Conv	25	13	12	0.013*
	SABR	14	13	1	
Mean Re-RT prescription dose (EQD2 Gy, $\alpha/\beta = 10$, range)		58.4 (51.8 - 96.3)	72.3 (51.8 - 96.3)	58.8 (51.8 - 83.3)	0.006*

4.3.2 Region of interest selection

Eight patients with locally recurrent disease were used to assess how to select the ROI. The whole lung ROI (ROI-WL) demonstrated more biologically plausible warp maps compared to the ROI restrained to 2cm around the PTV (ROI-PTV).

The direction vectors for the ROI-PTV and the ROI-WL are demonstrated in Figure 4.1 and Figure 4.2 respectively.

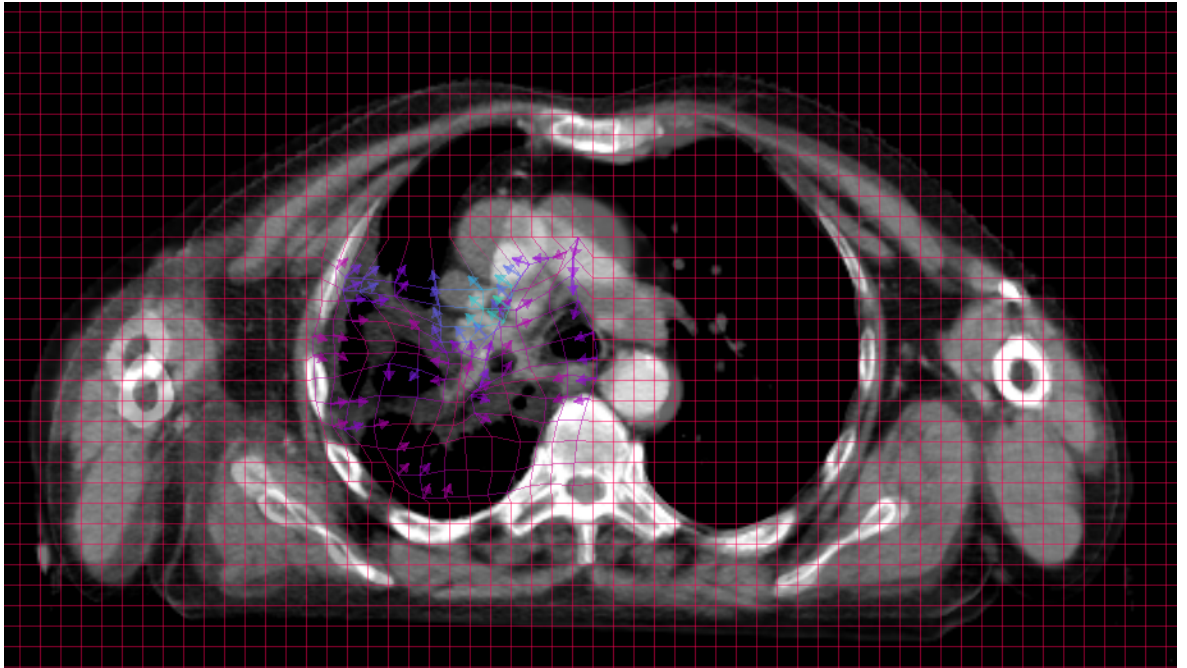


Figure 4.1 Direction vectors with a limited region of interest Region of interest was set to 2cm superior and inferior to the planning target volume. Purple lines demonstrate the direction the initial planning CT scan was warped to align with the re-irradiation planning CT.

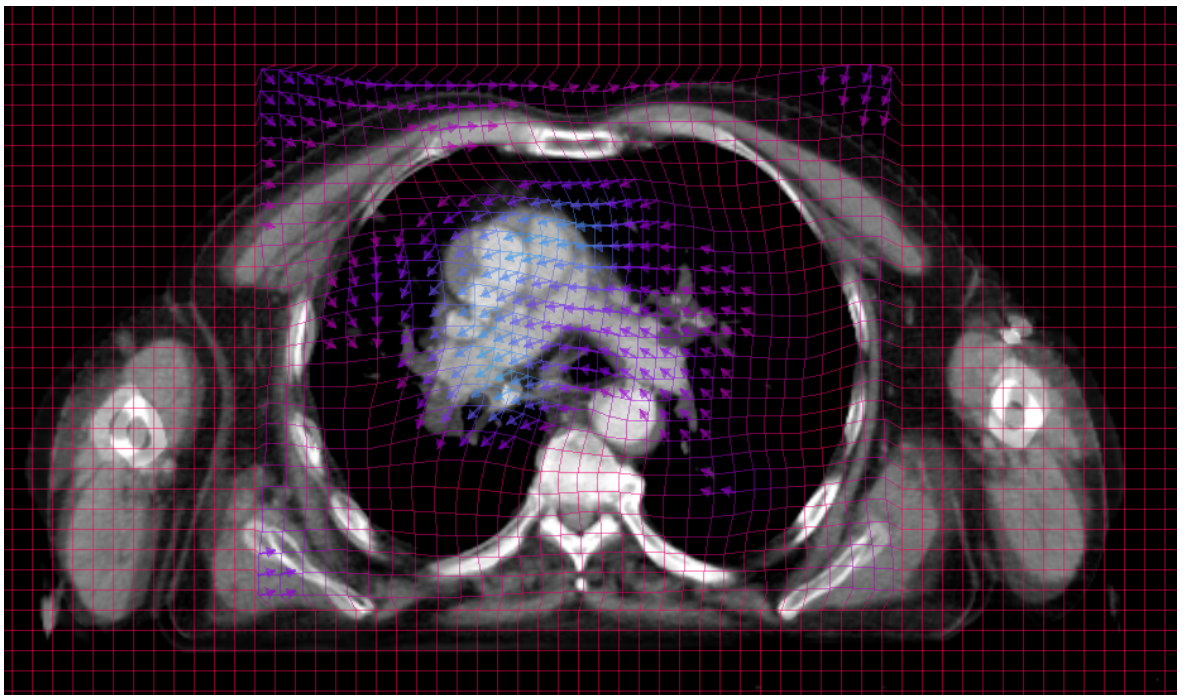


Figure 4.2 Direction vectors with a whole organ region of interest Region of interest was set to include the whole lung. Purple lines demonstrate the direction the initial planning CT scan was warped to align with the re-irradiation planning CT

The direction vectors with the ROI-WL are visually biologically plausible, with the zzCT1 image being warped in a consistent direction to match the area of fibrosis in the right lung. The ROI-PTV however does not have a consistent warp pattern, with some direction vectors moving away from the area of fibrosis. This implies an expansion of tissue which does not seem plausible.

The doses to the thoracic OARs (PBrT, oesophagus, mean lung dose, aorta, and spinal cord) were calculated using both ROI-WL and ROI-PTV.

Table 4.2 demonstrates the range of difference between the cumulative doses using both ROIs. There was no significant difference on paired t-tests between the two datasets. The difference in dose ranged between -9.73 to 2.07 EQD2 Gy, with the widest variance in the dose to the aorta. For all subsequent cumulative dose calculations, the ROI was set to the whole lung.

Table 4.2 Doses of OARs predicted by ROI-PTV subtracted from ROI-WL EQD2: equivalent dose in 2 Gray fractions, MLD: mean lung dose, OARs: organ at risk, Oes: oesophagus, PBrT: proximal bronchial tree, ROI-PTV: region of interest-planning target volume, ROI-WL: region of interest whole lung, negative values represent where ROI-PTV predicted a high cumulative dose than ROI-WL.

Patient number	PBrT (EQD2 Gy)	Oes (EQD2 Gy)	MLD (EQD2 Gy)	Aorta (EQD2 Gy)	Cord (EQD2 Gy)
6	1.75	2.07	-1.28	-8.24	1
8	0.27	-7.98	-0.29	-0.14	0.23
11	0.57	3.25	0.63	-0.26	-0.11
12	-1.25	0.96	-2.43	-9.73	0.52
23	-0.28	-0.2	-0.51	0.44	-0.16
25	0.36	-0.95	-1.59	-0.82	0.09
29	-0.1	-3.16	0.17	0.06	-0.88
34	1.79	0.26	-1.02	-0.97	-0.14
Mean difference	0.39	-0.72	-0.79	-2.46	0.07
T-test p-value	0.32	0.58	0.06	0.13	0.73

4.3.3 Re-irradiation toxicity

There were 7 (17.9%) grade ≥ 3 toxicity events at initial radiotherapy (5 chest infections and 2 oesophagitis leading to dysphagia) and 17 (43.6%) grade ≥ 3 toxicity events at re-irradiation. There were 8 (20.5%) events graded as “likely

re-irradiation toxicity”. The risk of toxicity at re-irradiation was higher than at initial radiotherapy (two-proportion comparison test re-irradiation toxicity rate (17/39) and initial-RT toxicity (7/39), $p=0.014$). The predominant toxicity seen after re-irradiation was grade 3 chest infections (70.5%, Table 4.3).

Table 4.3 Grade and number of observed re-irradiation toxic events PBrT: Proximal bronchial tree

	Lung toxicity (chest infections/ pneumonitis)	PBrT toxicity (stridor/ haemoptysis)	Arm lymphoedema	Chest pain
Grade 3	12	1	1	2
Grade 4	0	0	0	0
Grade 5	0	1	0	0

The most serious complication was a grade 5 episode of haemoptysis which occurred 71 days after the end of re-irradiation. There were 3 early grade ≥ 3 toxicities and 14 late. The median time to toxicity (of the 17 patients who experienced grade ≥ 3 toxicity) was 5.5 months (range 0.5 to 28.5 months).

Figure 4.3 summarises the results of an exploratory sub-group analysis using a Cox proportional hazards model. The likelihood of toxicity was increased in patients with stage III disease at re-irradiation (hazard ratio 66.56, 95% CI 3.73 - 1187.4, $p=0.004$). The PS 2 group and patients with CCI score of ≥ 6 also had an increased risk of developing grade ≥ 3 toxicity (hazard ratio 6.44, 95% CI 1.01 - 39.6, $p=0.045$, and hazard ratio 5.43, 95% CI 1.12 - 26.3m $p=0.036$ respectively).

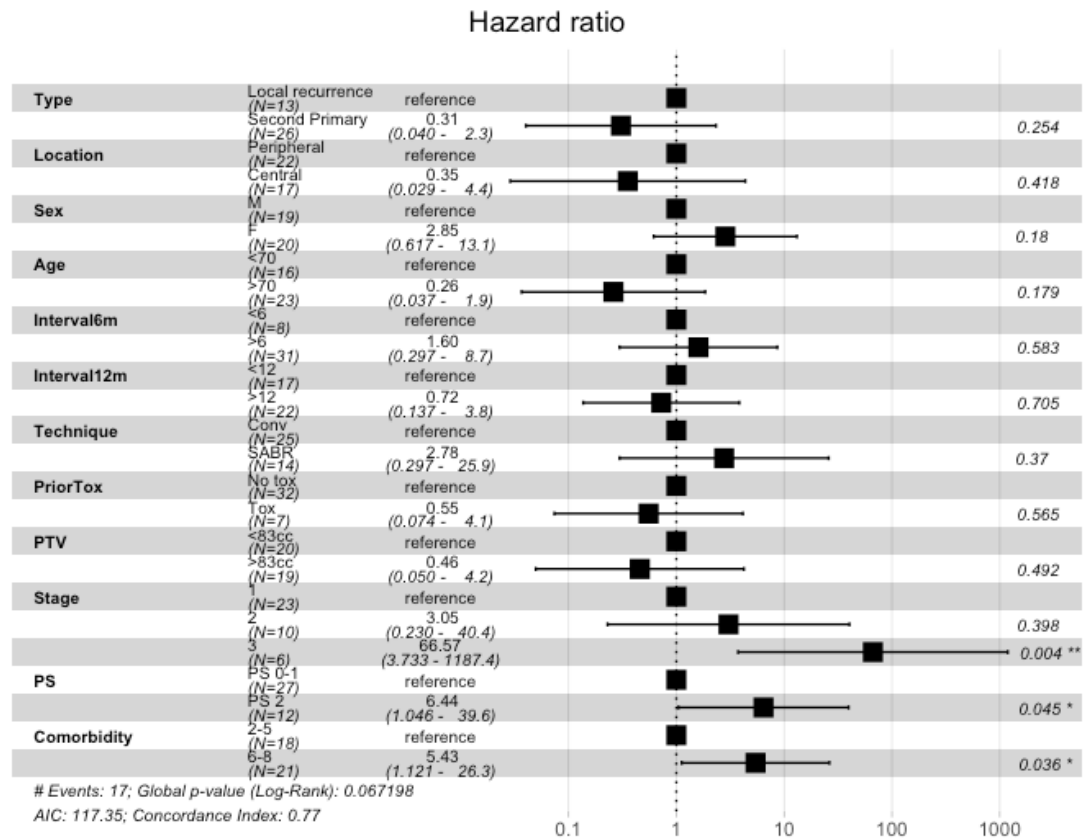


Figure 4.3 Subgroup analysis of the hazard ratio for toxicity Interval6m: interval between initial radiotherapy and re-irradiation split by less than and greater than 6 months, Interval12m: interval between initial radiotherapy and re-irradiation split by less than and greater than 12 months, PriorTox: experience of prior grade 3 or above toxicity at initial radiotherapy, PS: Performance status, PTV: planning target volume, SABR: stereotactic ablative radiotherapy

There was no statistical difference in the proportion of grade ≥ 3 re-irradiation toxicity seen between the SPLC and the LR groups (12/26 and 5/8 respectively, $p=0.74$). There was no significant difference in the rate of toxicity at re-irradiation between patients who had grade 3 toxicity from the initial course of radiotherapy and who did not (Fisher's exact test $p=0.483$, Table 4.4)

Table 4.4 Re-irradiation toxicity divided by grade 3 toxicity encountered at initial radiotherapy G3 tox: Grade 3 toxicity, Re-RT: re-irradiation

		Initial G3 tox	
		Yes	No
Re-RT G3 tox	Yes	2	15
	No	5	17

4.3.4 Cumulative doses

The cumulative EQD2 doses delivered to the thoracic OARs are summarised in Table 4.5. The cumulative doses to midline structures (cord, base of heart, PBrT, oesophagus and great vessels) were significantly higher in the LR versus the SPLC group. The MLD, lung V5Gy and lung V20Gy were not significantly different.

Table 4.5 Cumulative mean doses to thoracic organs at risk All doses measured in equivalent dose in 2 Gray fractions. BoH: base of heart, D20cc: dose to 20 cubic centimetres, Dmax: maximum dose received to an organ at risk, Dmean: mean dose to an organ at risk, LR: local recurrence, MLD: mean lung dose, Oes: oesophagus, PA: pulmonary artery, PBrT: proximal bronchial tree, PTV: planning target volume, SPLC: second primary lung cancer

	Whole group	SPLC	LR	P-value
Dmax Cord	28.82 (8.10 - 62.62)	25.97 (8.1 - 41.92)	34.5 (19.23 - 62.62)	0.039*
Dmax Brachial plexus	28.03 (0.09 - 89.780)	22.49 (0.09 - 82.18)	39.1 (0.99 - 89.78)	0.145
D20cc Chest wall	66.09 (25.71 - 119.21)	65.6 (25.71 - 119.21)	67.08 (34.52 - 110.35)	0.851
Dmax Chest wall	132.51 (53.48 - 279.80)	142.65 (53.74 - 279.80)	112.23 (53.48 - 240.43)	0.159
Dmean Heart	5.87 (0.07 - 27.16)	6.28 (0.07 - 27.16)	5.06 (1.14 - 18.21)	0.517
Dmax Heart	55.48(0.23 - 144.73)	47.49 (0.23 - 144.73)	71.45 (19.18 - 126.94)	0.069
Heart V5	30.14 (0 - 99.85)	34.76 (0 - 99.85)	20.89 (3.86 - 67.49)	0.098
Heart V30	3.41 (0 - 35.02)	3.53 (0 - 35.02)	3.18 (0 - 17.7)	0.869
Dmax BoH	55.59(0.81 - 137.71)	44.29 (0.81 - 80.98)	78.18 (19.18 - 137.71)	0.006*
MLD	11.75 (5.1 - 20.89)	11.54 (5.1 - 20.89)	12.17 (7.94 - 19.67)	0.661
Lung V5	48.9 (15.46 - 86.07)	48.85 (15.46 - 86.07)	48.99 (32.35 - 70.29)	0.976
Lung V20	18.23 (5.26 - 44.89)	17.94 (5.26 - 44.89)	18.79 (9.14 - 40.77)	0.815
Dmax PBrT	65.83 (2.1 - 135.96)	48.46 (2.1 - 82.81)	100.59 (50.83 - 135.96)	<0.001*
Dmax Oes	57.10 (10.16 - 118.66)	47.37 (10.16 - 84.43)	76.55 (15.75 - 118.66)	0.003*
Dmean Oes	17.33 (2.08 - 46.28)	13.77 (2.08 - 36.35)	24.45 (7.81 - 46.28)	0.014*
Oes V55	9.89 (0 - 56.62)	5.48 (0 - 37.33)	18.72 (0 - 56.62)	0.028*

Dmax Aorta	64.57 (4.08 - 135.43)	50.41 (4.08 - 88.87)	92.88 (18.08 - 135.43)	<0.001*
Dmax PA	66.46 (0.38 - 139.74)	53.26 (0.38 - 139.74)	92.86 (20.53 - 139.16)	0.001*
Dmax PTV	-	-	124.9 (108 - 172.2)	-

4.3.5 Survival

The median follow-up time using the reverse Kaplan Meier method is 49.53 (IQR 36 - 57.2). The median OS for the whole group 30.5 months (95% CI 19.5 - 46.7, Figure 4.4). There was no statistically significant difference in OS between LR and SPLC. The median OS for LR was 13.8 months (95% CI 7.03 to NR) and SPLC 35.8 months (95% CI 26.23 to NR, $p=0.15$, Figure 4.5). In the local recurrence group, there were 10 deaths (76.9%, five due to progressive lung cancer, three due to pneumonia, one re-irradiation related death and one unknown). In the SPLC group, there were 12 deaths (46.2%, four due to progressive lung cancer, four due to pneumonia, two from other cancers - ovarian and meningioma, one from liver failure and one from myocardial infarction).

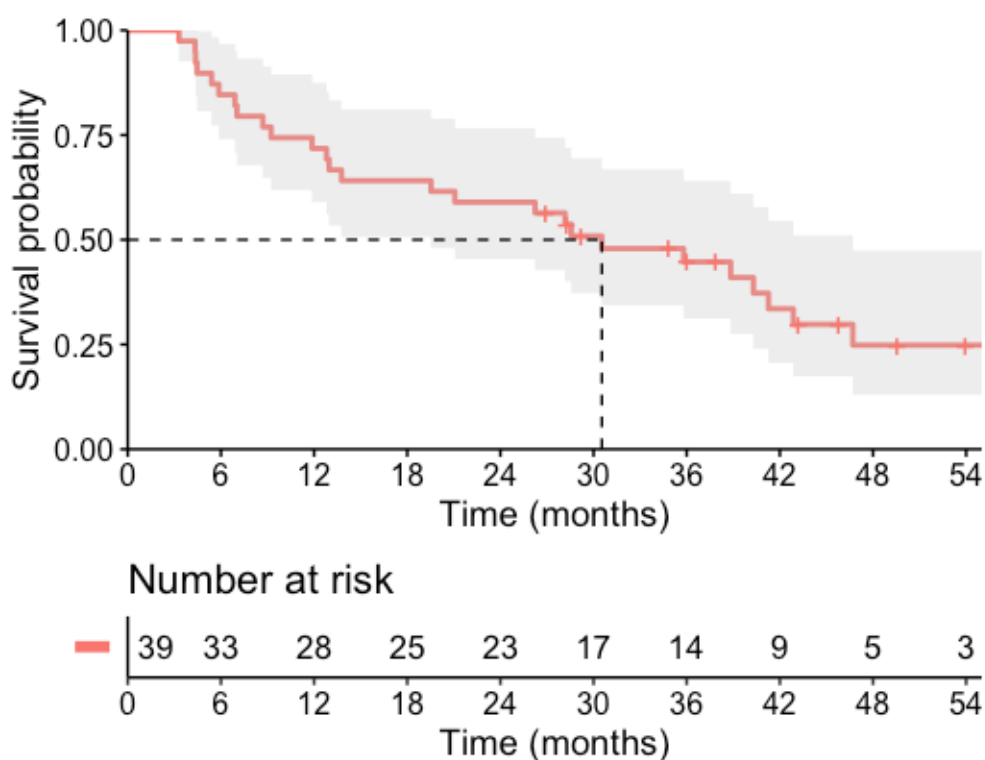


Figure 4.4 Kaplan-Meier plot of overall survival for the whole group

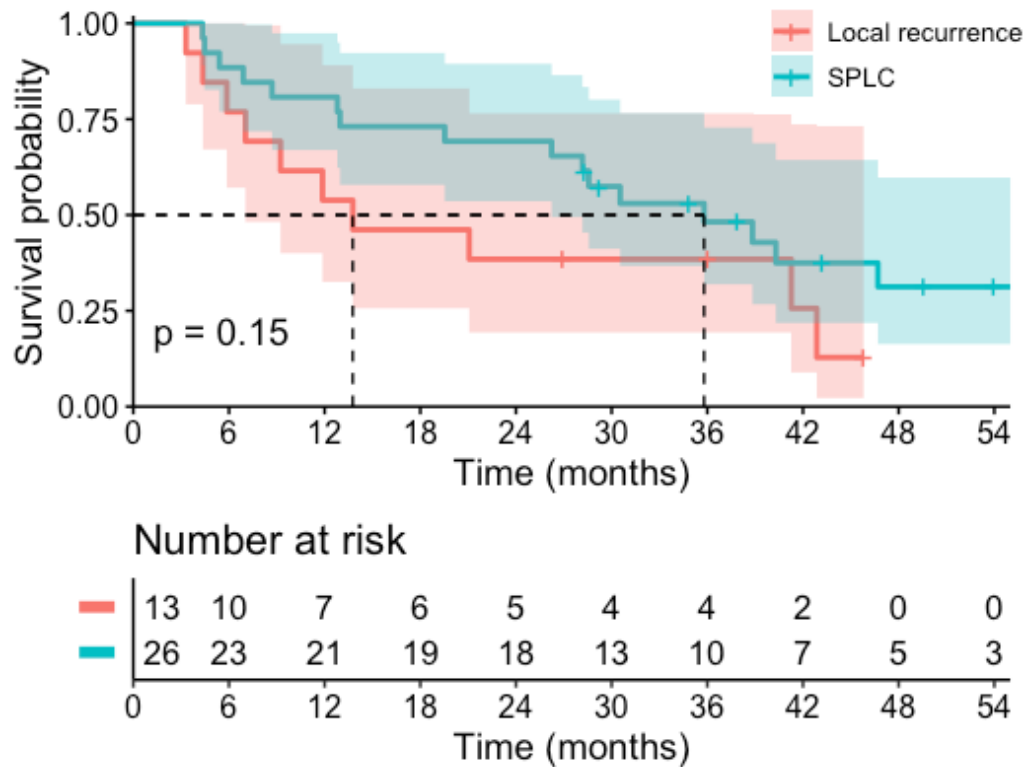


Figure 4.5 Kaplan-Meier plot of overall survival split by second primary and locally recurrent lung cancers SPLC: second primary lung cancer

On Cox proportional hazards regression analysis, the use of SABR for re-irradiation and having a radiological diagnosis of relapse were significantly associated with a higher hazard of death (Figure 4.6). Conversely, having a SPLC had a lower risk of death compared to LR (hazard for death 0.046 95% CI 0.007 - 0.30, $p=0.001$). A greater than 6-month interval between re-irradiation showed a significantly lower risk of death (hazard ratio 0.106 95% CI 0.02 - 0.72, $p=0.03$). There was also a significant trend for worsening survival as the stage of disease at re-irradiation increased. Stage II disease has a hazard ratio for death of 3.43 (95% CI 0.67 - 19.4, $p=0.16$) and stage III disease has a hazard ratio of 15.7 (95% CI 1.15 - 213.3, $p=0.039$). Developing likely re-irradiation toxicity, but not any toxicity, had a significantly higher risk of death (hazard ratio 14.3, 95% CI 2.13 - 96.0, $p=0.006$). The 2-year OS rate was 38.5% in the local recurrence group, and 69.2% in the SPLC group.

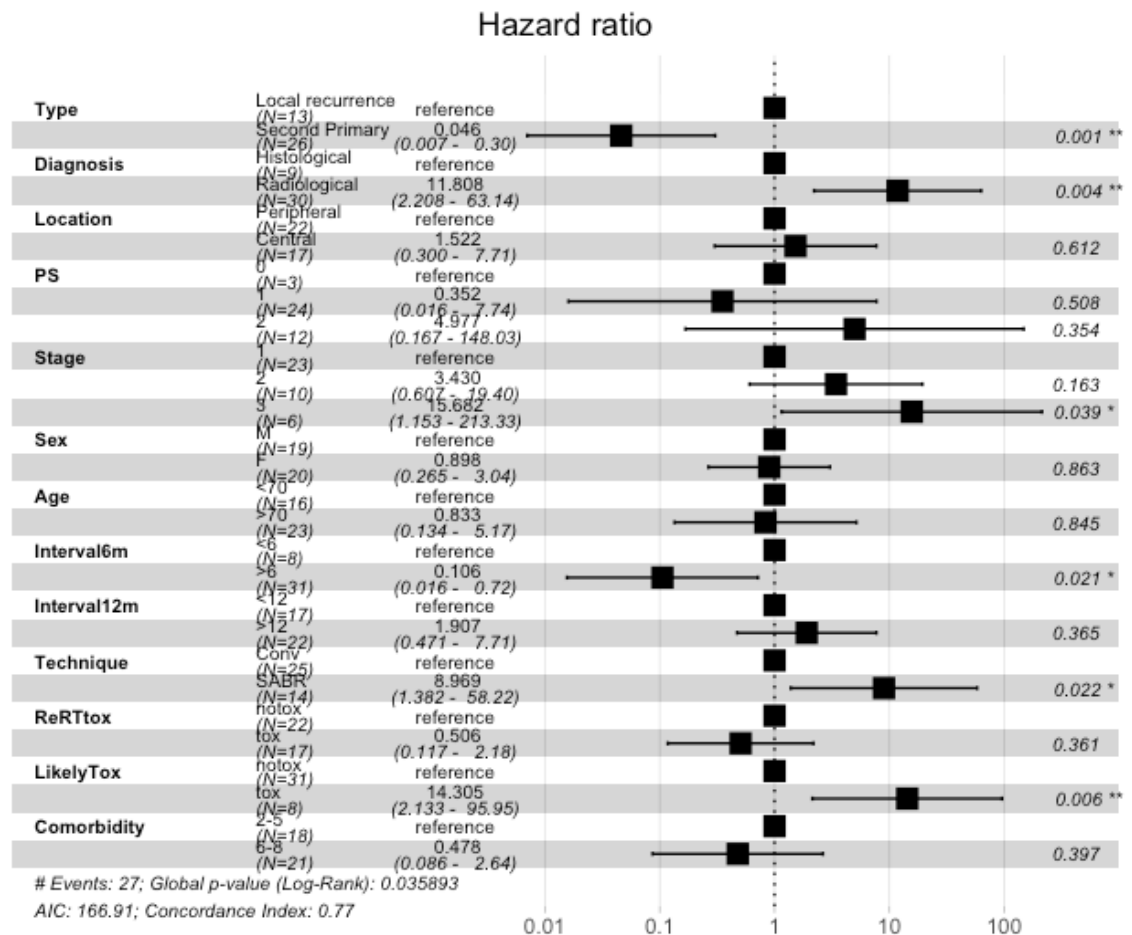


Figure 4.6 Sub-group analysis of hazard ratios for death Diagnosis: method of lung cancer diagnosis, Interval6m: interval between initial radiotherapy and re-irradiation split by less than and greater than 6 months, Interval12m: interval between initial radiotherapy and re-irradiation split by less than and greater than 12 months, LikelyTox: grade 3 or above toxicity investigator assessed to be due to re-irradiation, PS: Performance status, PTV: planning target volume, Re-RTtox: grade 3 or above toxicity without attribution to cause, SABR: stereotactic ablative radiotherapy

4.4 Discussion

This retrospective analysis of radical thoracic re-irradiation for NSCLC demonstrates that the median OS for the whole group is 30.5 months, with a grade ≥ 3 re-irradiation toxicity rate of 43.6%. There is a trend that SPLC have longer OS than LR, but this did not meet statistical significance. The risk of re-irradiation toxicity was similar for SPLC and LR. Patients with stage III disease or PS 2 at re-irradiation are at increased risk of developing grade ≥ 3 toxicity.

4.4.1 Outcomes in the context of other studies

There are eight studies which have a comparable group of patients (mainly or exclusively NSCLC, with locally recurrent disease, re-irradiated radically with conventional fractionation)^{114,119-126}. The median OS from these studies range between 7.1 to 31.4 months with a 2 year OS rate between 11-64%. The results of the Beatson cohort are similar at 13.8 months for the LR group. Sumita *et al.* reported the longest survival in the group of similar patient with a median OS of 31.4 months, which may be due to the good PS of the patients in that cohort (95% were PS 0-1), and a larger proportion of SCLC (33%) than this group.

Of those eight studies, the grade 3 toxicity rates range between 4.7 and 31.5%. The rate of grade ≥ 3 toxicity of our whole cohort is 43.6%. The reasons for this difference may be due to how the toxicities have been reported. Firstly, clinicians delivering re-irradiation may have been more concerned about toxicities as it is a non-standard treatment and may have followed these patients up more intensively. Secondly, due to the retrospective nature of this study, pneumonitis and chest infections were grouped together, but there is uncertainty in attributing radiotherapy as the cause of the chest infections. This group of patients are more likely to have chest infections due to their comorbidities (22 out of 39 patients had a pre-existing diagnosis of COPD). However, not including chest infections in the toxicity data may exclude patients who developed pneumonitis and were mis-diagnosed. Three chest infections occurred within 3 months of re-irradiation. However, two of the chest infections probably were pneumonitis as they resulted in patients requiring domiciliary oxygen. If only these are included (i.e., excluding the nine chest infections that occurred later than three months after re-irradiation), the rate of toxicity is 20.5% (8/39) and in keeping with the existing literature. It should be noted that the published data generally did not divide the toxicity into early and late groups. This makes comparisons between the Beatson cohort and other studies inaccurate.

One patient developed fatal haemoptysis 71 days after the last fraction of re-irradiation. The recurrent tumour was central and had 97.5% overlap with the original PTV. The cumulative EQD2 doses received by the PBrT, aorta and pulmonary artery were 119.7, 86.6 and 120.62 Gy₃. The patient did not undergo

an autopsy therefore it is not possible to determine the cause of the haemoptysis. The cumulative doses for the pulmonary artery and the PBrT exceed the suggested dose constraints from the clinician consensus, and the failure of either of these tissues could account for the haemoptysis. The re-irradiation was delivered before the dose constraints had been published. However, as the recurrent tumour was centrally located, it is also possible that the cancer progressed and led to the fatal bleeding. Two studies of central re-irradiation report a 20% risk of fatal haemoptysis, which demonstrate the high risk nature of these lesions, either from treatment or the natural course of the disease^{114,123}.

Comparison of the SPLC survival and toxicity is difficult as there is little data about this group. Ricco *et al.* describe the use of SABR re-irradiation in a group of 44 patients, 86% with out-of-field recurrences¹⁶⁸. The reported median OS is 36 months, similar to the median OS in the SPLC group in this study (35.8 months). The reported grade ≥ 3 toxicity rate was 13.7% at 6 years, which is lower than the toxicity of the SPLC group in this study (46.2%, 12/26). The toxicity in the SPLC group was 8 chest infections (one within 3 months of treatment), two episodes of chest pain, one stridor and one arm swelling. If the late chest infections are excluded, the overall grade 3 toxicity rate falls to 19.2% (5/26). There was no statistically significant difference between the SPLC and LR groups in this study, however there is a large difference in OS between them. This may reflect that the size of the cohort is too small to have sufficient power to reach significance.

4.4.2 Investigation of uncertainty from the clinician consensus

The use of a multivariable Cox proportional hazards regression analysis is limited in a cohort of this size. This approach was used to attempt to investigate multiple factors of interest, but any interpretation from this is limited by the large number of variables (13) and the limited number of cases (39). In addition, there may have been collinearity between the variables (e.g. comorbidity and performance status).

4.4.2.1 Interval

The minimum interval between courses of radiotherapy did not meet consensus, with some participants suggesting at least 12 months, and most suggesting at least 6 months. There is no increased risk of toxicity using a ≥ 6 month or ≥ 12 -month cut-off in this cohort. This may be due to higher number of SPLC where there is little overlap with the prior radiotherapy fields, therefore the amount of normal tissue receiving a large second dose is low. There is a significant trend for improved survival in patients who had re-irradiation with a minimum interval of 6 months (hazard ratio 0.11, 95% CI 0.016-0.72, $p=0.021$), whereas using a cut-off of 12 months had little influence (hazard ratio 1.91, 95% CI 0.47-7.71, $p=0.365$). The finding of improved survival with longer intervals has been replicated in several studies^{121,169}. In locally recurrent disease, a long interval may suggest a more indolent tumour and this could lead to longer OS regardless of treatment. It is unclear if a longer interval is associated with a greater response to re-irradiation as there is little data on response rates split by interval. In summary, from this cohort, there is some evidence to support using 6 months as a minimum cut-off interval for re-irradiation.

4.4.2.2 Prior grade 3 toxicity

In the clinician survey, concern was raised about re-irradiation in patients with previous grade 3 toxicity from initial radiotherapy. Radiobiologically, if a patient experienced grade 3 toxicity, this could indicate depletion of stem cells or other long lasting damage in the OAR and therefore impaired capacity to respond to further radiation. In this group, two patients experienced grade ≥ 3 toxicity in both courses of radiotherapy. One developed grade 4 pneumonia after the first course, and then subsequently had an infective exacerbation of COPD after re-irradiation. The other patient developed an infective exacerbation of COPD at the first course and developed a rib fracture and another chest infection after the second. Given the uncertainty as to whether these represent true radiation toxicity, this cohort of patients is unable to confirm if patients who had toxicity in the first course of radiation are at higher risk at re-irradiation.

4.4.2.3 Use of SABR

An unexpected finding in this cohort was that the use of SABR was significantly associated with worse survival on sub-group analysis (hazard ratio 8.97, 95% CI 1.38 to 58.2, $p=0.022$). This is unusual as SABR re-irradiation had better outcomes than conventional fractionation in other studies¹³⁴⁻¹³⁶. This may be due to several reasons: SABR is used for patients with smaller tumours; it delivers a higher EQD2 to the tumour for the same normal tissue EQD2 and; SABR treatment is complete in a shorter amount of time compared to conventional fractionation. In addition, the radiological diagnosis sub-group also had worse outcomes (hazard ratio 11.81, 95% CI 2.21-63.1, $p=0.004$). The clinician survey strongly supported SABR as the preferred radiation technique, and the use of highly conformal radiotherapy is a reasonable strategy to limit dose to normal tissue. One possible reason for these findings is that SABR was used more often with PS 2 patients. The SABR group had 42.8% PS 2 patients compared to 24% in the non SABR group. Similarly, the worse outcomes for the radiological diagnosis group may be due to these patients being unfit for biopsy due to comorbidities. As SABR has no minimum lung function requirements, it may indicate that some patients with poor PFTs would have been treated with SABR. Moreover, patients developing SPLC may indicate continued smoking (which this study did not assess), which could add to the poor prognosis in this group. Finally, it may be that previously treated tumours have a different α/β ratio and rate of repopulation which may limit the effect of SABR.

4.4.2.4 Different definition for SPLC and LR

Dividing re-irradiation into two groups (SPLC and LR) did not reach consensus. One issue raised was the lack of evidence to suggest that outcomes were different between the two categories. On Kaplan-Meier survival analysis using the single variable of SPLC and LR, there was no significant difference between the two groups despite SPLC having a longer median OS (35.8 months vs 13.7 months, $p=0.15$). However, on subgroup analysis where numerous other variables are included in the model, SPLC has a significantly lower risk of death compared to LR (hazard ratio 0.09, 95% CI 0.02 - 0.44, $p=0.003$). Interestingly, this supports some degree of treatment resistance in the locally recurrent arm resulting in the poorer overall survival. In addition, overall survival does not account for cancer-

specific mortality or death from other causes, although it is likely in this cohort that the death was due to recurrent cancer. Contrary to this, Griffioen *et al.* reported on 21 patients (46% second primaries and 54% local recurrences) and found no difference in survival on Kaplan-Meier analysis¹¹⁴. The size of both cohorts is small and therefore statistically underpowered to find a difference.

In terms of toxicity, SPLC had similar rates of toxicity as LR, which was not expected. There were 5 (62.5%) grade ≥ 3 toxicities in the LR group and 12 (46.2%) in the SPLC group. If the “likely re-irradiation toxicity” measure is used, 5/8 of the grade ≥ 3 toxic events happened in the SPLC, therefore this is likely to be a true effect. Possible explanations for this finding are the SPLC group have worse PS compared to the LR group and therefore have more co-morbidities, or that the total volume of lung exposed to radiation (over two treatments) increases the rate of toxicity (as opposed to LR where the irradiated lung tissue is more likely to be re-irradiated, implying that retreatment of previously damaged lung is less likely to cause additional new toxicity).

The clinician consensus was that re-irradiation was suitable for PS 0-2 patients. This is supported by this current data in terms of survival, with no significant difference in risk of death between PS 0-1 patients and PS 2 patients. However, PS2 patients or those who had a CCI score ≥ 6 were at a significantly increased risk of toxicity. Therefore, ensuring that patients have sufficient reserve to survive hospitalisation is an important consideration when offering re-irradiation.

4.4.3 Cumulative doses and constraints

There are several potential inaccuracies in generating the cumulative dose. There is no validated method to confirm the amount of dose any tissue has received. One source of inaccuracy is due to the dose accumulation process.

The cumulative doses delivered were calculated using a deformable dose registration. This process uses an elastic b-spline algorithm to apply a series of transformations to image data to morph one set of images (in this case the first CT planning scan) to the second set of images (the re-irradiation planning scan). This set of transformations is also called a deformation vector field (DVF). The

DVF is then applied to the dose maps. One flaw with this method is that the cumulative dose is dependent on the accuracy of the spatial transformations created by the image registration. The ROI is important to highlight the area where the transformation occurs. This is chosen by the operator and can include structures where an accurate image (and therefore dose) match is required. For example, if the ROI includes the PTV, then, because the PTV would be a different shape after initial radiotherapy, the transformations would “squeeze” dose into a space where the cells have disappeared. Similarly, if the ROI is focused on an OAR where there has been significant deformation after initial radiotherapy (e.g., lung fibrosis), the DVF may give an inaccurate dose. This may lead to variation in the true cumulative dose delivered. The magnitude of error has been investigated using proton plans for NSCLC, and six different deformable image registration algorithms. A study of seven patients who had repeated planning scans warped back on to their original planning scans, found that the average decrease in delivered dose to the PTV was 16%¹⁷⁰.

In the ROI evaluation, the most biologically plausible DVFs were seen when the ROI used the whole lung. The range of predicted cumulative doses varied by almost 10 Gy (EQD2) which is a significant margin of error. As there are no validated methods to assess a dose registration except visually reviewing the deformation maps, this method of dose accumulation is prone to error and should be applied cautiously.

Another source of error is the use of planning CT scans for dose registration. As patients go through treatment, they would be slightly different positions on the treatment couch, due to patient set-up and internal organ motion. This would lead to dose changes to the cumulative doses to the OARs. To better identify the true dose received by the patient, daily CBCT could be used and the applied doses for each plan merged, although to merge the doses from approximately 40 radiation treatments would be unwieldy, and also prone to registration error. If the radiation treatments required numerous shifts to improve patient positioning, this would imply that set-up was difficult, and that cumulative dose may be prone to a greater degree of error. Quantification of the error is difficult to do on this retrospective cohort because the daily CBCT required have not been performed as they were not standard of care at the time of treatment.

Despite the uncertainties of cumulative dose registration, and that the patients in the Beatson cohort were treated before the publication of any re-irradiation constraints, the doses delivered in this cohort are in keeping with the suggested constraints from the clinician survey (see Table 4.6) with some exceptions.

There is a consistent difference between the SPLC and LR group, with significantly higher doses delivered to the midline structures (cord, great vessels, heart, PBrT and oesophagus) in the LR group. This is due in part to the increased amount of conventionally fractionated radiotherapy and higher stage of patients in the LR group.

Table 4.6 Comparison of suggested dose constraints and delivered dose ALARA: as low as reasonably achievable Dmax: maximum dose received to an organ at risk, G3: grade 3, Gy: Gray, MLD: mean lung dose, V20Gy: volume of lung receiving at least 20Gy

	α/β	Delphi	Mean delivered dose (Gy α/β)	Range	Observed \geq G3 toxicity
Spinal cord	2	Dmax 60Gy	Dmax 28.82	8.10 - 62.62	0
Brachial plexus	2	Dmax 80-95Gy	Dmax 28.03	0.09 - 89.78	0
Skin/Chest wall	2.5	ALARA	Dmax 132.51	53.48 - 279.80	2
Heart	2.5	ALARA	Dmax 55.48	0.23 - 144.73	0
Lung	3	Individualised	MLD 11.75	5.1 - 20.89	12
Lung	3	Individualised	V20Gy 18.23%	5.26 - 44.89	
PBrT	3	Dmax <80-105Gy*	Dmax 65.83	2.1 - 135.96	2
Oesophagus	3	Dmax 75-100Gy	Dmax 57.10	10.16 - 118.66	0
Great vessels	3	Dmax 110 - 115Gy	Dmax Aorta 64.57	4.08 - 135.43	1

4.4.4 Strengths and limitations

The strengths of this data are that it provides detailed comorbidity information and cumulative dose data on a real-world cohort of re-irradiation patients. The sub-group analyses of toxicity give insights into possible drivers of reduced survival and toxicity. The data generated by this cohort of patients can be used in Chapter 5 (dose/toxicity modelling) as a validation cohort for any models, and in Chapter 7 (re-irradiation replanning).

There are several limitations to this retrospective review. Common to other series, the number of patients available for analysis is low, reducing the statistical strength of some findings. The use of a multivariable proportional hazards model potentially over-analyses the available data, and a univariable approach for fewer factors may have provided more statistically robust results.

The rate of histological confirmation of disease was low compared to other series. Diagnosing recurrent disease is difficult, especially in a group of patients with comorbidities that may preclude biopsy, therefore there may be some patients who did not have recurrent disease or had a different histological type of tumour than at initial radiotherapy.

Toxicity grading was retrospective, and the grade 3 severity depended on hospital admission data. There may be numerous grade 2 toxicity events that are undetected in this study. In addition, the attribution of toxicity to radiotherapy in this cohort was subjective (clinician-based), due to the lack of any prospective process. Some toxicity may be incorrectly labelled as due to radiotherapy when it may be attributable to tumour progression.

There was no formal follow-up scan protocol and scans were performed ad hoc by clinicians to determine local recurrence. This is understandable if the treating clinician felt that there were no other treatment options available and to pursue a symptom-based management strategy. However, cancer specific survival was not performed due to this, because of the risk that undiagnosed recurrent disease may be incorrectly labelled.

4.5 Summary

This retrospective review demonstrates that the toxicity and survival rates from other published data are replicated in the Beatson West of Scotland Cancer Centre re-irradiation cohort. There is some evidence on subgroup analysis to suggest there is a longer median OS in the SPLC arm which may provide some justification to define them as separate entities. Conversely, there were similar toxicity rates detected in both SPLC and LR cohorts. This review has also shown areas of uncertainty in cumulative dose registration, and the need for further

research as to optimal planning techniques to meet the suggested cumulative dose constraints.

5 Re-irradiation normal tissue analysis

5.1 Introduction

Dose constraints in radiotherapy planning exist to prevent unacceptable rates of toxicity. Normal tissue responds to radiation in several ways. There is a dose dependent response (e.g., a minimum dose required to cause DNA damage or induction of a cytokine response), but also a dose independent response which is poorly understood^{171,172}. Low doses rarely cause sufficient DNA damage to result in toxicity (or in the case of pneumonitis, induce the production of cytokines and subsequent inflammation), whereas high doses are very likely to result in large amounts of DNA damage and subsequent toxicity. This relationship is sigmoidal, and often the goal in dose/toxicity modelling is to identify the dose where the risk of toxicity is unacceptably high. It should be noted that choosing the risk level is a subjective process, as demonstrated in the Delphi consensus (Chapter 3).

Landmark dose constraints have evolved in radiation planning from the work of Emami *et al.* and subsequently the QUANTEC series of papers^{83,84}. The 1991 Emami paper described dose and volume constraints for a range of OARs. They reported the 5% toxicity rate and 50% toxicity rates at 5 years with doses given to the whole organ, two-thirds organ and one-third organ. However, as new radiotherapy techniques such as 3D planning and IMRT became available, the volume model of using a third of an organ receiving a uniform dose became obsolete. In addition, more data was available to update the dose volume constraints. The QUANTEC series of papers in 2010 updated these preliminary dose constraints for use where the dose to a normal tissue often was non-uniform and remain in common use today.

Both QUANTEC and Emami study used experimental evidence, retrospective data and clinical consensus to determine the dose constraints for initial courses of radiotherapy. Alternative methods include a dose finding study such as RTOG 0813 or using data from clinical trials¹⁷³. However, re-irradiation toxicity has additional variables in determining dose constraints. Normal tissue can recover radiation tolerance. Studies of re-irradiation of the primate spinal cord demonstrates the longer the duration between treatments, the higher the

tolerance^{139,140}. The size of the first dose is also important, with larger doses resulting in lower re-irradiation tolerance. However, evidence is lacking to predict the degree of normal tissue recovery for most OARs in the thorax. These uncertainties make modelling re-irradiation dose/toxicity difficult.

5.1.1 Current re-irradiation dose constraints

Re-irradiation has been practiced since the 1970s where the dose limits have been set according to the clinicians' experience. However, the high rate of toxicity implies that better patient selection and dose constraints are needed. There are several recently published re-irradiation dose constraints for OARs in the chest. The first publication in 2019 from the University of Michigan outlines their institutional re-irradiation process, where they convert the initial dose delivered to EQD2, apply a discount for recovery, and then convert the dose back into physical dose to use as a dose constraint for re-irradiation planning¹¹². In 2020, Troost reported the re-irradiation dose constraints used from an *in silico* study comparing photon and proton re-irradiation¹⁴⁶. Similar to the University of Michigan approach, these constraints were given in EQD2, but specified a minimum interval between treatments of 9 months. They also limited not only the maximum cumulative dose, but also the maximum dose that could be delivered at the re-irradiation. In the same year, the American Radium Society published the results of a consensus process with recommended composite doses in EQD2 but without any correction for recovery¹⁶⁰. In 2021, an expert consensus paper (Chapter 3) and a re-irradiation literature review also provided dose constraints with accompanying trials - both used EQD2 and no correction for recovery^{161,174}.

All these approaches used EQD2 to summate the dose, and used expert opinion based on a small number of key trials. Table 5.1 outlines the re-irradiation studies that have informed expert opinion on cumulative re-irradiation dose constraints.

Table 5.1 Overview of studies used to form re-irradiation dose constraints EQD2: equivalent dose in 2 Gray fractions, SABR: stereotactic ablative radiotherapy, V20: volume of lung receiving at least 20 Gray

Paper	n	Dose recommendation
<i>Lung</i>		
Ren ¹⁴⁷	67	Cumulative V20>28% had tox rate of 38.2%
Liu ¹⁴⁹	72	Cumulative V20<30%
Meijneke ¹⁷⁵	20	Cumulative V20 <15.2%
<i>Cord</i>		
Nieder ¹⁷⁶	48	0% risk if EQD2 <60Gy, 3% risk if EQD2 <68Gy, and interval >6 months, dose to cord EQD2 <49Gy in each treatment
Saghal ¹⁷⁷	19	EQD2 <70Gy to thecal sac, re-treatment max dose EQD2 25Gy with SABR, minimum interval 5 months, retreatment dose < 50% of total dose
<i>Oesophagus</i>		
Meijneke ¹⁷⁵	8	EQD2 median 85.3Gy (range, 71 - 123Gy) had no ≥G3 toxicities
<i>Proximal bronchial tree</i>		
Feddock ¹⁷⁸	17	EQD2 105Gy safe with initial SABR
<i>Great vessels</i>		
Evans ¹⁷⁹	35	Raw composite dose <120Gy
<i>Brachial plexus</i>		
Chen ¹⁸⁰	43	EQD2 <95Gy and interval >2 years is low risk

The numbers in these trials are low and are from a small number of centres. This could lead to biased dose estimates, especially where the predicted outcomes are rare, such as high-grade toxicity. In addition, the risk of toxicity from exceeding the dose constraints are not quoted. This would be useful when counselling patients in circumstances where dose constraints may need to be exceeded.

5.1.2 Aims of modelling

The aims of dose/toxicity modelling are to build models to predict the cumulative dose to an OAR for a pre-defined toxicity rate. The models will be used to predict the toxicity rate from the published dose constraints and suggest revised dose constraints.

5.2 Methods

5.2.1 Overview

A database was developed taking cumulative dose delivered to an OAR and associated toxicity from published studies. Associated data (e.g., use of concurrent chemotherapy, interval between treatments) was collected where available. Dose/toxicity models were created using logistic regression. The models primarily assessed the role of cumulative EQD2 and toxicity. Exploratory analysis of the interval, the ratio of dose delivered at re-irradiation to the total dose and the effect of chemotherapy was also performed.

5.2.2 Datasets used in modelling and model validation

Three types of data were used in creating and validating these re-irradiation dose toxicity models, outlined in Figure 5.1. The first two types are taken from a literature search of studies which re-irradiation toxicity and dose were given, the process of which is explained below. The data from the literature search could be divided into individual data (where exact patient level information was given) or grouped data (where median doses and toxicity rates for cohorts were reported). Both groups have cumulative doses to an OAR and the associated toxicity, but information on interval between radiation courses and use of concurrent chemotherapy may be missing. The third category of data is for model validation purposes. It is the cumulative dose and toxicity data from the 39 patients treated at the Beatson, the collection of which is outlined in Chapter 4. There are no missing data in this dataset.

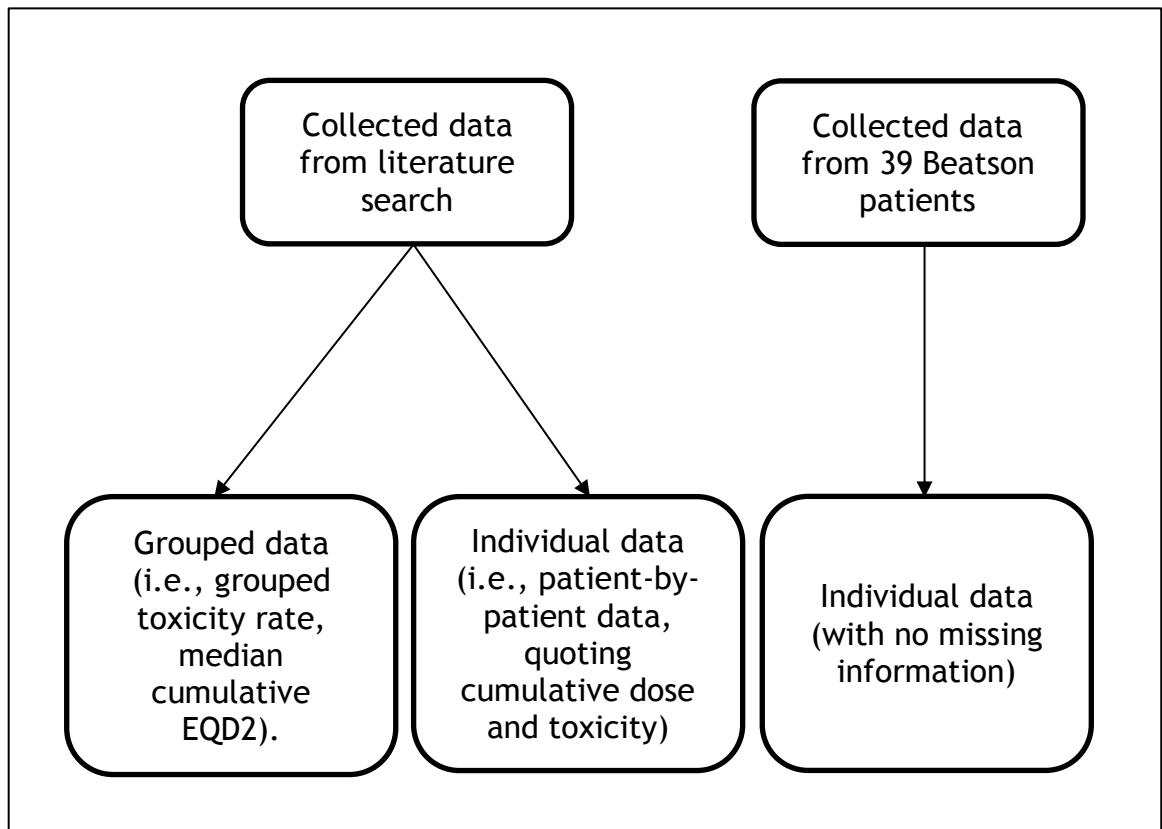


Figure 5.1 Diagram outlining sources of data used in modelling

5.2.3 Data collection and format

A literature search was conducted using MEDLINE and the Glasgow University search engine, identifying any English language studies from 1st January 1970 to 1st October 2018 which included adult humans who had two courses of radiotherapy for malignancy, where both the dose given to a given organ/tumour and the toxicity encountered were published. Animal models were excluded. The OARs which were searched for are as follows: aorta, oesophagus, spinal cord, proximal bronchial tree, lungs, heart, chest wall and brachial plexus.

The search strategy was performed in two phases. The first phase is to look for all published data involving thoracic re-irradiation specific to non-small cell lung cancer. The MEDLINE search strategy is ((lung AND cancer) OR non-small cell lung cancer) AND (retreatment OR re-treatment OR re-irradiation OR reirradiation) AND (dose constraints OR toxicit*). The second phase is to search each OAR specifically looking for re-irradiation data and toxicity e.g. (Lung OR pulmonary) AND (retreatment OR re-treatment OR re-irradiation OR reirradiation).

Duplicates were removed and dose/toxicity information was collected from the identified papers using a standardised data collection form. This search was repeated in December 2020 to identify more recent publications.

5.2.4 Method of deriving cumulative doses

EQD2 was chosen as the most suitable method to add doses from two treatments as it was more easily applied to a clinical setting than BED. Information regarding cumulative equivalent dose in 2 Gray fractions (EQD2), use of concurrent chemotherapy with re-irradiation, the interval between initial radiotherapy and re-irradiation, and the toxicity encountered were recorded from the selected papers. Toxicity was recorded by grade in the original studies and subsequently grouped into G1-2 and G3-5 toxicity. For lung re-irradiation, cumulative mean lung dose (MLD), volume receiving 5Gy or greater and volume receiving 20Gy or greater (cumulative V5 and cumulative V20 respectively) were also recorded.

Some studies did not report the cumulative normal tissue dose explicitly. However, in some papers it was reasonable to assume that the prescription dose would be the same the dose the normal tissue would have received e.g. (re-irradiation for locally recurrent oesophageal cancer where both courses treated the oesophagus with overlapping volumes). If the prescription dose for the two treatments were given in these instances, the EQD2 was calculated for the initial and re-irradiation courses using the following equation using the prescription dose:

$$EQD2 = D \cdot \frac{(d + \alpha/\beta)}{(2 + \alpha/\beta)}$$

Where D = total dose, d = dose per fraction, and α/β = the alpha/beta ratio for a given OAR. The EQD2 for each treatment was then added to generate the cumulative EQD2 e.g., for spinal cord dose, the calculated EQD2 from the first and second treatment were added together, assuming that part of the cord received the sum EQD2. Where data was presented as summary statistics e.g., median cumulative EQD2 to the cord 45 Gy₃ (range 30 to 60Gy₃), the median

value was taken as the dose delivered for all the patients from that study. No data imputation was performed for missing data. Therefore, where data was missing for both univariable and multivariable analysis, the data was excluded.

5.2.5 Choice of endpoints

The toxicity endpoints for each OAR are given in Table 5.2. Early and late toxicity were grouped together to ensure sufficient events occurred to allow modelling.

Table 5.2 Outline of outcome and predictor variables in modelling Dmax: maximum dose received to an organ at risk, MLD: mean lung dose, OAR: Organ at risk, Vx: volume of lung receiving at least xGy

OAR	Outcome variable	Predictor variables
Lung	≥Grade 3 pneumonitis/fibrosis	Cumulative V5
		Cumulative V20
		Cumulative MLD
		Interval
Cord	≥Grade 3 myelitis	Concurrent chemotherapy
		Cumulative Dmax
		Interval
Oesophagus	≥Grade 3 oesophagitis/fibrosis/ perforation	Concurrent chemotherapy
		Cumulative Dmax
		Interval
Proximal bronchial tree	≥Grade 3 haemoptysis/stenosis	Concurrent chemotherapy
		Cumulative Dmax
		Interval
Aorta	≥Grade 3 bleeding	Concurrent chemotherapy
		Cumulative Dmax
		Interval
Brachial plexus	Any toxicity	Concurrent chemotherapy
		Cumulative Dmax
		Interval
Heart	Any cardiac toxicity	Concurrent chemotherapy
		Cumulative Dmax
		Interval
Chest wall	≥Grade 3 chest wall pain	Concurrent chemotherapy
		Cumulative Dmax
		Interval
		Concurrent chemotherapy

5.2.6 Selection of α/β ratio

5.2.6.1 Spinal cord and brachial plexus

An α/β ratio of 2Gy was used for the spinal cord and brachial plexus. There are a range of different values that can be applied to the spinal cord, ranging between 0.87 to 4Gy¹⁸¹. The lower value was derived from a model used for the cervical cord, and a model for the thoracic cord was not possible, although the data suggested that it was less radiosensitive¹⁸². The most recent large study of dose-constraints used an α/β of 2Gy and therefore this value was chosen to use in this process¹⁸³. The α/β ratio of the brachial plexus was best explored in a study assessing the fractionation effects of treatment for breast cancer, which concluded that the likely α/β ratio is 2Gy however other groups have used an α/β of 3Gy^{136,180,184}. This study used the former value as it has more empirical evidence to support it.

5.2.6.2 Chest wall and heart

The α/β for the heart used in the QUANTEC papers was 2.5Gy for pericardial toxicity and 3Gy for ischaemic heart disease¹⁸⁵. Other papers have used a lower α/β of 2Gy¹⁸⁶. A study of a pragmatic approach to planning re-irradiation used an α/β ratio of 2.5 for both chest wall and heart, therefore for ease of comparison with this work, this study will use the same ratio¹¹².

5.2.6.3 Proximal bronchial tree, great vessels, oesophagus and lungs

An α/β of 3 has been used in the published dose constraint papers for toxicity from the proximal bronchial tree, great vessels, oesophagus and lungs. This modelling work will use the same value for ease of comparison.

The only exception is where early OAR toxicity is reported e.g. if early oesophagitis was reported, the α/β ratio used to calculate the EQD2 was 10, and for late stricture, the α/β ratio applied was 3.

5.2.7 Modelling process

The studies found by the literature search were critically assessed by the researcher and papers that gave a cumulative dose to an OAR (in EQD2 or BED)

after two radical courses of radiation were included. Studies were also included if they provided the dose and fractionation details such that the cumulative EQD2 to an OAR could be calculated using the LQ equation. The studies used in the modelling presented their data differently - some provided individual patient-by-patient data (e.g. dose given to each patient), and some used grouped data (e.g. the median dose to the study cohort). In order to accommodate both groups, the standard method of analysis of logistic regression models was adapted, and this is outlined below. All studies included provided toxicity data. The rate of concurrent chemotherapy at re-irradiation and the fractional split (the ratio of the amount of dose given in the 1st treatment to the total received dose), the interval between initial treatment and re-irradiation and the duration of follow-up were collected if available. The data was reviewed after collection to confirm correct transcription/calculation of dose.

The modelling process is outlined in Figure 5.2. The datasets used for each OAR model were a combination of the collected individual data and grouped data from published papers. For each OAR and sub-datasets, any missing data was identified and assessed if the missing data was different in terms of cumulative dose or toxicity compared to the dataset with no missing data (tested using a student's T-test and Fisher's exact test respectively). No imputation was performed for missing data (with the exception of the proximal bronchial tree model). The potential predictor variables (dose, chemotherapy, interval and fractional split) were split by their median values and evaluated using χ^2 or Fisher's exact test as suggested in a recent primer on radiotherapy modelling¹⁸⁷. A relative risk table described the numbers of toxic events split by dose ranges with p-values created using the Altman-Bland method¹⁸⁸.

Logistic regression modelling was performed on each dataset using the maximum likelihood estimation method. Univariable models were generated for each predictor. Univariable models which had a p-value < 0.2 were included in multivariable models.

Leave-one out cross validation (LOOCV) by cohort was used for model selection to determine the model that best fitted the data. This approach was chosen because the toxicity reporting from the collected studies in all cases was a crude rate, and therefore dependent on the length of follow-up of each study. An

actuarial approach was not possible because the time-to-toxicity was not regularly provided in the studies. The use of the crude rate is likely to lead to a greater centre-to-centre variation than expected, as the follow-up length will be uncontrolled (which an actuarial approach would account for). The expected high degree of overdispersion meant that using the Akaike's Information Criterion (AIC) would be inappropriate, whereas LOOCV would better account for the differences between each study. For the same reason, block bootstrapping was used to calculate the confidence intervals for model predictions rather than a binomial approach. This method of analysis would account for the difference in individual and grouped data.

For each modelled OAR, the LOOCV process was to remove the data of one study and fit a model to the remaining dataset. This model was then applied to the removed study. The accuracy of each putative model fit from the cohorts with a dataset removed was determined by calculating a log-likelihood score. This calculated (in a model distribution analogous to the model fitting technique) the difference between the predicted toxicity rate and the observed toxicity rate.

The log-likelihood calculation for a study which provided grouped data was:

$$OC_i \cdot \ln(MC_i) + (N_i - OC_i) \cdot \ln(1 - MC_i)$$

where:

OC_i is the observed toxicity rate for study cohort i

N_i is the number of patients in study cohort i

MC_i is the modelled toxicity rate for study cohort i

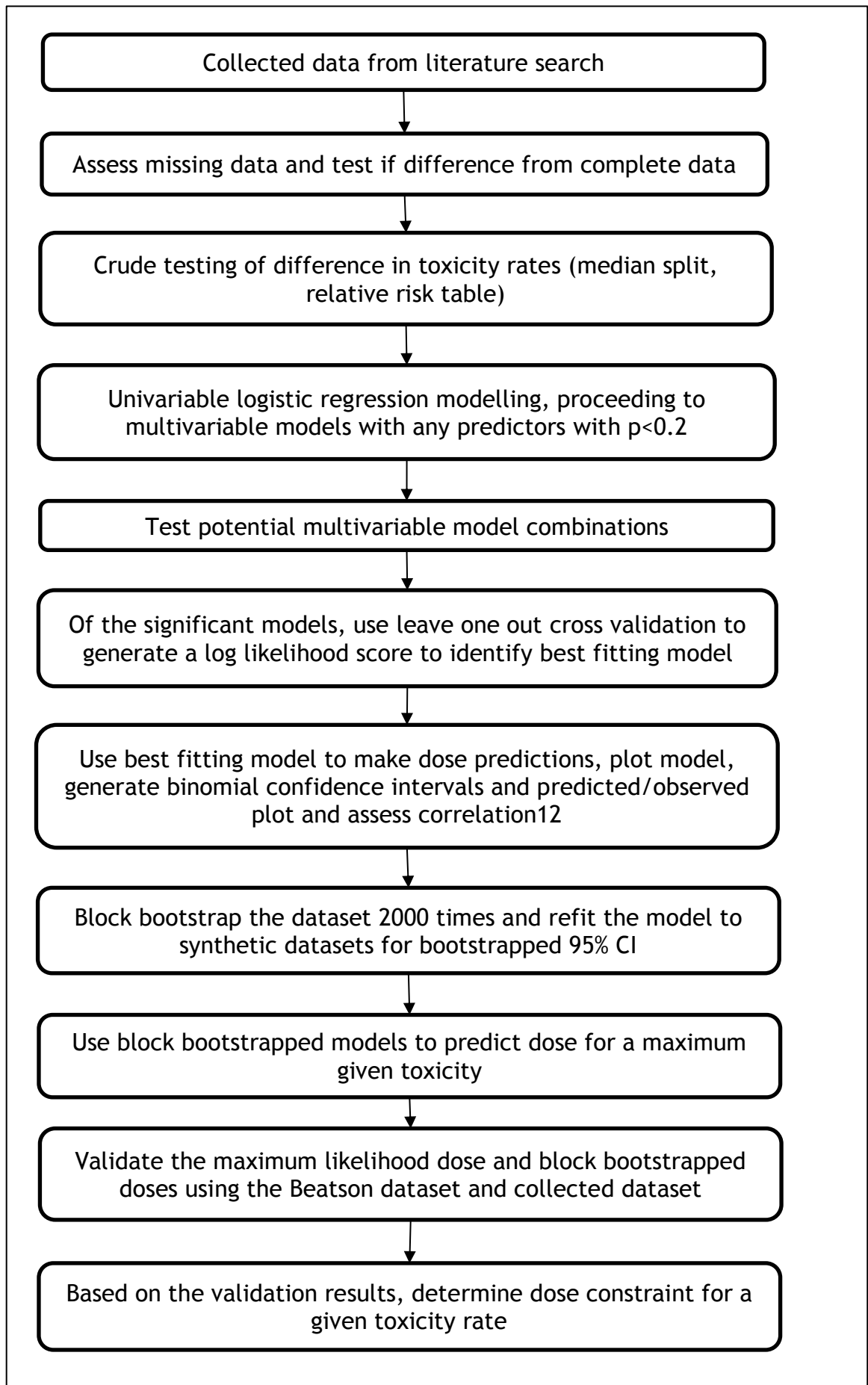


Figure 5.2 Flow chart detailing the process to select a dose constraint

The log-likelihood calculation for individual data if the patient had a toxicity was:

$$\ln(MC_i)$$

The log-likelihood calculation for individual data if the patient did not have a toxicity was:

$$\ln(1 - MC_i)$$

The log-likelihood scores for each different cohort were summed. The model with the lowest log-likelihood score implied a better fit to data and was chosen to make predictions.

The models were plotted and used to predict the maximum-likelihood 5% toxicity rate in all OARs (excepting lung fibrosis where a 20% rate was used). A binomial 95% confidence interval (CI) was not added to the graphs as this would be misleading and would not account for the differences between studies in follow-up. Additional toxicity rate and associated doses were predicted from the models if doing so would be clinically useful (e.g., 1% rate of cord toxicity). Each OAR dataset was block-bootstrapped 2000 times. Block-bootstrapping (where bootstrapped datasets were generated by selecting study cohorts with replacement) was chosen as this accounted for overdispersion. The bootstrapped samples were used to calculate the doses at the pre-determined toxicity rates for each OAR. The selected the lowest 2.5% and top 2.5% predictions were excluded to give the block-bootstrapped 95% CI on the dose leading to a 5% toxicity rate.

Assessment of model fit was performed by splitting the collected dataset into deciles (or if the dataset was small, by individual studies). This was graphically represented by plotting the model predictions (using variables from the collected dataset) of the rate of toxicity by decile (or individual study), against the observed rate of toxicity for the corresponding decile. This was assessed using a Pearson correlation coefficient. Cumulative dose constraints were developed by applying the model predicted dose that would give a 5% toxicity rate and calculating the 95% CI range of toxicity rates this dose would give. A

dose was then calculated which gave the upper limit of the 95% CI of the bootstrapped samples as a maximum of 5%.

To further evaluate the putative constraint, the external Beatson dataset and the individual data from published studies were divided using the putative dose constraint values, and the toxicity rate was calculated for above and below the dose constraint. The constraint was then adjusted to align with the validation data.

All analyses were performed using R version 3.6.1 (R Core Team (2013). R: A language and environment for statistical computing. R Foundation for Statistical Computing, Vienna, Austria). A p-value of <0.05 was used for significance for all tests.

5.3 Results

5.3.1 Structure of reports

Five OARs were modelled based on the collected database. Each OAR dose/toxicity analysis is presented in a similar way. A summary of relevant studies, lowest dose where toxicity was observed and a crude analysis using median splits of each variable are presented. Univariable and multivariable analysis and the optimal dose/toxicity model follow, with development of dose constraints using the bootstrapping results. Finally, the model is evaluated using a predicted vs observed toxicity plot and dose constraints validated using the dataset the model was developed from and external (Beatson) data.

5.3.2 Data collection

The literature search revealed 55 papers that were suitable for inclusion in the study (see Figure 5.3). The data collected from each paper is summarised in the tables at the beginning of each subsection.

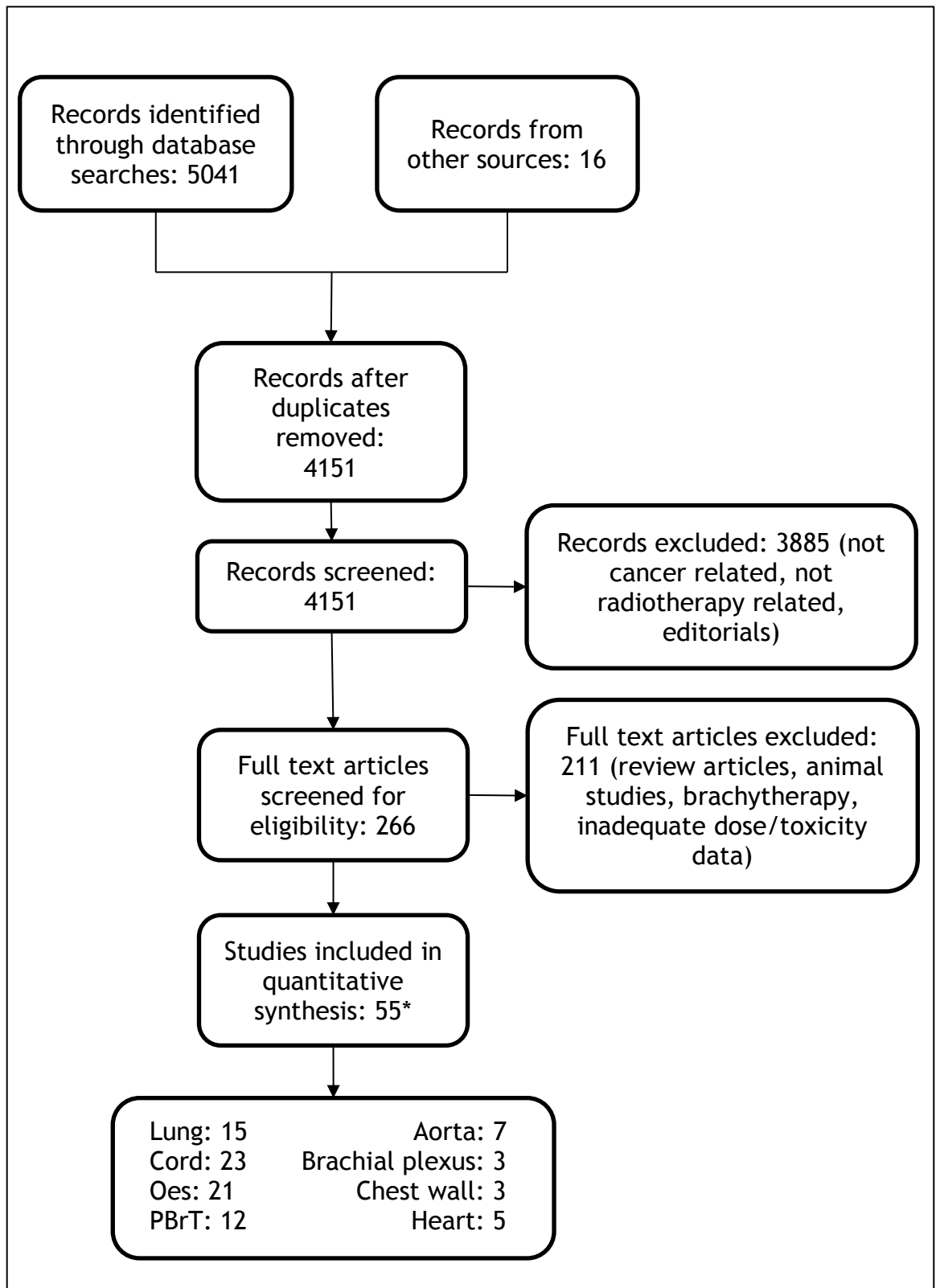


Figure 5.3 PRISMA diagram Some papers provided dose/toxicity data on more than one OAR

5.3.3 Models for cord

Dose/toxicity models were created for the spinal cord using a dataset created from the 23 papers listed in Table 5.3 and Table 5.4. The data was collected between 1955 - 2017. The lowest dose where grade 3 or above toxicity ($\geq G3$) was observed is an EQD2 of 63.3Gy.

5.3.3.1 Dose toxicity models using the complete dataset

There were 604 patients in the exact dataset and 18 $\geq G3$ toxic events, summarised in Table 5.5. There was a significant difference in the rate of toxicity above the median cumulative dose (EQD2 of 60.8Gy, $p=0.007$), but no difference in the rate of toxicity when the dataset was divided between the median fractional split and interval (Table 5.6).

The missing data group included 123 cases where either the interval and/or the fractional split were unable to be calculated. 481 cases had no missing data. The missing data group had a significantly lower mean cord cumulative EQD2 compared to the group with no missing data (44.43 Gy vs 64.70, t-test p -value <0.001). The missing data group had no toxicities, compared to the 18 seen in the no missing data group (Fisher's exact p -value 0.032). No data imputation was performed, and the missing cases were excluded from the relevant modelling process (e.g., if there was no interval data in a case, the whole case would be removed from the interval model, or any multivariable model including the interval).

Paper	n	Individual data/Grouped	Treatment span	Median initial prescription dose in Gy/median Gy per fr (range)	Median re-RT prescription dose (range)/ median fr (range)	Re-treatment Technique	Cord dose assumed/actual
Ryu ¹⁸⁹	1	Individual	1981 – 1993	46.8/26	45/25	APPA/Direct post	Actual
Grosu ¹⁹⁰	8	Individual	1990 – 1997	38(29-50)/2.25 (1.25-3)	30(29-38) Gy/2(1.8 – 4)Gy per fr	Direct post	Assumed
Sminia ¹⁹¹	8	Individual	est 1995 – 2002	24.5 (8-49.6)Gy/2.6 (1.5-8)	21 (16-50)Gy/3 (2-4)Gy per fr	NR	Assumed
Milker-Zabel ¹⁹²	18	Grouped	1997 – 2001	38 (28-46)/est 2Gy per fr	39.6 (24 – 45)Gy/2Gy per fr	IMRT, 3D-CRT	Assumed
Kuo ¹⁹³	1	Individual	1997 – 2001	45/22	50.4/28	IMRT	Actual
Magrini ¹⁹⁴	5	Individual	1966- 1989	30 (20-30)/1.7 (1.7-1.7)	36 (20-36)Gy/2(2-2)Gy per fr	APPA	Actual
Bauman ¹⁹⁵	4	Individual	1977-1993	32.5 (24 – 36.8)/1.3 (1-1.6)	35 (10-40)Gy/1.5 (1-2) Gy per fr	Direct post	Actual
Wong ¹⁹⁶	11	Individual	1955 – 1985	33.9 (16-47.9)/3.39 (1.25-4.88) (dose to cord)	22 (8.2-42.67)Gy/2.72 (1.04-7.3)Gy per fr (dose to cord)	APPA/Direct post	Actual
Jackson ¹⁹⁷	22	Individual	1981 – 1985	55(50-61)/2 (2-2.2)	30 (21-30)Gy/2 (2)Gy per fr	3D-CRT	Actual
Wright ¹⁹⁸	23	Individual	2000 – 2005	30 (21-66)/ 3 (1.6-21)	20 (20 – 55.8)Gy/4 (1.8-6)Gy per fr	IMRT	Actual
Nieder ¹⁷⁶	5	Individual	1990 – 2005	60 (44.8-70)/ 2(1.6 – 2)	56 (36-62)Gy/2 (1.8-2) Gy per fr	NR	Actual
Rades ¹⁹⁹	74	Both	1992 – 2003	28 (16-64)/4(2-8)	15 (8-30.6)Gy/3(1.8-8)Gy per fr	APPA/Direct post	Actual
Gwak ²⁰⁰	3	Individual	2002-2005	50.4 (30-50.4)/NR	33 (21-35.1)Gy/11 (7-11.7) Gy per fr	SABR	Actual

Choi ²⁰¹	42	Grouped	2002 – 2008	40 (24.2-50.4)/2 (1.8-3)	20 (10-30)Gy/10 (estimated) Gy/fr)	SABR	Actual
Maranzano ²⁰²	12	Individual	1998-2007	12 (8-16)/8	8 (4-20)Gy/8 (4-8) Gy per fr	APPA/Direct post	Actual
Saghal ¹⁷⁷	5	Individual	2003-2010	38.75 (14-50.4)/ 1.81 (1.8-14)	20 (16-33)Gy/10.5 (4-16)Gy per fr	SABR	Actual
Navarria ²⁰³	31	Grouped	2009-2010	30 (8-60)/10 (1-30) fractions	30 (19.8-45)Gy/11 (5-18) fractions	VMAT	Actual
Chang ²⁰⁴	54	Grouped	2002-2008	EQD2 (10) 50.7	EQD2 (10) 51.1	SABR	Actual
Wang ²⁰⁵	12	Grouped	2006-2010	estimated 40 (30 – 40)/2 (2-3)	est 21-24Gy/7-8 Gy per fr	SABR	Actual
Hashmi ²⁰⁶	215	Grouped	NR (published in 2016)	NR	EQD2 (10) 36 (12-66.7)	SABR	Actual
Kawashiro ²⁰⁷	23	Individual	2006-2013	40 (30-40)/2 (2-3) (estimated)	24.5 (14.7-50)Gy/5 (3-25) Gy per fr	IMRT	Actual
Kennedy ¹³⁶	21	Grouped	2008-2017	54 (50-54)/18 (10-18)	50 (50-54)Gy/10 (10-18)Gy per fr	SABR	Actual
Schroder ²⁰⁸	6	Grouped	2011-2017	NR	NR	SABR	Actual

Table 5.3 List of studies used to form cord dataset The total number of patients included is 604, from 23 studies. 3D-CRT: three dimensional conformal radiotherapy, APPA: anterior posterior-posterior anterior beam arrangement, EQD2: equivalent dose in 2 Gray fractions, Fr: fractions, IMRT: intensity modulate radiotherapy, NR: not recorded, Post: posterior, Re-RT: re-irradiation, SABR: stereotactic ablative radiotherapy, VMAT: volumetric arc therapy

Paper	Median cumEQD2 to cord (range)	Median Interval (months, range)	Median Fr split	Any Grade 3-5 toxicity (%)	Median follow-up post re-RT (months, range)	Uncertainty
Ryu ¹⁸⁹	87.21	120	0.510	0	60	
Grosu ¹⁹⁰	68.29 (60.1 - 102)	30 (6 – 63)	0.56 (0.4-0.61)	0	16 (5 – 44)	
Sminia ¹⁹¹	72.97 (62.5 – 88.35)	42 (4 – 154.67)	0.35 (0.29 – 0.66)	0	12.1 (1 – 53.3)	
Milker-Zabel ¹⁹²	66.17Gy	17.7 (6.2 – 108.2)	0.342	0	12.3 (3.5 – 33.1)	Calculated EQD2 based on median dose and median fractions for both treatments, dose to cord estimated from paper.
Kuo ¹⁹³	62.96	37	0.63433254	0	8	
Magrini ¹⁹⁴	57.8 (47.8 – 67.8)	24 (12 – 36)	0.435 (0.34 – 0.58)	0	168 (120 – 204)	
Bauman ¹⁹⁵	38.75 (37.7-52.2)	16.4 (8.4-28)	0.477 (0.375-0.759)	0	6 (2.5-9.1)	Estimated EQD2 from table of physical dose
Wong ¹⁹⁶	74.86 (64.2-85.8)	19 (2-71)	0.646 (0.234-0.877)	100	11 (4-25)	Used fixed field technique therefore dose calculation variable, quotes dose to cord, myelopathy not graded
Jackson ¹⁹⁷	55 (30-79)	15 (5.7 – 48.5)	NR	0	5.3 (0.5-25.1)	One case of myelopathy authors think was due to initial RT
Wright ¹⁹⁸	47.4 (11.0-52.4)	19 (2-125)	0.792	0	8 (1-51)	Reconstructed dataset excluding cauda equina retreats, but no location of cord lesion

Nieder ¹⁷⁶	55 (52.3-90.8)	31 (12-96)	0.51 (0.313-0.65)	0	7 (5-10)	Used BED as Cord max
Rades ¹⁹⁹	56.3 (38.8-71.3)	majority < 12 months	0.61 (0.4-0.67)	0	7 (1-29)	
Gwak ²⁰⁰	90.81 (90.4 – 154.5)	54 (18-120)	0.33 (0.31-0.53)	33	24 (8-32)	
Choi ²⁰¹	63.3 (26.6-101.65)	19 (2-219)	0.632	2.4	7 (2-47)	Converted from EQD2 Gy3 to Gy2
Maranzano ²⁰²	52.9 (40-60)	5 (2-31)	0.583 (0.33-0.87)	0	5 (1-24)	
Sahgal ¹⁷⁷	95.4 (77.1-154.9)	18 (11-81)	0.382 (0.219 – 0.462)	100	17 (3-55)	SABR doses at prescription lines, so second dose is an estimate – but was checked with median values provided and correlates. Quotes thecal sac doses
Navarria ²⁰³	51.3 (27.9-57.6)	17 (6-106)	0.734	0	9 (6-24)	Fractional split calculated using median dose/fr for both treatments
Chang ²⁰⁴	83.37	24.5 (3-80)	0.446	0	mean 17.3	Including cauda equina doses.
Wang ²⁰⁵	98.6	9 (4-16)	0.406	0	9.4m (2.5-45)	Includes 23% lumbar spine re-irradiation, uses spinal cord doses
Hashmi ²⁰⁶	60.8 (14 – 107.6)	13.5 (0.2 – 107.3)	0.595	0	8.1 (0.1 – 52.6)	pooled analysis of 7 studies
Kawashiro ²⁰⁷	59.1 (47.5-82.3)	13 (2-75)	0.679 (0.486 – 0.789)	0	10 (1-54)	3 lumbar patients included
Kennedy ¹³⁶	12.2 (3 -21.1)	23 (7-52)	NR	0	24 (3-60)	
Schroder ²⁰⁸	57.75 (53.58 – 68.30)	14 (2-184)	NR	0	13 (1-45)	only reported cord dose when above 50Gy and reported EQD2 in α/β of 3

Table 5.4 List of studies used to form cord dataset The total number of patients included is 604, from 23 studies. BED: biologically equivalent dose, EQD2: equivalent dose in 2 Gray fractions, Fr: fractions, NR: not recorded, Re-RT: re-irradiation, RT: radiotherapy, SABR: stereotactic ablative radiotherapy

Table 5.5 Summary of whole cord dataset Dmax: maximal dose received to an organ at risk, EQD2: equivalent dose in 2 Gray fractions

		Missing values
Number of trials:	23	
Number of patients:	604	
Number of \geq Grade 3 events	18	
Median interval from initial treatment and re-irradiation (months, range)	13.5 (2 - 154.7)	96
Median cumulative cord Dmax (EQD2 Gy, range)	60.8 (12.2 - 154.9)	0
Median fractional split (range)	0.60 (0.22 - 0.88)	49

Table 5.6 Results of χ^2 tests when whole dataset split using median values Gy: Gray

	No toxicity	Toxicity	p-value
Median dose (Gy), n=604			
<60.8	193	0	
>60.8	393	18	
			0.007*
Median fractional split, n=555			
<0.60	415	10	
>0.60	122	8	
			0.063
Median interval (months), n= 508			
<13.5	97	7	
>13.5	393	11	
			0.094

To calculate the relative risk, the dataset was split by 30Gy increments, with the lowest dose where toxicity occurred assigned as the reference risk. The relative risk of \geq G3 events increased as the dose increased over 90Gy, with the doses above 120Gy statistically significant (Table 5.7).

Table 5.7 Relative risk table for the whole dataset CI: confidence intervals, EQD2: equivalent dose in 2-Gray fractions, Gy: Gray, NA: not available

Dose range (EQD2, Gy)	Number	Grade \geq 3 events	Relative risk	Lower 95% CI	Upper 95% CI	P-value
<30	21	0	0	0	NA	NA
30-60	167	0	0	0	NA	NA
60-90	396	14	1	0.48	2.07	1
90-120	18	2	3.14	0.77	12.8	0.11
>120	2	2	28.29	16.91	47.32	0

The cumulative cord Dmax, the interval and fractional split univariable logistic regression models all had p-values<0.2 and proceeded to multivariable model (Table 5.8).

Table 5.8 Summary of complete dataset univariable and multivariable modelling cumDmax: cumulative maximum dose to the organ at risk

Predictor	Toxicity	p-value	Number
Univariable modelling results			
Interval	Grade ≥ 3	0.005*	508
Fractional split	Grade ≥ 3	0.012*	555
cumDmax	Grade ≥ 3	<0.001*	604
Initial multivariable modelling results			
Interval	Grade ≥ 3	0.025*	481
Fractional split	Grade ≥ 3	0.250	
cumDmax	Grade ≥ 3	<0.001*	
2-variable model (Interval split excluded)			
Fractional split	Grade ≥ 3	0.394	555
cumDmax	Grade ≥ 3	<0.001*	
2-variable model (cumDmax excluded)			
Interval	Grade ≥ 3	0.067	481
Fractional split	Grade ≥ 3	0.062	
Final multivariable model (Fractional split excluded)			
Interval	Grade ≥ 3	0.038*	555
cumDmax	Grade ≥ 3	<0.001*	

Interval and cumulative Dmax were significant in the initial multivariable model including all the variables. Two-variable models were assessed, with the cumulative Dmax and interval being the model where both variables were significant. This model was compared using LOOCV to the univariable cumulative Dmax model. The log-likelihood scores for the univariable and two-variable models were 84.27 and 84.21. The LOOCV was performed only on the cohorts which had the necessary data for both models. Therefore, the multivariable model with the interval and cumulative Dmax had the best fit to the data. The model expression is:

$$P(\geq G3 \text{ toxicity} | X_1, X_2) = \Phi(-9.055 + 0.0748X_1 + 0.0239X_2)$$

where X_1 =cumulative Dmax, and X_2 = interval. Using the median interval (13.5 months), the predicted cord Dmax for a 5% toxicity rate is an EQD2 of 77.42Gy (95% CI 70.10 - 84.74Gy). The predicted cord Dmax for a 1% and 10% toxicity rate is an EQD2 of 55.34Gy (95% CI 43.39 - 67.30) and 87.42 (95% CI 78.70 - 96.13). These confidence intervals do not take into account overdispersion whereas the block bootstrapped samples do. The 95% confidence intervals for cumulative dose that gives the 5% and 1% toxicity rate using 2000 block-bootstrapped samples using the median interval of 13.5 months, are 9.46 - 306.64Gy and -23.18 - 156.33Gy respectively. This is summarised in Table 5.9. The dose response of the multivariable model is plotted in Figure 5.4 showing the regression model, the standard error of the regression and the source data.

Table 5.9 Summary of multivariable model dose predictions The median interval (13.5 months) was used for predicting dose. CI: confidence interval, EQD2: equivalent dose in 2-Gray fractions

Toxicity rate	Model dose prediction (EQD2 Gy)	95% CI lower limit (EQD2 Gy)	95% CI upper limit (EQD2 Gy)	Bootstrapped 95% CI lower limit (EQD2 Gy)	Bootstrapped 95% CI upper limit (EQD2 Gy)
1%	55.34	43.39	67.30	-23.18	156.33
5%	77.42	70.10	84.74	9.46	306.64

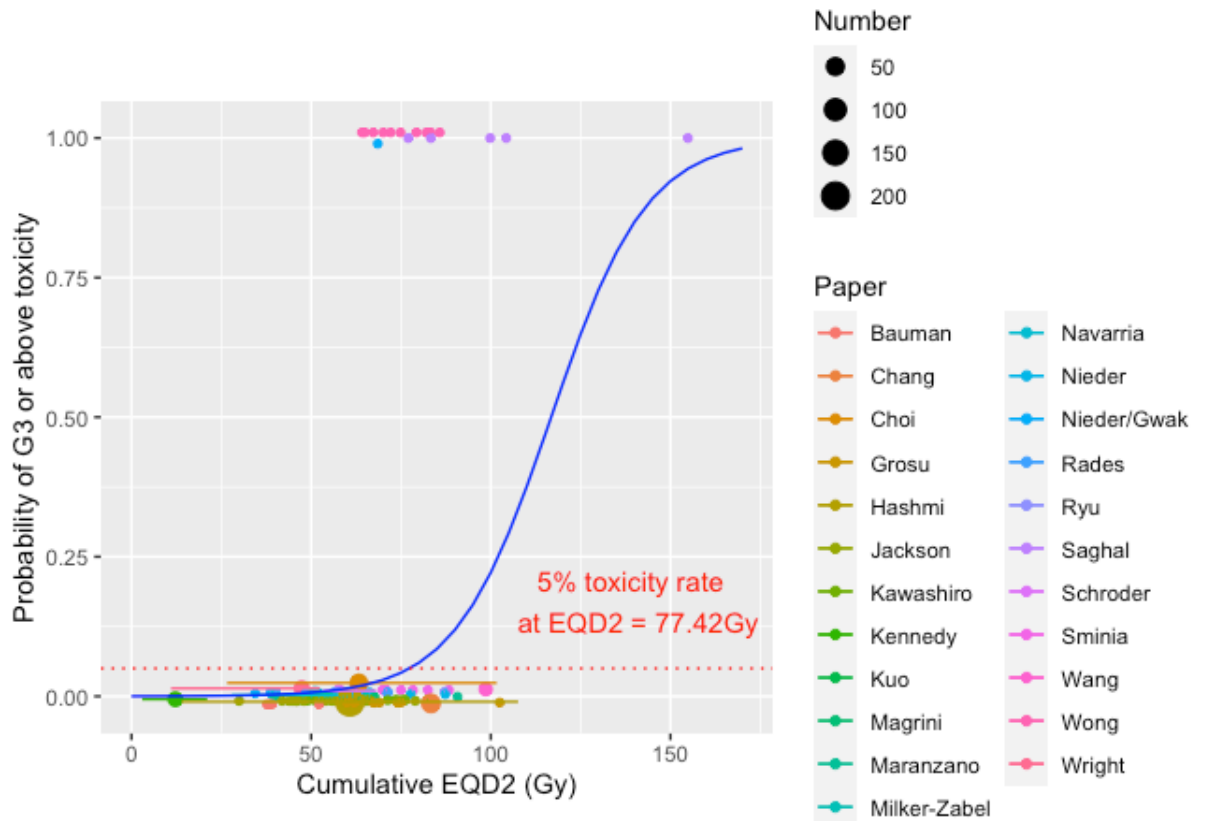


Figure 5.4 Plot of the cord multivariable model. The blue line is the fitted regression model, the red dotted line indicates the 5% toxicity level. The dots represent the toxicity rate from each individual paper coded by colour, with the size of the dots proportional to the number of patients in the study, horizontal bars represent the range of the doses where available, due to overlapping data point, the scatter plot has been jittered. The plot uses the median interval from the dataset.

5.3.3.2 Development of cord constraint values

The multivariable model maximum likelihood dose that gives a 5% rate of toxicity is 77.42Gy. When this dose is used to calculate the risk using the 2000 block-bootstrapped samples with the median interval of 13.5 months and no correction for different cohort sizes, the 95% CI for risk is 0.2% to 40.5%. Reducing the dose to 51.55Gy, gives a 95% CI for risk of 0.01% to 5%. The complete model maximum likelihood dose that gives a 1% rate of toxicity is 55.34Gy. When this dose is used to calculate the risk using the 2000 bootstrapped samples, the 95% CI for risk is 0.02% - 6.0%. Reducing the dose to - 2Gy gives a 95% CI for risk of <0.01% - 1%. These results are summarized in Table 5.10.

Table 5.10 Development of cord dose constraints using bootstrapping. CI: confidence intervals, EQD2: equivalent dose in 2-Gray fractions, Gy: Gray

Model dose (EQD2 Gy)	Risk	95% CI lower limit risk (%)	95% CI upper limit risk (%)
77.42	5%	0.2	40.5
51.55	Maximum 5%	0.01	5
55.34	1%	0.02	6
-2.0	Maximum 1%	<0.01	1

5.3.3.3 Evaluation of cord models and suggested dose constraints

The predicted against the observed toxicity rate by decile for the multivariable model was plotted in Figure 5.5. The Pearson correlation coefficient was 0.91 (p-value <0.01). This suggests that the model is a good fit to the data.

The 5% maximum likelihood dose (77.42Gy) and the bootstrapped maximum 5% (51.55Gy) dose from the multivariable model was applied to the external Beatson dataset to identify the rate in clinical practice. However, there were no cord toxicities in the validation set, therefore this was not contributory. These doses were then used as the cut-off points using the collected individual data (n=111) only to assess if the observed rate of toxicity above and below the cut-off matched the expected 5% rate (Table 5.11). The 51.55Gy bootstrapped constraint predicted <5% and the observed rate was 0%. Therefore, this use of this dose constraint may be too conservative. The 77.42Gy maximum likelihood constraint exceeded the predicted 5% toxicity rate with an observed rate of 7.7%. There is some uncertainty around this estimate given the small sample size of the individual data, with the true value possibly higher than this. The bootstrapped 95% upper confidence interval suggested that the rate could be as high as 40.5%. Due to this uncertainty, using this dose as a cut-off may result in excess toxicity. An exploratory cut-off of 67.3Gy (the upper 95% CI for 1% toxicity) had a 4.3% toxicity rate below the cut-off, and a 33.3% above it. The upper 95% confidence interval for this 67.3Gy is 12.2% and therefore may be a reasonable compromise.

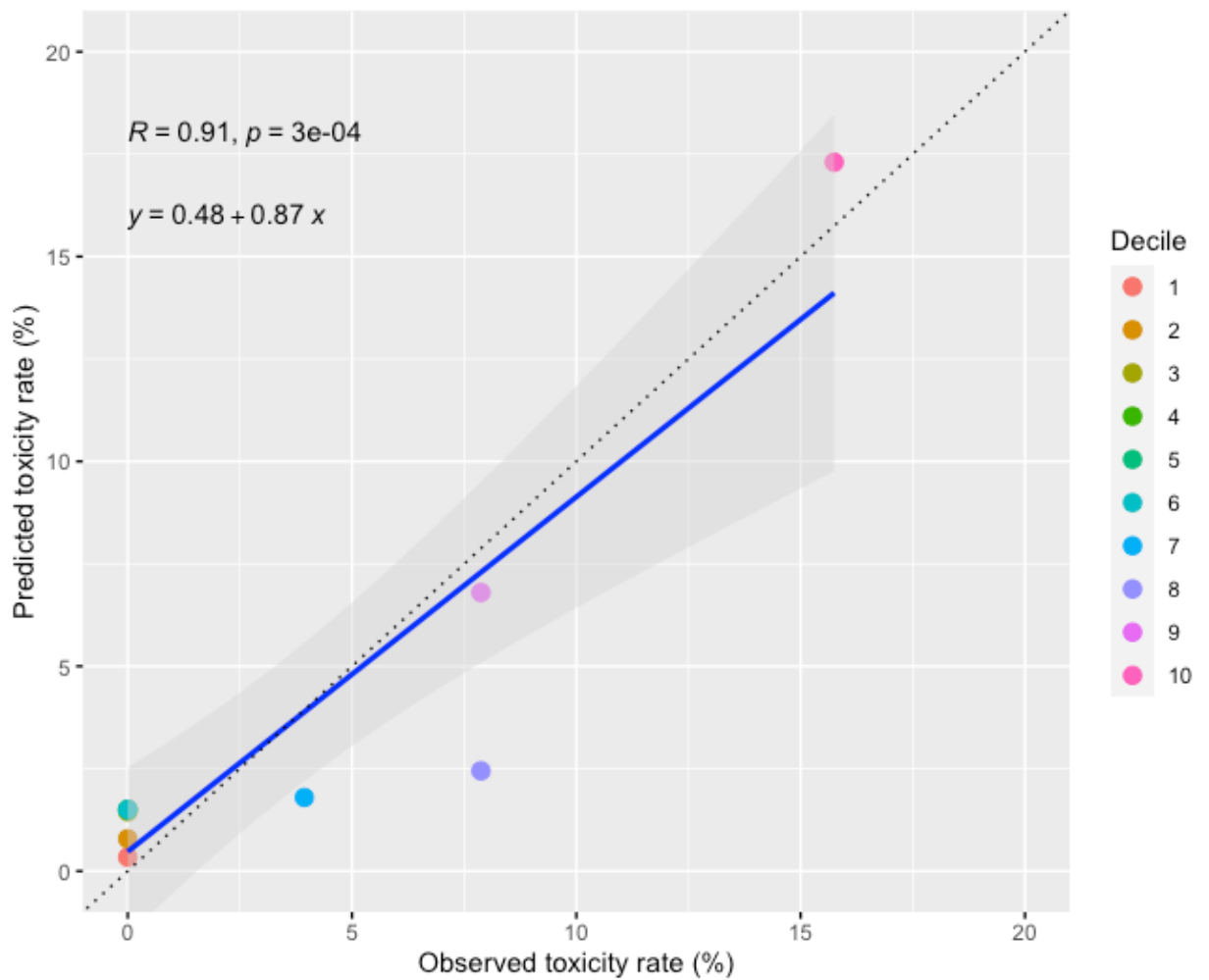


Figure 5.5 Predicted vs observed spinal cord grade 3 toxicity rate by decile using the multivariable model The blue line is the line of best fit and the black dotted line is the line of unity.

Table 5.11 Testing complete and individual model constraints on individual data Gy: Gray, total number of patients 111

	Number with no toxicity	Number with toxicity	Toxicity rate (%)
Maximum likelihood 5% toxicity			
≤77.42 Gy	82	7	7.7
>77.42 Gy	12	10	45.5
Bootstrapped maximum 5% toxicity			
≤51.55Gy	23	0	0
>51.55Gy	71	17	19.3
Exploratory cut-off (maximum likelihood upper limit of 1% toxicity)			
≤67.3Gy	66	3	4.3
>67.3Gy	28	14	33.3

5.3.3.4 Cord models discussion

Re-irradiation of the spinal cord has been extensively studied both in animal models and with human retrospective data. The QUANTEC spinal cord paper suggests a 0.2% toxicity rate at 50Gy in 2 Gy fractions, and a 6% toxicity rate at 60Gy with initial radiotherapy, and suggests 25% recovery of cord tolerance after 6 months¹⁸¹. Assuming an EQD2 of 50Gy was given in the initial treatment, then at 6 months the cumulative Dmax that could be delivered is 62.5Gy. This is a conservative estimate as pre-clinical data in primates and pigs demonstrate that the spinal cord recovers more than 25% of its radiation tolerance. Ang *et al.* treated primates with conventionally fractionated re-irradiation at 1, 2, 3 and 4 years after initial radiotherapy¹⁴⁰. The most conservative model from that dataset (which assumed all the recovery occurred during the 1 year after initial radiotherapy) suggested a 61.8% recovery in cord tolerance. The other models (which assumed some degree of recovery beyond the first year post-radiation) suggested that the cord could have complete recovery by 3 years. Assuming an initial EQD2 of 50Gy, the cumulative Dmax EQD2 using the conservative estimate would be 80.5Gy. Medin *et al.* studied SABR after conventional radiotherapy in using a swine spinal cord model. Initial radiotherapy was 30Gy in 10 fractions (EQD2 37.5Gy) and re-irradiation was performed a year afterwards. They found that a single dose of SABR with Dmax of 16Gy (EQD2 72Gy) and 17.1Gy (EQD2 81.7 Gy) was associated with a 1% and 5% toxicity rate respectively. This suggests a cumulative EQD2 Dmax for 1% toxicity of 109.5Gy.

Although both Medin and Ang treated the cervical or thoracic cord, there may be inter-species differences that limit the applicability of the animal models to human re-irradiation. Nieder et al. produced a risk model for re-irradiation using 48 patients, using the cumulative BED, an interval of less than 6 months, and size of one course less than a BED of 102Gy¹⁷⁶. They report a 3% toxicity rate with a BED of 135Gy₂ (an EQD2 of 67.5Gy) and no toxicity with a BED of 120Gy (EQD2 60Gy). Sahgal *et al.* studied SABR re-irradiation in 19 patients, 5 of whom developed radiation myelopathy¹⁷⁷. The group which developed radiation myelitis had a significantly higher mean cumulative EQD2 Dmax compared to the group that did not (105.8Gy vs 62.3Gy). This work was included in the guidelines for SABR re-irradiation, which suggested a minimum interval of 5 months, and a cumulative EQD2 Dmax of 70Gy to the thecal sac¹⁸³.

The suggested dose constraints from the published papers range between an EQD2 of 62.5 to 70Gy for a <5% toxicity risk with a minimum interval of approximately 6 months. The re-irradiation dose constraints from the expert bodies range from 57Gy (American Radium Society) and 67.5Gy (Hunter *et al.*)^{160,161}. The model prediction from the multivariable model is similar, giving a 1% and 5% risk at 55.34Gy (95% CI 43.39 - 67.30) and 77.42Gy (95% CI 70.10 - 84.74Gy), whereas the individual model is more conservative. A study published after the models were created re-irradiated 32 patients to a median EQD2 Dmax of 80.7Gy (range 61.1 - 95.6Gy) with no toxicity after a 12-month median follow-up²⁰⁹. Patients were counselled about the additional risk of toxicity against the possible benefit of improved local control. This study suggests that the re-irradiation dose constraints may be too conservative. However, the serious and likely permanent implications of myelitis such as paralysis means that a cautious approach with the cumulative cord dose constraint is warranted.

The 18 \geq G3 toxic events that formed the basis of the models are derived from 4 papers. Wong *et al.* reported on 11 patients re-irradiated with conventionally fractionated radiotherapy between 1955 to 1985 to a mean cumulative EQD2 Dmax of 74Gy (range 64 - 86Gy) who developed myelitis¹⁹⁶. This study gives the dose and fractionations for both initial and re-irradiation and used conventional radiotherapy, allowing calculation of the cumulative cord Dmax dose. Gwak *et al.* described three patients who had re-irradiation for chordoma with SABR, one of whom developed paraesthesia 8 months after re-irradiation. The cumulative cord dose was calculated by adding the conventional first treatment EQD2 (assuming either 1.8 or 2Gy were given per fraction) and the quoted re-irradiation cord Dmax (converting that from physical dose to EQD2). This assumed that the first treatment (using conventional radiotherapy) had some part of the cord in the PTV and that there was cord overlap between the two treatments²⁰⁰. Choi *et al.* reported one grade 4 myelitis after conventionally fractionated initial radiotherapy and SABR re-irradiation²⁰¹. This study quotes the cord dose from both treatments and confirmed the overlap of treatments. Sahgal *et al.* also provided thecal sac dose and fractionation for 5 patients who had SABR re-irradiation after conventionally fractionated radiotherapy¹⁷⁷.

There are several sources of error in the studies. There is no uniform toxicity grading used across the four studies, with Gwak *et al.* reporting a patient who had paraesthesia (which may be a grade 3 toxicity if using the LENT-SOMA scale if it was persistent), compared to the patient in Choi *et al.* who clearly developed grade 4 toxicity with urinary retention and paralysis. The dose is reported to the thecal sac in some studies, and the cord in the other studies. This may be of significance as given the high conformality of SABR treatments, the dose to the thecal sac may be higher than to the cord. This could falsely increase the dose that toxicity may occur in the model. The inclusion of SABR re-irradiation studies may introduce a volume factor which is uncontrolled for in the models. Conventionally fractionated radiotherapy is often to a larger volume than SABR. Although the spinal cord is seen as a serial organ, there is an increase in radiation tolerance where the length of cord irradiated is less than 1cm²¹⁰. The length of the cord treated was not recorded in the studies therefore the models do not account for this. The assessment of toxicity for spinal cord depends on the lesion arising in the radiation field and with other causes of myelopathy excluded²¹¹. Some of the studies included in the dataset would not have included MRI or electromyograms to assess any other causes for neural injury. Therefore, there is a risk that myelitis could be due to disease recurrence or another cause. Toxicity may also be due to the initial radiotherapy, rather than caused by the re-irradiation, which was the opinion of Jackson *et al.* who noted a grade 3 myelitis but on review, felt that it was caused by initial treatment rather than re-treatment.

In some of the grouped studies, there were some patients who had re-irradiation to the lumbar spine or cauda equina, which has a different α/B ratio. This could skew the modelling results as using an α/B ratio of 2 when an α/B of 4 is correct would give a lower dose. However, the number of patients with lumbar spine or cauda equina re-irradiation is estimated at 30 out of 604 therefore is unlikely to have a significant effect. In some of the earlier studies, the dose to the cord is assumed from the prescription dose and the beam arrangement as stated. For example, the EQD2 from Grosu *et al.* was calculated by the prescription dose assuming that this was a direct posterior field prescribed to the depth of the spinal cord¹⁹⁰. However, as this was a study of palliative treatment to the

vertebral bodies, the spinal cord may have received a higher dose depending on where the dose was prescribed to.

The multivariable model that best fitted the data featured both the interval and the cumulative cord Dmax. The univariable model of the cumulative Dmax was also very similar. Interestingly, in the multivariable model, the interval between treatments had a positive coefficient (i.e., the longer the interval between the initial radiotherapy and the re-treatment, the higher the risk of toxicity). This is the opposite of what the pre-clinical models predict, as the longer the time interval, the greater the normal tissue recovery. This unusual finding may be due to several issues. The patients who are re-irradiated with a longer interval may have biologically more indolent disease, and therefore may live longer after re-irradiation to experience toxicity. The longer interval may represent the pre-existing clinician bias to offer radiation to patients with a longer interval than those with shorter interval. This would lead to a disparity in the number of patients being retreated within 6-12 months, compared to patients being treated after 12 months, which would result in the difference in observed toxicity. Finally, this could simply be a random finding, as the dataset is subjected to multiple testing at a 5% significance level, meaning that 1 in 20 tests would be positive by chance.

The multivariable model performance by decile has a Pearson correlation coefficient of 0.91, suggesting a good correlation between the observed and predicted values. However, the bootstrapped 95% confidence intervals are extremely wide with the 5% and 1% toxicity rates between 9.46 - 306.64Gy and -23.18 - 156.33Gy respectively. This reflects the significant heterogeneity of the data. The studies used in the dataset are different across many variables such as length of follow up, dose calculation, treatment technique and different centres. For example, the median length of follow up in each study ranged between 5 to 168 months and would have significant ramifications on the detection of toxicity. Furthermore, there are unknown effects which are unable to be corrected for easily. Block bootstrapping takes these effects into account and demonstrates the large degree of uncertainty in the model fits.

The selection of dose constraints is a compromise of accepting a low risk of toxicity, balanced against the need to deliver a high enough dose for tumour

control. Patients that require doses close to the cord constraint will have recurrent disease close to the spinal cord, and therefore may be at risk of cord compression. Therefore, the risk of re-irradiation toxicity has to be balanced against the risk of not treating the patient. The time to toxicity also merits consideration. If untreated, disease close to the spinal cord may cause cord compression sooner than the time taken for re-irradiation toxicity to develop. The median time to radiation myelopathy seen in Wong *et al.* was 11.4 months, while with Saghal *et al.* the earliest toxicity was seen at 3 months post-re-irradiation^{177,196}. Therefore, there may be clinical benefit in exceeding any dose constraint, albeit at increased risk to the patient.

The multivariable model was used to determine a suitable re-treatment dose constraint. The maximum likelihood dose for a 5% toxicity rate (77.42Gy) has a large degree of uncertainty as shown by the 40% toxicity rate at the 95% confidence interval upper limit. The true toxicity rate may be close to 5% but there is insufficient data to narrow the confidence intervals at this dose range. When this dose was restricted to ensure that the risk was less than 5%, the limit of 51.6Gy was too conservative. The exploratory 5% toxicity constraint of 67.3Gy is close to the observed rate of 4.3% seen in doses <67.3Gy, is similar to the expert consensus values and is consistent with the recovery values seen in pre-clinical studies. This dose is a reasonable balance between efficacy and safety, with the proviso that in individual circumstances, it may be appropriate to exceed this.

5.3.3.5 Conclusion

A multivariable model was produced to predict the re-irradiation cord toxicity, using the interval between treatments and the cumulative Dmax. The complete dataset model and the individual dataset model predicts a 5% and 1% toxicity rate at an EQD2 of 77.42Gy and 55.34Gy respectively. The model was a good fit the data with a Pearson correlation coefficient of 0.91. An exploratory 5% toxicity constraint dose of 67.3Gy is similar to the observed rate (4.3%) and is a reasonable balance between efficacy and risk; therefore this is the recommended cord dose constraint.

5.3.4 Models for oesophagus

The dataset for the oesophageal toxicity was derived from 21 papers detailed in Table 5.12 and Table 5.13. The patient data was collected between 1996 and 2017. Two models were created from the dataset, a multivariable model using cumulative oesophageal EQD2 Dmax (cumDmax) and concurrent chemotherapy, and a univariable model using only the cumDmax. The lowest \geq grade 3 toxicity was seen at a cumulative Dmax of 60.4 EQD2 Gy and at an interval of 4 months. Table 5.14 summarises the oesophageal dataset.

There was a large amount missing data: 340 cases had data missing regarding fractional split and 4 regarding the interval. Patients with missing data had a statistically significant higher mean cumDmax compared to the included data (97.1 vs 69.1, t-test p-value <0.001). There was also a higher rate of toxicity in the group with no missing data with 26.1% compared to 1.8% in the missing data group (Chi sq test p-value <0.001). No data imputation was performed and these cases were excluded when modelling those variables.

Table 5.12 List of studies used to form the oesophageal dataset. The total number of patients included is 505, from 21 studies. 3D-CRT: three dimension conformal radiotherapy, BED: biologically equivalent dose, EQD2: equivalent dose in 2 Gray fractions, Fr: fractions, IMPT: intensity modulated proton therapy, IMRT: intensity modulated radiotherapy, NR: not recorded, RBE: relative biological effectiveness, Re-RT: re-irradiation, SABR: stereotactic ablative radiotherapy

Paper	n	Individual data/Grouped	Treatment span	Initial prescription dose/fr	Re-RT prescription dose/fr	Re-treatment Technique
Poltinnikov ²¹²	9	Individual	1999-2003	median 52 (50-66)Gy/assumed 2Gy/fr (estimated)	median 35 (17.5-40)Gy/ median 3.5Gy (3-4) fractions	3D-CRT
Yamaguchi ²¹³	12	Individual	1996-2008	median 60 (50.4-70)Gy/median 30 (28-35) fr	median 39 (30-60)Gy/median 24.5 (15-42) fr	3D-CRT
Kim ²¹⁴	10	Individual	2007-2011	median 50.4 (50.4-63)Gy/median 28 (27-35) fr	median 50.4 (50.4-63)Gy/median 28 (27-35)fr	3D-CRT
Katano ²¹⁵	4	Individual	2011-2016	50.4Gy/28fr for all	median 45 (30-50.4)Gy/median 25 (21-45) fr	3D-CRT
Hong ²¹⁶	39	Grouped	2000-2014	74.11 (48–86.32) Gy BED 10	60 (25.41–84.87) Gy BED 10	IMRT 56.4%, 3D-CRT 43.6%
Zhou ²¹⁷	55	Grouped	2003-2012	mean 61.2Gy/1.8-2Gy per fr	median 54 (18-66)Gy/1.8-2Gy per fr	IMRT or 3D-CRT
Chen ²¹⁸	36	Grouped	1996-2005	median 54 (54-63)Gy/32	50.4Gy/28 fr	IMRT
Kennedy ¹³⁶	21	Grouped	2008-2017	median 54 (50-54)Gy/ median 3 (3-5) fr	median 50 (50-54)Gy/ median 5 (3-5) fr	SABR
Schlammpp ¹²⁷	62	Grouped	2010-2015	median 60 (36-70)Gy/median 32 (13-38) fr (estimated)	median 38.5 (20-60)Gy/median 19 (3-30) fr (estimated)	IMRT
Schroder ²⁰⁸	30	Grouped	2011-2017	NR	NR	SABR
Meijneke ¹⁷⁵	8	Grouped	2005-2021	median 60 (30-60)Gy/median 3 (1-25)fr (whole group)	median 51 (20-60)Gy/median 5 (3-10) fr (whole group)	90% SABR, 10% Conventional

Owen ²¹⁹	18	Grouped	2006-2012	median 60 (39-70)Gy/median 30 (12-35) fr	median 50 (40-60)Gy/ median 4 (3-10) fr	SABR
Kilburn ¹³⁰	33	Grouped	2001-2012	median 60 (22.5-80.5)Gy/median 30 (1-37)fr	median 50 (20-70.2)Gy/median 10 (1-35) fr	SABR in 91%
Sumita ¹²⁴	21	Grouped	2007-2014	EQD2 median 60 (43.1-87.5)Gy (10)	EQD2 median 60 (50-87.5)Gy (10)	Conventional 90%, Proton 10%
Binkley ²²⁰	38	Individual	2008-2014	median 50 (20-74)Gy/median 4.5 (1-37)fr	median 50 (20-177.5)Gy/median 4 (1-54) fr (including multiple re-RT courses)	SABR 73.7%, Conventional 26.3%
Maranzano ²²¹	18	Grouped	2003-2013	40 (16-60)Gy/5 (2-30)fr	40 (25-50)Gy/5 fr	SABR
Ho ¹²⁶	27	Grouped	2011-2016	EQD2 median 60 (36-226.8)Gy	EQD2 median 66 (43.2-84)Gy	Proton (IMPT)
Hong ²²²	31	Grouped	2005-2016	EQD2 median 66 (43.13-125) Gy	EQD2 median 57.2 (36-110)Gy	IMRT 67.7%, SABR 32.3%
Ogawa ²²³	31	Grouped	2004-2017	BED median 112.5 Gy (10) (75-119.6)	BED median 105 Gy (10) (64.2-119.6)	SABR
Griffioen ¹¹⁴	1	Individual	2004-2013	60Gy/30f	60Gy/30f	Conventional
McAvoy ¹²²	1	Individual	2006-2011	63Gy/45fr	39.6(RBE)Gy/22fr	Protons

Table 5.13 List of studies used to form the oesophageal dataset. BED: biologically equivalent dose, cumDmax: maximum dose received to a given organ at risk, Dxcc: maximum dose to an organ at risk to a volume of xcc, EQD2: equivalent dose in 2 Gray fractions, f/u: follow-up, NR: not recorded, oes: Oesophagus, PTV: planning target volume, Re-RT: re-irradiation, RT: radiotherapy.

Paper	Median cumDmax	Interval (months, range)	Chemo % rate with re-RT	Any Grade 3-5 toxicity (%)	F/u post re-RT (months, range)	Uncertainty
Poltinnikov ²¹²	82.2 (66.8-96.3)	13 (2-39)	33.3	0	5.5 (2.5– 30) (f/u to death)	Assumed median dose for first treatment, calculated dose for second treatment, no direct data for cumulative oesophageal dose. Quoted toxicity is acute, so used the EQD2(10) for this effect, and only for 9 patients due to the other 8 not having significant dose to their oes
Yamaguchi ²¹³	93.8 (87.0-98.9)	8.5 (4-162)	100	50	4 (1-108)	54.5% of patients also had hyperthermia with re-irradiation (but paper showed that it had no influence on toxicity so included)
Kim ²¹⁴	98.7 (93.8-111.5)	15.6 (4.8-36.4)	30	30	4.9 (2.6-11.4)	Oes doses not quoted exactly but assumed PTV dose = oes dose (as oesophagus is the target)
Katano ²¹⁵	88.2 (71.9-97.9)	17.4 (6.4-59.2)	83.3	16.7	8.8 (1-30.4)	Oes doses not quoted exactly but assumed PTV dose = oes dose (as oesophagus is the target)
Hong ²¹⁶	112 (80-140)	16 (3--168)	50	7.7	87 (2 -206)	
Zhou ²¹⁷	115.2 (NR)	12 (6-56)	NR	20	20 (8-70)	Oes doses not quoted exactly but assumed PTV dose = oes dose (as oesophagus is the target)
Chen ²¹⁸	99.2 (99.2-107.7)	14.6 (4.5-165)	100	52.8	62 (8-192) (whole group including surgery patients)	Grouped Grade 2-4 toxicity together

Kennedy ¹³⁶	18.7 (4.9--37.2)	23 (7-52)	0	0	24 (3-60)	
Schlamp ¹²⁷	89.9 (NR)	14 (3-103)	3.2	4.8	8.2 (0-27)	Used α/β of 4 for EQD2 calculations
Schroder ²⁰⁸	81.0 (70.2--103.8)	14 (2-184)	0	0	13 (1-45)	Uses a subset of the original 42 patients
Meijneke ¹⁷⁵	85.2 (70.5--123.2)	17 (2-33)	0	0	12 (2-52)	Uses a subset of a larger group
Owen ²¹⁹	62.5 (38.9-78.4)	18.4 (1.5-112.8)	0	0	21.2 (3.4-50.2)	
Kilburn ¹³⁰	69 (11-129)	18 (6-61)	0	3	17 (NR)	
Sumita ¹²⁴	73 (NR)	26.8 (11.4-92.3)	5	0	22.1 (2.3-56.4)	Dose to Oesophagus given as D1cc for initial RT and D10cc for re-RT rather than Dmax
Binkley ²²⁰	44.1 (3.7--220.6)	16 (1-71)	23.7	2.6	17 (3-57)	Quotes EQD2 dose to D1cc therefore Dmax could be higher
Maranzano ²²¹	45 (4-138)	18 (6-90)	0	0	57 (6-132)	
Ho ¹²⁶	84.8 (57.1-121)	29.5 (0.1-212.3)	48	0	11.2 (2.4-48.5)	22/27 has composite doses
Hong ²²²	74.4 (NR)	15.1 (4.4-56.3)	9.7	0	17.4 (4.8-76.8)	
Ogawa ²²³	19.4 (0.8-146.8)	NR	0	0	26 (5.5-111)	
Griffioen ¹¹⁴	120	62	NR	100	6	Quotes dose to D1cc
McAvoy ¹²²	135.7	36	NR	100	29	

Table 5.14 Summary of the oesophageal dataset. Dmax: maximum dose received by an organ at risk.

		Missing values
Number of trials:	21	
Number of patients:	505	
Number of \geq Grade 3 events	49	
Median interval from initial treatment and re-irradiation	15.5 months (1-162)	4
Median concurrent chemotherapy rate	0	0
Median cumulative Dmax (range)	84.8Gy (3.7 - 220.6)	0
Median fractional split	0.53 (0.49 - 0.74)	340

The type of grade 3 or above events are subcategorised in Table 5.15. There were 57 events in total, but when grouped together, this number reduced to 49 as eight patients had both early and late toxicity. The variables were split by their median values. The rate of toxicity was significantly different for the interval, use of concurrent chemotherapy and the cumDmax (Table 5.16). The data was split into 35Gy dose ranges and the relative risk of toxicity increases significantly above the reference range (set at an EQD2 of 35-70Gy, Table 5.17).

Table 5.15 Type of Grade 3 or above toxicity. Gx: grade of toxicity at x level, NR: not recorded

	Number	Acute			Late		
		G3	G4	G5	G3	G4	G5
Yamaguchi ²¹³	12	3	1	0	2	0	1
Kim ²¹⁴	10	0	0	3	0	0	0
McAvoy ¹²²	1	NR	NR	NR	0	1	0
Griffioen ¹¹⁴	1	NR	NR	NR	1	0	0
Kilburn ¹³⁰	1	NR	NR	NR	0	0	1
Binkley ²²⁰	38	NR	NR	NR	1	0	0
Katano ²¹⁵	4	0	0	0	1	0	0
Hong ²¹⁶	39	0	0	0	3	0	0
Zhou ²¹⁷	55	NR	NR	NR	0	0	11
Chen ²¹⁸	36	19	NR	NR	NR	7	NR
Schlamp ¹²⁷	62	NR	NR	NR	1	1	0
Total (%)		22 (38.6)	1 (1.8)	3 (5.3)	9 (15.8)	9 (15.8)	13 (22.8)

Table 5.16 Results of χ^2 and Fisher's exact tests when oesophageal dataset split by median values. cumDmax: cumulative maximum dose to an organ at risk, G3: grade 3

	No \geq G3 toxicity	Any \geq G3 Toxicity (early or late, %)	P-value
Median cumDmax (n=505)			
<84.8	238	2 (0.8)	
>84.8	218	47 (17.7)	
			<0.001*
Median interval (n=505)			
<15.5	209	41 (16.4)	
>15.5	247	8 (3.1)	
			<0.001*
Median concurrent chemotherapy rate (n=505)			
0	245	18 (6.8)	
>0	211	31 (12.8)	
			0.003*
Median fractional split (n=165)			
<0.53	18	21 (53.8)	
>0.53	104	22 (17.5)	
			<0.001*

Table 5.17 Relative risk table for the oesophageal dataset. CI: confidence interval, Gy EQD2: Equivalent dose in 2 Gy fractions, NA: not applicable

Range (Gy, EQD2)	Number	Grade 3+ events	Relative risk	Lower 95% CI	Upper 95% CI	P-value
<35	69	0	0	0	NA	NA
35-70	79	1	1	0.06	15.71	1
70-105	248	28	8.92	1.23	64.51	0.03
105-140	107	20	14.77	2.02	107.73	0.01
>140	2	0	0	0	NA	NA

5.3.4.1 Dose/toxicity oesophageal model

Concurrent chemotherapy and cumDmax were statistically significant on both univariable and multivariable logistic regression modelling (Table 5.18). The univariable cumDmax model was compared to the multivariable model (cumDmax and concurrent chemotherapy) using LOOCV. The log likelihood scores were 265.33 and 274.91 for the univariable model and the multivariable model

respectively, therefore suggesting that the univariable model better described the data.

Table 5.18 Results from univariable and multivariable modelling. cumDmax: cumulative maximum dose to an organ at risk

Predictor	Toxicity	P-value	Number
Univariable modelling results			
Interval	Grade ≥ 3	0.991	501
Chemotherapy	Grade ≥ 3	<0.001*	505
cumDmax	Grade ≥ 3	<0.001*	505
Fractional split	Grade ≥ 3	0.386	165
Multivariable modelling results			
Chemotherapy	Grade ≥ 3	<0.001*	505
cumDmax	Grade ≥ 3	<0.001*	

The univariable model expression is:

$$P(\geq G3 \text{ toxicity} | X_1, X_2) = \Phi(-6.2964 + 0.0446X_1)$$

where X_1 =cumulative Dmax.

The multivariable model expression is:

$$P(\geq G3 \text{ toxicity} | X_1, X_2) = \Phi(-7.0065 + 0.0431X_1 + 2.2065X_2)$$

Where X_1 =cumulative Dmax, X_2 = concurrent chemotherapy. Despite the cumDmax model having a better fit, it is useful to model the effect of chemotherapy on dose and toxicity, as chemotherapy is associated with

oesophageal toxicity²²⁴. Therefore, both models will be used to make predictions.

5.3.4.2 Univariable model predictions

The predicted 5% grade 3 oesophageal toxicity rate was 75.10Gy (95% CI 63.70 - 86.50). The predicted doses for 10%, 20% and 30% are summarised in Table 5.19.

5.3.4.3 Multivariable model predictions

The dose predicted to give a 5% grade 3 or above toxicity rate without chemotherapy is 94.23Gy (95% CI 82.10, 106.37Gy). The block bootstrapped 95% CI is 79.64 to 142.77Gy. The dose prediction for 5% toxicity with chemotherapy is 43.04Gy (95% CI 14.65, 71.44Gy), with a block bootstrapped 95% CI of -18.47 to 108.79. The predicted doses, 95% CI and bootstrapped 95% CI for 10, 20 and 30% toxicity rates are given in Table 5.19. There is a strong effect of chemotherapy with approximately a 40-50Gy reduction in dose for the same toxicity rate. The dose response of the multivariable model without chemotherapy is plotted with in Figure 5.6 and with chemotherapy in Figure 5.7. The chemotherapy rate in the studies in the models are fitted to, and the multivariable model plots with and without chemotherapy are plotted in Figure 5.8. The risk of toxicity increases at earlier doses with the model fit with chemotherapy suggesting a radiosensitising effect to the normal oesophagus with concurrent chemotherapy.

Table 5.19 Summary of multivariable model dose predictions with and without chemotherapy. CI: confidence interval, EQD2 Gy: equivalent dose in 2-Gray fractions, MV: multivariable, UV: univariable

Toxicity rate for \geq G3 toxicity	Model dose prediction (EQD2 Gy)	95% CI lower limit (EQD2 Gy)	95% CI upper limit (EQD2 Gy)	Block bootstrapped 95% CI lower limit (EQD2 Gy)	Block bootstrapped 95% CI upper limit (EQD2 Gy)
UV model					
5%	75.10	63.70	86.50	51.27	97.63
10%	91.84	84.40	99.28	74.05	117.97
20%	110.00	101.91	118.10	93.12	146.88
30%	122.08	110.91	133.25	99.22	168.10
MV model-- without concurrent chemotherapy					
5%	94.23	82.10	106.37	79.64	142.77
10%	111.57	98.86	124.28	96.14	174.44
20%	130.38	112.45	148.32	104.51	212.04

30%	142.89	120.28	165.49	109.64	236.72
MV model-- with concurrent chemotherapy					
5%	43.04	14.65	71.44	-18.47	108.79
10%	60.38	39.02	81.74	14.97	120.61
20%	79.19	64.34	94.05	51.56	135.99
30%	91.70	79.56	103.83	73.72	149.03

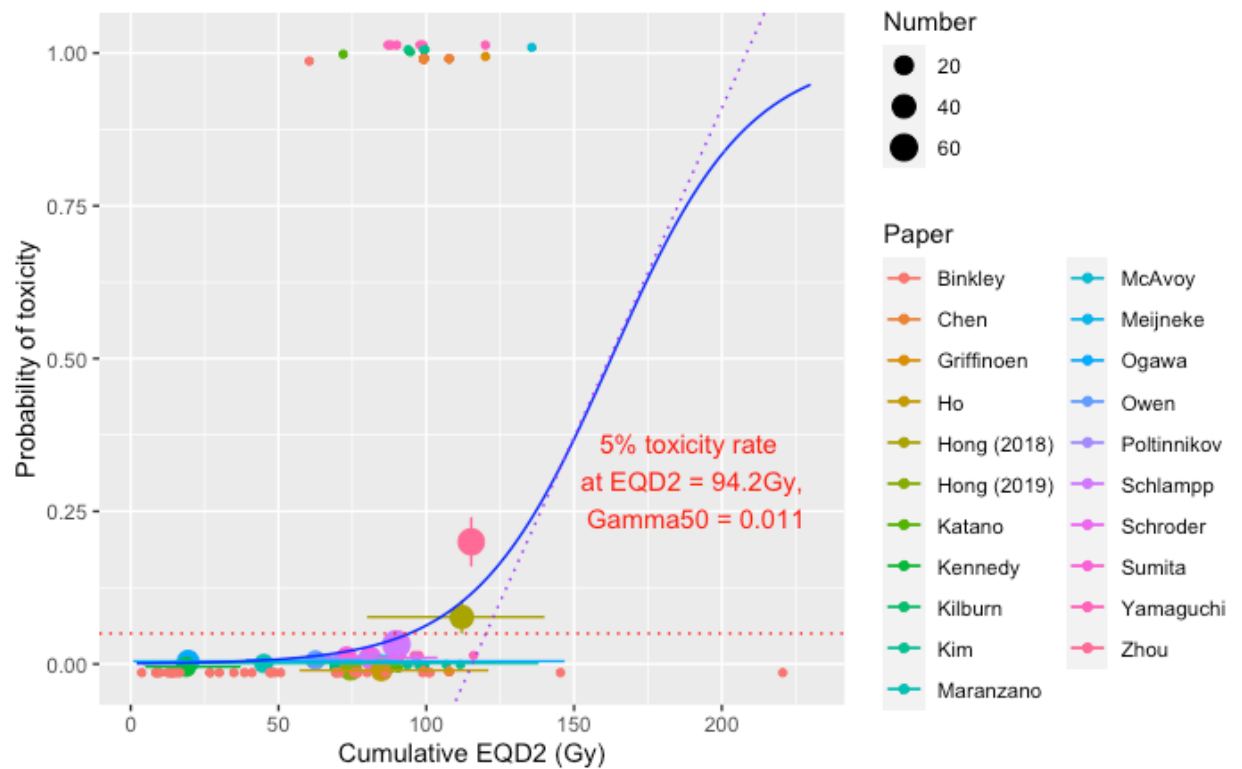


Figure 5.6 Plot of the oesophageal multivariable model without concurrent chemotherapy. The blue line is the fitted regression model, the red dotted line indicates the 5% toxicity level, and the purple dotted line is drawn at the gradient at 50% probability of toxicity (the Gamma or γ_{50} value). The dots represent the toxicity rate from each individual paper coded by colour, with the size of the dots proportional to the number of patients in the study, vertical bars are the 68% binomial confidence interval, horizontal bars represent the range of the doses where given. Due to overlapping data points, the scatter plot has been jittered. This model plot did not use concurrent chemotherapy.

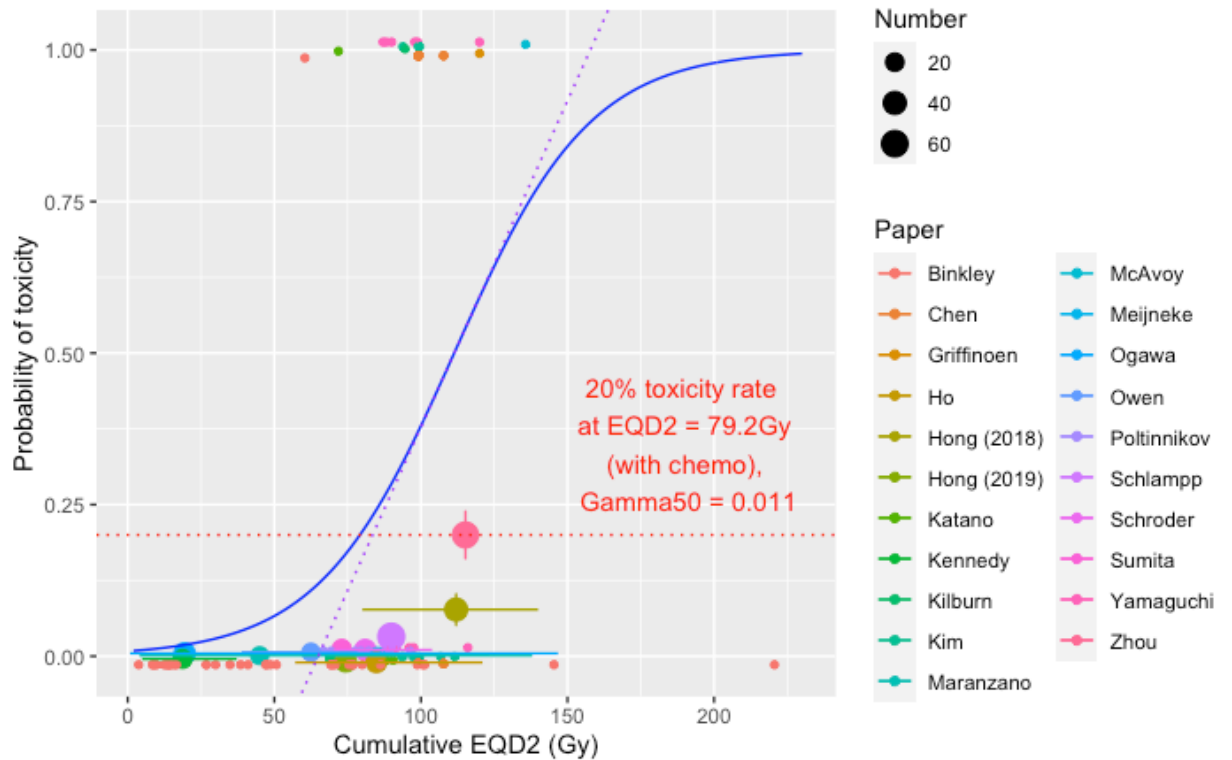


Figure 5.7 Plot of the oesophageal multivariable model with concurrent chemotherapy. The blue line is the fitted regression model, the red dotted line indicates the 20% toxicity level and the purple dotted line is drawn at the gradient at 50% probability of toxicity (the Gamma50 or γ_{50} value). The dots represent the toxicity rate from each paper coded by colour, with the size of the dots proportional to the number of patients in the study, vertical bars are the 68% binomial confidence interval, horizontal bars represent the range of the doses, due to overlapping data points, the scatter plot has been jittered. This model plot uses concurrent chemotherapy.

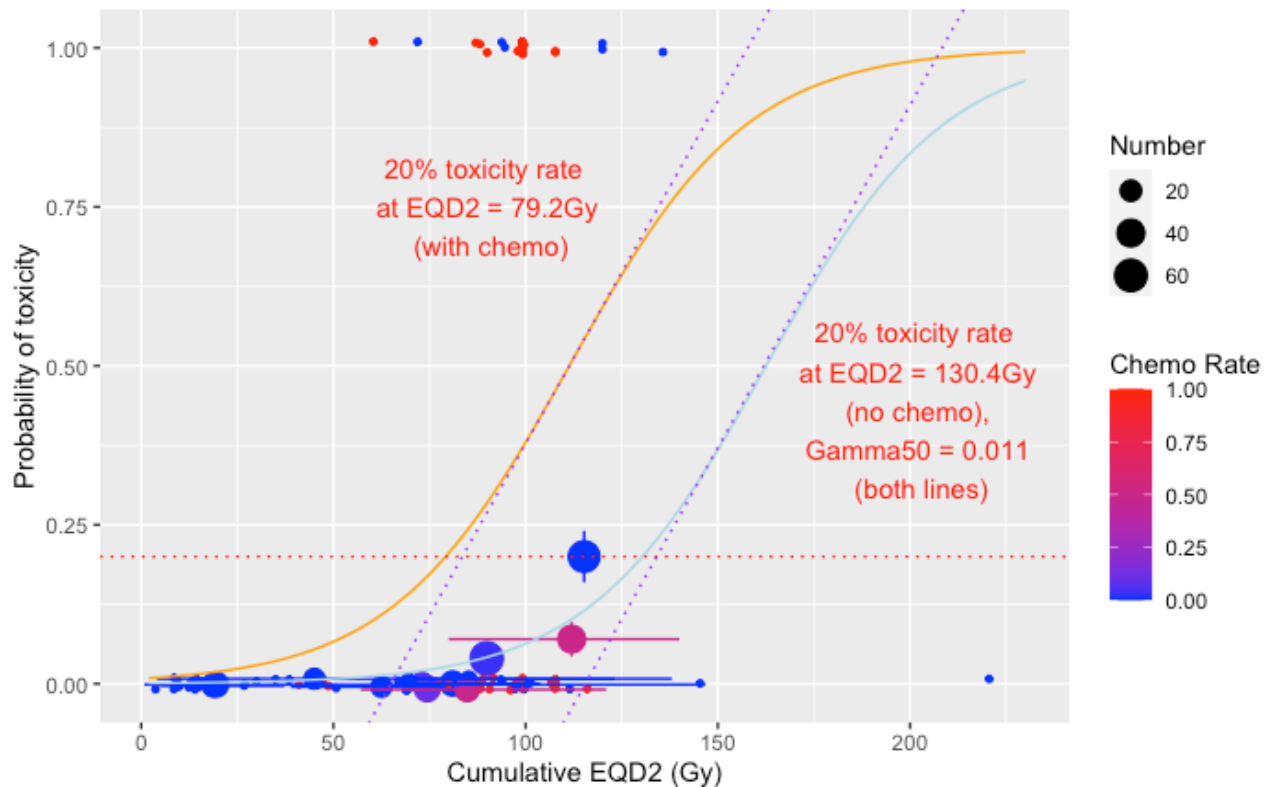


Figure 5.8 Plot of the oesophageal multivariable models with and without concurrent chemotherapy. The orange line is the fitted regression model with chemotherapy, the light blue line is the fitted regression model without chemotherapy, the red dotted line indicates the 20% toxicity level and the purple dotted lines are drawn at the gradient at 50% probability of toxicity (the Gamma50 or γ_{50} value). The dots represent the toxicity rate from each paper (labelled), with the size of the dots proportional to the number of patients in the study, vertical bars are the 68% binomial confidence interval, horizontal bars represent the range of the doses. The chemotherapy rate for each study is represented on a blue/red scale, with red indicating 100% rate of concurrent chemotherapy, and blue representing a 0% rate. Due to overlapping data points, the scatter plot has been jittered.

5.3.4.4 Development of oesophageal constraint values

The multivariable model estimated dose that gives a 5% rate of toxicity with no chemotherapy is 94.23Gy. When this dose is used to calculate the risk using the 2000 block bootstrapped samples, the 95% CI for risk is 1.2% to 9.5%. Reducing the dose to 78.81Gy, gives a 95% CI for risk of 0.6% to 5%. The same process was used to develop bootstrapped dose constraints for the multivariable model with chemotherapy (for a 5% and 20% toxicity rate). The results are summarized in Table 5.20.

Table 5.20 Development of oesophageal dose constraints using bootstrapping. CI: confidence interval, EQD2 Gy: equivalent dose in 2 Gray fractions

Model	Model dose (EQD2 Gy)	Risk	95% CI lower limit risk (%)	95% CI upper limit risk (%)
Multivariable (no chemo)	94.23	5%	1.2	9.5
	78.81	Maximum 5%	0.6	5
Multivariable (with chemo)	43.04	5%	0.02	16.7
	-16.1	Maximum 5%	<0.01	5
Multivariable (with chemo)	79.19	20%	0.6	32.6
	52.25	Maximum 20%	0.05	20

5.3.4.5 Validation of the multivariable oesophageal model

To evaluate the multivariable model, the dataset the model was developed on (i.e. excluding data points that were missing concurrent chemotherapy data) was split into deciles by the modelled risk of toxicity. The cases were not grouped into pre-specified risk bands. The actual and model predicted rate of toxicity was calculated for each decile. For example, the modelled toxicity risk in the 15 cases that made up the first decile was between 0.1 and 0.2%, with no observed toxicity events. The multivariable model had a Pearson correlation coefficient of 0.75 ($p=0.013$) suggesting a good correlation between the model predictions and the actual rate of toxicity by decile. This was plotted in Figure 5.9. This demonstrates a close correlation between the predicted and observed toxicity deciles up to the 20% toxicity rate. Above this, the confidence intervals become wider suggesting a less good fit to the data.

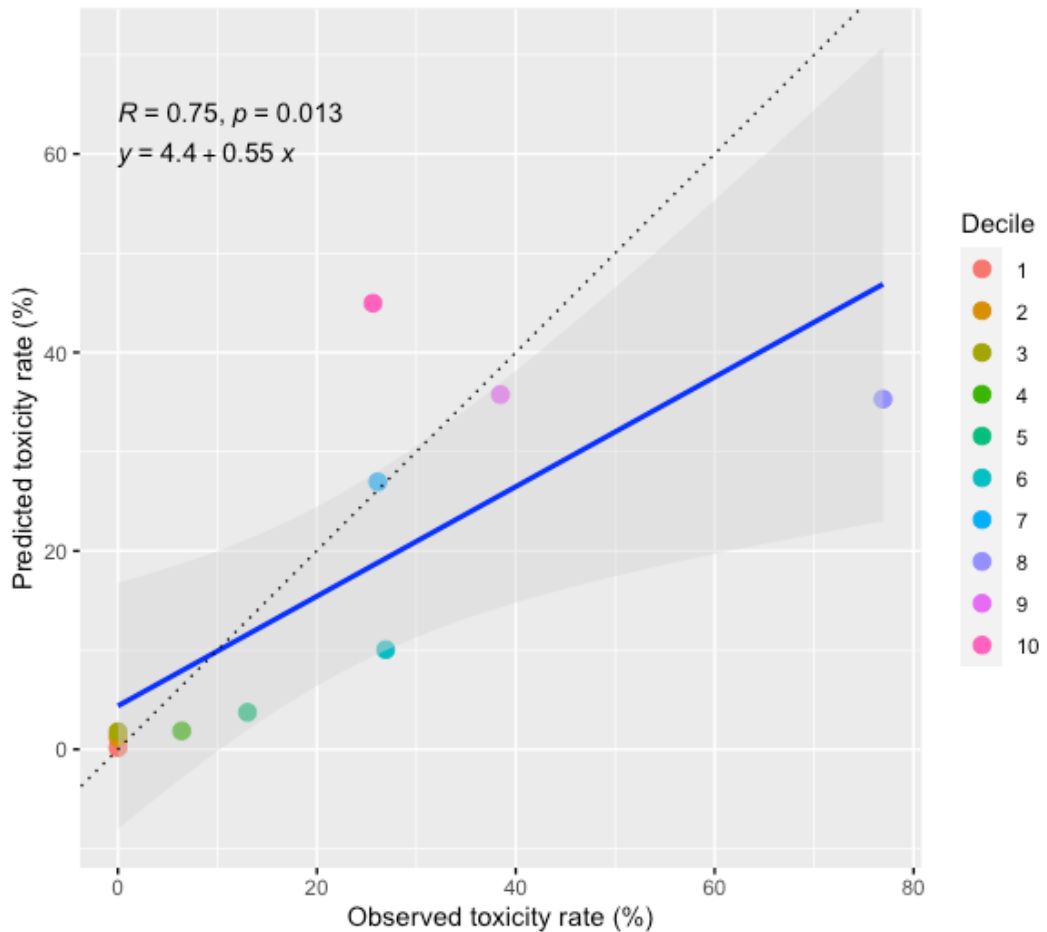


Figure 5.9 Plot of the actual and predicted oesophageal multivariable model toxicity rates. The blue line is the line of best fit, with the shaded grey area the 95% confidence interval. The black dotted line represents the line of unity. The dots represent the toxicity rate from each decile.

There were no oesophageal toxicities in the Beatson dataset so application of putative dose constraints was not performed. Therefore, a subset of the whole dataset that had individual patient level data was used to validate possible constraints. The chosen doses were the maximum 5% dose (78.8Gy) and the maximum-likelihood dose (94.2Gy) for the multivariable models. The predicted 5% toxicity rate was exceeded using the 94.2Gy cut off (albeit by 2%), but was met by the 78.8Gy limit (Table 5.21). Both the toxicity rate and the rate of chemotherapy were much higher in the patients treated above the putative constraints, with a rate of toxicity of 40.3% above 78.8Gy. It is difficult to separate how much of the increased toxicity is due to the concurrent chemotherapy and how much is due to the increased dose. It seems reasonable to use 94.2Gy (without chemo) as a dose constraint for several reasons. Firstly, 78.8Gy is too low a cumulative dose to facilitate radical re-irradiation doses.

There is a relatively small 4% increase in toxicity with the higher dose constraint with the observed values, which may be due to random variation. Finally, the upper 95% bootstrapped confidence interval is 9.5%, indicating that the true toxicity rate is likely to be within an acceptable range.

The multivariable model predicted a significant increase in toxicity where concurrent chemotherapy was used. Therefore, it may be prudent to limit the use of concurrent chemotherapy in the re-irradiation setting to patients who had a low oesophageal dose at initial radiotherapy, where the cumulative Dmax to the oesophagus is less than 43Gy EQD2.

Table 5.21 Testing multivariable model constraints on individual data. Gy: Gray, MV: multivariable model

	Number with no toxicity	Number with toxicity	Observed Toxicity rate (%)	Concurrent chemo rate (%)
Source of cut-off: MV model max 5% toxicity (no chemotherapy)				
<78.8 Gy	65	2	3.0	7.5
≥78.8 Gy	46	31	40.3	74.0
Source of cut-off: MV model max-likelihood 5% toxicity (no chemotherapy)				
<94.2	80	6	7.0	19.8
≥94.2	31	27	46.6	77.6

5.3.4.6 Oesophageal models discussion

The multivariable model predicts a 5% risk of toxicity with no chemotherapy at a cumDmax EQD2 of 94.2Gy (95% CI 82.10, 106.37Gy). This analysis demonstrated a large risk increase with concurrent chemotherapy, where if given, the 20% and 30% toxicity rates with chemotherapy were predicted at 79.2 and 91.7Gy respectively, doses that could be reasonably given in a clinical situation. The model predictions (when split by decile) have a strong correlation (R=0.75) with the corresponding actual toxicity rate.

Of the variables assessed, the cumulative dose and the use of concurrent chemotherapy were significant factors. Interestingly, the model that has the best fit to the data was the univariable model with the cumulative dose, suggesting that chemotherapy did not improve the model fit. However, there is

significant clinical data that chemotherapy does affect toxicity rates, and is a relevant clinical question, as chemotherapy may have a role in recurrent disease to radiosensitise tumours. Therefore, the multivariable model was chosen for further analysis to assess the toxicity rates with and without chemo. In the multivariable model, chemotherapy reduces the dose at which toxicity occurs is unsurprising given that concurrent chemotherapy are radiosensitisers. The magnitude of change is useful to know, as it allows for better counselling of patients and stricter planning constraints. Ultimately, patients would have been given concurrent chemotherapy for central nodal disease, therefore it would be very difficult to spare the oesophagus due to the likely proximity to the disease.

There are no pre-clinical models assessing oesophageal re-irradiation, and the existing re-irradiation dose constraints suggest a cumDmax EQD2 range between 75Gy and 110Gy^{161,174}. Using 110Gy as the modelled dose (without concurrent chemotherapy) predicts a \geq G3 toxicity rate of 9.4% (95% CI 5.7, 15.1%) implying that treating at 110Gy will be high risk. Even exceeding 105Gy using the cruder relative risk table is associated with a 14.8 times increased risk of toxicity (95% CI 2.0 - 107.8, p-value=0.01) compared to a cumDmax between 35-70Gy. However, the largest distance between the predicted and actual values in Figure 5.9 is when the predicted toxicity rate is above 20%, suggesting that the model is less accurate beyond this. Nevertheless, the models and the data would support a more conservative cumulative oesophageal dose constraint than the highest current expert opinion of 110Gy EQD2.

The toxicity which was modelled in the models are derived from 10 studies. Six studies presented data from re-irradiation of recurrent oesophageal cancer²¹³⁻²¹⁸. These studies accounted for 43 (87.8%) of the toxicities in the model. The use of concurrent chemotherapy was common in these patients (median rate 66%, range 0 - 100%). The techniques used were 3D-conformal therapy in three studies, either 3D-CRT or IMRT in two studies and exclusively IMRT in one study. The other four studies were retrospective reviews of re-irradiation in NSCLC which quoted oesophageal dose and toxicity^{114,122,127,220}. The lung studies accounted for 6 \geq G3 events. The re-irradiation treatment technique was IMRT in two studies, SABR and passive scatter proton therapy in one study each. The

concurrent chemotherapy rate was similar to the oesophageal re-treatment group (median 65.8%, range 24-100%).

The difference in the tumour type re-irradiated is likely to significantly affect the model predictions. Re-irradiation of the oesophagus is likely to involve a longer part of the oesophagus and to a higher dose compared to the lung re-irradiation plans where the dose and treated oesophageal volume will be minimised. In support of this, Yamaguchi *et al.* quoted a median field area of 29cm² (range 21-40cm²) for oesophageal re-irradiation, and Schlampp *et al.* gave a median length of oesophagus at lung re-irradiation of 1cm (range 0-17cm). The presence of an oesophageal tumour may also predispose patients to fistulate or perforate, making re-irradiation toxicity harder to accurately discern. Unfortunately, the volume of oesophagus irradiated was rarely quoted in the other studies. This means that the volume of oesophagus, which is likely to be an important factor in toxicity, was unable to be modelled.

When the bootstrapped toxicity rate was limited to 5% (with no toxicity), the multivariable model predicted a maximum 5% toxicity rate at approximately 78.8Gy, which was similar to the observed rate in the individual dataset (3.0%). In addition, the external Beatson cohort (where there was no concurrent chemotherapy) had 6 patients who exceeded this cut-off and had no toxicity. Only three patients exceeded the max-likelihood cut off of 94.2Gy and also had no toxicity. The low numbers in this cohort limit how much can be concluded from this. Given the uncertainty about the role of the oesophageal volume and the role of concurrent chemotherapy, both the maximum-likelihood and the maximum 5% dose constraints may be conservative when applied to re-irradiation of lung recurrences. This may be due to the volume of oesophagus involved is likely to be less compared to the data the models were built on, and the models are most representative of re-irradiation where a longer length of the oesophagus is irradiated.

However, the gradient of the plotted curves for both models between 5% and 10% are shallow (with the multivariable model predicting 5 and 10% toxicity at 94.2 and 111.6Gy respectively). Therefore, exceeding the dose constraints will have a small increase in risk which may be acceptable to clinicians and patients when weighed against the risk of progressive disease.

The dataset has other sources of inaccuracy. Several studies quote dose to 1cc (D1cc) rather than cumulative Dmax. The effect of this would be to underestimate the delivered Dmax. In addition, one study combined hyperthermia with re-irradiation²¹³. The data from this study were included as the study authors found that hyperthermia had no influence on toxicity. Another study grouped Grade 2-4 toxicity together, therefore a small number of toxic events may be grade 2 rather than \geq G3 events²¹⁸. In some studies, the actual oesophageal dose was not quoted^{214,215,217}. As these studies were relating to oesophageal retreatment, it was assumed that the oesophageal Dmax is equivalent to the PTV dose. This may underestimate the dose as there may be dosimetric hot-spots in the PTV which could make the cumDmax higher than the prescription dose. The grouping of early and late toxicity can be misleading. Early grade 3 oesophageal toxicity (oesophagitis) is likely to recover (although is severe enough to warrant hospitalisation), whereas late oesophageal toxicity (stricture, fistula, perforation) is likely to be permanent. This was done to ensure that any serious toxicity was included in the model and to ensure large enough events for the modelling to be statistically valid. To compensate for the different outcomes, where early toxicity was quoted, the EQD2 was calculated using an α/β of 10 to ensure that the dose and biological effect are congruent. Early Grade 3 toxicity represented 38.5% of the toxicity in the dataset, with early or late grade 4 and 5 toxicity with 45.6% , therefore the model should be viewed as more representative of higher grade toxicity.

The evaluation of the model fit shows a high correlation when using the rate of toxicity when split by deciles. This was calculated by grouping the predicted and the actual toxicity rate together. This method therefore does not accurately assess each individual data points' accuracy. This approach was used because some data points are derived from cohorted study data, and the number of patients in each cohort was generally small, and in some cases, was only one patient. The low numbers involved would result in the binomial variance of the observed rate for each cohort being very large. This would create significant uncertainty around each data point. By grouping the observed data into deciles, this reduces the uncertainty inherent in a cohort-by-cohort analysis with low numbers and allows for an evaluation of model performance.

In summary, the bootstrapped maximum-likelihood 5% toxicity risk dose from the multivariable model is 94.2Gy without chemotherapy. The maximum-likelihood constraint was chosen over the maximum 5% dose limit as this dose constraint was probably too cautious and allows the clinician to give 15Gy more dose at re-irradiation with little increase in risk. The model is largely based on oesophageal retreatments and therefore assume a large volume of oesophagus is re-irradiated. Therefore, these predictions may be too cautious when applied to re-irradiation for lung cancer where the oesophageal volume may be less.

5.3.4.7 Conclusions

Multivariable dose toxicity models were derived from the oesophageal re-irradiation dataset. The use of concurrent chemotherapy increases the likelihood of \geq G3 toxicity using the multivariable model. The bootstrapped dose constraints for the multivariable model (no chemotherapy) suggested a maximum-likelihood 5% toxicity rate at 94.2Gy.

5.3.5 Models for lung

Lung dose/toxicity models were created using a dataset from 15 studies summarised in Table 5.22 and Table 5.23. The data was collected between 2005 and 2021. The lowest median values where \geq Grade 3 toxicities were seen were cumulative MLD (cumMLD) of 11.5Gy, cumulative V5 (cumV5) of 28.9% and cumulative V20 (cumV20) of 13.2%. These were the cumulative doses quoted in the studies; no modifications were made when transcribing the cumulative doses into the database.

There were missing data in each potential lung predictor variable. There were 71 missing cases in the cumMLD data from a total of 476 patients. There was no significant difference in the rate of toxicity in the missing cumMLD data group (2/71 events in the missing data, 35/405 events in the no missing cumMLD group, Fisher's exact p-value 0.145).

There were 215 cases with no cumV5 data, and there was a significantly lower rate of toxicity in the missing cumV5 group than the group which reported

cumV5 (5/215 event in the missing data, 32/261 in the cumV5 reported group, Fisher's exact p-value <0.001). There were 93 cases with no cumV20 data and 383 with cumV20 data, but there was no significant difference in the rate of toxicity between those groups (3/93 events in the missing data, 34/383 in the no missing data group, Fisher's exact p-value 0.083).

For all cases with missing data, no data imputation was performed, and when modelling using those variables, those cases with missing data were excluded from the analysis.

Table 5.22 List of studies used to form the lung dataset. The total number of patients included is 476, from 15 studies. EQD2: equivalent dose in 2 Gray fractions, est: estimated, Fr: fractions, IMPT: intensity modulated proton therapy, IMRT: intensity modulated radiotherapy, NR: not recorded, RBE: relative biological effectiveness, Re-RT: re-irradiation, SABR: stereotactic ablative radiotherapy

Paper	n	Individual data/Grouped	Treatment span	Median initial prescription dose/fr	Median re-RT prescription dose/fr	Re-treatment Technique
Meijneke ¹⁷⁵	20	Grouped	2005-2021	60 (30-60)Gy/3 (1-25)fr	51 (20-60)Gy/5 (3-10) fr	90% SABR, 10% Conventional
McAvoy ¹²²	33	Grouped	2006-2011	63 (40-74)Gy/ 33 (4-59)fr	66 (16.4-75)Gy RBE/32 (9-58) fr	Proton (passive scatter)
Owen ²¹⁹	18	Grouped	2006-2012	60 (39-70)Gy/30 (12-35) fr	50 (40-60)Gy/4 (3-10) fr	SABR
Kilburn ¹³⁰	33	Grouped	2001-2012	60 (22.5-80.5)Gy/30 (1-37)fr	50 (20-70.2)Gy/ 10 (1-35) fr	SABR in 91%
Sumita ¹²⁴	21	Grouped	2007-2014	EQD2 60 (43.--87.5)Gy (10)	EQD2 60 (50-87.5)Gy (10)	Conventional 90%, Proton 10%
Binkley ²²⁰	38	Individual	2008-2014	50 (20-74)Gy/4.5 (1-37)fr	50 (20-177.5)Gy/ 4 (1-54) fr (including multiple re-RT courses)	SABR 73.7%, Conventional 26.3%
Karube ²²⁵	29	Individual	2007-2014	46 (34-61.2)Gy RBE/1 (1-9)fr	60 (54-72)Gy/12 (12) fr	Carbon ion
Ren ¹⁴⁷	67	Grouped	2010-2017	EQD2 56 (3--260)Gy (10)	EQD2 54 (14-240)Gy (10)	Conv IMRT 89.6%, SABR 10.4%
Ho ¹²⁶	27	Grouped	2011-2016	EQD2 60 (36-226.8)Gy	EQD2 66 (43.2-84)Gy	Proton (IMPT)
Hong ²²²	31	Grouped	2005-2016	EQD2 66 (43.13-125) Gy	EQD2 57.2 (36-110)Gy	IMRT 67.7%, SABR 32.3%
Kennedy ¹³⁶	21	Grouped	2008-2017	54 (50-54)Gy/ 3 (3-5) fr	50 (50-54)Gy/5 (3-5) fr	SABR
Ricco ¹⁶⁸	44	Grouped	2012-2017	54 (45-70.2)Gy/3 (NR) fr	50 (39-54)Gy/4 (NR) fr	SABR
Schlampp ¹²⁷	62	Grouped	2010-2015	60 (36-70)Gy/32 (13-38) fr (est)	38.5 (20-60)Gy/19 (3-30) fr (est)	IMRT
Schroder ²⁰⁸	30	Grouped	2011-2017	NR	NR	SABR
Yang ¹²⁸	2	Individual	2009-2017	NR	NR	IMRT

Table 5.23 List of studies used to form the lung dataset. cumMLD: cumulative mean lung dose, cumVx: cumulative volume receiving at least x Gray, f/u: follow-up, NR: not recorded, Re-RT: re-irradiation

Paper	cumMLD	cumV5	cumV20	Interval (months, range)	Chemo % rate with re-RT	Any Grade 3-5 toxicity (%)	F/u post re-RT (months, range)	Uncertainty
Meijneke ¹⁷⁵	15 (4.2-27.6)	41 (8-72)	15 (3-47)	17 (2-33)	0	0	12 (2-52)	
McAvoy ¹²²	17.8 (6.94-37.4)	45 (23-81)	24 (12-65)	36 (2-376)	24	15.2	11 (1.4-32.4)	
Owen ²¹⁹	17.8 (6-26.6)	62.4	29.6	18.4 (1.5-112.8)	0	0	21.2 (3.4-50.2)	
Kilburn ¹³⁰	NR	NR	26 (5-40)	18 (6-61)	0	6.1	17 (NR)	
Sumita ¹²⁴	12	30	17	26.8 (11.4-92.3)	5	4.8	22.1 (2.3-56.4)	
Binkley ²²⁰	NR	NR	15.6 (3.8-38.4)	16 (1-71)	31.6	0	17 (3-57)	
Karube ²²⁵	7.3 (2.6 - 14)	15.1 (7.4-27.6)	9.8 (4.1-19.7)	20 (8-99)	0	0	29 (4-88)	
Ren ¹⁴⁷	17.3 (NR)	68.1 (NR)	28 (NR)	16 (2-96)	28.4	26.9	9 (4-76)	
Ho ¹²⁶	14.5 (7-22.5)	48.9 (0.4-71.7)	23.8 (0-36.7)	29.5 (0.1-212.3)	48	7.4	11.2 (2.4-48.5)	Composite plans were available for only 1 of the 2 patients who had grade 3 toxicity

Hong ²²²	9.77 (NR)	NR	NR	15.1 (4.4-56.3)	61.3	0	17.4 (4.8-76.8)	
Kennedy ¹³⁶	5.5 (3-9)	NR	12 (6.4-16.5)	23 (7-52)	0	0	24 (3-60)	
Ricco ¹⁶⁸	11.5 (4.55-26.52)	37.45 (14.2-78)	13.2 (3.8-46.1)	7 (NR)	0	4.5	24 (4-84)	Multiple courses to the lung (30 had only 2, 14 had 3 or more)
Schlapp ¹²⁷	19 (8.1-33)	NR	NR	14 (3-103)	0	4.8	8.2 (0-27)	
Schroder ²⁰⁸	11.1 (3.3-17.9)	NR	14.9 (2.7-36.7)	14 (2-184)	0	0	13 (1-45)	Uses a subset of the original 42 patients
Yang ¹²⁸	19.9--23.2	28.9-93.4	28.8-38.2	NR	0	100	NR	Uses a subset of 50 patients which give the cumulative doses

There were 476 patients included in the dataset with 37 \geq G3 toxic events (Table 5.24). There was a significant difference in the rate of toxicity when the cumMLD, cumV5, cumV20 and concurrent chemotherapy rate were split by their median values (Table 5.25) with higher toxicity rates seen in the group that exceeded the median values.

Table 5.24 Summary of lung dataset. MLD: mean lung dose, Vx: volume of lung receiving at least x Gray

		Missing values
Number of trials:	15	
Number of patients:	476	
Number of \geq Grade 3 events	37	
Median interval from initial treatment and re-irradiation	16 months (1-71)	4
Use of concurrent chemotherapy	66/476 (13.9%)	0
Median MLD (range)	14.5Gy (5.5 - 23.2)	71
Median V5 (range)	45% (15.1 - 93.4)	215
Median V20 (range)	17.6% (3.8 - 38.4)	93

Table 5.25 Results of χ^2 and Fisher's exact tests when lung dataset split by median values. cumMLD: cumulative mean lung dose, cumVx: cumulative volume receiving at least x Gray, G3: grade 3

	No toxicity	\geq G3 Toxicity (% rate)	p-value
Median cumMLD (Gy, n=405)			
\leq 14.5	198	5 (2.5)	
$>$ 14.5	172	30 (14.9)	
			$<0.001^*$
Median cumV5 (% , n=261)			
\leq 45%	137	11 (7.4)	
$>$ 45%	92	21 (18.5)	
			0.011*
Median cumV20 (% , n=383)			
\leq 17.6	189	3 (1.6)	
$>$ 17.6	160	31 (16.2)	
			$<0.001^*$
Median interval (months, n=472)			
\leq 16	228	25 (10.0)	
$>$ 16	207	12 (5.5)	
			0.109

Median concurrent chemotherapy rate (%; n=476)			
0	282	9 (3.1)	
>0	157	28 (15.1)	
			<0.001*

The lung metrics (cumMLD, cumV5, cumV20) interval and concurrent chemotherapy had p-values of <0.2 on univariable logistic regression but all were non-significant on multivariable modelling. Concurrent chemotherapy was significant on univariable logistic regression (Table 5.26) and was combined with each lung metric to form multivariable models. The lung metrics all had p-values <0.001 and therefore were all combined into a multivariable model; none of the predictors were significant. The lung metrics were combined to form two variable models (cumMLD/cumV5, cumMLD/cumV20 and cumV5/cumV20). Only cumMLD was significant in these models. Subsequently, the lung metrics were combined individually with concurrent chemotherapy to form two-variable multivariable models. The cumMLD/concurrent chemotherapy model was significant, but concurrent chemotherapy was not significant when paired with cumV5 and cumV20, albeit with p-values <0.2.

Table 5.26 Summary of lung dataset univariable and multivariable modelling. cumMLD: cumulative mean lung dose, cumVx: cumulative volume receiving at least x Gray

Predictor	Toxicity	P-value	Number
Univariable modelling results			
cumMLD	Grade ≥ 3	<0.001*	405
cumV5	Grade ≥ 3	<0.001*	261
cumV20	Grade ≥ 3	<0.001*	383
Interval	Grade ≥ 3	0.181	472
Chemotherapy	Grade ≥ 3	0.037*	476
Multivariable modelling results			
cumMLD	Grade ≥ 3	0.073	261
cumV5	Grade ≥ 3	0.480	
cumV20	Grade ≥ 3	0.870	
Interval	Grade ≥ 3	0.314	
Chemotherapy	Grade ≥ 3	0.104	
Multivariable combinations			
cumMLD	Grade ≥ 3	0.046*	261
cumV5	Grade ≥ 3	0.623	
cumV20	Grade ≥ 3	0.739	
Chemotherapy	Grade ≥ 3	0.139	
Multivariable combinations with chemotherapy			
<i>MLD/Chemo</i>			

cumMLD	Grade ≥ 3	<0.001*	405
Chemotherapy	Grade ≥ 3	0.002*	
<i>V5/Chemotherapy</i>			
cumV5	Grade ≥ 3	0.002*	261
Chemotherapy	Grade ≥ 3	0.177	
<i>V20/Chemotherapy</i>			
cumV20	Grade ≥ 3	<0.001*	383
Chemotherapy	Grade ≥ 3	0.128	
Multivariable combinations with lung indices			
MLD/V5/V20			
cumMLD	Grade ≥ 3	0.093	261
cumV5	Grade ≥ 3	0.697	
cumV20	Grade ≥ 3	0.894	
MLD/V5			
cumMLD	Grade ≥ 3	0.010*	261
cumV5	Grade ≥ 3	0.450	
MLD/V20			
cumMLD	Grade ≥ 3	0.045*	312
cumV20	Grade ≥ 3	0.546	
V5/V20			
cumV5	Grade ≥ 3	0.997	261
cumV20	Grade ≥ 3	0.055	

The univariable models for cumMLD, cumV5 and cumV20 were compared against the following multivariable models (cumMLD/chemo, cumV5/chemo and cumV20/chemo) using leave one out cross validation to identify the model with the best fit to the data. The cumMLD/chemo, the univariable cumV5 and cumV20 models had a better fit to the data (see Table 5.27) and were further assessed to find putative dose constraints.

Table 5.27 Leave one out cross validation values for univariable and multivariable chemotherapy models. cumMLD: cumulative mean lung dose, cumVx: cumulative volume receiving at least x Gray, LOOCV: leave one out cross validation

	LOOCV value
MLD models	
cumMLD	124.31
cumMLD/chemo	121.61
cumV5 models	
cumV5	92.44
cumV5/chemo	102.30
cumV20 models	
cumV20	106.31
cumV20/chemo	107.00

5.3.5.1 Cumulative MLD model

The relative risk of toxicity was divided into 3Gy subgroups between a cumMLD of 10 and 19Gy, with the reference category 10-13Gy. There was a significant increase in relative risk between a cumMLD of 16-19Gy (Table 5.28).

Table 5.28 Relative risk table for the cumulative mean lung dose dataset. CI: confidence interval, NA: not applicable.

Range	Number	Grade 3+ events	Relative risk	Lower 95% CI	Upper 95% CI	P-value
<10	81	0	NA	NA	NA	NA
10-13	95	3	1	0.21	4.83	1
13-16	47	2	1.35	0.23	7.79	0.75
16-19	118	25	6.71	2.09	21.55	<0.01
>19	64	5	2.47	0.61	9.99	0.20

The multivariable model expression is:

$$P(\geq G3 \text{ toxicity} | X) = \Phi(-9.9872 + 0.4218X_1 + 4.3753X_2)$$

Where X_1 =cumulative MLD and X_2 =concurrent chemotherapy rate. This model is plotted in Figure 5.10. The 20% toxicity rate with chemotherapy is predicted at a cumMLD of 10.02Gy (95% CI 8.45, 11.58Gy). The 20% toxicity rate without chemotherapy is predicted at a cumMLD of 20.39Gy (95% CI 18.83, 21.95). The 10% and 30% toxicity rates without chemotherapy are 18.47Gy (95% CI 17.06, 19.87) and 21.67Gy (95% CI 19.71, 23.63) respectively. The 95% confidence interval for cumulative MLD that gives 20% toxicity rate using 2000 block bootstrapped samples with and without chemotherapy are -36.23, 32.74Gy and 15.90, 34.68 respectively.

The multivariable model unexpectedly found that concurrent chemotherapy was a significant factor, whereas it was not significant with the other lung metrics. The addition of concurrent chemotherapy in a large meta-analysis did not increase the incidence of pneumonitis, therefore the most likely cause of lung toxicity is the mean lung dose⁵⁷. To better explore this, the univariable cumulative mean lung dose was also assessed.

The univariable cumulative MLD model expression is:

$$P(\geq G3 \text{ toxicity} | X) = \Phi(-9.9872 + 0.4218X_1)$$

Where X_1 =cumulative MLD. This model is plotted in Figure 5.11. The 20% toxicity rate at a cumMLD of 19.26Gy (95% CI 17.56, 20.96Gy). The 10% and 30% toxicity rates are 16.31Gy (95% CI 14.98, 17.65) and 21.21Gy (95% CI 18.79, 23.64) respectively. The 95% confidence interval for cumulative MLD that gives a 20% toxicity rate using 2000 block bootstrapped samples are 16.60, 29.41Gy.

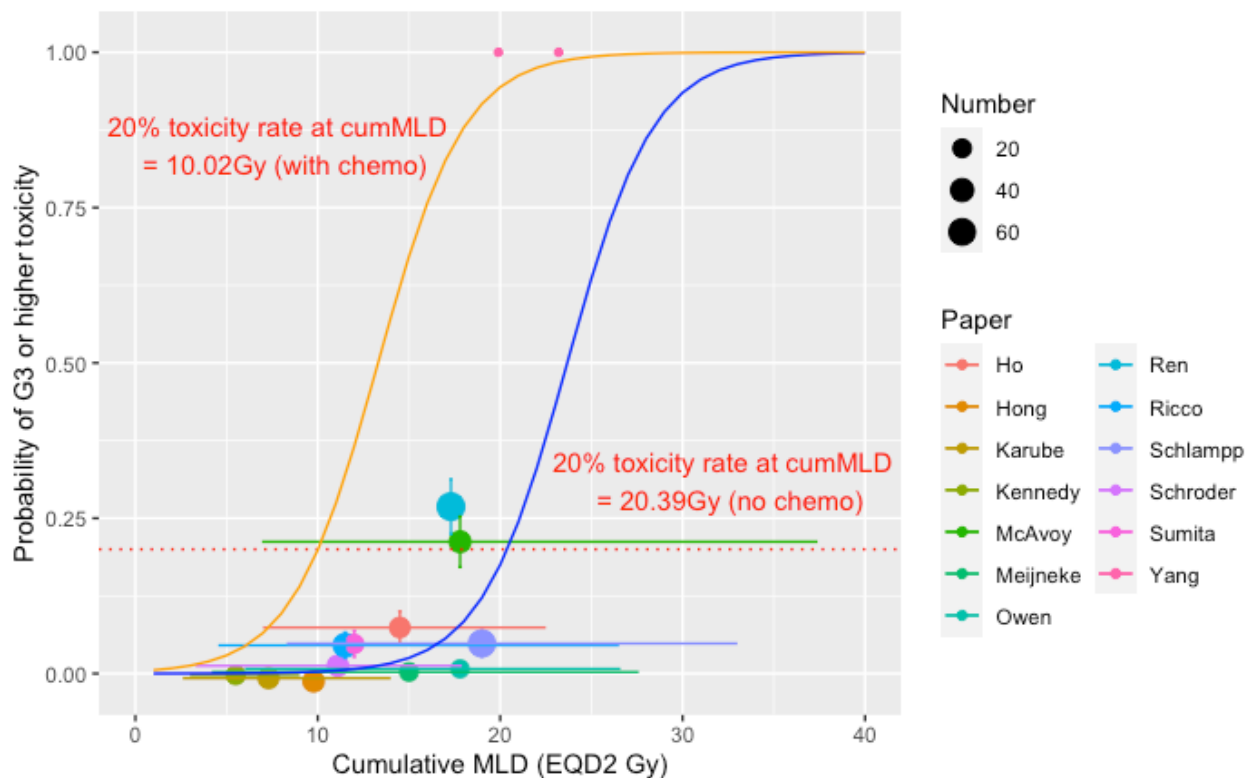


Figure 5.10 Plot of cumulative mean lung dose multivariable model. The blue line is the fitted regression model without chemotherapy, the orange line represents the fitted regression model with chemo, the red dotted line indicates the 20% toxicity level. The dots represent the toxicity rate from each individual paper coded by colour, with the size of the dots proportional to the number of patients in the study, vertical bars are the 68% binomial confidence interval, horizontal bars represent the range of the doses, due to overlapping data points, the scatter plot has been jittered.

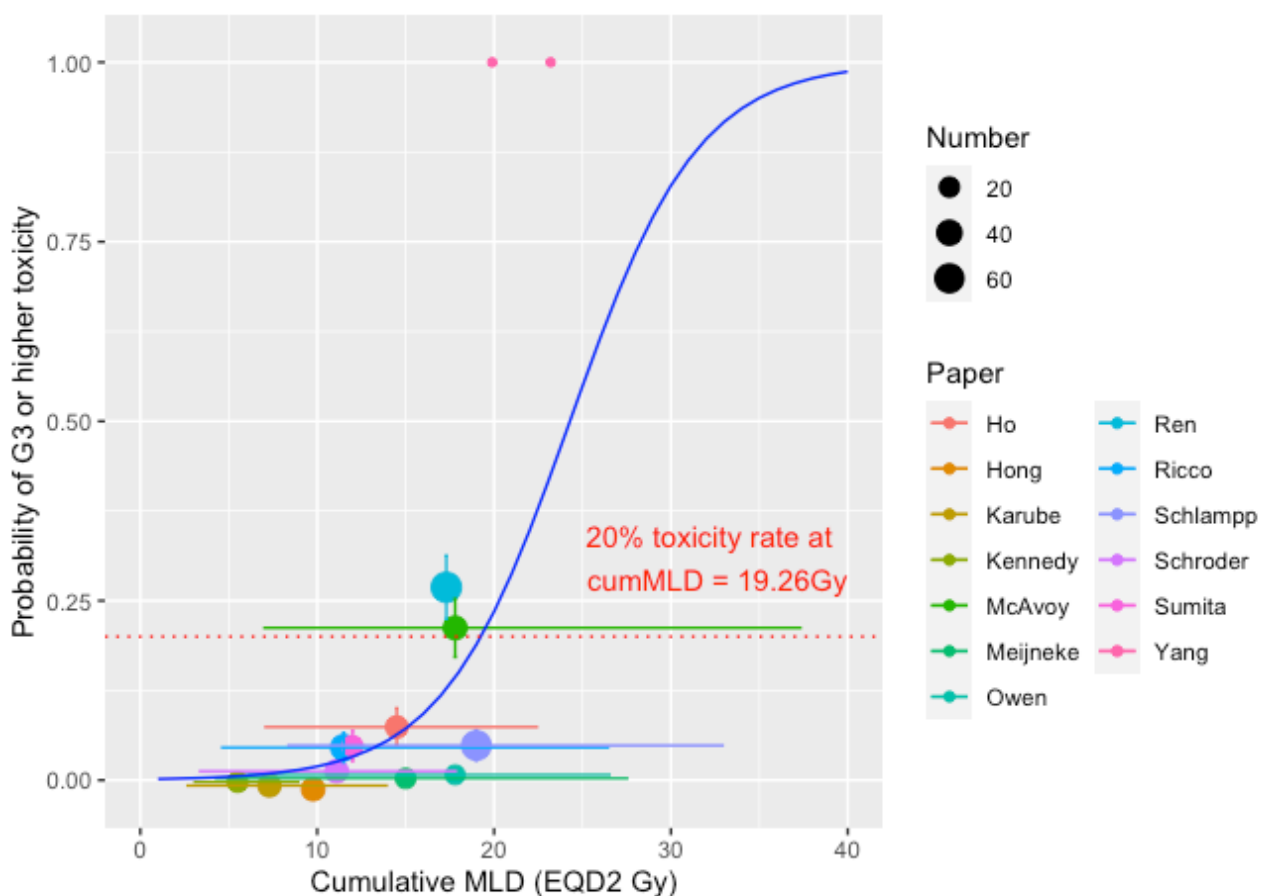


Figure 5.11 Plot of cumulative mean lung dose univariable model. The blue line is the fitted regression model without chemotherapy and the red dotted line indicates the 20% toxicity level. The dots represent the toxicity rate from each individual paper coded by colour, with the size of the dots proportional to the number of patients in the study, vertical bars are the 68% binomial confidence interval, horizontal bars represent the range of the doses, due to overlapping data points, the scatter plot has been jittered.

5.3.5.2 Cumulative V5 model

There was no significant change in the relative risk of Grade 3 toxicity with increasing cumV5 when divided into 15% bins between 15-- 60% with the cumV5 15-30% as the reference risk (Table 5.29). However, the relative toxicity risk is significantly higher (8.64, 95% CI 1.21, 61.56) when the cumV5 exceeds 60% compared to a cumV5 between 15-30%.

Table 5.29 Relative risk table for the grouped cumulative V5 dataset. CI: confidence interval, NA: not applicable.

Range	Number	Grade 3+ events	Relative risk	Lower 95% CI	Upper 95% CI	P-value
<15	0	0	NA	NA	NA	NA
15-30	30	1	1	0.07	15.26	1
30-45	85	3	1.06	0.11	9.79	0.96
45-60	60	9	4.5	0.60	33.89	0.14
>60	66	19	8.64	1.21	61.56	0.03*

Model expression:

$$P(\geq G3 \text{ toxicity} | X) = \Phi(-4.7294 + 0.0531X)$$

Where X=cumulative V5. This model is plotted in Figure 5.12. The 20% toxicity rate is predicted at a cumV5 of 62.95% (95% CI 55.07, 70.82%). The 95% confidence interval for cumulative V5 that gives 20% toxicity rate, using 2000 block bootstrapped samples, is 13.14 - 148.93%. The 10 and 30% toxicity rates are estimated at 47.68 (95% CI 39.13, 56.22) and 73.10 (95% CI 62.15 - 84.04) respectively.

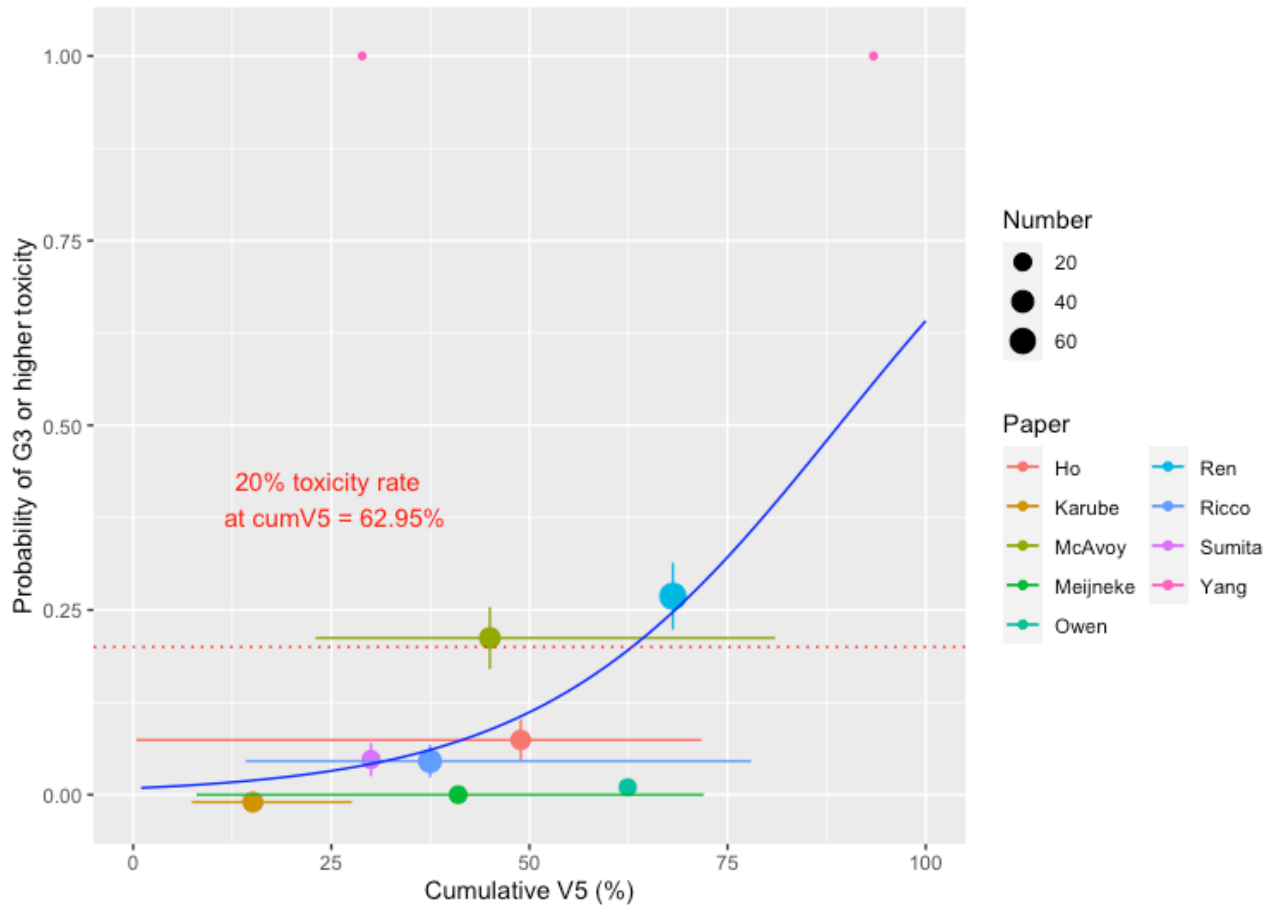


Figure 5.12 Plot of cumulative V5 univariable model. The blue line is the fitted regression model, and the red dotted line indicates the 20% toxicity level. The dots represent the toxicity rate from each cohort or individual coded by colour, with the size of the dots proportional to the number of patients in the study, vertical bars are the 68% binomial confidence interval, horizontal bars represent the range of the doses, due to overlapping data points, the scatter plot has been jittered.

5.3.5.3 Cumulative V20 model

The relative risk table for cumulative V20Gy demonstrates a trend for increasing relative risk as the cumV20 increases, and values over 24% have a significantly higher risk compared to the reference range (12-18%, Table 5.30). The relative risk of \geq G3 toxicity of the cumV20 24-30% group is approximately 9 times higher when using cumV20 between 12-18% as the reference risk.

Table 5.30 Relative risk table for the grouped cumulative V20 dataset. CI: confidence interval, NA: not applicable.

Range	Number	Grade 3+ events	Relative risk	Lower 95% CI	Upper 95% CI	P-value
<12	40	0	NA	NA	NA	NA
12-18	152	3	1	0.21	4.88	1
18-24	35	2	2.90	0.50	16.68	0.24
24-30	153	28	9.27	2.88	29.86	<0.01*
>30	3	1	16.89	2.39	119.13	<0.01*

The model expression for the cumulative V20 model is:

$$P(\geq G3 \text{ toxicity} | X) = \Phi(-6.2712 + 0.1720X)$$

Where X=cumulative V20. The 20% toxicity rate is predicted at a cumulative V20 of 28.41% (95% CI 25.92, 30.00%). The 10% and 30% toxicity rates are predicted for 23.69 (95% CI 21.43, 25.95) and 31.54 (95% CI 28.17 - 34.91) respectively. The bootstrapped 95% confidence interval is for the 20% toxicity rate is 25.63, 47.80%. This model is plotted in Figure 5.13.

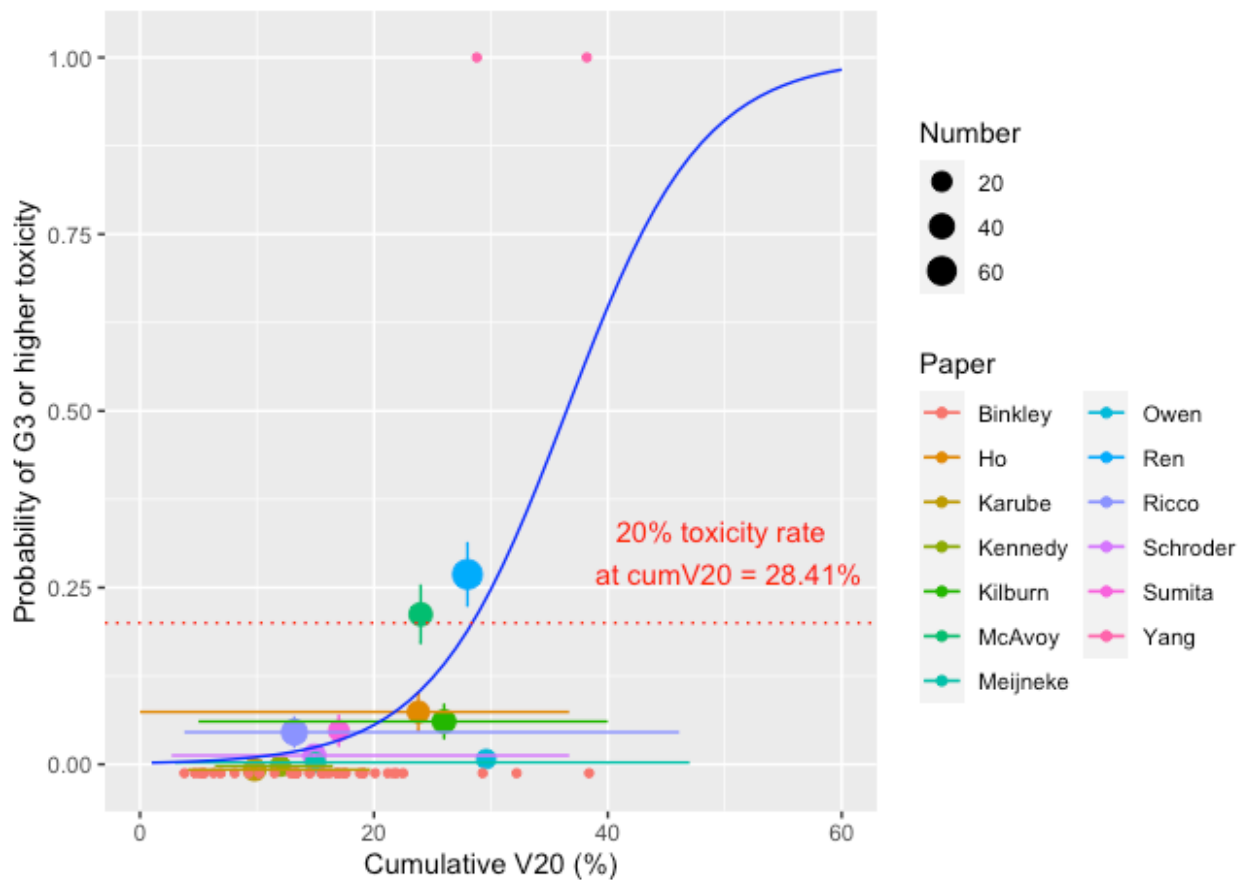


Figure 5.13 Plot of cumulative V20 univariable model. The blue line is the fitted regression model, and the red dotted line indicates the 5% toxicity level. The dots represent the toxicity rate from each cohort or individual coded by colour, with the size of the dots proportional to the number of patients in the study, vertical bars are the 68% binomial confidence interval, horizontal bars represent the range of the doses, due to overlapping data points, the scatter plot has been jittered.

5.3.5.4 Development of lung constraint values

The cumMLD multivariable model estimated the dose that gives a 20% rate of toxicity is 20.39Gy. When this dose is used to calculate the risk using the 2000 bootstrapped samples, the 95% CI for risk is 4.2% to 99.5%. The upper limit of risk for the bootstrapped samples was fixed at 20% and the highest dose which meets this criterion is 16.02Gy (95% CI for risk of <0.1% to 20%). The same process was used to develop bootstrapped dose constraints for the cumMLD univariable model, cumV5 and cumV20 model and the results are summarized in Table 5.31.

Table 5.31 Development of lung dose constraints using block bootstrapping. All models assumed no concurrent chemotherapy. CI: confidence interval, cumMLD: cumulative mean lung dose, cumVx: cumulative volume receiving at least x Gray, MV: multivariable model, UV: univariable model.

Model	Model dose	Risk	95% CI lower limit risk (%)	95% CI upper limit risk (%)
cumMLD (MV model - no chemo)	20.39 Gy	20%	4.2	99.5
	16.02 Gy	Maximum 20%	<0.1	20
cumMLD - UV model	19.26	20%	5.4	52.3
	16.65	Maximum 20%	3.4	20
cumV5Gy	62.95%	20%	4.6	50.6
	48.36%	Maximum 20%	3.5	20
cumV20Gy	28.41%	20%	5.5	31.1
	25.70%	Maximum 20%	4.1	20

5.3.5.5 Evaluation of lung models

All three models were assessed using a Hosmer Lemeshow goodness of fit test. The cumMLD and cumV20 models were non-significant indicating a good fit between the model predictions and the observed toxicity. The cumV5 model was significant suggest that the predictions were not a good fit (Table 5.32). Likewise, the Pearson correlation coefficients for the cumMLD and V20 models were over 0.7 (and significant) suggesting that the predictions had reasonable correlation with the observed rates, whereas the cumV5 model did not correlate well. The observed against predicted toxicity rates are plotted for each model in Figure 5.14, Figure 5.15, Figure 5.16 and Figure 5.17.

Table 5.32 Summary of Hosmer Lemeshow and Pearson correlation tests for lung models. CI: confidence interval, cumMLD: cumulative mean lung dose, cumVx: cumulative volume receiving at least x Gray, MV: multivariable model, UV: univariable model.

Model	Hosmer-Lemeshow p-value	Pearson correlation coefficient	Pearson p-value
cumMLD (MV model)	0.625	0.75	0.01*
cumMLD (UV model)	0.628	0.81	<0.01*
cumV5Gy	<0.01*	0.54	0.10
cumV20Gy	0.938	0.71	0.02*

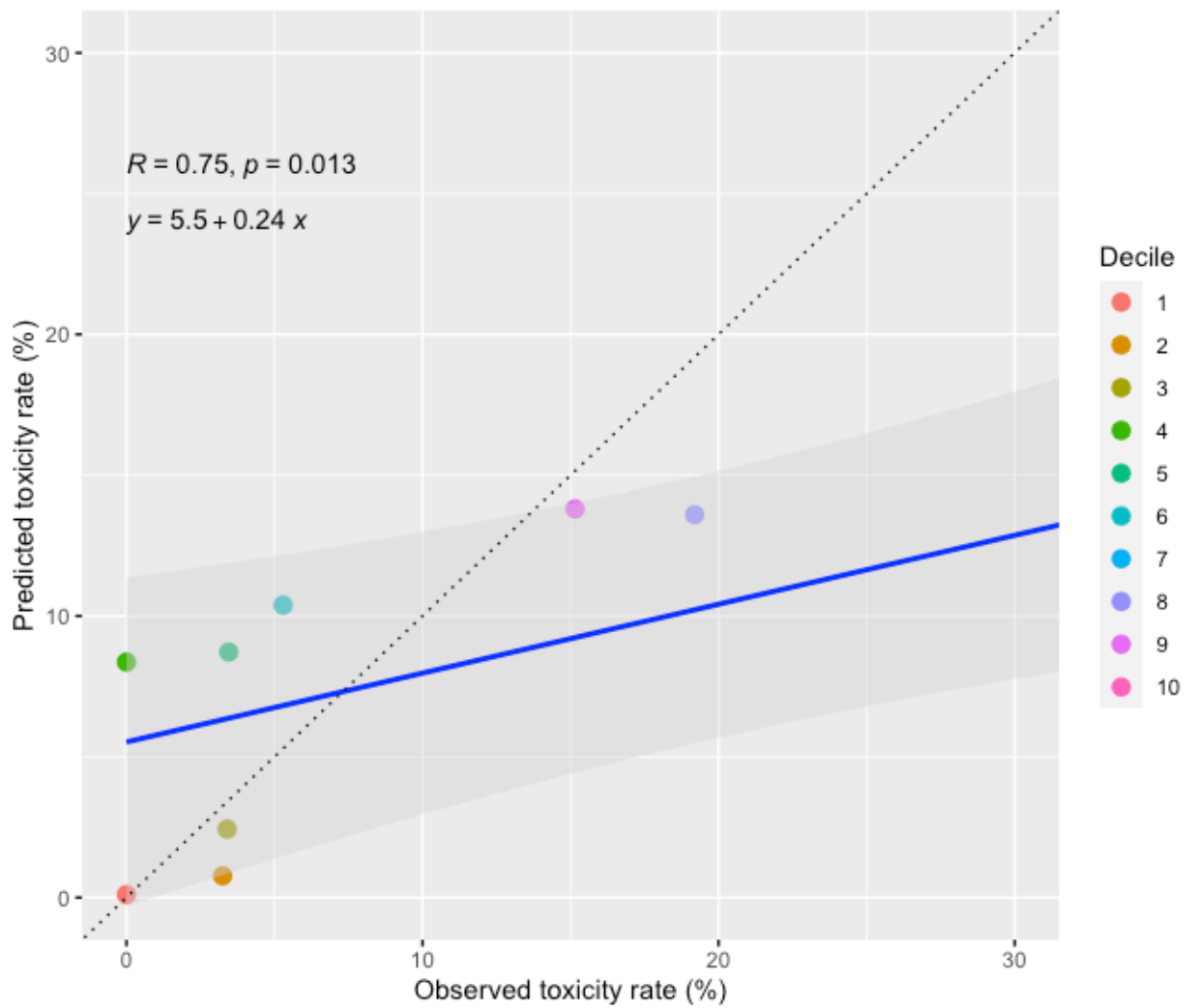


Figure 5.14 Plot of the actual and predicted cumulative mean lung dose multivariable model toxicity rates. The blue line is the line of best fit, with the shaded grey area the 95% confidence interval. The black dotted line represents the line of unity. The dots represent the toxicity rate from each decile.

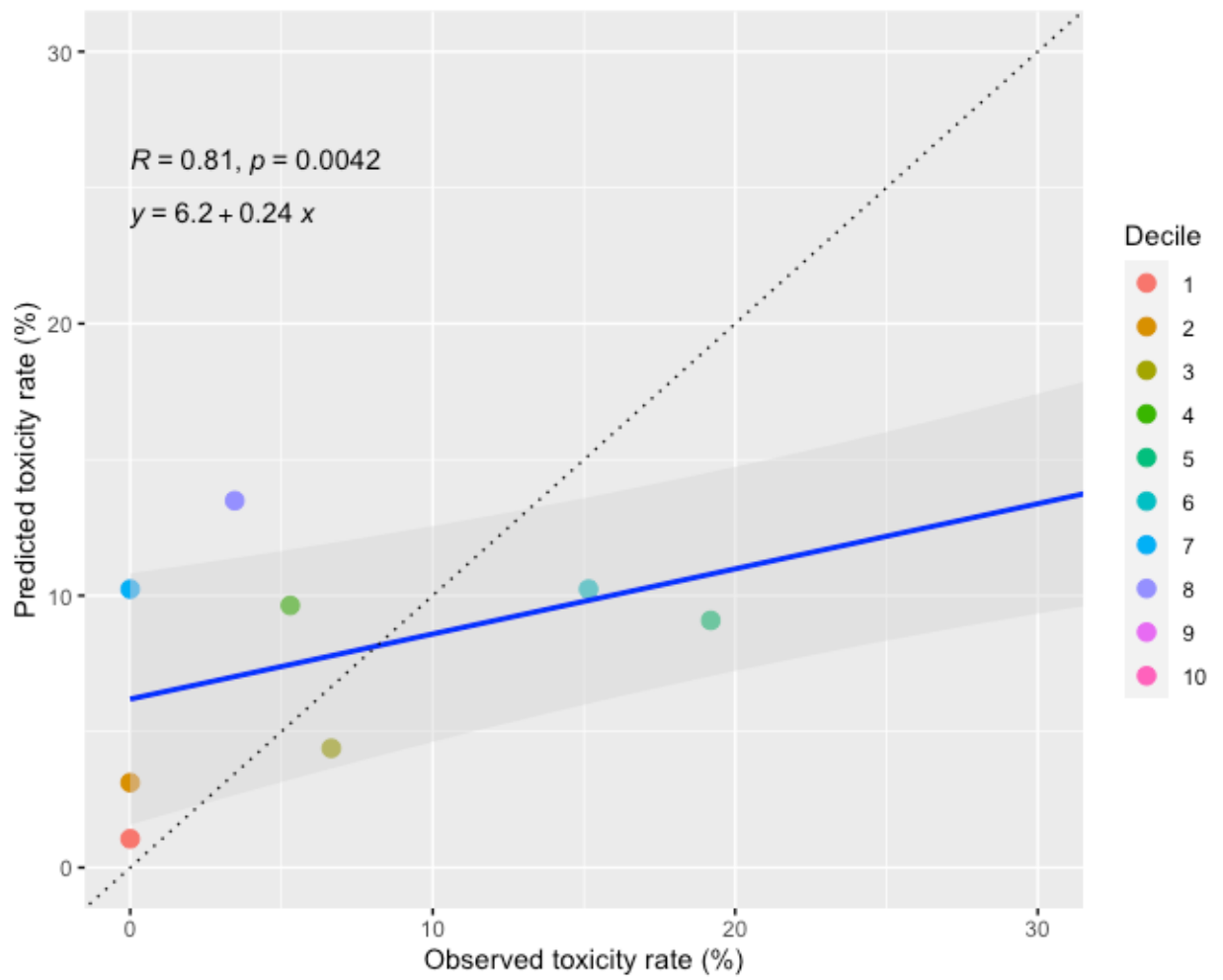


Figure 5.15 Plot of the actual and predicted cumulative mean lung dose univariable model toxicity rates. The blue line is the line of best fit, with the shaded grey area the 95% confidence interval. The black dotted line represents the line of unity. The dots represent the toxicity rate from each decile.

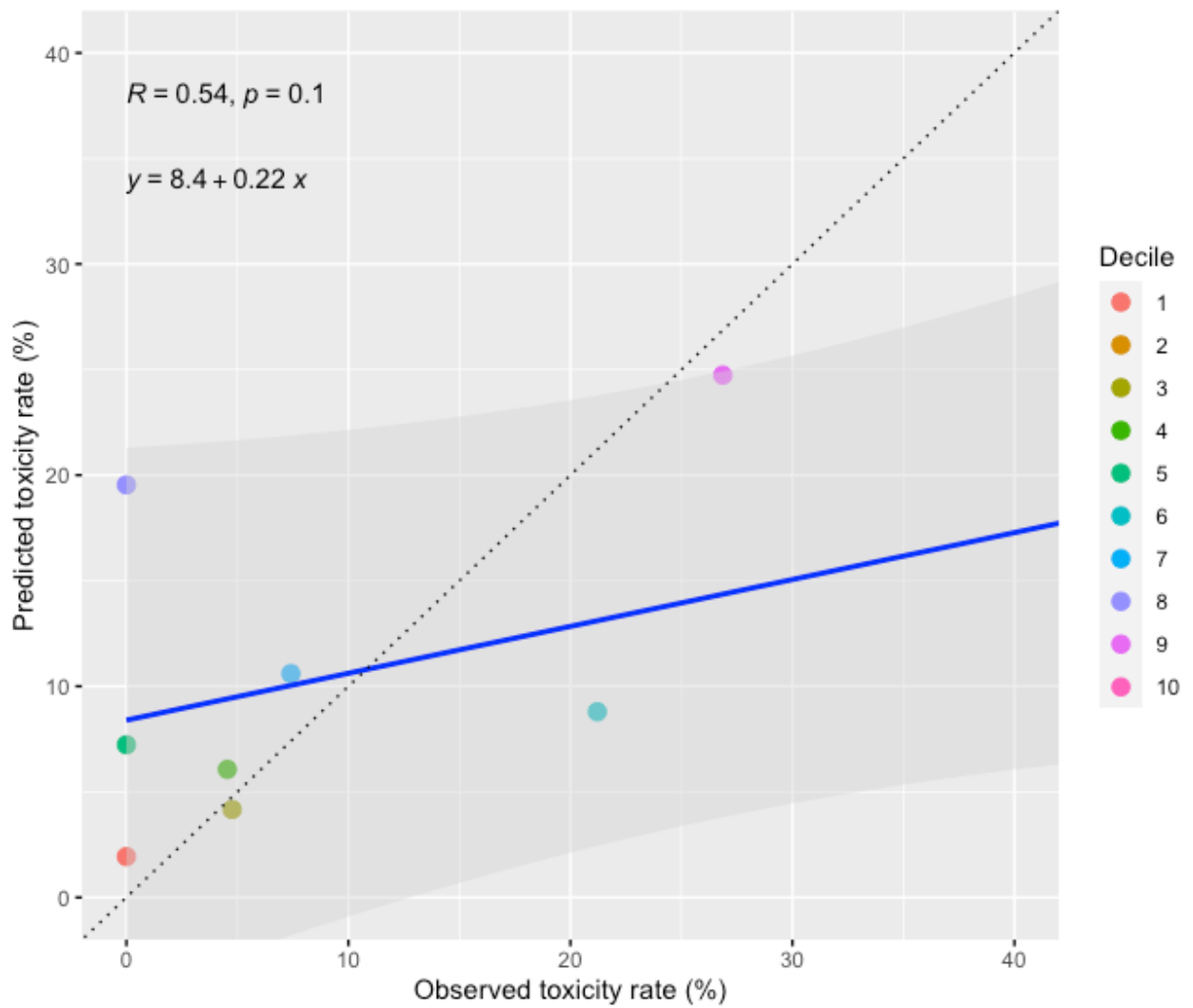


Figure 5.16 Plot of the actual and predicted cumV5Gy model toxicity rates. The blue line is the line of best fit, with the shaded grey area the 95% confidence interval. The black dotted line represents the line of unity. The dots represent the toxicity rate from each decile.

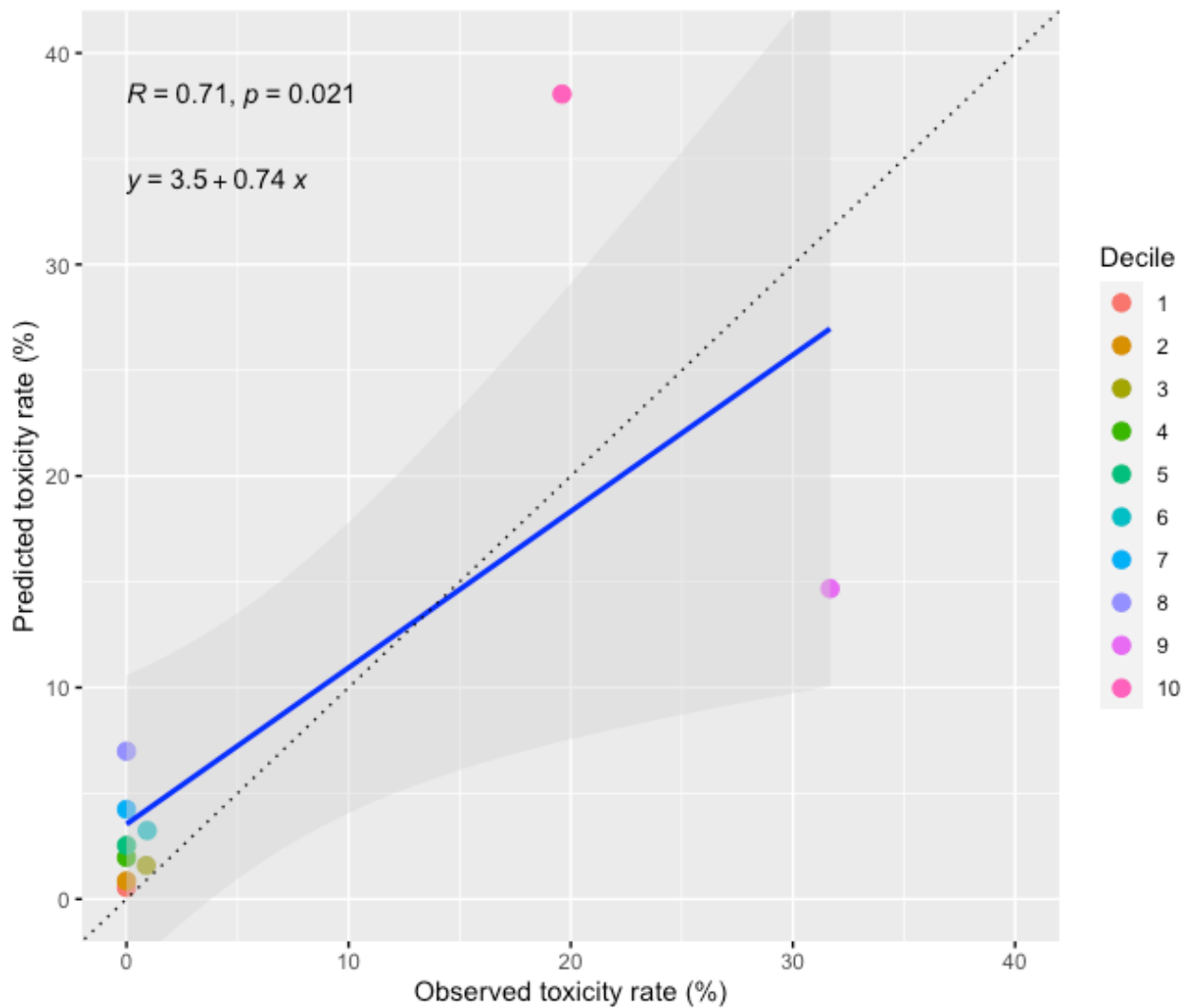


Figure 5.17 Plot of the actual and predicted cumV20Gy model toxicity rates. The blue line is the line of best fit, with the shaded grey area the 95% confidence interval. The black dotted line represents the line of unity. The dots represent the toxicity rate from each decile.

The model 20% dose predictions and the bootstrapped 20% maximum constraints were tested against the external Beatson cohort for all models. The cumV20 dose constraints were also applied to the individual data (as this was the only lung metric that had individual data). None of the suggested dose constraints offered good discrimination between the higher and lower doses when tested with the external cohort, with some showing a higher toxicity rate below the cut-off than above it (e.g., the cumMLD and cumV20 models, Table 5.33). The cumV20 cut-offs predicted a low toxicity rate of 5.9% below both cut-offs, and 50% above them, when applied to the individual data (Table 5.34).

Table 5.33 Testing lung dose constraints on external Beatson cohort. CI: confidence interval, cumMLD: cumulative mean lung dose, cumVx: cumulative volume receiving at least x Gray, MV: multivariable model, UV: univariable model.

	Number with no toxicity	Number with toxicity	Toxicity rate (%)
cumMLD MV model 20% toxicity			
<20.4 Gy	26	12	31.2
>20.4 Gy	1	0	0
cumMLD MV model maximum 20% toxicity			
<16.0 Gy	21	11	34.4
>16.0 Gy	6	1	14.3
cumMLD UV model 20% toxicity			
<19.3 Gy	25	11	30.6
>19.3 Gy	2	1	33.3
cumMLD UV model maximum 20% toxicity			
<16.7 Gy	21	11	34.4
>16.7 Gy	6	1	14.3
cumV5 model 20% toxicity			
<63.0%	23	9	28.1
>63.0%	4	3	42.9
cumV5 model maximum 20% toxicity			
<48.4%	11	5	31.3
>48.4%	16	7	30.4
cumV20 model 20% toxicity			
<28.4%	22	11	33.3
>28.4%	5	1	16.7
cumV20 model maximum 20% toxicity			
<25.7%	20	9	31.0
>25.7%	7	3	30.0

Table 5.34 Testing cumV20 constraints on individual dataset. CI: confidence interval, cumMLD: cumulative mean lung dose, cumVx: cumulative volume receiving at least x Gray, MV: multivariable model, UV: univariable model.

	Number with no toxicity	Number with toxicity	Toxicity rate (%)
cumV20 model 20% toxicity			
<28.4%	32	2	5.9
>28.4%	2	2	50
cumV20 model maximum 20% toxicity			
<25.7%	32	2	5.9
>25.7%	2	2	50

5.3.5.6 Lung models discussion

Four models were created to model the cumulative MLD, cumulative V5 and cumulative V20 and \geq G3 lung toxicity. Interestingly, the dose predictions for a 20% risk of grade 3 toxicity are lower than the dose constraints at initial radiotherapy (grade two or above toxicity seen at $MLD < 20-23Gy$ and $V20 < 30-35\%$), as suggested in the QUANTEC lung study²²⁶. This implies that there is little or no lung recovery over time, and possibly that a lower dose results in severe toxicity with repeated radiotherapy. It may also reflect that the re-irradiation models used a \geq G3 toxicity endpoint, whilst QUANTEC used a \geq G2 toxicity.

The QUANTEC predictions are similar to other studies that analyse the risk of re-irradiation pneumonitis. Liu *et al.* also found that the cumulative V20 $>30\%$ had a higher risk of toxicity in 72 patients, previously treated with conventionally fractionated radiotherapy and re-irradiated with SABR¹⁴⁹. Schlamp et al. reported a median cumMLD of 19Gy and had a \geq G2 toxicity risk of 19.3%. Ren *et al.* found that a cumulative V5 $>68.3\%$ had a higher risk of \geq G3 pneumonitis from a cohort of 67 patients who had either local or SPLC¹⁴⁷. The cumV5 model, using an outcome of grade 3 or above toxicity, is similar to the Ren paper. The cumMLD and cumV20Gy model results predict grade 3 toxicity, therefore making comparisons to Schlamp and Liu's studies difficult.

The model findings are potentially congruent with the pre-clinical research on lung re-irradiation. Terry *et al.* irradiated whole mice lungs with a priming dose of either 6, 8 or 10Gy and then repeated the dose at monthly intervals until 6 months¹⁴¹. A marked reduction in radiation tolerance was seen for all groups at 1 month, but the mice primed with 6 and 8Gy doses, recovered almost complete lung tolerance by 3 months. However, the mice treated initially with 10Gy never recovered complete tolerance. Both the groups treated with 10Gy and 6Gy after the 3-month time point had reduced re-irradiation tolerance by month 6. This was the trend for all groups. The radiation dose given in the first treatment had a significant effect on the subsequent re-irradiation tolerance.

One criticism of this murine study is that the follow up period was too short. Pathophysiologically, the acute transient inflammation peaks after 3-4 months post-radiotherapy, followed by the slower fibrotic process that starts nine

months after irradiation²²⁷. If the experiment follow-up was longer, it may have shown further reduction in re-irradiation tolerance, especially given the trend for decreasing re-irradiation tolerance in all groups at 6 months. However, the follow-up time is sufficient to investigate the influence of the size of the initial radiation dose. This finding from the mouse study has been replicated in clinical practice by Ren *et al.*, who identified initial MLD as having the highest effect on hazard ratio of toxicity at re-irradiation¹⁴⁷. Additionally, Terry *et al.* treated the whole mouse lung, and therefore it may be difficult to extrapolate the data to humans, where partial lung irradiation is commonplace.

The dose predictions of the models are similar to the expert dose constraints proposed by Hunter *et al.* although other groups suggesting individualised dose limits¹⁶¹. The American Radium Society guidelines suggest cumulative V20<40%¹⁶⁰. If a patient was treated with a cumulative V20 of 40%, the model predicts a toxicity risk of 64.7%.

There are several sources of potential error in the lung models. The cumulative lung doses are difficult to measure. This is because of the way the V20 and V5 lung metrics are calculated. The lung V20 measurement at the first course of radiation is a measurement of the number of voxels receiving $\geq 20\text{Gy}$ in the volume contoured as lung. The cumulative V20 is difficult to calculate because the initial radiotherapy may have caused lung fibrosis thereby changing the shape of the lungs, or the planning scan was in a different phase of respiration. Therefore, the re-irradiation lung contours and dose contours would have to undergo deformable image registration to the volume of lung at initial radiotherapy. This process is prone to error, as deformable dose registration uses an algorithm to warp the re-irradiation image into the shape of the lung at initial treatment. This may cause underdosing or overdosing, depending on the deformation. In addition, there are different commercial programs which do this, and each may give a different solution depending on the proprietary algorithms used¹⁷⁰. This would lead to dosimetric uncertainty in all the studies in the lung dataset.

The outcome measures are inconsistent. The RTOG toxicity scale describes grade 2 toxicity as persistently symptomatic, and grade 3 as needing steroids or

oxygen. The CTCAE uses activities of daily living as a guide, with impaired self-care being the hallmark of grade 3 toxicity. The SWOG grading defines steroid use as grade two, and oxygen as grade 3. Therefore, there may be misrepresentation of the true toxicity patients experienced as there was no consistent toxicity scale used. This discrepancy is highlighted in a study where the RTOG and CTCAE scales were applied to the same group of 50 patients. The rate of grade three toxicity in the RTOG and CTCAE groups were 23% and 0% respectively²²⁸. This could affect the dose estimates made by the models.

Other sources of error include the description of V20 and V5. The V20 whole lung minus PTV ($V20_{WL-PTV}$) or V5 whole lung minus PTV ($V5_{WL-PTV}$) are used and quoted in clinical practice. However, this is difficult in the re-irradiation context, as there is uncertainty in whether to exclude both the re-irradiation PTV and the initial PTV, or just the re-irradiation PTV. Most studies reported the V20 and V5 without any subtraction of PTV, apart from Kennedy *et al.* who quoted PTV minus ITV in their study of 21 patients having SABR re-irradiation¹³⁶. Some studies also corrected the V20, V5 and MLD to EQD2 values but the remaining studies used the physical dose^{168,208,220}. The effect of this was analysed by Ricco *et al.* who noted that V5 to V5(EQD2) resulted in lower doses, MLD to MLD(EQD2) resulted in higher doses, and V20 to V20(EQD2) were approximately the same¹⁶⁸. As the majority of the dose information comes from physical doses, assuming the correct approach is to use the EQD2 values, the cumV5 model would give a higher dose for a given toxicity rate, the cumMLD model would give a lower dose, and the cumV20 model would remain unchanged.

The models also fail to include several factors that are likely to have an influence on the risk of re-irradiation toxicity, such as initial MLD, previous surgery, type of re-treatment, comorbidities and lung function tests. These were not included because the data was not available in the studies. The moderate correlation of the cumMLD and cumV20 models, and the poor discrimination when putative cut-offs were tested against the external Beatson cohort and the individual data, may be due to these uncontrolled factors. Interestingly, when the cumMLD multivariable model prediction cut-off was used, there was a trend that higher dose resulted in less toxicity, whereas the univariable model supported the model findings. This is in part due to the univariable model having

a flatter gradient by removing the effect of chemotherapy. However, only 3 patients were re-classified by the change in dose cut-off from the multivariable to the univariable model, highlighting how the low numbers in the external group can lead to significant changes. In the external Beatson cohort, there were 12 \geq G3 toxic events, occurring, with the lowest values of cumMLD, cumV5 and cumV20 of 5.1Gy, 15.5% and 5.3% respectively. These values are similar to the dataset derived from published data and are below the suggested constraints, suggesting that there are other factors that influence toxicity development.

The degree of overlap may be important in lung re-irradiation and these models do not include this factor. The lung is considered a parallel organ and is composed of functional sub-units. These can be damaged independently but the remaining undamaged units can still oxygenate blood. The organ fails once there are too few undamaged FSU to adequately transfer oxygen into the blood. In re-irradiation where the PTVs overlap, the FSUs damaged by the initial radiotherapy will receive another large dose. However, if they are already non-functional from the first dose of radiotherapy, it may make little difference to the lung function. However, in SPLC where the PTVs are spatially different, FSUs that were undamaged after the first course of radiotherapy are damaged by the second course. Therefore, in re-irradiation for SPLC, the total volume of lung treated may be greater than high overlap re-irradiation for local recurrence. Clinical evidence for this effect is seen in Ren *et al.* who found that the greater the overlap between the initial V5 and re-irradiation V5, the lower the risk of \geq G3 toxicity¹⁴⁷.

There would need to be many events in the dataset to produce reliable models exploring these multiple variables, requiring a large data collection of hundreds of patients. The amount and quality of data at present is not available to perform these analyses. Therefore, these models cannot be used in isolation to give the risk of toxicity to an individual patient. One limitation of the current data is that only 64 out of 405 (15.8%) of the cumMLD dataset and 3 out 383 (0.8%) of the cumV20 dataset exceed the dose constraints used for initial radiotherapy. Therefore, the models have insufficient evidence to predict the toxicity rates at doses above these constraints as shown by the wide 95%

bootstrapped confidence intervals for both the cumMLD and cumV20 models at higher doses.

The \geq G3 toxic events came from eight studies, four using conventionally fractionated radiotherapy, two using SABR and two using protons. Most of the events came from patients treated with CFRT (n=24, 68.6%) with only 4 (11.4%) from SABR studies. This disparity is likely due to the small treatment volumes and high conformality of SABR treatments. The detection of pneumonitis or fibrosis is difficult, as there is a risk that these can be misdiagnosed as other conditions, most often chest infections. All the studies included in this dataset are retrospective reviews so this is a source of inaccuracy. The effect on the models if toxic events were overestimated would be to make the dose constraints more conservative than necessary.

Despite the lack of correlation with the external Beatson datasets, the crude testing (median split and relative risk tables) indicate a proportional relationship of increasing toxicity with increasing dose. The median splits suggest higher toxicity at higher cumulative MLD, V5Gy or V20Gy and the relative risk tables show a significantly raised risk of toxicity at higher dose levels. On logistic regression, the cumMLD/chemo, the univariable cumMLD and the cumV20 models were significant and fit the observed data well according to the Hosmer-Lemeshow and Pearson correlation tests. The cumV5 model however fits poorly and this may be because the dataset used to form the model was smaller (n=261) than the other two models. Other multivariable models with more than one lung metric were not significant, likely due to missing data leading to lower numbers in the multivariable models, or possibly due to collinearity between the metrics.

In part, the lack of correlation of the models with the external data may be because the metrics studied are not the most useful to detect re-irradiation toxicity. Re-irradiation specific lung metrics may be needed to better discriminate between low and high risk than the standard metrics used in *de novo* radiotherapy. Candidate re-irradiation lung metrics may include the critical volume, the functional MLD/V5/V20 or the cumulative Dmax. The critical volume has been used in SABR studies and is the volume of lung receiving a given dose or less²¹⁹. The concept of this metric is to identify a volume of normal lung

undamaged by radiotherapy (and therefore remains functional). This concept has been used in RTOG 0813 where a planning constraint of at least 1500cc of lung should be treated to 12.5Gy or less was applied²²⁹. The basis of this constraint is anecdotal from post-pneumonectomy surgical studies where a residual lung volume of 1.5 litres is sufficient for acceptable lung function²³⁰. Another option is to use functional MLD, V5 and V20 as metrics. These metrics are based on a four-dimensional ventilation/perfusion positron emission tomography-computed tomography (4D-V/Q PET-CT) pre-treatment. This scan allows delineation of functional lung, and therefore excludes the fibrotic lung post-initial radiotherapy, therefore providing a more accurate description of the actual MLD, V5 and V20. This approach has been demonstrated to reduce the dose to functional lung in initial lung radiotherapy but is yet to be applied in the re-irradiation setting²³¹. In addition, the cumulative Dmax is not well explored in this setting. Anecdotally, once lung has been treated to a high dose, it is fibrosed and considered inactive. Therefore, repeated higher doses through fibrosed lung may not cause more toxicity. However, the re-irradiation modelling results suggest that the lung may have greater sensitivity to repeat doses of radiation, which may indicate that the pre-treated fibrosed lung is not physiologically inactive.

In summary, although the cumMLD and cumV20 models fit the data well, the cut-offs when tested on the external dataset show poor discrimination. This may reflect several other factors which may influence toxicity. However, the model predictions suggest that there is little lung recovery therefore dose constraints for initial radiotherapy should be applied in the re-irradiation setting.

5.3.5.7 Conclusions

Three models were created to predict the \geq G3 lung toxicity from re-irradiation. A 20% rate of toxicity is predicted at a cumMLD of 20.4Gy, a cumV5 of 63.0% and a cumV20 of 28.4%. The cumV5 model had a poor fit to the dataset whereas the cumMLD and cumV20 models had a good fit. The maximum likelihood predictions from the models and the bootstrapped maximum 20% dose constraints when applied to the external Beatson data did not provide discrimination in the toxicity rates above or below the constraints. However, the cumV20 model dose constraints did provide better discrimination when tested on the individual data

(cumV20<28.4% the toxicity rate was 5.9%, cumV20>28.4%, the toxicity rate was 50%). The models give predict high grade toxicity at doses lower than the dose constraints used in initial radiotherapy. Due to the technical uncertainties of the models, more robust data in terms of outcome grading and cumulative dose calculation is required before dose/toxicity can be modelled accurately. In the interim, it is reasonable to try and limit the cumulative dose to the QUANTEC dose limits for initial radiotherapy.

5.3.6 Models for proximal bronchial tree

A proximal bronchial tree model was created using a dataset based on 13 studies summarised in Table 5.35 and Table 5.36. The data in the studies were collected between 1979 - 2017.

There were 52 missing data regarding the use of concurrent chemotherapy. There was no difference in cumEQD2 between the group with missing data and the group with no missing data (t-test p-value 0.264) but there was a significant difference in the rate of toxicity (7/52 in the missing data group, and 3/102 in the no missing data group (Fishers exact p-value 0.03). These missing cases were excluded from any concurrent chemotherapy models.

There were four cases missing interval data from two papers (Repka *et al.*, and Tetar *et al.*^{123,232}) and all had toxic events associated with them. This was significantly different from the group with no missing data who had a significantly lower rate of toxicity (fishers p-value <0.001), although the range of EQD2 was not different (t-test p-value 0.16). The exclusion of these four toxic events would lead to 40% of the toxic events being excluded from any including the interval as a variable. Given the low number of events in this dataset, this had the potential to alter the modelling results. Therefore, the missing interval data for the four cases was replaced with the median interval values quoted in the respective papers. The three cases from Tetar *et al.* were assigned an interval of 29.7 months and the single case from Repka *et al.* was assigned an interval of 23.3 months.

To assess the effect of imputed the data on the prediction, one model used the imputed dataset, and another model excluded the four cases.

Table 5.35 List of studies used to form the proximal bronchial tree dataset. The total number of patients included is 154, from 13 studies. 3D-CRT: three dimensional conformal radiotherapy, BED: biologically equivalent dose, EQD2: equivalent dose in 2 Gray fractions, Fr: fractions, IMPT: intensity modulated proton therapy, IMRT: intensity modulated radiotherapy, NR: not recorded, Re-RT: re-irradiation, SABR: stereotactic ablative radiotherapy.

Paper	n	Individual data/Grouped	Treatment span	Initial prescription dose/fr	Re-RT prescription dose/fr	Re-treatment Technique
Okamoto ¹¹⁹	6	Individual	1979-2000	60 (30-80)Gy/median (1.5-2)Gy per fr	50 (10-70)Gy/(1.8-3)Gy per fr	3D-CRT
McAvoy ¹²²	2	Individual	2006-2011	66 (40-74)/33 (4-59)fr	66(16.4-75)/32 (9-58)fr	Protons
Schroder ²⁰⁸	24	Grouped	2011-2017	NR	NR	SABR
Sood ²³³	2	Individual	2009-2017	66/33	57.5 (50-65)/10fr	SABR
Meijneke ¹⁷⁵	7	Grouped	2005-2021	median 60 (30-60)Gy/median 3 (1-25)fr	median 51 (20-60)Gy/median 5 (3-10) fr	90% SABR, 10% Conventional
Kilburn ¹³⁰	19	Grouped	2001-2012	median 60 (22.5-80.5)Gy/median 30 (1-37)fr	median 50 (20-70.2)Gy/median 10 (1-35) fr	SABR in 91%
Sumita ¹²⁴	21	Grouped	2007-2014	EQD2 median 60 (43.1-87.5)Gy (10)	EQD2 median 60 (50-87.5)Gy (10)	Conventional 90%, Proton 10%
Binkley ²²⁰	34	Individual	2008-2014	median 50 (20-74)Gy/median 4.5 (1-37)fr	median 50 (20-177.5)Gy/median 4 (1-54) fr (including multiple re-RT courses)	SABR 73.7%, Conventional 26.3%
Repka ²³²	1	Individual	2004-2014	NR	45Gy	SABR
Griffioen ¹¹⁴ /Tetar ¹²³	4	Grouped	2004-2015	59.9 (59.9-70)Gy/25 (25-28)	60 (60)/30 (20-30)	IMRT
Peulen ¹⁴⁵	3	Individual	1994-2004	40 (30-40)/4 (3-4)	40 (33-45)/3 (3-5)	SABR
Ogawa ²²³	31	Grouped	2004-2017	BED median 112.5 Gy (10) (75-119.6)	BED median 105 Gy (10) (64.2-119.6)	SABR

Table 5.36 List of studies used to form the proximal bronchial tree dataset. cumDmax: maximum dose received to a given organ at risk, Dxcc: maximum dose to an organ at risk to a volume of xcc, EQD2: equivalent dose in 2 Gray fractions, Fr: fraction, f/u: follow-up, NR: not recorded, PBrT: proximal bronchial tree, PTV: planning target volume, Re-RT: re-irradiation.

Paper	Median cumDmax (EQD2, Gy)	Interval (months, range)	Chemo % rate with re-RT	Any Grade 3-5 toxicity (%)	F/u post re-RT (months, range)	Uncertainty
Okamoto ¹¹⁹	120 (90-150)	41.5 (8-69)	0	0	35 (20-58)	Derived EQD2 using assumed 2Gy/fr, dose to trachea not explicitly stated but extrapolated from central location of tumour
McAvoy ¹²²	136.3 (132.7 - 140)	42 (36-48)	0	100	11 (1.4-32.4) (whole group)	Uses a subset from 33 patients
Schroder ²⁰⁸	81.99	14 (2-184)	0	0	13 (1-45)	Uses a subset of the original 42 patients
Sood ²³³	158.5 (153-164)	10.7 (8.2-13.2)	0	0	NR	Uses a subset of patients where the cumulative PBrT dose is given
Meijneke ¹⁷⁵	89.2	17 (2-33)	0	0	12 (2-52)	Subset of 7 patients with PBrT dose reported
Kilburn ¹³⁰	60	18 (6-61)	0	0	17 (NR)	Subset of 19 patients who had cumulative doses recorded
Sumita ¹²⁴	128	26.8 (11.4-92.3)	5	0	22.1 (2.3-56.4)	D1cc and D10cc cumulative dose so approximation of Dmax
Binkley ²²⁰	63.4 (1.3-228.3)	16.5 (1-71)	31.6	0	17 (3-57)	4 excluded due to multiple courses of re-irradiation
Repka ²³²	128	NR	NR	100	35	single report of haemoptysis
Griffioen ¹¹⁴ /Tetar ¹²³	124.6 (124.6-130)	NR	NR	100	NR	Estimated from two reports of central re-treatments
Peulen ¹⁴⁵	196.4 (192-240)	13 (12-36)	0	100	3 (1.5-10)	
Ogawa ²²³	226.7 (1.7-322.3)	NR	0	0	26 (5.5-111)	

5.3.6.1 Dose toxicity model

The complete dataset is summarised in Table 5.37. There are 10 \geq G3 events and 154 patients. The lowest \geq grade 3 toxicity was seen at a cumulative Dmax of 124.6 EQD2 Gy and at an interval of 12 months.

Table 5.37 Summary of proximal bronchial tree dataset. Dmax: maximum dose received to an organ at risk

		Missing values
Number of trials:	13	
Number of patients:	154	
Number of \geq Grade 3 events	10	
Median interval from initial treatment and re-irradiation	18 months (1-124)	4
Median rate of concurrent chemotherapy	0 (0-1)	52
Median cumulative Dmax (range)	87.4Gy (1.3 - 240)	0

There is a significant difference in the rate of toxicity between the cumulative Dmax and interval where split at the median value, but there is no significant difference with use of concurrent chemotherapy (Table 5.38).

Table 5.38 Results of Fisher's exact tests when the dataset is divided using median values. This table includes imputed data. cumEQD2: cumulative equivalent dose in 2-Gray fractions

	No toxicity	Toxicity	P-value
Median cumEQD2 (n=154)			
\leq 87.4	69	0	
$>$ 87.4	75	10	
			0.002*
Median interval (n=154)			
\leq 18	104	2	
$>$ 18	40	8	
			0.001*
Median chemotherapy rate (n=102)			
\leq 0	94	3	
\geq 0	5	0	
			1

There was no significant increase in relative risk as the dose increased. This was due to the reference group (cumulate Dmax 120-130) having a similar rate of toxicity as the group >130Gy (Table 5.39). However, toxic events were only seen beyond a cumulative dose of 120Gy suggesting that this dose may be a promising initial cut-off.

Table 5.39 Relative risk table for the complete proximal bronchial tree dataset. CI: confidence interval, EQD2 Gy: equivalent dose in 2-Gray fractions

Range (EQD2 Gy)	Number	Grade 3+ events	Relative risk	Lower 95% CI	Upper 95% CI	P-value
<120	84	0	0	0	NA	NA
120-130	27	4	1	0.28	3.59	1
>130	43	6	0.94	0.29	3.03	0.93

The interval was significant on univariable logistic regression. The cumulative Dmax had a p-value <0.2 and so also was included in a multivariable model. Both variables were significant in the multivariable model (Table 5.40).

Table 5.40 Results from univariable and multivariable modelling (using the imputed data). This table includes imputed data. cumDmax: cumulative maximum dose to an organ at risk.

Predictor	Toxicity	P-value	Number
Univariable modelling results			
Interval	Grade ≥ 3	0.007*	154
Chemotherapy	Grade ≥ 3	0.996	102
cumDmax	Grade ≥ 3	0.091	154
Multivariable modelling results			
Interval	Grade ≥ 3	0.007*	154
cumDmax	Grade ≥ 3	0.050*	

Leave one out cross validation was used to compare the fit of the cumEQD2 univariable model and the cumEQD2/interval multivariable model. The MV model had a better fit to the data with a LOOCV score of 89.97 compared to the UV model (108.25). The multivariable model expression is :

$$P(\geq G3 \text{ toxicity} | X_1, X_2) = \Phi(-6.0611 + 0.0117X_1 + 0.0710X_2)$$

Where X_1 is cumulative Dmax EQD2 and X_2 is the interval. The multivariable model predicts a 5% toxicity rate at a cumulative EQD2 Dmax of 157.5Gy (95%CI 86.99, 228.11) when the interval is set to the median (18 months). The block

bootstrapped 95% CI is -367.21, 740.94 EQD2 Gy. If the interval value is extended to 36, the 5% toxicity rate is estimated at a cumEQD2 of 48.12Gy (95% CI -67.54 - 163.78). This model therefore suggests that a longer interval is associated with lower radiation tolerance. The model is plotted in Figure 5.18 using the median interval (18 months).

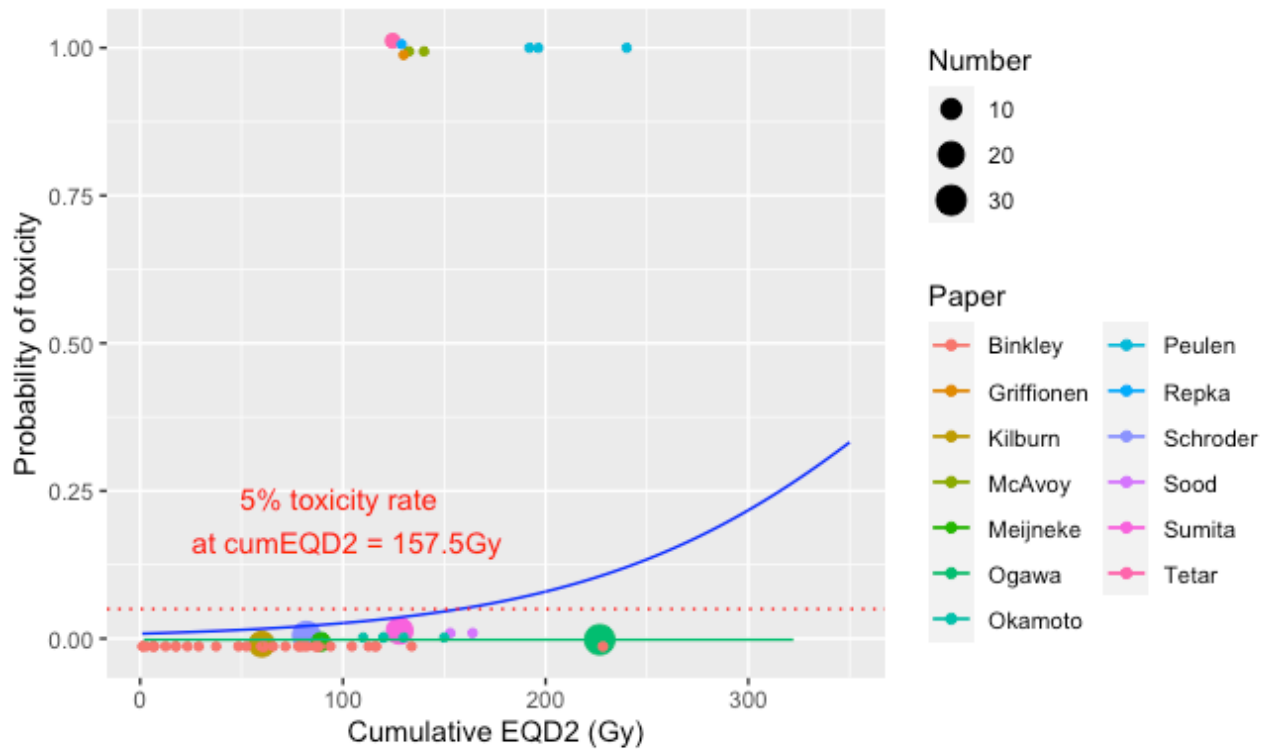


Figure 5.18 Plot of the proximal bronchial tree multivariable model. The blue line is the fitted regression model, and the red dotted line indicates the 5% toxicity level. The dots represent the toxicity rate from each cohort or individual coded by colour, with the size of the dots proportional to the number of patients in the study, vertical bars are the 68% binomial confidence interval, horizontal bars represent the range of the doses, due to overlapping data points, the scatter plot has been jittered. The median interval value was used (18 months).

An exploratory multivariable model with interval and cumulative dose was made that excluded the four cases where toxicity occurred but no interval data was available. This model had only six toxic events and predicted a 5% toxicity rate at a cumulative EQD2 Dmax of 200.1Gy (95%CI 146.45 - 253.72) when the interval is set to the median (18 months).

5.3.6.2 Development of proximal bronchial tree constraints

The imputed PBrT multivariable model estimated the dose that gives a 5% rate of toxicity at 157.5 EQD2 Gy. When this dose is used to calculate the risk using the 2000 block bootstrapped samples, the 95% CI for risk is <0.1% to 60.4%. Due to the influence of the interval on the equation, the minimum bootstrapped risk was 8.5% when the interval was 18 months, and this was reached at a dose of 90Gy. The non-imputed multivariable model estimates a 5% rate of toxicity at 200.1 EQD2 Gy, and the dose that gives a maximum bootstrapped toxicity rate of 5% is 125.6Gy, using an interval of 18 months. The results are summarized in Table 5.41.

Table 5.41 Development of proximal bronchial tree constraints using block bootstrapping. CI: confidence interval, EQD2 Gy: equivalent dose in 2-Gray fractions

Model	Model dose (EQD2 Gy)	Risk	95% CI lower limit risk (%)	95% CI upper limit risk (%)
Imputed multivariable model (18-month interval)				
	157.5	5%	<0.1	60.4
	90	Maximum 8.5%	<0.1	8.5
Non-imputed multivariable model (18-month interval)				
	200.1	5%	<0.1	100
	125.6	Maximum 5%	<0.1	5

5.3.6.3 Evaluation of proximal bronchial tree model and suggested constraints

The Hosmer Lemeshow test for the imputed model had a p-value 0.02 suggesting a poor fit. However, the Pearson correlation coefficient suggests a good fit with an R-value of 0.79 (p-value <0.01). The predicted and observed toxicity rates by decile plot is shown in Figure 5.19. The model 5% dose predictions and the bootstrapped 8.5% maximum constraint were tested against the dataset the model was derived from, a data subset with only the patient level information was provided and the external Beatson cohort. The toxicity rates above and below the suggested dose constraints are summarised in Table 5.42, Table 5.43 and Table 5.44. The 157.5Gy constraint gives a higher than 5% risk in the patient level and overall datasets, whilst the 90Gy constraint has no toxicity in any

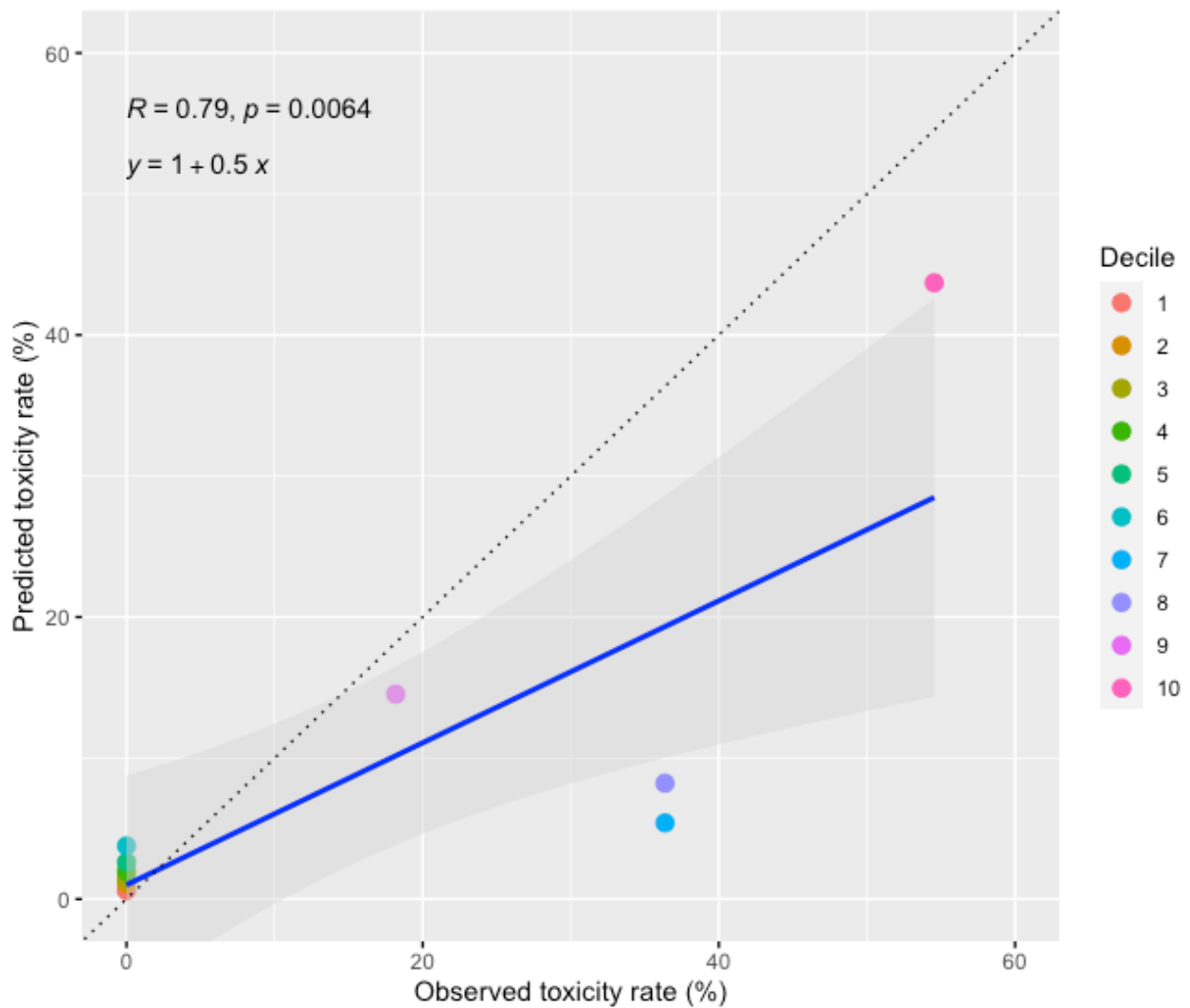


Figure 5.19 Plot of the actual and predicted imputed PBRT model toxicity rates. The blue line is the line of best fit, with the shaded grey area the 95% confidence interval. The black dotted line represents the line of unity. The dots represent the toxicity rate from each decile.

datasets. Therefore, the maximum likelihood dose (157.5Gy) is too aggressive and the 5% maximum dose (90Gy) is too conservative. As a compromise, 115Gy was selected to be explored as a potential dose constraint, on the basis that it is slightly less than the lowest dose where toxicity was observed of 119Gy (in the Beatson validation dataset or the dataset derived from published studies). The model toxicity prediction for 115Gy (using a median of 18 months) is 3.1% (95% CI 1.1%, 8.3%). This exploratory constraint continues to offer good discrimination between the rate of toxicity above and below it (0% toxicity below 115Gy) but allows the re-irradiation dose to be increased by 25Gy with minimal increase in the toxicity risk.

Table 5.42 Testing proximal bronchial tree dose constraints on complete dataset. (Based on 154 patients).

	Number with no toxicity	Number with toxicity	Toxicity rate (%)
Multivariable model 5% toxicity			
≤157.5 Gy	111	7	5.9
>157.5 Gy	33	3	8.3
Multivariable model maximum 8.5% toxicity			
≤90 Gy	78	0	0
>90 Gy	66	10	13.2
Lowest observed dose			
≤115 Gy	82	0	0
>115 Gy	62	10	13.9

Table 5.43 Testing proximal bronchial tree dose constraints on individual dataset. (Based on 49 patients).

	Number with no toxicity	Number with toxicity	Toxicity rate (%)
Multivariable model 5% toxicity			
≤157.5 Gy	40	4	9.1
>157.5 Gy	2	3	60
Multivariable model maximum 8.5% toxicity			
≤90 Gy	28	0	0
>90 Gy	14	7	33.3
Lowest observed dose			
≤115 Gy	32	0	0
>115 Gy	10	7	41.2

Table 5.44 Testing proximal bronchial tree dose constraints on external Beatson cohort. (Based on 39 patients).

	Number with no toxicity	Number with toxicity	Toxicity rate (%)
Multivariable model 5% toxicity			
≤157.5 Gy	38	1	2.6
>157.5 Gy	0	0	0
Multivariable model maximum 8.5% toxicity			
≤90 Gy	31	0	0
>90 Gy	7	1	12.5
Lowest observed dose			
≤115 Gy	33	0	0
>115 Gy	5	1	16.7

5.3.6.4 Proximal bronchial tree discussion

A multivariable model with two predictors, EQD2 Dmax to the proximal bronchial tree and the interval between treatments, was developed using the proximal bronchial tree dataset. It found the longer the interval, the lower the re-irradiation tolerance. The 95% confidence interval for the dose prediction from the model was extremely wide, suggesting that the uncertainties were so large that any prediction would be inaccurate. Therefore, as the lowest dose toxicity was observed at was 119Gy, a slightly reduced constraint of 115Gy was explored as a constraint. This dose discriminated well between toxicity in the collected data and in the external validation data, with the benefit of increasing the scope of the dose that could be delivered at re-irradiation, but also maintaining similar risk.

Assuming that the longer the time interval, the more sensitive the PBrT is to re-irradiation is a true effect, pre-clinical evidence is lacking to describe the recovery of the proximal bronchial tree. One explanation could be that, as the bronchial tree is cartilage, that the cellular turnover is slow, and any effect of radiotherapy on the stem cells of the tissue, would take time to manifest. Alternatively, this finding may be an error of the model process or a result of the large number of statistical tests performed on the data. The effect of the interval on the model remains small and may not be of significance. There are only 10 events in the model, and a low number of events are more likely to generate unreliable models¹⁸⁷. Furthermore, the extremely wide block bootstrapped confidence intervals indicate that the data is overdispersed and has a large degree of variability between studies.

Four cases which had toxicity had interval data imputed from the source studies. The median values of those studies may be misleading as the range of the time interval for both papers were broad (the median intervals and ranges for Repka *et al.* and Tetar *et al.* were 23.3 (2.6 - 93.6) and 29.7 (5 - 189) months respectively). Another possibility is that there is confounding in the dataset. The interval between initial radiotherapy and re-irradiation is proportional to survival after re-irradiation. The patients who had longer intervals may have lived longer after re-irradiation, and by having longer follow-up, experienced more late toxicity than patients who had shorter follow-up. However, as most

toxicities in the dataset occurred within 9 months, it is unlikely that longer overall survival would change the detection of toxicity.

If the interval is removed from the model, and univariable modelling using cumulative EQD2 as the sole predictor variable on the complete dataset is performed, the 5% toxicity rate is predicted at 154.67 Gy which is similar to the dose predicted with the multivariable model using an 18 month interval.

Four studies had the toxic events included in the model. McAvoy *et al.* treated 33 patients with proton re-irradiation, two of whom developed tracheal necrosis. The length of trachea involved at re-irradiation was 2.5cm and 4.25cm¹²². Peulen *et al.* and Repka *et al.* reported 4 patients with haemoptysis after SABR re-irradiation^{145,232}. Griffioen and Tetar *et al.* described 4 patients who died from haemoptysis after conventionally fractionated radiotherapy^{114,123}. In these patients, alternative causes of haemoptysis were not explored as no autopsies were performed. This would have been important to rule out tumour recurrence as an alternative cause of fatal bleeding. Therefore, re-irradiation may not be the cause of all the toxicities described.

There was a large difference between the model developed using imputed data for four toxic events, and the model that excluded those events. The four cases developed toxicity between 124 and 129 EQD2 Gy. The imputed model suggested a 5% toxicity rate at 157.5Gy accounting for these cases, whereas the non-imputed model predicted 5% toxicity at 200.1Gy. The difference between the imputed and non-imputed models indicates that the proximal bronchial tree may tolerate higher cumulative doses. From the data available, the 10 toxic events occurred at doses ranging from 124.6Gy to 240Gy EQD2, and the toxic event in the external Beatson cohort occurred at 119Gy. Most of these doses are far exceeded by the non-imputed model's prediction of 200.1Gy. This suggests that the non-imputed model is underestimating the toxicity rate when compared to the published data. Therefore, in clinical practice, a cautious approach using the lower dose constraints may be warranted.

In summary, for patients having re-irradiation, the model predictions have a high degree of uncertainty therefore limiting the cumulative Dmax to the proximal

bronchial tree to 115Gy based on empiric evidence is likely to have a <5% toxicity rate and can be considered a safe re-irradiation constraint.

5.3.6.5 Conclusions

A multivariable proximal bronchial tree dose/toxicity model was created using data imputation for four cases. The multivariable model predicted lower re-irradiation tolerance the longer the time interval between treatments. The multivariable model predicted a 5% toxicity risk at a cumulative EQD2 Dmax of 157.5Gy (with interval at the median 18 months). The model predicted a 3.1% risk of toxicity with an exploratory constraint of 115Gy. When applied to the overall and external datasets, this constraint had no toxic events suggesting that this dose gives a <5% risk of \geq G3 toxicity and would be reasonable to use as a constraint.

5.3.7 Models for aorta

Aorta models were created using a dataset based on 7 studies summarised in Table 5.45 and Table 5.46 with a total of 142 patients. The data in the studies were collected between 1993 - 2017. The dataset included patients who had been treated with SABR twice, conventionally fractionated radiotherapy twice, or a combination. The lowest dose Grade 3 toxicity was seen was at 114.3Gy and the shortest interval was 3 months.

There were no missing interval data. There were 75 cases that had missing concurrent chemotherapy data. The missing data group had a higher mean EQD2 (109.41) compared to the complete data group (90.64Gy, student's t-test p-value 0.004). The rate of toxicity was not significantly different between the chemo missing and chemo complete dataset (complete data 2/67, incomplete data 2/75, Fisher's exact p-value 1).

Table 5.45 List of studies used to form the aorta dataset. The total number of patients included is 142, from 7 studies. 3D-CRT: three-dimensional conformal radiotherapy, BED: biologically equivalent dose, EQD2: equivalent dose in 2 Gray fractions, Fr: fractions, NR: not recorded, Re-RT: re-irradiation, SABR: stereotactic ablative radiotherapy.

Paper	n	Individual data/Grouped	Treatment span	Initial prescription dose/fr	Re-RT prescription dose/fr	Re-RT Technique
Evans ¹⁷⁹	35	Grouped	1993-2008	54 (45-70)/30 (15-58)	60 (30-70)/30 (10-42)	NR
Trombetta ²³⁴	1	Individual	1998-2008	114Gy brachytherapy	45/25	3D-CRT
Schroder ²⁰⁸	19	Grouped	2011-2017	NR	NR	SABR
Sumita ¹²⁴	21	Grouped	2007-2014	EQD2 median 60 (43.1--87.5)Gy (10)	EQD2 median 60 (50-87.5)Gy (10)	Conventional 90%, Proton 10%
Kilburn ¹³⁰	1	Individual	2001-2012	74Gy	54/3	SABR
Binkley ²²⁰	34	Individual	2008-2014	median 50 (20-74)Gy/median 4.5 (1-37)fr	median 50 (20-177.5)Gy/median 4 (1-54) fr (including multiple re-RT courses)	SABR 73.7%, Conventional 26.3%
Ogawa ²²³	31	Grouped	2004-2017	BED median 112.5 Gy (10) (75-119.6)	BED median 105 Gy (10) (64.2-119.6)	SABR

Table 5.46 List of studies used to form the aorta dataset. cumDmax: cumulative dose received to a given organ at risk, DVH: dose-volume histogram, D_{xxx}: maximum dose to an organ at risk to a volume of xxx, EBRT: external beam radiotherapy, EQD2: equivalent dose in 2 Gray fractions, Fr: fraction, f/u: follow-up, NR: not recorded, Re-RT: re-irradiation.

Paper	Median cumDmax (EQD2 Gy)	Interval (months, range)	Chemo % rate with re-RT	Any Grade 3-5 toxicity (%)	F/u post re-RT (months, range)	Uncertainty
Evans ¹⁷⁹	100.3	30 (1-185)	60	5.7	42 (14-70)	Converted normalised isoeffective doses with recovery factor, so approximate Aorta D1cc dose
Trombetta ²³⁴	154.4	3	0	100	19	Brachytherapy implant then EBRT 3 months afterward - dose estimated from data
Schroder ²⁰⁸	79.1 (70.9 - 216.1)	14 (2-184)	0	0	13 (1-45)	Uses a subset of the original 42 patients, interval and follow up for whole group
Sumita ¹²⁴	152	26.8 (11.4-92.3)	5	0	22.1 (2.3-56.4)	D1cc and D10cc cumulative dose so approximation of Dmax
Kilburn ¹³⁰	200	12	0	100	6	Estimate of cumDmax EQD2 based on DVH
Binkley ²²⁰	44.6 (2.3 - 211.4)	16.5 (1-71)	31.6	0	17 (3-57)	4 excluded due to multiple courses of re-irradiation
Ogawa ²²³	111.1 (9.3 - 317.1)	NR	0	0	26 (5.5-111)	

5.3.7.1 Dose toxicity models using the complete dataset

The complete dataset is summarised in Table 5.47. There are 4 \geq G3 events and 142 patients. This is low number of events and is less than the 10% event rate which is commonly applied as a minimum number of events required to generate robust models using logistic regression. There were no significant differences in the rate of toxicity when each variable was split by its median value (Table 5.48). However, there was a significant nine times increase in relative risk when the dose to the aorta was over a cumulative EQD2 of 160Gy compared to the reference dose group between 80-120Gy (Table 5.49). The increase in risk as dose increases implied a strong relationship may exist despite the low event rate and was explored further using logistic modelling.

Table 5.47 Summary of complete aorta dataset. Dmax: maximum dose received to an organ at risk, EQD2: equivalent dose in 2-Gray fractions.

		Missing values
Number of trials:	7	
Number of patients:	142	
Number of \geq Grade 3 events	4	
Median interval from initial treatment and re-irradiation (range)	18 months (1-71)	0
Median rate of concurrent chemotherapy	0	75
Median cumulative Dmax (EQD2 Gy, range)	100.3Gy (2.3 - 211.4)	0

Table 5.48 Results of Fisher's exact tests when the complete dataset is divided using median values. cumEQD2: cumulative equivalent dose in 2-Gray fractions.

	No toxicity	Toxicity	P-value
Median cumEQD2			
\leq 100.3	81	2	
$>$ 100.3	57	2	
			1
Median interval			
\leq 18	70	2	
$>$ 18	68	2	
			1
Chemotherapy rate (%)			
0	62	2	
$>$ 0	5	0	
			1

Table 5.49 Relative risk table for the aorta dataset by dose. CI: confidence interval, EQD2 Gy: equivalent dose in 2-Gray fractions, NA: not applicable.

Dose range (EQD2 Gy)	Number	Grade 3+ events	Relative risk	Lower 95% CI	Upper 95% CI	P-value
<40	13	0	0	0	NA	NA
40-80	29	0	0	0	NA	NA
80-120	72	2	1	0.14	6.91	1
120-160	24	1	1.5	0.14	15.82	0.11
>160	4	1	9	1.02	79.55	0.05

The cumulative EQD2 aorta Dmax was close to significance on univariable logistic regression modelling, with no other variables having a p-value of <0.2 (Table 5.50). As this was the only variable that was significant, this model was used for dose predictions.

Table 5.50 Summary of complete aorta dataset univariable modelling. cumEQD2: cumulative equivalent dose in 2-Gray fractions.

Predictor	Toxicity	P-value	Number
Univariable modelling results			
Interval	Grade ≥ 3	0.474	142
Chemotherapy	Grade ≥ 3	0.996	75
cumEQD2	Grade ≥ 3	0.052	142

The model expression is:

$$P(\geq G3 \text{ toxicity} | X) = \Phi(-6.4692 + 0.0247X)$$

Where X is cumEQD2. The 5% toxicity estimate is 142.53Gy (95% CI 100.94 - 184.13). The block bootstrapped 95% CI is -880.47, 400.93Gy. The model is plotted in Figure 5.20.

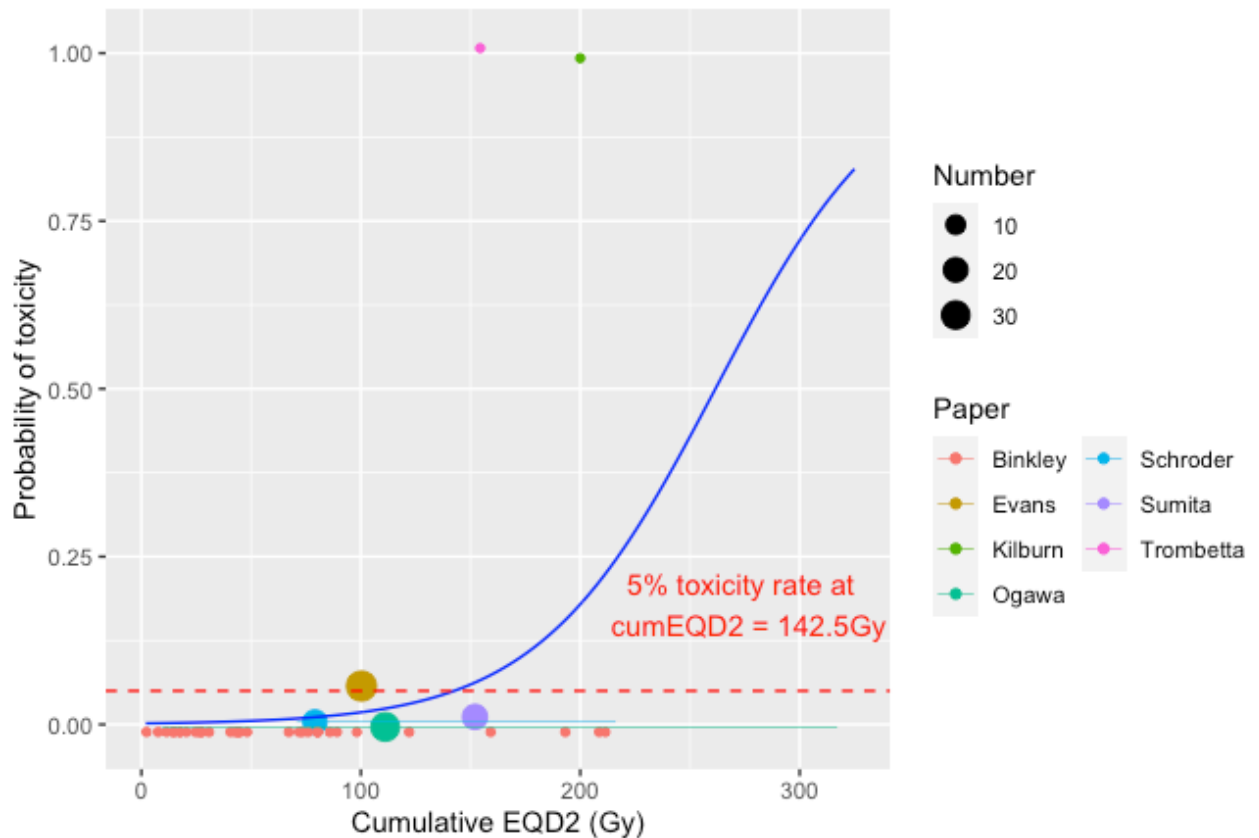


Figure 5.20 Plot of cumulative aorta EQD2 Dmax univariable model. The blue line is the fitted regression model, and the red dotted line indicates the 5% toxicity level. The dots represent the toxicity rate from each paper coded by colour, with the size of the dots proportional to the number of patients in the study, vertical bars are the 68% binomial confidence interval, horizontal bars represent the range of the doses, due to overlapping data points, the scatter plot has been jittered.

5.3.7.2 Development of aorta dose constraints

The aorta univariable model estimated the dose that gives a 5% rate of toxicity at 142.5 EQD2 Gy. When this dose is used to calculate the risk using the 2000 block bootstrapped samples, the 95% CI for risk is <0.1% to 100%. The upper limit of risk for the block bootstrapped samples was fixed at 5% and the highest dose which meets this criterion is 100.17Gy (95% CI for risk of 0.0% to 5%). The results are summarized in Table 5.51.

Table 5.51 Development of aorta constraints using block bootstrapping. CI: confidence interval, EQD2 Gy: equivalent dose in 2-Gray fractions.

Model	Model dose (EQD2 Gy)	Risk	95% CI upper limit risk (%)	95% CI lower limit risk (%)
Univariable model				
	142.1	5%	0.1	10.5
	100.2	Maximum 5%	0.0	5

5.3.7.3 Evaluation of aorta model and suggested constraints

The Hosmer Lemeshow test for the aorta model had a p-value of 0.94 suggesting that the model did fit the data well. The predicted and observed toxicity rates by decile is plotted in Figure 5.21. The Pearson correlation coefficient was 0.84 (p-value <0.01) which indicated a good model fit.

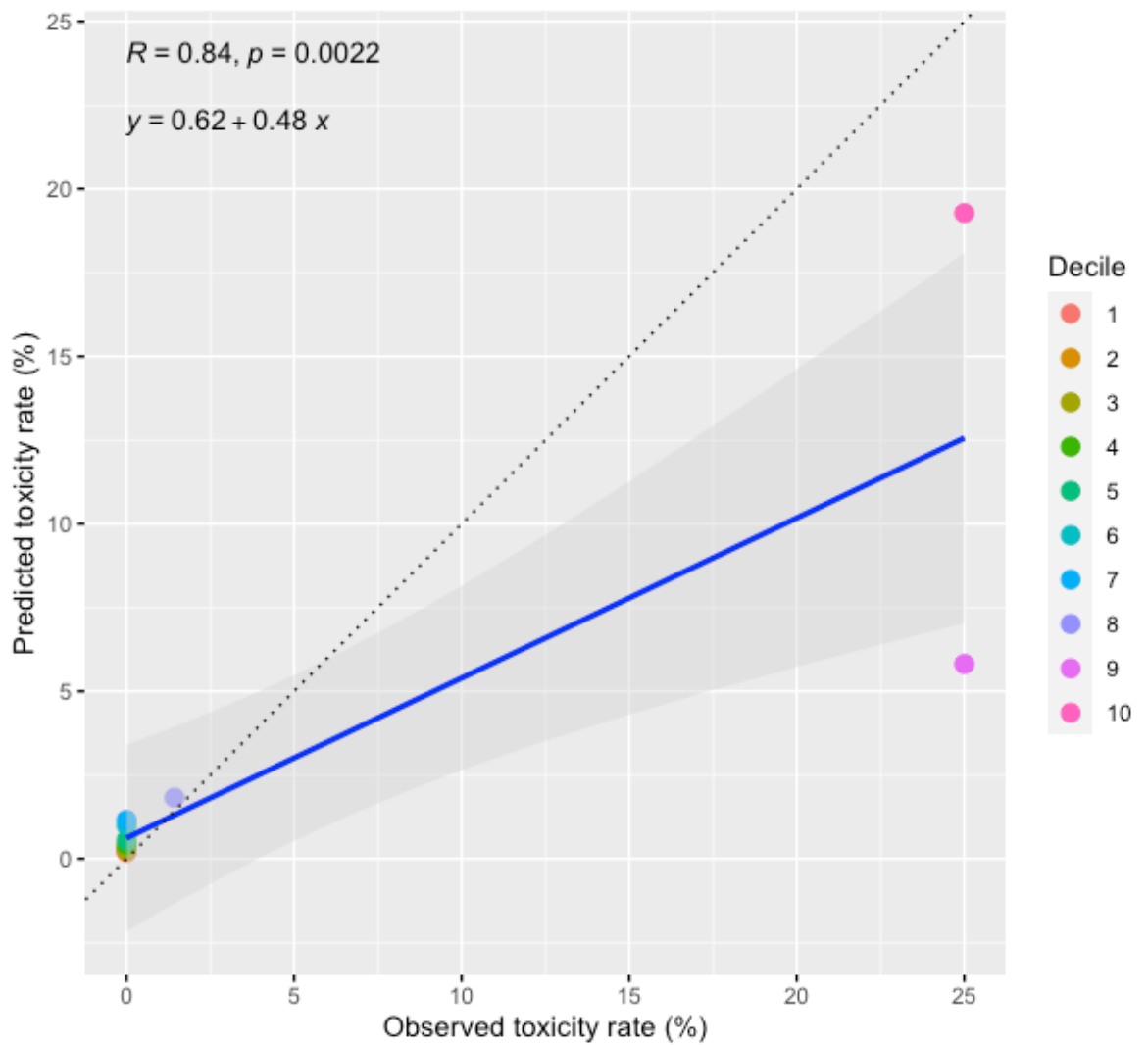


Figure 5.21 Plot of the actual and predicted aorta model toxicity rates. The blue line is the line of best fit, with the shaded grey area the 95% confidence interval. The black dotted line represents the line of unity. The dots represent the toxicity rate from each decile.

The model prediction doses for 5% toxicity and the maximum 5% toxicity from the bootstrapped samples were applied to the complete dataset, the individual data subset and the external Beatson cohort. The results are summarised in Table 5.52 and Table 5.53. When the 5% maximum toxicity dose of 100.2Gy was used as a constraint, it had a toxicity rate of <5% when in all datasets, whereas the higher 5% model prediction of 142.5Gy had a rate of 6.3% in the individual dataset. There was no aortic toxicity in the external Beatson cohort therefore the model predictions could not be validated using that dataset.

Table 5.52 Testing aorta dose constraints on complete dataset.

	Number with no toxicity	Number with toxicity	Toxicity rate (%)
Univariable model 5% toxicity			
≤142.5 Gy	113	2	1.7
>142.5 Gy	25	2	7.4
Univariable model maximum 5% toxicity			
≤100.2 Gy	48	0	0
>100.2 Gy	90	4	4.3

Table 5.53 Testing aorta dose constraints on individual dataset.

	Number with no toxicity	Number with toxicity	Toxicity rate (%)
Univariable model 5% toxicity			
≤142.5 Gy	30	0	0
>142.5 Gy	4	2	33.3
Univariable model maximum 5% toxicity			
≤100.2 Gy	29	0	0
>100.2 Gy	5	2	28.6

5.3.7.4 Aorta model discussion

A univariable model was derived from the aorta dataset with cumulative dose being the only significant predictor. Critically, the number of events is low in the aorta dataset. For a univariable model, a minimum of 10 events should be included, otherwise the models are prone to error²³⁵. Therefore, the model predictions have extremely wide confidence intervals and the maximum likelihood prediction of 142.5Gy is unlikely to be useful. However, where the model is helpful is when the upper limit of the confidence limit is limited to 5%, the dose of 110.2Gy can be considered safe. This prediction is slightly lower than the suggested dose limits from the expert groups, who suggested a maximum dose of 110 - 120Gy. Hunter *et al.* divided their dose limits into 110Gy for the pulmonary artery and 120Gy for the aorta¹⁶¹. This may be because the aorta wall is thicker than the pulmonary artery. A study of re-irradiation in recurrent head and neck cancer looked at 381 patients, 32 of whom had carotid blowout syndrome (8.4%)²³⁶. The estimated median cumDmax EQD2 to the carotid was 134Gy, although on multivariable modelling, the dose was not a significant factor when split into groups above and below and EQD2 of 117Gy. These data were not included in the modelling dataset as the carotid artery is different to

the aorta. However, it implies that the cumulative dose to major arteries lies similar to the dose constraint suggested from the modelling. The most compelling evidence specific to aorta doses comes from Evans *et al.*, who found that a cumulative aortic dose $\geq 120\text{Gy}$ is associated with a 25% risk of grade 5 toxicity, in a dataset of 35 patients, which is similar to the current analysis¹⁷⁹.

The four toxic events in the dataset are derived from three papers. Evans *et al.* reported two grade 5 bleeding events from a cohort of 35 patients¹⁷⁹. The two patients died from massive haemoptysis with no evidence of recurrent tumour on imaging. This study reported the cumulative dose to D1cc, therefore the Dmax could be higher. Trombetta *et al.* described one fatal bleeding event where the Iodine¹²⁵ brachytherapy implant and external beam radiation overlapped, leading to a aorta dose of approximately 154.4Gy ²³⁴. Kilburn *et al.* reported an aorto-oesophageal fistula after SABR to the thorax and a cumulative dose of 200Gy . Given the severe nature of the toxicity, a 5% toxicity rate may be considered too high. However, the model prediction for a 1% toxicity rate is 75.8Gy (95% CI 2.5, 149.1Gy) which may be too restrictive in terms of the ability to deliver a dose for meaningful tumour control.

The model fitted the data well when measured using the Hosmer Lemeshow test and Pearson correlation coefficient. However, these results should be viewed cautiously. Most of the data had no toxic events and the model appropriately gave a low risk to. For the deciles where the 4 toxic events were, the model also gave reasonable predictions. However, with such a small number of toxic events in a small dataset (each decile was 14 patients in number), if any additional information was added, this could significantly alter the results. The block bootstrapping method highlighted the wide variety across different centres in terms of and follow-up, resulting in extremely wide bootstrapped confidence intervals. Nevertheless, the suggested constraint of 100.2Gy (using the bootstrapped samples) does seem to be a reasonable cut-off when applied to the complete and individual datasets, with no toxicity below it, and a 4.2% rate above it, close to the 5% rate the model predicted. This dose constraint may be over cautious, with the lowest dose toxicity seen in the studies at an EQD2 of 114.3Gy . The collected data had 82 patients treated with a dose less than 100Gy with no toxicities, which suggests that this limit is safe. When 114.3Gy was used

as a cut off, the toxicity rate in the dataset below this dose was 1.8% (2 events out of 114 patients). The expert consensus suggests a dose of 120Gy, likely to be based on the Evans *et al.* paper, which used 35 patients. The model for this higher dose gives a 95% confidence interval upper limit of 8.2%. On balance however, given the severity of the toxicity seen, and the relatively small numbers in the Evans paper, a more cautious cut off seems reasonable.

Sources of inaccuracy in the data include slightly different metrics to describe the dose to the aorta in Sumita *et al.* (D1cc and D10cc) and Evans *et al.* (D1cc) which may underestimate the Dmax dose^{124,179}. A potential source of inaccuracy that applies to all the dataset is the dose to the aorta ideally should consider the aorta wall, as this is the part of the organ that fails. It is possible that the cumulative Dmax falls in the lumen of the aorta i.e., in the bloodstream, and the actual dose to the wall is lower. This is of relevance to highly conformal treatments like SABR. However, given the small diameter of the aorta, it is unlikely to have a significant change in the reported dose.

In summary, the low number of events make the dose/toxicity models for the aorta prone to error. Given the severity of aortic toxicity, it is prudent to limit the dose to below 100.2Gy based on the 5% maximum toxicity bootstrapped dose.

5.3.7.5 Conclusion

A univariable model was created from the aorta dataset with the predictor variable of cumulative dose. The 5% model toxicity and the bootstrapped maximum 5% risk are predicted at a dose of 142.5Gy and 100.2Gy respectively. The 100.2Gy dose constraint gave a rate of <5% toxicity on all the datasets it was applied to and would be reasonable to use as a re-irradiation dose constraint.

5.3.8 Thoracic organs at risk not modelled

5.3.8.1 Brachial plexus

The dataset for the brachial plexus included three studies and 98 patients (Table 5.54). There were 13 any grade events of brachial plexopathy. The main paper in the dataset was Chen *et al.* which analysed 43 patients after high dose re-

irradiation for head and neck cancer¹⁸⁰. They found 12 ungraded toxicities using a questionnaire at follow-up appointments. 85% of the toxic events were sensory (pain/numbness) and 15% were motor deficits. No effects on activities of daily living were recorded, therefore the toxicities were unable to be graded using the CTCAE toxicity scale. They created a model suggesting patients with low risk of any toxicity (approximately 9%) in patients where the interval between treatment was >2 years and the cumulative EQD2 Dmax was <95Gy, and a high-risk group where the interval was <2 years and the cumulative EQD2 Dmax was >95Gy (47% risk of toxicity). They also found that dose was not associated with toxicity when evaluated as either a categorical or continuous variable.

Table 5.54 Summary of the brachial plexus dataset. Dmax: maximum dose to an organ at risk.

		Missing values
Number of trials:	3	
Number of patients:	98	
Number of any grade events	13	
Median interval from initial treatment and re-irradiation	23 months (1-145)	0
Use of concurrent chemotherapy	5/55 (9.1%)	43
Median cumulative Dmax (range)	47.6Gy (0 - 242.5)	0

Binkley *et al.* reported a G3 brachial plexopathy in a patient who had conventional radiotherapy followed by SABR²²⁰. The brachial plexus received a D0.2cc of 242.5Gy (EQD2).

Modelling was not performed on this dataset for the following reasons. The imprecision of toxicity grades would make any model result difficult to interpret and potentially may suggest a low dose. If clinicians were to use an inappropriately low dose constraint, then they could under-dose the tumour and fail to provide local tumour control. In addition, the bulk of the toxicity data comes from head and neck patients who may have had prior surgery. Therefore, the dataset does not represent patients undergoing thoracic re-irradiation.

In summary, the toxicity model suggested by Chen *et al.* is a reasonable toxicity model to apply to thoracic re-irradiation, in the absence of thorax specific data. This is similar to the dose limits suggested by the expert groups.

5.3.8.2 Chest wall

The chest wall dataset consists of three studies using 62 patients (Table 5.55). There was one G3 chest wall pain reported at 193.3Gy in a patient who had SABR for a recurrent lung cancer. Due to the low number of events, dose/toxicity modelling was not performed. One expert group recommended limits to the chest wall at D0.1cc <116Gy¹¹².

Table 5.55 Summary of the chest wall dataset. Dmax: maximum dose to an organ at risk.

		Missing values
Number of trials:	3	
Number of patients:	62	
Number of Grade ≥ 3 events	1	
Median interval from initial treatment and re-irradiation	18.4 months (1-71)	1
Use of concurrent chemotherapy	5/19 (26.3%)	43
Median cumulative Dmax (range)	93.3Gy (0.3 - 193.3)	0

5.3.8.3 Heart

There were five studies that reported cumulative EQD2 Dmax to the heart with 129 patients (Table 5.56). The median dose delivered was 62Gy. However, none of the studies reported major adverse cardiovascular events or pericarditis therefore modelling was impossible.

The expert groups have suggested a range of different heart constraints. Paradis *et al.* suggested a dose constraint of D0.1cc 86.1Gy, Troost *et al.* used a Dmax <70Gy in their study while the American Radium Society recommend a V40<50%^{112,146,160}. None of the expert groups provided study data to support their recommendations. An added complication is that a heart dose constraint has not been adopted for initial radiotherapy, although 85Gy has been suggested¹⁸⁶.

Table 5.56 Summary of the heart dataset. Dmax: maximum dose to an organ at risk

		Missing values
Number of trials:	5	
Number of patients:	129	
Number of any grade events	0	
Median interval from initial treatment and re-irradiation	18 months (1-71)	0
Use of concurrent chemotherapy	5/108 (4.6%)	21
Median cumulative Dmax (range)	62Gy (0.2 - 118.3)	0

5.4 Discussion

5.4.1 Main findings

Thoracic re-irradiation dose/toxicity models have been developed for the lungs, oesophagus, spinal cord, proximal bronchial tree and aorta. There was insufficient data to create models for the brachial plexus, the chest wall and the heart. Table 5.57 summarises the expert groups suggested dose limits, the lowest dose where toxicity occurred from each dataset, and the bootstrapped doses that predict the maximum 5% toxicity rate (20% for lung) with 95% confidence. The bootstrapped doses form the basis of possible re-irradiation dose constraints. Table 5.58 uses the models created to predict the risk of toxicity using the maximum expert groups dose limits for each OAR.

The suggested constraints are similar to the expert dose recommendations in the case of the spinal cord and lung. In the lung re-irradiation models, the toxicity rates exceed 20% when the cumulative doses exceed those which are recommended for initial radiotherapy (e.g. MLD<22Gy and V20<30-35%). This suggests that there is no or little recovery of tolerance in the lung, therefore dose constraints used for initial radiotherapy should be adhered to. The highest cumulative V20 dose constraint (a cumulative V20 of $\leq 40\%$) predicts a $\geq G3$ toxicity rate of 60.7% and is likely to be considered too dangerous. The proximal bronchial tree constraint at 119Gy is higher than the expert recommendations (<110Gy). The oesophageal and great vessels constraints are lower than the expert recommendations, both by 15-20Gy. The oesophageal model suggests that the 5% toxicity rate is at a lower dose than the maximum dose suggested by the expert panels (94.2Gy compared to 110Gy). The oesophageal model predicts a

9.4% risk of \geq G3 risk of toxicity if re-treating to 110Gy reflecting the shallow gradient of the model fit. The great vessel constraint is 100.2Gy, although the expert recommendation of <120Gy has \geq G3 toxicity rate of 2.9%.

There are no clear guidelines on how to develop dose constraints. The dose constraints used in conventional fractionation are based in a combination of normal tissue complication probability modelling, such as the QUANTEC series of papers, clinical trials and clinical experience. This process is demonstrated in the development of SABR dose constraints. The first dose constraints for SABR were the AAPM 101 guidelines which were “based on toxicity observation and theory, there is a measure of educated guessing involved as well.”²³⁷ The UK SABR consortium published dose constraints in 2018 based on these and then updated in 2022 with the 2021 HyTEC modelling data paper²³⁸⁻²⁴⁰. Throughout these landmark publications, studies such as LungTECH, ROSEL, SABR-COMET reported and allowed for further refinement of the dose constraints²⁴¹⁻²⁴³. The models from HyTEC allow prediction of a toxicity rate for SABR, as do the re-irradiation dose/toxicity models presented in this chapter.

The aorta dose constraint was modified from the 5% maximum toxicity rate predicted by block bootstrapping. This method was unsuccessful with the other models because of the overdispersion of the datasets, leading to very wide bootstrapped confidence intervals. This method was useful in the aorta model, possibly because the few toxic events occurred at very high doses so the large reduction in dose when the toxicity rate was limited to 5% resulted in a clinically acceptable dose. However, in the other models, to reduce the risk to a maximum of 5%, the dose reduction required led to over-conservative constraint suggestions. When validated with the information in the collected data and the Beatson cohort, it seemed appropriate to increase the dose constraint and accept a slightly higher potential risk, for a much larger increase in the dose that could be delivered. Ultimately, the maximum likelihood model prediction for 5% toxicity is an estimate of the dose that gives a 5% complication rate, with the true value possibly higher or lower than this value. By limiting the upper bound of the 95% confidence interval, the dose is likely to be safer, but also may limit the dose given to the tumour. Therefore, a clinically useful dose constraint

would lie somewhere between these values and would be guided by the risk appropriate to each individual situation.

These dose constraints are set to arbitrary limit, set by the clinician. The dose constraints do not take in to account the risks patients wish to accept. However, dose constraints set in this method would be variable because different patients will have individual levels of risk. Nevertheless, it is worth exploring the patient's perspective on risk and what they would accept. Specific to re-irradiation constraints, it is also worth considering what the risk of tumour related toxicity is if re-irradiation was not attempted. For example, if the risk of fatal haemoptysis due to recurrent tumour at the PBrT is 30%, then it is not unreasonable to exceed the suggested 5% dose constraint of 119Gy to gain better control of the tumour. This nuanced discussion of the potential risks and benefits of re-irradiation is essential when considering re-treatment, and the attitude of patients to re-irradiation will be further explored in Chapter 8.

Table 5.57 Comparison of expert dose constraints and modelling dose constraints. ALARA: as low as reasonably achievable, BP: brachial plexus, cumMLD: cumulative mean lung dose, cumVx: cumulative volume receiving at least x Gray, CW: chest wall, Dmax: maximum dose received by an organ at risk, Dmean: mean dose received by an organ at risk, Dxcc: maximum dose to an organ at risk to a volume of xcc, EQD2: equivalent dose in 2-Gray fractions, GV: great vessels, Ind: Individualised dose, NA: not applicable, PA: pulmonary artery, PBrT: proximal bronchial tree, § Paradis quoted doses in D0.1cc, *Uses median interval (13.5 months), ^Multivariable model with no chemotherapy, † Multivariable model using median interval (18 months), ††<80 (if <24m), ^^V60<40%, §§ <110 for pulmonary artery, <120 for great vessels

	α/β	Expert dose constraints (Gy, EQD2)					Rulach analysis (Gy, EQD2)		
		Delphi 2021	Troost 2020	Paradis 2019§	ARS 2020	Hunter 2021	Lowest dose tox observed	Constraint for ≥G3 toxicity	Estimated ≥G3 tox rate
Dmax Spinal cord	2	60	<65	<61.6	<57	<67.5	63.3	67.3*	5%
Dmax BP	2	80-95	<85	<86.9	<85	<95 (>24m) ††	n/a	n/a	n/a
D0.1cc Skin/CW	2.5	ALARA	n/a	<116	n/a	n/a	n/a	n/a	n/a
Heart	2.5	ALARA	Dmax<70	D0.1cc<86.1	V40 <50%	n/a	n/a	n/a	n/a
Lung cumV20	3	Ind	n/a	Ind	<40%	<30-35%	8.5%	35%	20%
Lung cumV5	3	n/a	n/a	n/a	n/a	n/a	15.1%	Est 70%	20%
Lung cumMLD	3	Ind	Dmean<22	Ind	n/a	n/a	7.3	22	20%
Dmax PBrT	3	<80-105*	<110	<85.8	<110	<105	124.6	119†	5%
Dmax Oes	3	75-100	<100	<87.5	<110^^	<110	60.4	94.2^	5%
Dmax GV	3	110 - 115	<110	<116.5	<120	<110/120§§	114.3	100.2	5%

Table 5.58 Existing dose constraint toxicity rate predictions using models. CI: confidence interval, CW: chest wall, Dmax: maximum dose received by an organ at risk, D_{cc}: maximum dose to an organ at risk to a volume of xcc, EQD2: equivalent dose in 2-Gray fractions, LL: lower limit, MLD: mean lung dose, NA: not applicable, PBrT: proximal bronchial tree, UL: upper limit, V_x: volume receiving at least x Gray.

	α/β	Maximum constraint	Model risk prediction for $\geq G3$ toxicity	95% CI LL	95% CI UL
Spinal cord	2	Dmax <67.5Gy	2.4% (interval 13.5 months)	1.3%	4.5
Brachial plexus	2	Dmax <85Gy	n/a	n/a	n/a
Skin/Chest wall	2.5	n/a	n/a	n/a	n/a
Heart	2.5	D _{0.1cc} <86.1Gy	n/a	n/a	n/a
Lung	3	V20<40%	60.7%	37.3%	85.9%
Lung	3	MLD<22Gy	33.0% (no chemo)	16.8%	54.3%
PBrT	3	Dmax <110Gy	2.9% (interval 18 months)	1.0%	8.2%
Oesophagus	3	Dmax <110Gy	9.4% (no chemo)	5.7%	15.1%
Great vessels	3	Dmax <120Gy	2.9%	1.0%	8.2%

5.4.2 Data issues affecting all models

Accurate dose/toxicity models are useful in re-irradiation planning. If the dose an expected toxicity occurs at is too low, this may compromise the dose to the PTV, leading to lower tumour control. Conversely, if the dose constraint is too high, then patients would develop serious toxicity from their treatment.

Modelling re-irradiation toxicity is more complex compared to modelling for a single course of treatment. The interval between the first and second radiation course determines how much normal tissue repopulation occurs. The longer the interval, the more repopulation occurs thereby increasing the tolerance of the organ at risk. The amount of dose delivered in the first treatment may also influence the tolerance at re-treatment, as seen in spinal cord re-irradiation of primates and in the murine lung re-irradiation.

However, the quality of data in every dataset is not detailed enough to quantify the effects of all these factors for each endpoint. There was a large amount of missing data regarding the interval and concurrent chemotherapy, therefore when adding these variables to a multivariable model, a large amount of data was discarded. For example, in the oesophagus multivariable model, 245 out of

505 (48.5%) patients' information had to be discarded. This issue is less when using univariable models, as there is no additional data that is excluded. However, for multivariable models, data on the entire case is excluded if only one variable in the multivariable model is missing. Data imputation could be performed to fill in the absent data, but this would significantly undermine the results. In addition, the ratio of number of events in comparison to the number of non-events in each model is relatively low (the oesophagus has the highest with a 9.7% ratio, aorta the lowest with 2.8%). The combination of limited sample size and low numbers of events can cause the models to be biased. Corrections can be applied in rare events data, which may increase the risk of a given variable, but again, these advanced statistical approaches add added uncertainty by shifting the dataset away from the empirical evidence²⁴⁴.

There are several sources of error that apply to every dataset, and this can be separated into issues affecting the dose and issues affecting the toxicity. Firstly, the doses in the datasets may deviate from the actual dose delivered. Some studies gave a prescription dose to the PTV, and it was assumed that this was the dose that the OAR received e.g. oesophageal re-irradiation or spinal metastases re-irradiation. This prescription dose was converted into EQD2. However, the prescription dose can vary between 95-107% using the ICRU guidelines. This would affect the spinal cord and oesophageal datasets mainly. This error is minimised because most studies quoted the actual dose received by the OAR.

However, determining the cumulative dose an OAR receives is also prone to error. Often after an initial course of radiation, the anatomy is distorted. Rigid image registration and dose accumulation may lead to inaccurate cumulative doses, as the dose may not align with the new position of the OAR after the first treatment. Deformable image registration uses an algorithm to better match the images from the first course to the second course and the associated dose maps compared to rigid deformation²⁴⁵. However, there is no gold standard to confirm the dose a tissue has received, therefore most of the work has been performed on contour matching, rather than actual dose deposition. The true accuracy of the using deformable dose registration is unknown. For some organs at risk, the

contouring is non-standardised. This is an added area of variance between the studies.

The dose data is inaccurate when using grouped data. The grouped doses in the datasets are the median dose for the whole cohort. This means that the true dose delivered maybe higher or lower than what was used in the models. The rate of toxicity will be higher in a group of patients treated to a range of doses with a median X compared to a group all treated at the median dose X . This is because the rate of toxicity will likely be higher in those patients treated above the median value. This effect means that dose predictions from models using grouped median data will overestimate the true toxicity rate, and therefore be more cautious. In addition to using the bootstrapped samples to find the maximum 5% toxicity rate, the models' dose predictions may be more conservative. It was necessary to use grouped data as there was not enough data of the more accurate individual doses to produce models. If the grouped data (and the toxicity information therein) was ignored, as seen in the models for the spinal cord, the more accurate data gives an over-cautious estimate of the dose for 5% toxicity.

The sources of the datasets are from treatments delivered between 1955 to 2017. Radiation treatment has changed significantly over that time. The radiotherapy technique, the size of normal tissue irradiated, and the dose calculation methods have all changed. This is an inherent flaw in collecting data across such a wide time period, and unavoidable as the number of events are rare. This variation is accounted for in the block bootstrapping process, where a random selection of the cohorts are resampled with replacement to form 2000 synthetic datasets. The synthetic datasets have the selected model re-fitted to them, and used to generate new predictions. The 2.5% and 97.5% predicted values are used as the block bootstrap confidence interval. The differences from each cohort in terms of treatment, follow-up and unknown factors across each synthetic dataset are reflected in the width of this interval. For all the models, the block bootstrapped confidence intervals were very wide. This suggests that there is significant uncertainty about all of the presented models due to wide variability over the data.

The recording of toxicity has significant uncertainties. This is critical in the dose/toxicity models because there are relatively few events, a few mischaracterised toxicities can have a large influence on the model predictions. The recording of re-irradiation toxicity is complicated. For example, in the proximal bronchial tree, it is difficult to attribute the severe bleeding events as re-irradiation toxicity where there is still recurrent disease. In lung models, comorbid conditions like COPD could result in the need for additional oxygen (causing a grade three toxicity) but it may not be caused by the re-irradiation. Prospective studies can improve this by investigating the cause of toxicity, but the data used in these models are from retrospective reviews so may not have performed those tests. The effect of mis-labelling a toxicity as due to re-irradiation may cause the models to predict higher toxicity levels at lower doses.

Conversely, missing re-irradiation toxicity will have the opposite effect. Reasons why re-irradiation toxicity is missed is due to lack of follow-up, on short duration of follow-up. Early toxicity is apparent within three months. All the papers studied had a median follow-up longer than this (shortest median follow-up was 4 months), although there would be a small number of patients who would not have this. Late toxicity can take years to develop. The cord, oesophagus, lung, proximal bronchial tree and aorta datasets have 2, 1, 3, 3 and 2 studies that have median follow-up of greater than 2 years respectively. Therefore, late toxicity may be underestimated. Finally, the grading of toxicity is not consistent between the papers, with some studies using published criteria, and others not grading the toxicity. Moreover, some toxicity scales give different results than others. For example, there are four possible grading systems for pneumonitis, which are all subtly different²⁴⁶. This can lead to some toxicities being graded a G2 toxicity as opposed to G3 and vice versa.

5.4.3 Issues related to modelling technique

Logistic regression modelling has been used extensively for dose constraints in radiation oncology. The application of this technique for re-irradiation modelling introduces some sources of inaccuracy. The number of patients and events in the re-irradiation datasets are relatively small. Standard practice in logistic regression is to split each dataset into training and test sets. However, the limited data available would introduce significant bias in the training set, as

removing the low number of events to fit the model to adds greater bias. Using the external cohort of 39 Beatson re-irradiation patients allows the models to be tested on a real-world, accurate dataset. However, the lack of toxic events in the validation cohort meant that the AUC of some models could not be assessed.

The choice of endpoints for logistic regression is important. The endpoint of \geq Grade 3 toxicity was chosen because in most toxicity scales this results in hospitalisation and is significant for patients. Grade 3-5 toxicity was grouped together to increase the chance of having enough events to form models. The exploration of other toxicity endpoints such as grade 1-2 toxicity was not possible due to lack of data. However, grade 2 toxicity is likely to be of importance to patients but is not assessed in these models. The used of patient reported outcome measures were not recorded in any of the re-irradiation studies but would have given a valuable patient perspective on the toxicities of treatment.

The modelling performed in this study summed the dose of two treatments into one EQD2 value using the linear-quadratic equation. The α/β values use in the LQ equation are not absolute values. The values used in this study are commonly used, using an α/β of 3 for late responding tissues. However, the α/β for late oesophageal toxicity was tested on a canine model and found to be 3.3Gy²⁴⁷. For lung, pneumonitis having a α/β of 4Gy and fibrosis of 3.07Gy^{226,248}. The possible variations of α/β ratios may affect the dose calculations by a small amount. Moreover, data is lacking on if a course of radiation changes the α/β ratio of a tissue. For example, the α/β ratio of unirradiated lung may be 3Gy, but after radiation, it may fibrose. This may change its fraction sensitivity. This has not been investigated. Additionally, the calculation of EQD2 does not consider the use of concurrent chemotherapy, which can act as a radiosensitiser. This could be useful when planning re-irradiation after an initial course of concurrent chemoradiotherapy. It might be assumed that the re-treatment dose should be less to avoid toxicity given the previous intensive treatment, but again, data is lacking to support this approach.

The datasets include data from conventionally fractionated radiotherapy, two course of SABR or a combination of both. The LQ model was applied to all these

treatments to calculate the EQD2. The mechanistic underpinning of the LQ formalism however does not apply to SABR treatments, which have different radiobiological effects (on hypoxia, immunologically and the vasculature of the tumour)¹⁶². Furthermore, where the dose per fraction is greater than 15Gy, the LQ model underestimates the effect²⁴⁹. Applying the LQ formalism to calculate EQD2 values from the published data may therefore be a source of error.

However, for most *in vivo* research, the LQ model is accurate between a range of 2-15Gy, and the use of more complicated models (the linear-quadratic-linear model or the universal survival curve) were not significantly better^{162,250}. Therefore, although the LQ model may not mechanistically match the radiobiological processes at higher doses per fraction, it still accurately predicts the effect. One area that remains controversial is the effect of SABR doses on normal tissue, as much of the research has focused on tumour control probabilities. High fraction doses affect endothelial function and blood flow in tumours but there is little data on how normal tissue respond biologically to these changes^{251,252}. One putative mechanism is that SABR-related normal tissue damage is akin to a surgical wound, and normal tissue recovery depends on the tissue architecture, innate regenerative abilities, the amount of stem cell depletion and vasculature damage²⁵³.

The use of the LQ model for SABR treatments can increase the EQD2 values significantly. SABR delivers high dose per fraction treatments, which can potentially skew the dose delivered. For example, 60Gy in 2Gy fractions gives an EQD2 of 60Gy, while 60Gy in 7.5Gy fractions gives an EQD2 of 126Gy to late responding tissue. According to Lyman's power law as applied to partial volume irradiation, as the volume reduces, higher doses are tolerated^{254,255}. For SABR treatments, the dose to give a certain toxicity may be higher than that for with conventionally fractionated radiotherapy data. However, the models did not have sufficient data to split into SABR only or conventional fractionation only re-irradiations to explore this.

The selection of papers included in this study was based on a large literature search. There may be other papers that report dose and toxicity that were omitted. To capture all the relevant data, the search was repeated on two occasions (in 2018 and 2020). The data was extracted by a single researcher and

was reviewed to ensure that the correct data was entered. However, the use of a large literature review introduces publication bias into the results. As re-irradiation is a novel and technical treatment, it is more likely to be performed in large-volume centres. Therefore, there may be missing information from other centres which perform re-irradiation but have not published it. Additionally, there may be a bias to publish papers where significant toxicity was seen. However, there were several studies which were published with no toxicity. It is difficult to quantify this effect. Once the models were created, they were bootstrapping (re-sampled with replacement) 2000 times to generate a bootstrapped 95% confidence interval. This process assumes that the sample is representative of the population - this may not be the case.

5.4.4 Conclusions

Dose/toxicity models were built for lung, spinal cord, oesophagus, proximal bronchial tree and aorta and were used to predict the dose that gives a 5% or 20% toxicity rate (Table 5.57). There are several sources of potential inaccuracy although the results of the modelling are largely in agreement with the expert groups dose constraints. The models will be used to predict the estimated toxicity rates for the replanned treatments. This may be useful in clinical practice as it allows clinicians to counsel patients about re-irradiation with a greater awareness of toxicity risks.

6 Re-irradiation tumour control models

6.1 Introduction

The 2-year overall survival rates of radical thoracic re-irradiation range between 11-64% with conventionally fractionated radiotherapy, and 37 -79% with SABR (see Table 1.1 in introduction). There are several factors that may influence survival. These can be divided into factors that are within the treating clinician's control such as use of concurrent chemotherapy and cumulative dose^{169,222,256}, or less controllable factors such as size of the tumour and whether the new disease is a local recurrence or a second primary^{126,257,258}. As demonstrated in the previous chapter, dose and concurrent chemotherapy are also associated with increased toxicity rates and are controllable factors. The competing objectives of maximising tumour control while minimising toxicity is a fundamental challenge in radiation therapy. In the re-irradiation setting, dose constraints may need to be exceeded to achieve a high re-irradiation dose, but it is not clear what dose is required to achieve a particular outcome.

Historically, it was thought that higher dose equates to improved tumour control in *de novo* radiotherapy for lung cancer⁵⁹. However, the RTOG 0617 study demonstrated no benefit of dose escalation from 60Gy to 74Gy in 2Gy fractions to the lung primary in terms of local control or overall survival, which were significantly lower in the escalated arm⁶⁰. This unexpected finding may be due to excess unreported cardiac mortality, longer treatment time or inherent biological factors of radioresistance^{62,259}. Conversely, in *de novo* SABR treatments for T1-2 NSCLC, there is a well-defined PTV target dose of 43-50Gy in 3-5 fractions⁷⁵.

Data from some retrospective studies suggest that higher dose at re-irradiation leads to better outcomes. Kruser *et al.* analysed the outcomes of 37 patients retreated with palliative and radical intent re-irradiation for NSCLC and demonstrated that higher re-treatment dose and good performance status were associated with better outcomes in a multivariable Cox regression analysis¹⁶⁹. Hong *et al.* demonstrated in a cohort of 31 patients that a cumulative BED of >145Gy₁₀ and re-irradiation dose of >68.7Gy₁₀ (or an EQD2 of 57.25Gy) were associated with significantly longer OS and local control²²². These findings were

mirrored in a proton re-irradiation study: 27 patients re-treated with 66Gy EQD2 or above had a significantly better 1-year freedom from local failure (100% vs 49%, $p=0.013$)¹²⁶. These data are based on a relatively small sample size yet suggest a dose target for radical re-irradiation of approximately 60Gy EQD2.

However, this target does not provide an estimate of the local control or overall survival rate of re-treatment at this dose. It is important to predict the possible benefit of re-treatment when counselling a patient, especially given the historical high toxicity rates of re-irradiation. Thoracic re-irradiation is used in selected patients on a non-protocolised basis and counselling the patients extensively beforehand is recommended¹⁷⁴. This discussion may include what level of risk a patient would accept for a projected benefit.

6.1.1 Aims of tumour control modelling

The aim of dose/efficacy modelling was to predict the benefit of re-irradiation across a range of cumulative doses. The models were derived from a database of published studies that detail the cumulative dose given to a tumour and the outcome, either as local control or overall survival. Data from all modalities used in re-irradiation (e.g., photons, protons and carbon ions) were included. Logistic regression was performed to predict the dose required for 30% and 50% local control or overall survival rates at 2 years. Exploratory analyses were performed on the effect of interval between treatments, concurrent chemotherapy and tumour size. The doses predicted for a given effect were assessed in a feasibility study to see if the retreatment dose could be escalated without breaching published dose constraints.

6.2 Methods

6.2.1 Datasets used in modelling and model validation

Three datasets were used in creating and validating the dose/outcome models. The primary sources of information are the published studies of re-irradiation, identified by a literature search. The information collected from this exercise can be divided into grouped data (where median doses and outcome measures were quoted) and discrete data (where individual patient-by-patient level information was available). For validation purposes, the cumulative dose and outcome data was taken from the 39 patients treated at the Beatson, the collection of which is outlined in Chapter 4.

6.2.2 Data collection and dose combinations

Studies were identified using the literature search strategy outlined in Chapter 5.2.2. Studies were included in the database if greater than 50% of the patients treated in the study were NSCLC (as opposed to SCLC and re-irradiation of metastases), quoted the cumulative dose delivered at re-irradiation, and gave an outcome of treatment measured either in local control or overall survival rate at one- or two-years post-re-irradiation. The cumulative dose to the tumour was converted to EQD2 using the method outlined in Chapter 5.2.3. Additional data tabulated when available were the use of concurrent chemotherapy, the size of the tumour (either as GTV, CTV, ITV or PTV) and the interval between treatments.

6.2.3 Selection of α/β ratio for tumour

The α/β value for lung cancer is difficult to due to the heterogeneity of the tumours. For stage I NSCLC, the α/β has been estimated at 8.2Gy (95% CI 7 - 9.4)²⁶⁰. By contrast, a modelling study using a dataset of 2319 patients with stage I NSCLC of varying histologies, suggested an α/β ratio of 3.9Gy (68% CI 2.2 - 9.0, $p>0.005$)²⁶¹. This highlights that the α/β ratio for lung cancer is difficult to obtain precisely. As the tumour histologies and stages of lung cancer of the data in this study vary, the accepted α/β of 10Gy will be used.

6.2.4 Choice of endpoints

The endpoints selected are local control at 2 years and overall survival at 2 years. These were chosen as they are of clinical relevance and frequently stated in the studies the database is derived from. The outcomes and predictors are summarised in Table 6.1.

Table 6.1 Outline of the outcome and predictor variables. PTV: planning target volume.

Outcome variable	Predictor variables
Local control/overall survival at 2 years	Cumulative dose to the PTV
	Initial dose
	Retreatment dose
	Size of PTV
	Interval between treatments
	Concurrent chemotherapy
	Local recurrence

6.2.5 Modelling process

The studies identified by the literature search were critically assessed and only those which met the inclusion criteria as described in section 6.2.2 were added to the database. The grouped data regarding outcome rates were converted into individual events (e.g., if a study of 30 patients quoted a two-year OS rate of 10%, the database would have 30 cases with the grouped median dose and other variables if given and 3 patients would be assigned a value of 0, denoting that those cases were alive, and 27 would be assigned a value of 1, denoting that those cases were dead). The database was manually re-checked to ensure that all the data was correctly transcribed.

Descriptive statistics and missing data analysis were performed on the final database. The dataset was subdivided into two subsets, one with the outcome variable of local control at two years and the other with overall survival at two years. Each subset was split by the median of the predictor variables and evaluated using χ^2 or Fisher's exact test as suggested in a recent primer on radiotherapy modelling¹⁸⁷.

6.2.5.1 Data collection

Cumulative doses were taken from the studies in EQD2. For studies that used carbon ions and protons, the relative biological effectiveness (or EQD2 dose) as quoted in the papers was used to correct for the difference in modality. The median retreatment dose (RT dose) in EQD2 was calculated from the studies using the linear/quadratic equation unless stated in the study. The rate of concurrent chemotherapy was taken from the studies only if explicitly stated. If no rate of concurrent chemotherapy was noted, this was ascribed as missing data. As studies reported different measures of tumour volume (e.g., some studies reported the GTV, whilst others reported the PTV), the reported tumour volume (RTV) included the quoted measurement of tumour volume (GTV, CTV, ITV or PTV) given in the study.

6.2.5.2 Corrections for limited follow-up

The outcome measures under investigation are the 2-year local control rate and the 2-year overall survival rate. For studies where the duration of follow-up is less than 2 years, the data would be incomplete and would lead to inaccurate predictions. This is because although the survival or overall control rate would be correct for that study, the raw number of patients reaching 2 years survival or local control would be overestimated. If these crude rates were used, this would result in an increase in the number of patients where the endpoint did not occur, and give undue prominence to that cohort inappropriately when fitting a model to the data. This was corrected for by making an estimate of the patients alive at 2 years (N_{eff}) where the follow-up was shorter than 2 years.

The following process was used to estimate the number of patients alive at 2 years. For studies where the median follow-up was equal or greater than 2 years, no correction was made. If the study quoted a 2 year OS rate and gave a 95% CI, the effective number of patients alive at 2 years were calculated using the following equation:

$$N_{eff} = \frac{OS(1 - OS)}{(95\% CI/3.92)^2}$$

where N_{eff} = Effective number alive at 2 years, OS = the quoted 2 year survival probability, 95% CI = the quoted 95% CI, and 3.92 is derived from 1.96×2 to represent the 2 standard deviations which the 95% CI represents. For local control, the local control rate was used instead of the OS.

If the study follow-up was less than 2 years, and had a Kaplan-Meier survival plot, the plot was digitised using an online graphics digitiser (<https://apps.automeris.io/wpd/>). The plot was traced and reconstituted into a life table using the method and R algorithm described by Guyot *et al.*²⁶² The life table was then used to derive the 2 year survival and the associated 95% confidence intervals. The above equation was then used to determine the N_{eff} .

If the study quoted a 2 year OS rate but gave no confidence intervals and had no Kaplan-Meier plot, the N_{eff} was estimated by multiplying the total number of patients in that study by the N_{eff}/N of a similar study in the dataset with similar follow-up duration. The N_{eff} values for each study were then multiplied by the quoted 2 years OS or LC rate to give the number of events. If the number of events were not integers, they were rounded to the nearest whole number. These cases were then used in the modelling process.

6.2.5.3 Exploratory estimation of concurrent chemotherapy rates and PTV

To improve the accuracy of the data, two exploratory analyses were performed. In studies where a measure of tumour volume other than PTV was given, the PTV was estimated from these values using the following process. The tumours were assumed to be spherical. The radius was calculated from the given ITV/CTV/GTV, then expanded using the data given in the methods sections of each study. The expanded radius was then used to generate the PTV. The results of the modelling using the reported target volumes (RTV) and the estimated PTV values are both presented.

According to the UK and US SABR guidelines, the use of concurrent chemotherapy is not used with SABR and in stage I NSCLC^{263,264}. Authors of studies that report re-irradiation using this technique or stage of disease may not explicitly mention that no chemotherapy was given, as it may be taken as obvious to the reader. Therefore, it could be assumed that patients having SABR

or treatment for stage I tumours did not have concurrent chemotherapy. Datasets and models with the estimated PTV and the assumed concurrent chemotherapy rates were created using the same technique as the unamended dataset and were reported in the results section.

6.2.5.4 Model fitting and selection

Logistic regression modelling was performed on each dataset using the maximum likelihood method. Univariable models were generated for each predictor. Univariable models which had a p -value < 0.2 were included in multivariable models. Where multivariable models were formed, backwards variable selection was used to ensure that the most parsimonious model was used. The model that best balanced goodness-of-fit against parsimony was selected according to the lowest Akaike's information criterion (AIC).

In contrast to the dose/toxicity models in Chapter 5, the outcomes of local control and overall survival were calculated on an actuarial basis. As the difference in follow-up time was corrected, overdispersion of the data was likely to be less, and therefore it is more reasonable to use a more standard approach, of model selection using the AIC, rather than cross-validation.

The models were plotted and used to predict the cumulative dose required to give 30% and 50% two-year local control and two year OS rates with a 95% confidence interval (CI). Both the LC and OS model datasets were bootstrapped 2000 times and the 30% and 50% rates were recalculated. For these bootstrapped predictions, the 95% CI was calculated by removing the lowest and highest 2.5% of the predictions. The minimum dose that would ensure a 30% or 50% survival rate was calculated using the bootstrapped datasets.

Assessment of model fit was performed by calculating the Hosmer Lemeshow goodness of fit test p -value using the model predictions against the complete dataset split into 10 deciles. To graphically demonstrate model performance, model predictions of 2 year local control or 2 year overall survival probability were generated using the predictor variables from each study that made up the dataset the models were derived from. These predictions were plotted against

the observed local control or overall survival rate of each study. These were then evaluated using a Pearson correlation coefficient.

The model dose predictions for 30% and 50% were validated against doses in the collected dataset and against the Beatson cohort. These datasets were split by the dose predicted for a 30%/50% local control or overall survival rates and the outcome rate was calculated. All analyses were performed using R version 3.6.1 (R Core Team (2013). R: A language and environment for statistical computing. R Foundation for Statistical Computing, Vienna, Austria). A p-value of <0.05 was used for significance for all tests.

6.2.6 Dose escalation feasibility

This feasibility study escalated the re-treatment dose until an OAR dose constraint was exceeded. The dose constraints used were the highest dose allowed by the expert consensus for each OAR (see Chapter 5). The local control and overall survival models then were used to predict the likely efficacy of the treatment, and the dose/toxicity models were used to predict the likely toxicity.

The feasibility study used the patients with local recurrence data ($n=13$) from the Beatson cohort. The cumulative dose received by four OARs (cord, proximal bronchial tree, aorta and oesophagus) in the primary and re-irradiation courses were collated using the methods described in Chapter 4. In short, this involved converting the initial and re-irradiation plans into EQD2 dose maps using a dose conversion and image registration software (Velocity version 3.1, Varian Medical System, Palo, Alto, US). The CT images from the initial and re-irradiation were registered using deformable dose registration and the deformations was applied to the EQD2 dose maps. The initial, re-irradiation and cumulative doses in EQD2, for each OAR were recorded.

The proportion of the cumulative dose attributable to the retreatment was calculated by subtracting the initial dose from the cumulative dose. It is assumed that the second dose overlaps to a degree with the first dose, which is likely for some but not all OARs. Doses were escalated using the following procedure. The maximum retreatment dose that could be delivered per patient per OAR was calculated by subtracting the OAR dose from the first treatment

from the maximum dose constraint for the OAR and dividing this by the proportion of the dose given by the second treatment. This was then divided by the proportion of the prescription dose to the OAR dose in the second treatment, to give a maximum retreatment prescription dose.

The maximum retreatment doses for each OAR per patient were collated and the lowest dose selected (as this represented the maximum dose possible before a constraint was breached). The maximum retreatment dose was then applied to the other OARs to determine their cumulative dose at this prescription dose. The additional dose was added by increasing the number of fractions, not by changing the dose per fraction. No correction was made for the longer treatment duration of the higher dose treatments.

Using the OAR dose toxicity models as described in Chapter 5, the predicted target dose cumulative OAR doses and the actual delivered cumulative OAR doses were entered into the model. Where the dose/toxicity model required additional variables (e.g. interval, use of concurrent chemotherapy), these were taken from the Beatson cohort. The model output therefore gave the original risk of toxicity to the OAR (from the delivered treatment) and the new risk if the maximum retreatment dose was used. The efficacy was also predicted of the maximum retreatment dose and the delivered dose using the LC and OS models.

6.3 Results

6.3.1 Data collection

The literature search identified 20 studies that had cumulative dose and outcome data suitable for use in dose/outcome modelling (Figure 6.1). These 21 studies are summarised in Table 6.2 and Table 6.3.

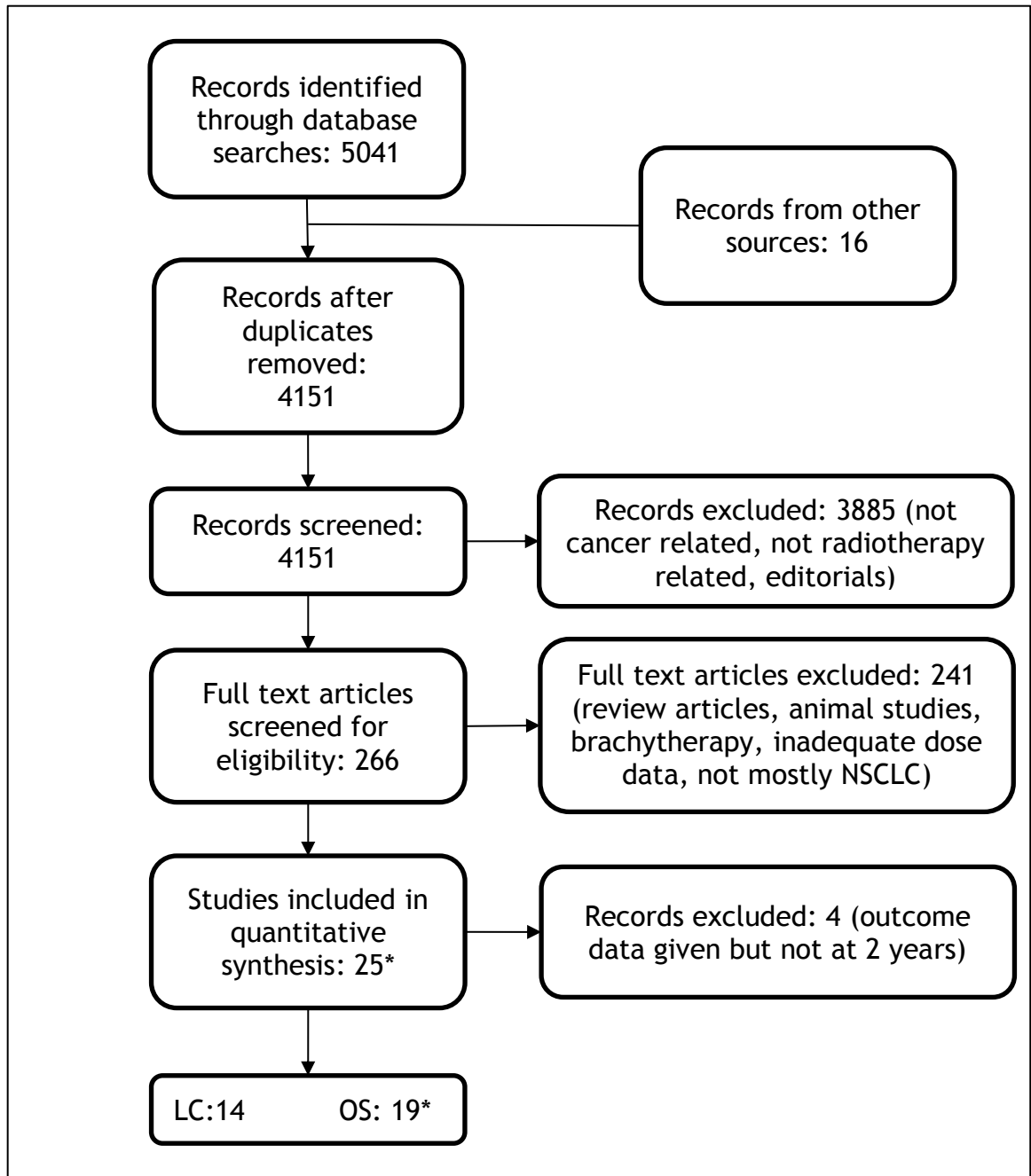


Figure 6.1 PRISMA diagram. LC: local control, NSCLC: non-small cell lung cancer, OS: overall survival. *Some papers provided dose/outcome data for both 2-year local control and overall survival.

Table 6.2 List of studies used in the local control and overall survival dataset. The total number of patients included is 693, from 21 studies. 3D-CRT: three dimension conformal radiotherapy, EQD2: equivalent dose in 2 Gray fractions, Fr: fractions, IMRT: intensity modulate radiotherapy, LR: Local recurrence, (1 – all local recurrence, 2 – local and non-local recurrence), NR: not recorded, NSCLC: non-small cell lung cancer, Re-RT: re-irradiation, SCLC: small cell lung cancer.

Paper	n	Individual data/Grouped	Treatment span	Median initial prescription dose/fr	Median re-RT prescription dose/fr	Re-treatment Technique	Type of tumour	All LR or not
Wu ¹²⁰	23	Grouped	1999 - 2001	66 (30-78) Gy/1.8-2Gy/fr	51 (46-60) Gy/1.8-2Gy/fr	3D-CRT	69.5% NSCLC, 30.5% SCLC	1
Tada ¹²¹	19	Grouped	1992 - 2002	50 -69.6Gy/NR	50 (50-60) Gy/25fr (25-30)	3D-CRT	100% NSCLC	1
Meijneke ¹⁷⁵	20	Grouped	2005 - 2012	median 60 (30-60) Gy/median 3 (1-25) fr	median 51 (20-60) Gy/median 5 (3-10) fr	90% SABR, 10% Conventional	75% NSCLC, 10% SCLC, 15% Mets	1
Ester ²⁶⁵	13	Grouped	2006 - 2012	61.2 (12 - 70) Gy/ NR	45 (45-50)/5	SABR	83.3% NSCLC, 8.3% SCLC, 8.3% Wilms	1
McAvoy ¹²²	33	Grouped	2006 - 2011	median 63 (40-74) Gy/median 33 (4-59) fr	median 66 (16.4–75) Gy RBE/median 32 (9–58) fr	Proton (passive scatter)	100% NSCLC	2
Trovo ¹²⁹	17	Grouped	NR (<2014)	50-60Gy/ 20-30 fr	30Gy/5-6 fr	SABR	100% NSCLC	1
Griffioen ¹¹⁴ /Tetar ¹²³	30	Grouped	2004 - 2015	59.9 (24 - 70) Gy/25 (3-35) fr	60 (39-66) Gy/30 (13-33) fr	IMRT	100% NSCLC	2
McAvoy ²⁵⁸	102	Grouped	2006 - 2013	70 EQD2 Gy (33-276)	60.5 EQD2 Gy (25.2 - 155)	IMRT or Protons	100% NSCLC	2

Owen ²¹⁹	18	Grouped	2006 - 2012	median 60 (39-70) Gy/median 30 (12-35) fr	median 50 (40-60) Gy/median 4 (3-10) fr	SABR	77.8% NSCLC, 5.5% SCLC, 16.7% mets	2
Kilburn ¹³⁰	33	Grouped	2001 - 2012	median 60 (22.5-80.5) Gy/median 30 (1-37) fr	median 50 (20-70.2) Gy/median 10 (1-35) fr	SABR in 91%	75.8% NSCLC, 12.1% SCLC, 12.1% mets	1
Patel ¹³¹	26	Grouped	2008 - 2011	61.2 (30 - 74)/NR	30 (15-50)/5 (3-5) fr	SABR	88.5% NSCLC, 11.5% other	1
Binkley ²²⁰	25	Grouped	2008-2014	median 50 (20-74) Gy/median 4.5 (1-37) fr	median 50 (20-177.5) Gy/median 4 (1-54) fr (including multiple re-RT courses)	SABR 73.7%, Conventional 26.3%	100% NSCLC	1
Karube ²²⁵	29	Grouped	2007-2014	median 46 (34-61.2) Gy RBE/median 1 (1-9) fr	median 60 (54-72) Gy/median 12 (12) fr	Carbon ion	100% NSCLC	1
Ceylan ²⁶⁶	28	Grouped	2005 - 2015	54 (40 - 57) Gy/ NR	30 (20-60) Gy/5 (3-9) fr	SABR	100% NSCLC	2
Caivano ²⁶⁷	22	Grouped	2011 - 2016	81 EQD2 Gy (32.5 - 100)	93.8 EQD2 Gy (40 - 126)	SABR	54.5% NSCLC, 4.5% SCLC, 40.9% Mets	2
Hayashi ²⁶⁸	95	Grouped	2006 - 2016	52.8 (28 - 76Gy)/1-16 fr	66 (48 - 72) Gy/ 12-16 fr	Carbon ion	76.8% NSCLC, 23.2% mets	1

Hong ²²²	31	Grouped	2005 - 2016	EQD2 median 66 (43.13-125) Gy	EQD2 median 57.2 (36-110) Gy	IMRT 67.7%, SABR 32.3%	77.4% NSCLC, 22.6% SCLC	2
Kelly ²⁵⁷	36	Grouped	2004 - 2008	61.5 (30 - 79.2)/NR	50 (40-50) Gy/4 fr	SABR	94.4% NSCLC, 5.6% other	2
Liu ¹⁴⁹	72	Grouped	2004 - 2010	63 (30 - 79.2)/NR	50Gy/4fr	SABR	79.2% NSCLC, 6.9% SCLC, 13.9% other	2
Kennedy ¹³⁶	21	Grouped	2008-2017	median 54 (50-54) Gy/ median 3 (3-5) fr	median 50 (50-54) Gy/ median 5 (3-5) fr	SABR	100% NSCLC	1

Table 6.3 Further details of studies used in the local control and overall survival dataset. CTV: clinical target volume, cumEQD2: cumulative dose in equivalent dose in 2-Gray fractions, f/u: follow-up, GTV: gross tumour volume, ITV: internal target volume, LC: local control, NR: not recorded, OS: overall survival, PTV: planning target volume, Re-RT: re-irradiation.

Paper	Median cumEQD2 to tumour ($\alpha/\beta = 10$)	Median re-irradiation dose (EQD2, $\alpha/\beta = 10$)	Median interval (months, range)	Chemo % rate with re-RT	2-yr LC (%)	2-yr OS (%)	PTV size	F/u post re-RT (months, range)	Neff	
									LC	OS
Wu ¹²⁰	117	51	13 (6-42)	0	42	42	.	15 (2-37)	10	16
Tada ¹²¹	110	50	16 (5-60)	89	.	11	64 (30 - 204)	All patients had died at time of reporting	N R	12
Meijneke ¹⁷⁵	216	83	17 (2-33)	0	50	33	46 (4-1734)	12 (2-52)	14	14
Ester ²⁶⁵	132.45	71.25	19.7 (4.7 - 84.7)	0	92	36	37.9 (19.5-119.6)	11.4 (1.6 - 38.3)	9	9
McAvoy ¹²²	128.86	66	36 (2-376)	24	24	33	.	11 (1.4-32.4)	14	28
Trovo ¹²⁹	108	40	18 (1-60)	0	.	29	.	18 (4 - 57)	N R	9
Griffioen ¹¹⁴ /Tetar ¹²³	122	60	29.7 (5 - 189)	6.67	.	23	237 (29 - 1140)	25	N R	21
McAvoy ²⁵⁸	130.48	60.48	17 (1 - 376)	33	34.2	32.6	94.2 (7.8-1356.3) ITV	6.5 (0-72)	50	73
Owen ²¹⁹	148	88	18.4 (1.5-112.8)	0	90	.	19.2 (6.4-79.6)	21.2 (3.4-50.2)	13	N R
Kilburn ¹³⁰	122.5	62.5	18 (6-61)	0	67	45	.	17 (NR)	15	24
Patel ¹³¹	101.2	40	8 (3 - 26)	0	65.5	37	.	.	11	22

Binkley ²²⁰	141.1	93.8	16 (1-71)	31.6	.	57.3	.	17 (3-57)	N R	17
Karube ²²⁵	201.56	85.3	20 (8-99)	0	66.9	69	112 (27-304)	29 (4-88)	29	29
Ceylan ²⁶⁶	94	40	14 (4-56)	0	.	42	24.2 (2.3-156.3) (GTV)	9 (3-93)	N R	13
Caivano ²⁶⁷	174.8	93.8	18 (6-66)	0	54	63	30.8 (2.7 - 260.7) (GTV)	13 (13 -65)	18	16
Hayashi ²⁶⁸	210.25	85.3	17 (6 - 139)	.	54	61.9	79.5 (7.1 - 452.8) (CTV)	18 (1-89)	58	70
Hong ²²²	123.33	57.4	15.1 (4.4- 56.3)	61.3	43.7	39.4	51.3 (13-299.3)	17.4 (4.8-76.8)	24	26
Kelly ²⁵⁷	155.25	93.8	22 (0 - 92)	0	92	59	.	15 (4-45)	17	31
Liu ¹⁴⁹	156.75	93.8	21 (0-106)	0	.	74.4	.	16 (4-56)	N R	61
Kennedy ¹³⁶	168.3	126	23 (7-52)	0	81	68	.	24 (3-60)	15	17

6.3.2 Dose/2-year local control model

6.3.2.1 Dataset description and initial assessment

There were 502 patients from 14 studies included in the dose/local control model. These studies only presented grouped data. The crude 2-year local control rate was 55.2%. Papers that reported only re-irradiation of local recurrences (i.e., in-field relapses) accounted for 51.8% of the cases. Local recurrences were also included in the remaining 48.2% of studies, but they also comprised data for second primary lung cancers and re-irradiation of metastatic disease. The grouped median follow-up for the local control dataset is 15 months (range 6.5 - 29 months). As the local control is measured at 2 years, the estimated effective number of patients (N_{eff}) was used to account for censoring. This reduced the number of cases in the dataset from 502 to 297. This is summarised in Table 6.4.

Table 6.4 Summary of the local control dataset. cumDmax: cumulative maximum dose to the organ at risk, EQD2: equivalent dose in 2-Gray fractions, LC: Local control, PTV: planning target volume, RTV: reported target volume.

		Missing values
Number of trials:	14	
Number of patients:	502	
Effective number of patients at 2 years:	297	
LC at 2 years (%)	166 (55.9)	0
Local recurrence (%)	131 (44.1)	0
Median interval from initial treatment and re-irradiation (months, range)	17 (8 - 36)	0
Concurrent chemotherapy rate	0.33 (0 - 0.613)	186
Median cumDmax to PTV (EQD2 Gy, range)	155.2 (101.2 - 216)	0
Median initial treatment dose (EQD2 Gy, range)	70 (42.3 - 133)	0
Median retreatment dose (EQD2 Gy, range)	85.3 (40 - 126)	0
Median RTV size (cc, range)	79.5 (19.2 - 112)	67
Median estimated PTV size (cc, range)	112 (19.2 - 234.5)	67

The dataset was divided into a group with concurrent chemotherapy data (n=111), and with missing/excluded data (n=186). The missing data group had a significantly higher mean cumulative dose (180.2Gy compared to 129.6Gy in the complete group, t-test p-value <0.001). The missing data group also had a significantly higher rate of local control at two years (64.5% vs 41.4%, p-value<0.001). There were 67 cases that had missing target volume data. The mean cumulative dose was significantly lower in the missing target volume data group (127.8Gy compared with 171.0Gy in the complete group, t-test p-value<0.001). However, there was no significant difference in the rate of local control at two years between the two groups (59.7% in the missing group and 45.2% in the group with PTV data, p-value 0.57). Four studies out of 14 studies gave non-PTV measurements of tumour volume^{258,266-268}. These studies were modelled as reported target volumes. Subsequently, they were expanded using the technique outlined in the methods to form the estimated PTV.

When the dataset was split according to the median values of the other predictor variables (cumulative dose, interval and target volumes), there was a statistically significant difference between the low and high cumulative dose and target volume groups (see Table 6.5). There was no significant difference in the rate of local control in patients who had concurrent chemotherapy and those who did not.

Table 6.5 Results of χ^2 tests when local control dataset split using median values. cumDmax: cumulative maximum dose to the organ at risk, EQD2: equivalent dose in 2-Gray fractions, PTV: planning target volume, RT: retreatment, RTV: reported target volume.

	Local control	Progression	P-value
Median cumDmax (EQD2 Gy)			
≤155.2	71	75	
>155.2	95	56	
		n=297	0.018*
Median initial dose (EQD2 Gy)			
≤70	82	46	
>70	84	85	
		n=297	0.018*
Median RT dose (EQD2 Gy)			
≤85.3	66	81	
>85.3	100	50	
		n=297	<0.001*

Median interval (months)			
≤17	21	24	
>17	145	107	
		n=297	0.234
Median RTV (cc)			
≤79.5	59	34	
>79.5	67	70	
		n=230	0.041*
Median estimated PTV (cc)			
≤112	59	34	
>112	67	70	
		n=230	0.041*
Median concurrent chemotherapy rate			
≤0.33	19	18	
>0.33	27	47	
		n=111	0.196

6.3.2.2 Local control logistic regression modelling using estimated PTV

On univariable modelling, the retreatment dose, PTV size and concurrent chemotherapy rate had p-values <0.2. On multivariable modelling, 210 cases had to be removed from the model as they missed either PTV or concurrent chemotherapy data, and the model that used all three terms was significant for retreatment dose only (based on 87 cases). As the concurrent chemotherapy data had the largest amount of missing data (186 cases), a model was built using only the PTV and retreatment dose variables thereby using more of the data available (based on 230 cases). Both variables were significant in the multivariable model. Backward variable selection confirmed that the model with the lowest AIC included both the estimated PTV size and retreatment dose as predictors (Table 6.6).

Table 6.6 Univariable and multivariable modelling of the local control dataset. Predictions made using estimated PTV. AIC: Akaike's information criterion, LC: local control, NA: not applicable, PTV: planning target volume, RT: retreatment.

Predictor	Local control	n	P-value	AIC
Univariable modelling results				
Initial dose	2-year LC	297	0.421	410.95
RT dose	2-year LC	297	<0.001*	396.3
Interval	2-year LC	297	0.852	411.56
PTV size	2-year LC	230	<0.001*	NA
Concurrent chemo rate	2-year LC	111	0.077	NA

Multivariable modelling results				
PTV size	2-year LC	230	0.030*	NA
RT dose	2-year LC	230	0.052	

The multivariable model expression is:

$$P(2 \text{ year local control} | X_1, X_2) = \Phi(-0.7542 - 0.0048X_1 + 0.0190X_2)$$

Where X_1 = estimated PTV size and X_2 = retreatment dose.

Using the median retreatment dose at 85.3Gy EQD2, the model predicted a 50% rate of 2-year local control for a PTV of 181.55cc (95%CI 88.40 - 274.70), and a 30% rate of 2 year local control for a PTV of 358.46cc (95% CI 120.2 - 596.72). The RT dose predicted to give a 50% 2 year local control rate (assuming the median PTV of 112cc) was 67.8Gy (95% CI 49.43, 86.16). This was bootstrapped 2000 times and the 95% CI was (-404.91, 569.94Gy). For 30% local rate, the predicted RT dose was 23.29 (95% CI -34.91, 81.49) and the bootstrapped 95% CI was (-508.97, 857.24). The predicted 2 year local control rate and the bootstrapped 95% confidence intervals are shown in Table 6.7, using the median PTV size. The model is plotted in Figure 6.2 with the source data and standard error of the regression.

Table 6.7 Predicted 2 year local control rate by increasing retreatment dose. CI: Confidence interval, EQD2: equivalent dose in 2 Gray fractions, Gy: Gray, LCR: local control rate, PTV: planning target volume. Median PTV of 112cc used for all predictions.

Retreatment dose (Gy, EQD2)	Maximum likelihood prediction 2-year LCR (%)	95% CI lower limit (%)	95% CI upper limit (%)
30	32.7	14.4	57.6
40	37.1	19.8	57.7
50	41.6	26.9	57.8
60	46.3	35.4	57.9
70	51.0	43.4	59.1
80	55.8	49.1	62.5
90	60.4	51.9	68.8
100	64.9	53.4	75.8

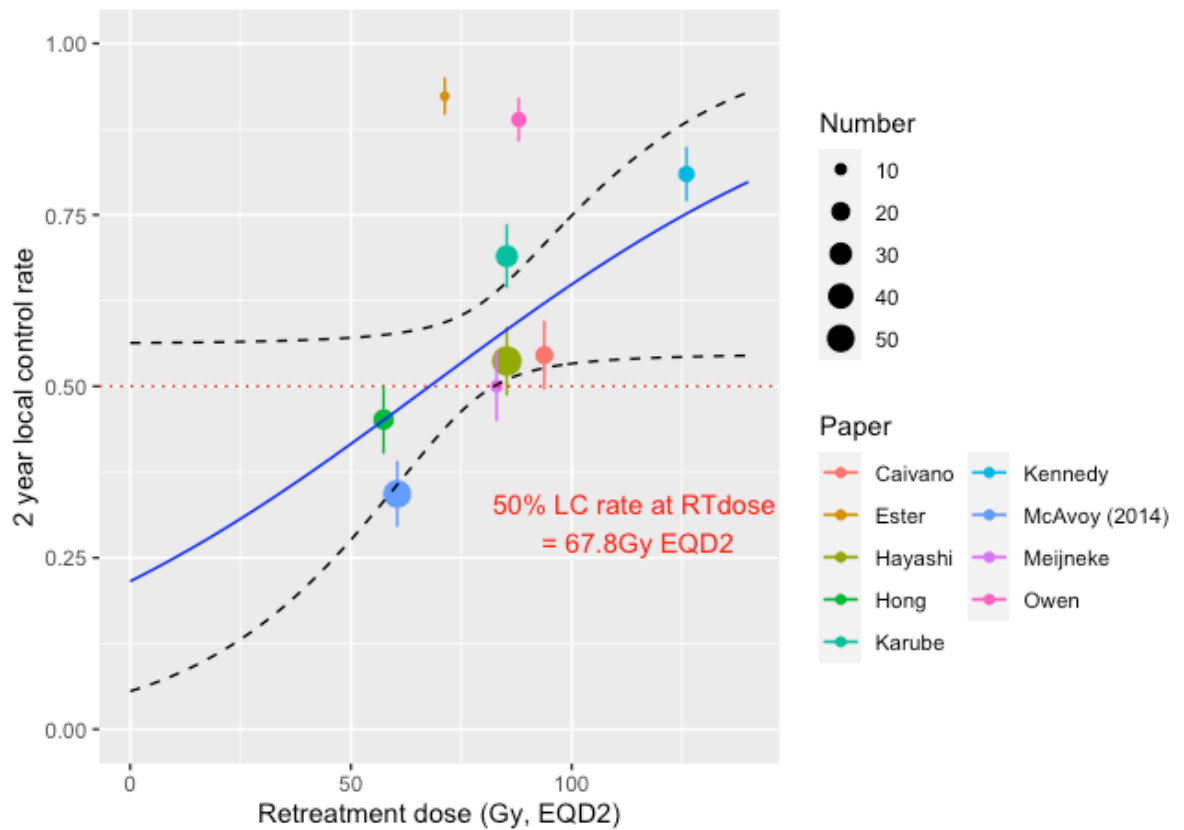


Figure 6.2 Plot of the local control multivariable model (estimated PTV and re-treatment dose). The blue line is the fitted regression model, black dotted lines represent the standard error of the regression, the red dotted line indicates the 50% local control rate. The dots represent the toxicity rate from each individual paper coded by colour, with the size of the dots proportional to the number of patients in the study, vertical bars are the 68% binomial confidence interval. There are only 9 data points included in the plot five of the 14 studies lacked PTV data and were excluded from the multivariable model. This model uses the median PTV of 112cc.

6.3.2.3 Reported target volumes and estimated PTV

The reported target volumes were used instead of the estimated PTV values to explore if this resulted in a difference in the modelling results. The RTV modelling resulted in a similar multivariable model including both the target volume and the RT dose. The predicted RT dose for 30 and 50% local control using the model was slightly higher. The RTV model a 50% 2-year rate of local control (using the median RTV) at 73.9Gy (95% CI 62.88 - 84.93) and a 30% rate at 40.92Gy (95% CI 13.60 - 68.23).

6.3.2.4 Estimated concurrent chemotherapy models

The modelling process was repeated using the dataset with the assumption that the rate of concurrent chemotherapy for patients treated with SABR and with stage I disease was zero. The modelling results are summarised in Table 6.8. The retreatment dose, PTV size and concurrent chemotherapy were significant on univariable modelling. On multivariable modelling PTV size and the estimated concurrent chemotherapy rate had $p < 0.2$. A subsequent model was made using only the PTV size and concurrent chemotherapy and both were significant.

Table 6.8 Univariable and multivariable modelling of the local control dataset. Model prediction using estimated PTV. AIC: Akaike's information criterion, LC: local control, PTV: planning target volume, RT dose: retreatment dose.

Predictor	Local control	n	P-value	AIC
Univariable modelling results				
Initial dose	2-year LC	297	0.421	410.95
RT dose	2-year LC	297	<0.001*	396.3
Interval	2-year LC	297	0.852	411.56
PTV size	2-year LC	230	<0.001*	n/a
Est. Concurrent chemo rate	2-year LC	297	<0.001*	394.44
Multivariable modelling results				
PTV size	2-year LC	230	0.014*	304.44
RT dose	2-year LC	230	0.946	
Est. Concurrent chemo rate	2-year LC	230	0.143	
Final multivariable model				
PTV size	2-year LC	230	0.003*	302.45
Est. Concurrent chemo rate	2-year LC	230	0.014*	

The multivariable model expression is:

$$P(2 \text{ year local control} | X_1, X_2) = \Phi(1.1005 - 0.0059X_1 - 1.6191X_2)$$

Where X_1 = estimated PTV size and X_2 = concurrent chemotherapy rate.

This model was used to predict the PTV size to give the 30% and 50% 2-year local control rates. The concurrent chemotherapy rate used was the median value median value (0). The model predicted a 50% 2 year local control rate with a

PTV size of 187.9cc (95% CI 110.38, 245.41) and a 30% 2 year local control rate with PTV 332.56cc (95% CI 171.48, 493.65). This model was plotted in Figure 6.3.

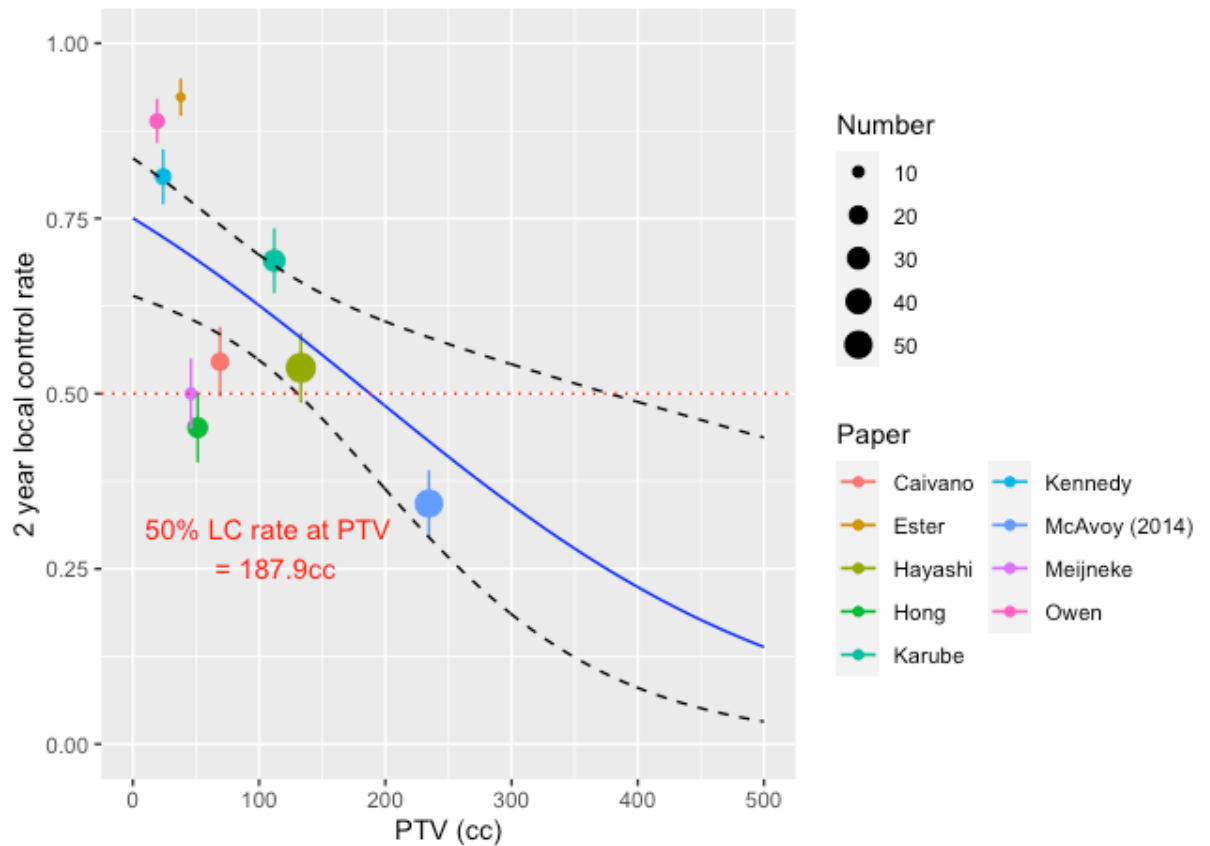


Figure 6.3 Plot of the local control multivariable model (PTV and assumed concurrent chemotherapy). The blue line is the fitted regression model, black dotted lines represent the standard error of the regression, the red dotted line indicates the 50% local control rate. The dots represent the toxicity rate from each individual paper coded by colour, with the size of the dots proportional to the number of patients in the study, vertical bars are the 68% binomial confidence interval. The median concurrent chemotherapy rate of zero was used.

6.3.2.5 Multivariable model validation

The multivariable model from the unadjusted dataset (with retreatment dose and PTV size as the predictors) had a Hosmer Lemeshow p-value of 0.758, suggesting a reasonable fit to the data. The expected and observed 2-year local control rates by model prediction decile is plotted in Figure 6.4. The Pearson correlation coefficient was 0.69 (p-value 0.041) suggesting that the line of best fit correlates reasonably with the observed local control rates. The multivariable model from the dataset with the assumed concurrent chemotherapy rate also

had a non-significant Hosmer Lemeshow test p-value (0.613) and the expected and observed plot is shown in Figure 6.5. Both models had similar performance, albeit the predictions from the assumed model had better correlation with the observed values with a Pearson correlation coefficient of 0.79 (p-value 0.011). However, the model with most clinical utility is the unadjusted model as it included the retreatment dose, which is the major modifiable factor when planning re-irradiation.

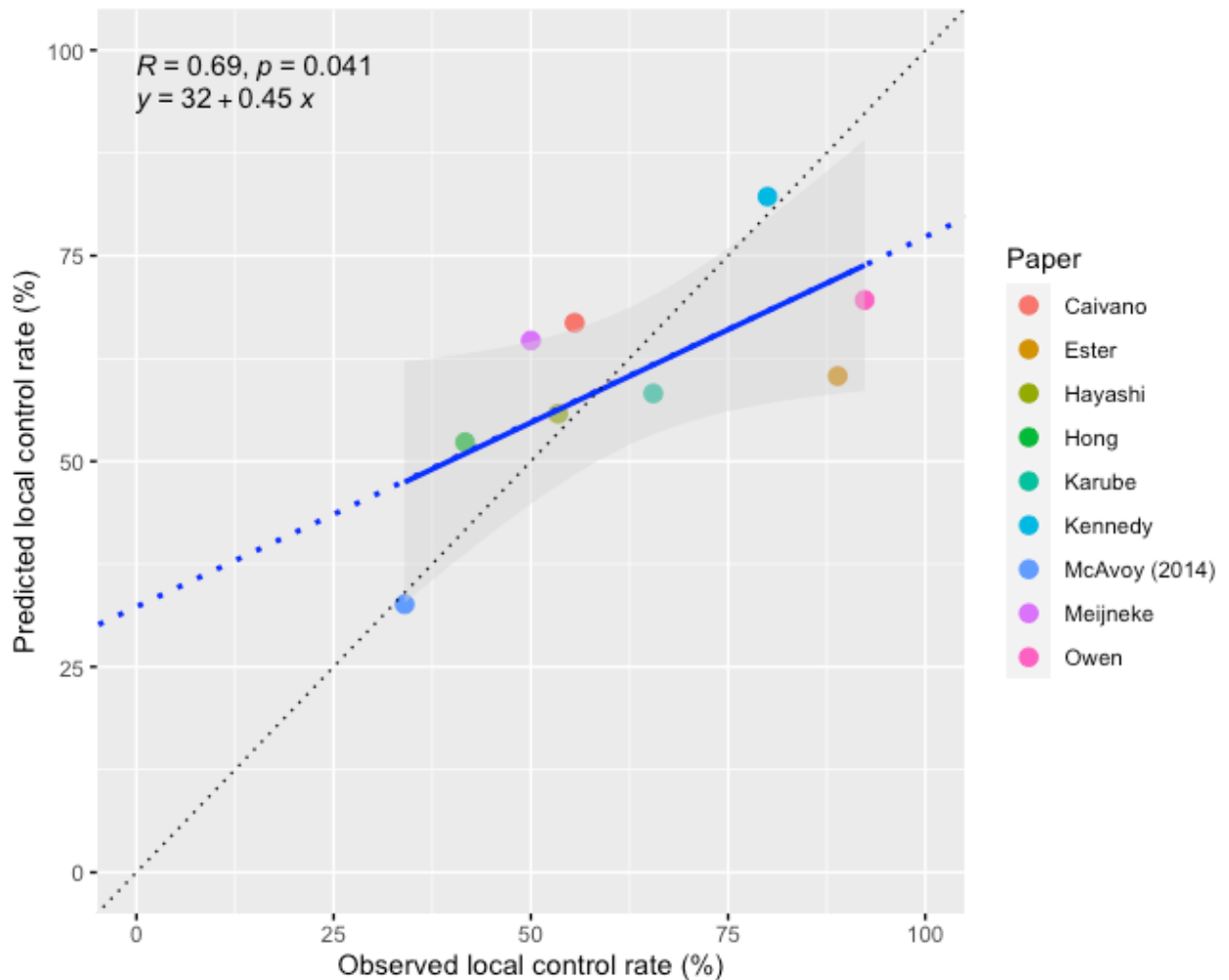


Figure 6.4 Predicted and observed 2 year local control rate by decile of model prediction (unadjusted multivariable model using PTV and retreatment dose). The blue line is the line of best fit and the black dotted line is the line of unity, n=230.

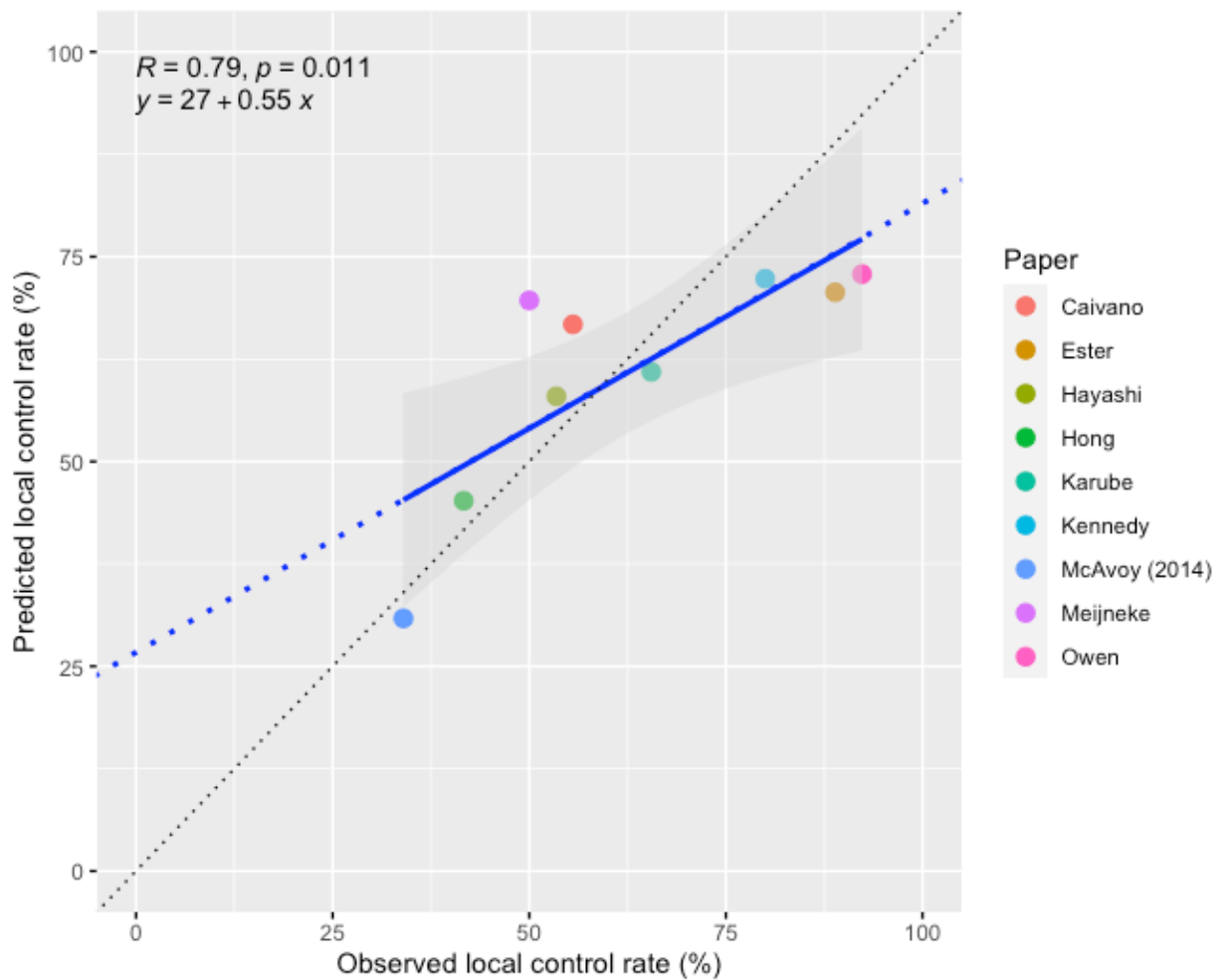


Figure 6.5 Predicted and observed 2 year local control rate by decile of model prediction (chemo-assumed and PTV multivariable model). The blue line is the line of best fit and the black dotted line is the line of unity, n=230.

The unadjusted model results for the 50% local control for PTV and RT dose were tested on the dataset. The model prediction for 50% local control is a PTV of 181.6cc (with the median RT dose of 85.3Gy). This cut-off was applied to the dataset and there was a statically significant difference, with a higher rate of local control below PTV size of 181.6cc compared to above (60.6% and 34.0% respectively, p-value 0.001, Table 6.9). If the assumed concurrent chemotherapy model was used with a PTV cut-off of 187.9cc, the local control and local failures rates are the same. However, there was only one study that reported a higher PTV size (234.5cc) than either of the 50% predictions, limiting the strength of the conclusions that can be drawn.

Table 6.9 Testing maximum-likelihood PTV cut-off for 50% 2-year local control. LC: local control, LCR: local control rate, LF: local failure,

	LC	LF	LCR at 2yr (%)	P-value
≤181.6cc	109	71	60.6	
>181.6cc	17	33	34.0	
			n=230	0.001*

The unadjusted model predicted a 2-year rate of local control at a RT dose 67.8Gy (with a median PTV of 112cc). This dose was used as a cut-off, and there was a statistically significant higher rate of local control with patients treated above compared to below this dose (63.5% and 36.5% respectively, $p < 0.001$, Table 6.10).

Table 6.10 Testing maximum-likelihood RT dose cut-off for 50% 2 year local control. LC: local control, LCR: local control rate, LF: local failure,

	LC	LF	LCR at 2yr (%)	P-value
≤67.8Gy	27	47	36.5	
>67.8Gy	99	57	63.5	
			n=230	<0.001*

6.3.3 Dose/overall survival model

6.3.3.1 Dataset description and initial assessment

There were 675 cases from 19 studies included in the overall survival dataset. These studies only presented grouped data. The crude 2-year overall survival rate was 48%. Papers that reported only re-irradiation of local recurrences (i.e., in-field relapses) accounted for 47.6% of the cases. Local recurrences were also included in the rest of the cases, but this subset of the data also included second primary lung cancers and re-irradiation of metastatic disease. The rate of concurrent chemotherapy and the target volume sizes were calculated as per the local control dataset. The grouped median follow-up for the local control dataset is 16 months (range 6.5 - 29 months). As the overall survival rate is

measured at 2 years, the estimated effective number of patients (N_{eff}) was used to account for censoring. This reduced the number of cases in the dataset from 675 to 506. This is summarised in Table 6.11.

Table 6.11 Summary of the overall survival dataset. cumDmax: cumulative maximum dose to the organ at risk, EQD2: equivalent dose in 2-Gray fractions, PTV: planning target volume, RT: retreatment, RTV: reported target volume.

		Missing values
Number of trials	19	
Number of patients	675	
Effective number of patients at 2 years	506	
OS at 2 years (%)	245 (48.4)	0
Death rate at 2 years (%)	261 (51.6)	0
Median interval from initial treatment and re-irradiation (months, range)	17 (8 - 36)	0
Median concurrent chemotherapy rate	0.33 (0 - 0.613)	315
Median cumulative Dmax (EQD2 Gy, range)	141.1 (94 - 216)	0
Median initial dose Dmax (EQD2 Gy, range)	65.9 (42.3 - 133)	0
Median retreatment dose Dmax (EQD2 Gy, range)	83 (40 - 126)	0
Median RTV size (cc, range)	79.5 (24 - 237)	208
Median estimated PTV size (cc, range)	133.1 (24 - 237)	208

There were 315 cases that had missing concurrent chemotherapy. The mean cumulative dose in the group with concurrent chemotherapy data was significantly lower in the missing group (127.0Gy vs 166.0Gy in the complete data subset, p-value <0.001). The two-year overall survival rate was also significantly lower in the missing group (32.3% vs 58.4% in the complete group, p-value<0.001).

There were 208 cases that had no target volume data. The mean cumulative dose was again significantly lower in the missing target volume group (136.6Gy vs 161.4Gy in the complete group, p-value<0.001). There was no significant difference in the rate of two year overall survival between the missing and complete target volume group (51.7% vs 46.3% respectively, p-value 0.272).

When the variables of the dataset were split by the median values, there was a significant difference between the higher and lower interval, and the retreatment and cumulative dose to the target volumes groups (Table 6.12).

Table 6.12 Results of χ^2 tests when overall survival dataset split using median values. PTV: planning target volume, RTV: reported target volume.

	Alive	Dead	P-value
Median cumulative dose			
≤141.1	82	168	
>141.1	164	92	
		n=506	<0.001*
Median retreatment dose			
≤83	82	168	
>83	164	92	
		n=506	<0.001*
Median initial dose			
≤65.9	127	126	
>65.9	119	134	
		n=506	0.506
Median concurrent chemotherapy rate			
≤ 0.33	52	114	
>0.33	16	9	
		n=191	0.003*
Median interval			
≤17	27	60	
>17	218	201	
		n=506	<0.001*
Median RTV			
≤79.5	45	59	
>79.5	93	101	
		n=298	0.517
Median estimated PTV			
≤133.1	65	68	
>133.1	73	92	
		n=298	0.497

6.3.3.2 Logistic regression modelling

PTV size, concurrent chemotherapy rate, retreatment dose and initial dose to the PTV had p-values <0.2 on univariable modelling and were included in the multivariable model. A multivariable model including concurrent chemotherapy rate was non-significant as only 191 cases could be included due to missing data.

Therefore, concurrent chemotherapy was removed from the model. The subsequent multivariable analysis found the initial and retreatment dose to have p-values <0.2 and the RTV size was non-significant with a p-value of 0.506 (Table 6.13). RTV was removed to form a model using the initial dose and retreatment dose. With this model, the retreatment dose was significant (p-value <0.001) and the initial dose not significant (p-value 0.404). Removal of the initial dose from the model improved the AIC from 662.49 to 661.2, therefore the final model included only the retreatment dose.

Table 6.13 Univariable and multivariable modelling of the overall survival dataset. AIC: Akaike's information criterion, OS: overall survival, RTV: reported target volume *Not comparable to cumDmax, retreatment dose and interval due to missing data

Predictor	OS	n	P-value	AIC
Univariable modelling results				
Initial dose	2-year OS	506	0.029*	701.58
Retreatment dose	2-year OS	506	<0.001*	661.19
Interval	2-year OS	506	0.824	706.36
RTV size	2-year OS	298	0.084	n/a
Concurrent chemotherapy rate	2-year OS	191	0.047	n/a
Multivariable modelling results				
Initial dose	2-year OS	298	0.079	n/a
Retreatment dose	2-year OS	298	<0.001*	
RTV size	2-year OS	298	0.506	
Final multivariable modelling results				
Initial dose	2-year OS	506	0.404	n/a
Retreatment dose	2-year OS	506	0.044*	

The final univariable model expression is:

$$P(\text{2-year OS} | X_1) = \Phi(-2.5929 + 0.0318X_1)$$

Where X_1 = retreatment dose.

The model was used to predict the initial dose and retreatment dose required for 30% and 50% 2-year overall survival. For a 30% 2 year OS rate, the model predicted the necessary retreatment dose at 49.84Gy (95% CI 40.28, 59.39). The retreatment dose for a 50% OS rate was 76.47Gy (95% CI 70.71, 82.22). The

dataset was bootstrapped 2000 times and the 95% CI using the bootstrapped samples for the 30% and 50% OS 2 year rate were 36.40 to 58.03Gy and 70.76 to 82.69Gy respectively. The model is plotted in Figure 6.6 with the source data and the standard error of the regression.

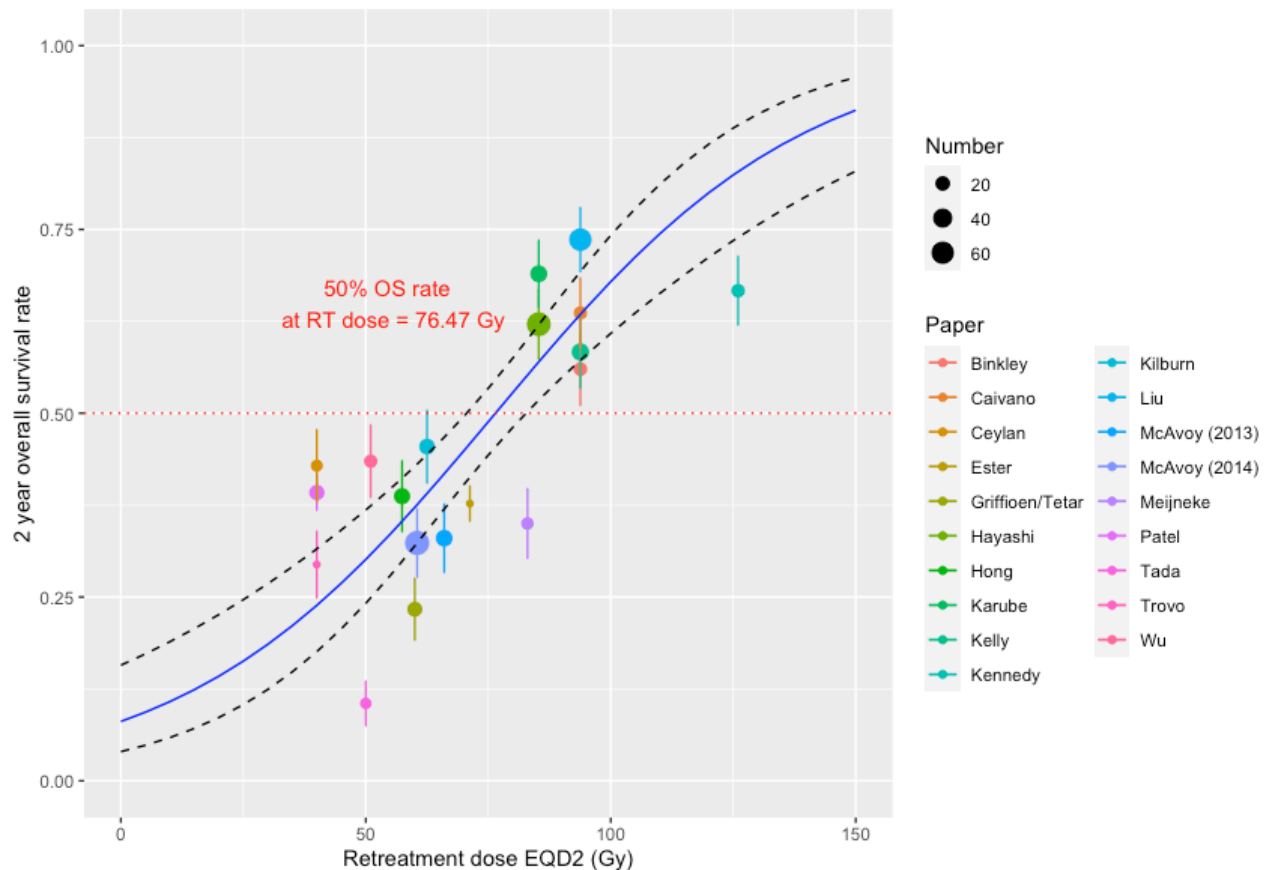


Figure 6.6 Plot of the 2 year overall survival univariable model by retreatment dose. The blue line is the fitted regression model, black dotted lines represent the standard error of the regression, the red dotted line indicates the 50% 2 year overall survival rate. The dots represent the toxicity rate from each individual paper coded by colour, with the size of the dots proportional to the number of patients in the study, vertical bars are the 68% binomial confidence interval.

6.3.3.3 OS Modelling using estimated PTV and assumed concurrent chemotherapy rate

The modelling process was repeated using a dataset that used the estimated PTV and the assumed concurrent chemotherapy rate. Only re-treatment dose was included in the final model. Therefore, as the concurrent chemo rate and the

PTV were not included, the model predictions remained the same as when using the unadjusted dataset.

6.3.3.4 Model validation

The unadjusted univariable model has a Hosmer Lemeshow test p-value of 0.385, suggesting a reasonable fit to the data. The plot of predicted vs observed 2-year overall survival rates by each study (Figure 6.7) has a Pearson correlation coefficient of 0.78 (p-value <0.001) which indicates the line of best fit correlates well with the observed data.

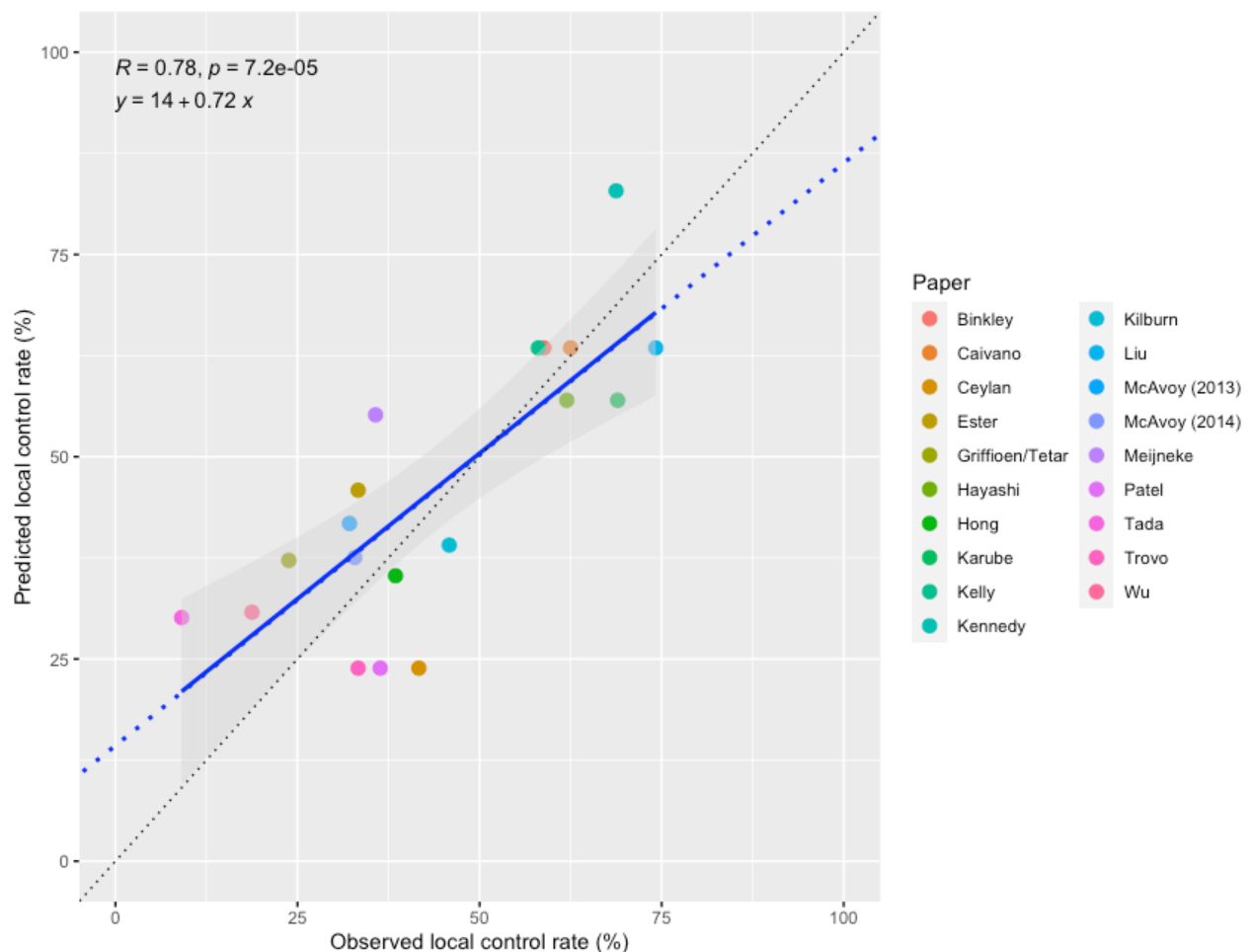


Figure 6.7 Predicted and observed 2 year overall survival rate by study using the unadjusted model. The blue line is the line of best fit, the blue dotted line is the extrapolated line, and the black dotted line is the line of unity, n=506.

To recap, the maximum-likelihood model predictions for the 30% and 50% overall survival rate at 2 years with 95% CIs (expressed as survival rates) are 49.84Gy (24.0, 36.7%) and 76.47Gy (45.4, 54.6%) respectively. These doses were

validated on data from the collected dataset (Table 6.14). This demonstrated that patients who had a retreatment dose of greater than 76.47Gy had a statistically significant higher rate of 2 year overall survival at 64.1%, compared to patients who received less than 76.47Gy. There was a smaller non-significant difference between the groups when divided using the 30% 2 year OS target dose, with an OS rate of 37.2% below 49.84Gy and 49.7% above ($p=0.16$). Although the observed OS rate below 49.8Gy is slightly higher than the 30% predicted rate, this is based on 43 patients and is likely to be within the 95% confidence interval for this prediction. The target doses could not be assessed on the external Beatson cohort because only one patient had a dose higher than 76.47Gy and no patients had a dose less than 49.8Gy therefore dividing them using the suggested doses would be non-contributory.

Table 6.14 Testing maximum likelihood retreatment dose on the overall survival dataset. OS: Overall survival.

50% 2 year OS dose (Gy)			
	Alive	Dead	OS rate at 2 years (%)
≤76.47	82	168	32.8
>76.47	164	92	64.1
		n=506	$p<0.01^*$
30% 2- year OS dose (Gy)			
	Alive	Dead	OS rate at 2 years (%)
≤49.84	16	27	37.2
>49.84	230	233	49.7
		n=506	$p=0.16$

6.3.4 Feasibility of dose escalation

Thirteen patients with locally recurrent disease were selected from the Beatson re-irradiation cohort. The median prescription dose for the initial treatment and at re-irradiation was 58.44Gy (EQD2). For the initial treatment, 10 patients were treated with 55Gy in 20 fractions and three with 54Gy in 36 fractions. At re-irradiation, nine patients were treated with 55Gy in 20 fractions, three with

54Gy in 36 fractions, and one with 50Gy in 5 fractions. The median PTV size was 179.78cc (range: 52.75 - 417.45cc). The location of the tumours at initial radiotherapy and at re-irradiation are listed in Table 6.15. The median 2-year LC and OS rate predicted from the efficacy models were 37.69% (range: 14.57 - 64.09) and 36.04% (range: 31.29 - 55.44%) respectively (Table 6.16).

Table 6.15 Location and PTV size of the locally recurrent Beatson re-irradiation cases. UC: ultracentral, C: central, LUL/LLL: left upper/lower lobe, P: peripheral, PTV: planning target volume, RUL/RML/RLL: right upper/middle/lower lobe.

Trial number	Initial tumour location	Re-irradiation tumour location	PTV size (cc)
1	Right hilum (UC)	RLL (P)	179.78
6	Right hilum (UC)	Right hilum (UC)	155.46
8	LUL (UC)	LUL (UC)	244.09
11	LLL (P)	RML (C)	217.47
12	LUL (UC)	LUL (UC)	417.45
15	RUL (UC)	RUL (P)	66.49
20	LUL (UC)	LUL (C)	84.84
23	LLL (UC)	LLL (UC)	223.9
27	LUL (P)	LUL (UC)	374.7
28	RUL (P)	RLL (P)	52.75
29	LUL (UC)	LUL (UC)	254.58
41	RUL (UC)	RUL (P)	61.5
44	LUL (UC)	LUL (P)	135.13
Median (range)			179.78 (52.75 - 417.45)

Table 6.16 Predicted 2-year overall survival and local control rates using delivered dose. EQD2: equivalent dose in 2-Gray fractions, LC: local control, OS: overall survival

Trial number	Max retreatment dose (EQD2 Gy)	Predicted 2-year LC rate (%)	Predicted 2-year OS rate (%)
1	58.44	37.69	36.04
6	58.44	40.46	36.04
8	51.75	28.13	31.29
11	58.44	33.55	36.04
12	51.75	14.57	31.29
15	58.44	50.99	36.04
20	58.44	48.80	36.04
23	58.44	32.87	36.04
27	58.44	19.21	36.04
28	83.33	64.09	55.44
29	58.44	29.71	36.04
41	51.75	48.41	31.29
44	58.44	42.83	36.04
Median	58.44	37.69	36.04

Range	51.75 - 83.33	14.57 - 64.09	31.29 - 55.44
-------	---------------	---------------	---------------

6.3.4.1 Efficacy

When the prescription doses were recalculated to give the maximum dose possible before exceeding an OAR constraint, six plans had a higher dose than originally delivered (patients 1, 15, 20, 28, 41 and 44). The other seven patients had dose reductions to keep within the dose constraints. The proximal bronchial tree was the most common OAR to limit dose (76.9% of patients). For the six patients where dose escalation was possible, the re-irradiation area was in a less central location compared to the initial radiotherapy plan. The maximum dose that could be escalated to was 348.17 Gy. However, this dose only considers the four serial OARs and is unlikely to be deliverable. The predicted 2-year LC and OS rates from the maximum retreatment dose group were 36.7% (range: 13.43 - 99.47%) and 33.14% (range: 21.42 - 99.98%) respectively (Table 6.17). There were no significant differences in predicted 2 year LC or OS between the delivered dose and maximum retreatment dose (Student's t-test 0.11 and 0.12 respectively). However, in the six patients where dose was increased, there was a significant difference in predicted outcomes when compared to the delivered dose (2 year LC rate 73.73% vs 48.8%, t-test p-value 0.03, and 2 year OS rate 73.45% vs 38.48%, t-test p-value 0.02).

Table 6.17 Maximum retreatment doses and predicted 2 year local control and overall survival rates. EQD2: equivalent dose in 2 Gray fractions, LC: local control, OAR: organ at risk, OS: overall survival, PBrT: proximal bronchial tree

Trial number	Max retreatment dose (EQD2 Gy)	Predicted 2-year LC rate (%)	Predicted 2-year OS rate (%)	Dose limiting OAR
1	68.22	42.15	43.48	PBrT
6	50.11	36.70	30.18	PBrT
8	46.08	26.00	27.55	PBrT
11	38.53	25.69	23.03	PBrT
12	46.76	13.43	27.99	PBrT
15	68.06	55.55	43.36	Cord
20	155.53	85.82	92.52	PBrT
23	51.07	29.85	30.83	PBrT
27	54.41	18.05	33.14	PBrT
28	169.10	90.13	95.01	PBrT
29	35.61	21.49	21.42	PBrT
41	97.80	69.27	66.35	Aorta
44	348.17	99.47	99.98	Aorta

Median	54.41	36.7	33.14	
Range	35.61 - 348.17	13.43 - 99.47	21.42 - 99.98	

6.3.4.2 Safety

The OAR dose/toxicity models from Chapter 5 were used to determine the toxicity rates from the delivered treatment and from the maximum retreatment doses. The mean doses by OAR are summarised in Table 6.18. There was no significant difference in the risk of OAR toxicity between the delivered dose and the maximum retreatment dose groups. In a sub-group analysis of the six patients who had an increased dose in the maximum retreatment group, there also was no significant difference in toxicity seen (Table 6.19).

Table 6.18 Comparison of the mean predicted toxicity risk between the delivered dose and maximum retreatment dose groups. G3: grade 3, PBrT: proximal bronchial tree.

	Cord \geq G3 toxicity risk (%)	Oesophagus \geq G3 toxicity risk (%)	PBrT \geq G3 toxicity risk (%)	Aorta \geq G3 toxicity risk (%)
Delivered dose group mean risk	0.55	3.66	5.26	1.88
Maximum retreatment dose group mean risk	0.79	3.17	5.16	1.86
t-test p-value	0.18	0.49	0.56	0.93

Table 6.19 Comparison of predicted toxicity between the delivered dose and maximum retreatment dose. Dose escalated sub-group only. G3: grade 3, PBrT: proximal bronchial tree.

	Cord \geq G3 toxicity risk (%)	Oesophagus \geq G3 toxicity risk (%)	PBrT \geq G3 toxicity risk (%)	Aorta \geq G3 toxicity risk (%)
Delivered dose group	0.88	1.83	5.98	1.14
Maximum retreatment dose group	1.46	2.85	6.36	1.89
t-test p-value	0.13	0.10	0.07	0.08

The cumulative doses from the delivered treatment and the predicted doses if the maximum retreatment dose was used to the four OARs are summarised in Table 6.20 and Table 6.21 respectively.

Table 6.20 Summary of dose and predicted risk to the cord, oesophagus, proximal bronchial tree and aorta from the delivered treatment. Oes: oesophagus, PBrT: proximal bronchial tree.

Trial number	Cord		Oes		PBrT		Aorta	
	Dose (Gy)	Tox (%)	Dose (Gy)	Tox (%)	Dose (Gy)	Tox (%)	Dose (Gy)	Tox (%)
1	48.52	0.53	76.08	2.35	104.09	1.38	96.89	1.67
6	37.86	0.31	99.93	6.30	119.73	3.56	86.75	1.31
8	26.79	0.12	75.45	2.29	115.50	2.50	99.97	1.80
11	22.78	0.10	118.66	13.11	132.11	3.63	134.53	4.14
12	35.09	0.40	71.17	1.91	114.31	11.71	100.26	1.82
15	62.62	4.12	86.84	3.69	78.90	18.29	89.31	1.39
20	31.8	0.16	76.02	2.34	83.80	1.31	81.84	1.16
23	38.26	0.29	103.54	7.29	118.32	2.68	124.55	3.26
27	32.88	0.21	75.49	2.29	115.67	3.01	79.47	1.09
28	19.23	0.08	15.75	0.18	68.85	1.88	18.08	0.24
29	41.27	0.44	84.95	3.41	135.96	5.41	135.43	4.23
41	28.96	0.30	71.39	1.93	69.54	11.54	95.58	1.62
44	22.49	0.10	39.86	0.50	50.83	1.45	64.77	0.76
Median	32.88	0.29	76.02	2.34	114.31	3.01	95.58	1.62
Range	19.23 - 62.62	0.08 - 4.12	15.75 - 118.66	0.18 - 13.11	50.83 - 135.96	1.31 - 18.29	18.08 - 135.43	0.24 - 4.23

Table 6.21 Summary of dose and predicted risk to the cord, oesophagus, proximal bronchial tree and aorta from the maximum retreatment dose. Oes: oesophagus, PBrT: proximal bronchial tree.

Trial number	Cord		Oes		PBrT		Aorta	
	Dose (Gy)	Tox (%)	Dose	Tox	Dose	Tox	Dose	Tox
1	50.25	0.60	77.23	2.47	110	1.48	101.32	1.86
6	35.60	0.26	93.43	4.84	110	3.19	80.93	1.13
8	25.75	0.11	74.30	2.18	110	2.35	96.50	1.66
11	21.38	0.09	96.92	5.58	110	2.83	111.76	2.40
12	34.82	0.39	70.87	1.89	110	11.20	97.40	1.69
15	67.50	5.83	90.60	4.31	81.47	18.74	92.37	1.50
20	42.35	0.36	94.39	5.03	110	1.77	101.53	1.87
23	35.80	0.24	96.00	5.37	110	2.44	115.72	2.64
27	31.22	0.18	71.20	1.91	110	2.82	74.91	0.98
28	21.70	0.09	16.21	0.18	110	3.00	17.44	0.24
29	33.16	0.24	75.62	2.30	110	4.06	109.95	2.30
41	29.04	0.30	73.02	2.07	70.62	11.67	120	2.93
44	60.22	1.58	82.05	3.02	52.07	1.47	120	2.93
Median	34.82	0.26	77.23	2.47	110	2.83	101.32	1.86
Range	21.38 - 67.5	0.09 - 5.83	16.21 - 96.92	0.18 - 5.58	52.07 - 110	1.47 - 18.74	17.44 - 120	0.24 - 2.93

6.3.4.3 Summary of dose feasibility

A dose escalation strategy was applied to 13 patient plans who had been re-irradiated for locally recurrent disease, to increase the retreatment dose to the maximum possible before an OAR constraint was breached. Six plans were able to receive an increased dose, and seven had a dose reduction. The main OAR that limited dose escalation was the PBrT. The dose escalated plans had a significantly higher 2-year LC and OS rate with no increase in predicted grade 3 or above toxicity. The patients who were suitable for dose escalation all had tumours that had recurred such that the re-irradiation PTV was further away from the patients' midline structures. Therefore, dose escalation may be feasible in this group, although other OARs must be considered (e.g. lung dose) to further evaluate this strategy.

6.4 Discussion

6.4.1 Main findings

Models were created to predict local control and overall survival after re-irradiation. In the local control model, the significant variables were the PTV and RT dose (or only the PTV size in the exploratory model). In the OS model, RT dose was the only significant variable. The 50% 2 year local control and overall survival rates were predicted at RT doses of 67.8 Gy (assuming a PTV of 112cc) and 76.5 Gy respectively. A feasibility study assessing if retreatment dose could be increased identified six patients out of a cohort of 13 who could have had a higher retreatment dose with no significant increase in toxicity of the OARs evaluated.

6.4.2 Local control models

6.4.2.1 Summary of data

Fourteen studies were included in the local control dataset, but five were excluded as they had no PTV data (three SABR studies, one CFRT study and one proton study). The local control models are based on nine papers. The re-irradiation techniques used in these studies were SABR (5), carbon ion (2), a combination of IMRT and SABR (1), and protons (1).

The five SABR studies included 94 patients, had a range of cumulative EQD2 to the PTV of 97.3 - 216Gy and a 2-year local control rate between 50-92%^{136,175,219,265,267}. Interestingly, the two studies with the highest local control rates (of 90 and 92%) used a strategy of CFRT followed by SABR. Accordingly, the cumulative doses in those two studies were 132Gy and 148Gy. The two carbon ion studies included 124 patients, had a range of cumulative EQD2 to the PTV of 201.6 - 210Gy, and two year local control rates of 54-66.9%^{225,268}. One paper examined carbon ion re-irradiation for stage I NSCLC and the other had broader inclusion criteria of locoregional recurrence, second lung primaries or metastatic lung lesions, albeit with all in-field or marginal field failures. Both studies used a re-irradiation fraction size of approximately 4Gy RBE. This suggests that even with high hypofractionation and high cumulative dose, local control is difficult to achieve.

The proton study reported a local control rate of 34.2% in 102 patients with a median cumulative dose of 130.5Gy²⁵⁸. In this study, the use of concurrent chemotherapy was associated with better overall survival and having an in-field recurrence was also associated with worse local control, suggesting an element of radioresistance when using a similar fractionation scheme to the initial radiotherapy. The final study included reported a two year local control rate of 43.7% from 31 patients, treated with a median cumulative dose of 123Gy²²². This study also reported that patients treated over an EQD2 of 121Gy₁₀ had statistically significant longer OS. Although not included in the final model due to lack of PTV data, the lowest local control rates of 24% and 34% were seen in two studies that used conventional fractionation, one with photons and the other with protons^{120,122}. The source data for the model therefore is more reflective of patients retreated with SABR, hypofractionated carbon ion or proton treatments rather than with conventional photon 2Gy fractionation.

6.4.2.2 Model results

The unadjusted LC model found that PTV and the RT dose are significant on multivariable modelling. The bootstrapped confidence intervals were very wide indicating a large amount of overdispersion, and this is expected given the relatively small number of patients after correction for short follow-up. The assumed LC model (that made assumptions regarding concurrent chemotherapy)

found that PTV and concurrent chemotherapy were the only significant predictors, but both were negative predictors (where any increase in the rate of chemotherapy or the size of PTV reduced the likelihood of local control. The former finding is unexpected, given that concurrent chemotherapy is a radiosensitiser. Chemotherapy was probably associated with lower control because the patients who received concurrent chemotherapy would have had more advanced disease therefore would have worse outcomes. In addition, smaller tumours were more likely to be treated with SABR, which were assumed to have no chemotherapy. Therefore, there is likely to be some collinearity between PTV and concurrent chemotherapy making this model unreliable. Moreover, the unadjusted model seems biologically plausible, is based on less assumptions and is more clinically useful as the RT dose is a controllable variable for clinicians. In conclusion, the RT dose and PTV model, despite the large uncertainties, is the more useful model.

The biological rationale for PTV being a factor in re-irradiation is that larger tumours may be more hypoxic and therefore less likely to respond to radiation. The models predicted that the smaller the PTV, the higher the rate of local control. The significance of RT dose is consistent with the earlier studies^{169,222}. Interestingly, the cumulative dose was not significant in the multivariable model. This could be due to the data used in the model was not from exclusively locally recurrent disease. In disease where there is no overlap between the initial and the re-irradiation PTV, the cumulative dose would not be a factor. Another radiobiological explanation is that recurrent tumours have recovered after the initial course of radiation, and “forgotten” the previous dose from the first treatment.

The RT dose is of great interest, as it is a variable that a treating clinician can influence when planning re-irradiation. The median split of the RT dose suggested a significant increase in local control in patients who had RT doses above 85.3Gy EQD2. The model prediction is lower than this with a RT dose of 67.8 Gy for a 50% 2-year local control rate. However, the model prediction is comparable to the 2-year local control rate seen in RTOG 0617. This study of *de novo* radiotherapy had a local control rate of 61.4% with 74Gy in 2Gy fractions⁵⁸. One possible implication is that tumours retain most of their radiosensitivity

after an initial course of radiotherapy. This conclusion may be incorrect as in the modelling dataset, it is difficult to separate the influence of radiotherapy technique on the dose delivered. Smaller tumours are likely to be treated with SABR, which gives a higher dose in EQD2 than CFRT, and works in a different way to fractionated radiotherapy. The model prediction is based on a PTV of 112cc, and RTOG 0617 included patients with stage III lung cancer, which would likely have a much larger PTV than this. Another reason why the modelling data may be incorrect is that the data was not exclusively local recurrences, thereby any comment made on the radiosensitivity of re-irradiated tumour may be inaccurate.

The objective of the local control modelling was to provide some guidance to a target re-irradiation dose. The multivariable model predicted a 50% local control rate at 67.8Gy but with wide 95% bootstrapped confidence intervals (-404.91, 569.94Gy). This may be due to the unavailability of variables which may influence local control to include in the model such as degree of PTV overlap. Additionally, there was a large amount of missing data pertaining to the PTV size, and concurrent chemotherapy which reduced the number of cases that could be included in the modelling. The missing concurrent chemotherapy data had a significantly higher cumulative dose, which would suggest that a treatment like SABR was used more often in this group, and by indication, would have smaller tumour sizes than the group with concurrent chemotherapy data.

To improve the quality of the target volume data, the estimated PTVs were calculated where target volumes were non-PTVs. This did not significantly change the modelling results. This supports the use of this approach and the assumptions made to estimate the PTV seem plausible. However, the use of assumed concurrent chemotherapy data formed a model that excluded the RT dose in favour of the concurrent chemotherapy variable. This may be due to some collinearity with low concurrent chemotherapy rates seen with SABR/stage I disease and high doses, and higher concurrent chemotherapy rates with higher stage disease and CFRT. Therefore, the unadjusted model is more clinically useful. For further investigation of the role of concurrent chemotherapy in tumour control, focusing the dataset on a given stage (e.g., stage III disease only) may give more accurate results. The result of the local control modelling

implied that to achieve a 50% rate of 2 year local control, a dose above 67.8Gy EQD2 was required and small PTVs responded better. This is higher than the doses usually given with CFRT but is readily achievable with SABR. Therefore, the results of these models suggest that early detection of recurrent disease (to identify low volume recurrence) and use of hypofractionated SABR may be result in better local control rates.

6.4.3 Overall survival

6.4.3.1 Summary of data

The overall survival model used the RT dose. The 19 papers that were used to develop the model used the following re-irradiation techniques: SABR (11), CFRT with photons (4), Carbon-ion (2), and protons (2)

The 11 SABR studies included 313 patients and reported a 2-year OS rate between 29 and 74.4% using a RT dose between 40-126Gy^{175,265-267}. The paper which had a two year local control rate of 90% had a corresponding 2 year OS rate of 36%²⁶⁵. The deaths were due to metastatic disease, demonstrating the efficacy of SABR at local control may not translate to an OS benefit. The four CFRT with photon studies analysed 103 patients, treated with a RT dose EQD2 of 50-60Gy with a 2 year OS rate of 11-42%^{114,121,123}. The carbon ion and proton studies were the same as described in the local control section, with a 2 year OS rate of 32.6-69%. As with the local control model, the dataset used for the OS model is based largely on outcomes from carbon ions, protons, and SABR. The data from the studies using photon CFRT was a minority of the dataset and had the lowest 2 year OS rates.

6.4.3.2 Model results

The median split analysis of OS dataset suggested that the higher cumulative dose, higher RT dose and the longer the interval, were associated with a higher 2 year OS rate. At logistic regression, only the RT dose was associated with a higher 2 year OS rate. The model predicted a 2 year overall survival rate of 30% and 50% at 49.84Gy and 76.47Gy respectively. The 95% bootstrapped CI for the 50% OS rate was 70.76 to 82.69Gy, which is narrower than the LC model. This is due to there being more data in the OS model, resulting in more precise

predictions. Nevertheless, as with the local control model, the RT doses for a 2 year OS of 50% are difficult to attain using CFRT only. Therefore, two courses of SABR or CFRT followed by SABR would be most commonly available technique to achieve this re-treatment dose.

The model has good performance, with the Hosmer Lemeshow test suggesting a reasonable fit to the data, and a significant line of best fit when plotted with an R-value of 0.78. The observed vs predicted plot (Figure 6.7) demonstrates that most rates observed from the studies are close to the model predicted line. The 50% OS prediction dose provided reasonable dose discrimination, with a significant difference in 2 year OS above the target dose of 76.47Gy (Figure 6.6). Therefore, the OS model does seem to predict outcomes accurately.

The 50% dose for 2 year OS is similar to the dose for local control (76.47Gy and 67.8Gy respectively). Conceptually, as radical re-irradiation is mostly given in the context of no distant disease, both doses should be similar. They are slightly different, possibly due to the different datasets they models have been built from. There are two technical reasons why the local control model is less accurate than the overall survival model. For the overall survival data, the endpoint of death is definitive. For the local control data, local failure after radiotherapy is difficult to diagnose and often needs serial CT scans or biopsies, making it a less clear endpoint, more so in the absence of a robust post-re-irradiation surveillance schedule.

The second reason why the overall survival model is superior is that the local control model would censor deaths from other causes, thereby limiting the sample size of cases that could be included for local control. The overall survival data would count all deaths as events, and therefore have a larger sample size compared to the local control model.

In conclusion, the modelling and analysis of the OS after re-irradiation demonstrate that higher RT doses are associated with a higher 2 year OS rate. The target RT dose to achieve a 2 year OS rate of 50% is 76.47Gy and this would necessitate the use of SABR as the re-treatment technique.

6.4.4 Feasibility study

The feasibility study demonstrated that dose escalation was possible in six of the 13 patients (46.2%) with local recurrence from the Beatson cohort, without exceeding the published cumulative dose constraints. The technique chosen to explore dose escalation used pre-existing plans and multiplied the dose to the OARs as a ratio of the prescription dose. This is not a comprehensive replanning study (due to resource constraints) and therefore should be considered as preliminary data only.

The six plans that had an increased dose did not have a statistically significantly larger amount of overlap than those that did not (average percentage PTV overlap 36.07% vs 46.38%, t-test p-value 0.64). However, the direction of recurrence was different. All six patients had recurrent disease that had moved peripherally away from midline structures. For example, trial patient 1 had central disease initially, then had a relapse in the right upper lobe. There was overlap in PTV, but much of the re-irradiation dose was superior to the original field. While this spares the dose to the central organs, this increases the volume of lung retreated, and could result in higher lung toxicity.

The conclusion that dose escalation is feasible in these patients should be taken with significant caution. If the recurrent disease is further away from the central OARs in the mediastinum, then it is likely that lung will be the dose limiting OAR. Lung toxicity was not calculated in this preliminary study as it was impossible to calculate accurately how dose escalation would change a volumetric dose using the proportions of a dose. This would require replanning the 13 studies completely, and then converting the doses to EQD2s and summing the doses to predict the risk in the context of a robust re-planning study. Therefore, the maximum retreatment dose (which was up to 348Gy in one patient) is clearly impractical as the lung dose would be far exceeded. Indeed, the results of all the re-plans may fail the lung (or other) constraints other than the four OARs analysed. However, this feasibility study does demonstrate that for a sub-group of patients, dose escalation may be an option, but needs further evaluation.

The OARs chosen (proximal bronchial tree, oesophagus, aorta and spinal cord) are all serial organs and were selected as the Dmax would increase proportionately as the prescription dose was increased. A limitation of this feasibility study methodology is the assumption that the Dmax of the initial and re-irradiation plans overlap exactly. This allows the cumulative dose to be summed from the first and second treatment. This is unlikely to be the case, even in local recurrences, as the Dmax of one plan may be in a different location. This makes the results of this study conservative, and it may be possible that dose escalation is possible for more of the patients.

The safety of re-irradiation was assessed using the dose/toxicity models. It is interesting that seven of the 13 patients exceeded an OAR constraint in the actual treatment that was delivered. However, the models predicted a generally low rate of \geq G3 toxicity whichever dose solution was used. The delivered dose risk ranged between 0.5 and 5.2% and the maximum retreatment dose risk was between 1 to 6.4%. It is unclear what risks patients may be willing to accept, and this is likely to be an individualised decision. The dose/toxicity models also fail to determine whether it is an early toxicity (and may be temporary) or a late toxicity (which would likely be permanent). This would be important as this would shape patients' attitude to retreatment. Chapter 8 of this thesis explores this issue through patient interviews.

In conclusion, the retreatment feasibility study implies that a subgroup of patients where the disease recurrence grows peripherally may be suitable for dose escalation. This result requires verification with a complete re-planning study to assess the effects on the lung doses.

6.4.5 Data limitations

There are several issues with the data that may affect the validity of the results. The dataset incorporated data from patients who had local recurrence of NSCLC and patients who had second primaries, re-irradiation for metastatic disease and for different histologies (e.g., small cell lung cancer). This mixture of pathologies means that interpreting the dose predictions from the models is difficult for an individual patient. However, 88.6% of the tumours included in the reports are NSCLC. The remaining 11.4% consist of small cell lung cancer and

metastatic lesions. Local recurrence is the main indication of re-irradiation in 73.9% of cases, with 26.1% of cases representing outcomes from second primaries and re-irradiation of metastases. Therefore, although most of the cases are local recurrence from NSCLC, there is a significant amount of data which reflect outcomes from other histologies and out-of-field recurrences or second primaries. This can affect the models if these groups have a significantly better or worse response to re-irradiation. Unfortunately, the studies do not provide enough information to analyse this.

The dataset contains only grouped data. The modelling used median values for the doses delivered and for the PTV size. This is a potential source of inaccuracy as it assumes that the local failure happened at the median dose, when it may be that local failure occurred at lower doses. Without individual patient level data, more accurate exploration of the dose/outcome relationship is not possible. In addition, four studies quoted GTV, CTV and ITV sizes, and these were used to calculate the PTV, assuming the tumour was spherical. The methods sections of the four papers described the expansions used and these were applied to predict the PTV. However, there may be unforeseen errors and the estimated PTVs may vary from the actual PTV.

The dataset collected information from patients using a variety of radiotherapy techniques including protons, carbon ions, and SABR conventionally fractionated radiotherapy. The models did not include treatment technique as factors in the logistic regression model as the sequence of the radiotherapy (e.g., SABR followed by SABR, or CFRT followed by SABR, or CFRT followed by protons) was not possible to derive from the studies accurately., but further exploration of the optimal technique was not possible.

There were missing data regarding concurrent chemotherapy and PTV size in both the local control and overall survival datasets. The missing data group with concurrent chemotherapy had a significantly lower dose and worse outcomes (possibly reflecting the use of CFRT, as concurrent chemotherapy is unlikely to be used with SABR). Additionally, a grouped rate of concurrent chemotherapy was used as it was not possible to attribute local control with the use of chemotherapy on a patient-by-patient basis. This is a source of inaccuracy, especially given that some studies had heterogenous patient groups where for

individual patients, concurrent chemotherapy would not have been an option e.g. studies that reported both SABR and CFRT. Interestingly, the concurrent chemotherapy rate may have some collinearity with both the PTV size and the dose (with concurrent chemotherapy being used for small lesions, and not being used with SABR treatments). This compromises any conclusions that can be drawn about the use of concurrent chemotherapy with re-irradiation.

The group missing PTV data also had a significantly lower cumulative dose compared to the complete data group, but there was no significant difference in the local control or overall survival rates. This missing data was excluded in the multivariable modelling. The effect of these missing data on the local control and overall survival models would have removed some lower doses from the dataset, therefore both models may overestimate the dose required for a given effect.

The choice of endpoints was constrained by the availability of data. Five studies reported the one-year local control and overall survival rates but did not report the rates at two years. These studies were excluded from the dataset but would have provided useful additional data. In addition, the predictor variable was the maximum cumulative dose to the PTV. However, the minimum cumulative dose to the PTV is a more useful measurement, as it is the minimum dose that defines the tumour control probability. The local control rate is dependent on the post-re-irradiation surveillance CT scan schedule. The details of these were not consistently reported and may be prone to error as most of the studies used retrospectively collected data. However, local control is the outcome that best reflects the effect of the radiotherapy as it is less prone to confounding by other factors. In addition, the detection of local recurrence is difficult. Fibrosed tissue can surround the re-irradiated volume and the diagnosis of recurrence on CT alone may require a combination of serial scans, metabolic imaging or a biopsy.

The overall survival model is a less precise endpoint when assessing tumour control probability. Many factors can influence overall survival, such as disease stage at re-irradiation, patient comorbidities, and further treatment. None of these factors were included in the modelling due to lack of data. An alternative explanation for why there is increased survival with higher doses is that to deliver such a high dose implies that either one of two courses of SABR were

used in those patients' re-irradiation. SABR treatments can only be given to patients whose tumours are relatively low volume and with no nodal involvement. Therefore, SABR is a likely confounder in the dose/response relationship. SABR (and therefore higher dose) is only given to patients with lower disease stages and lower volume recurrences. In addition, much of the data used to build the models are from SABR studies. This is a crucial potential source of error of the dose/outcome models.

6.4.6 Conclusions

Using logistic regression modelling, models were developed to predict the local control and OS rates at two years post-re-irradiation. The OS model found that RT dose was a significant factor, while the PTV and the RT dose were the significant factors for local control. Interval between treatments was not significant. Concurrent chemotherapy was unable to be modelled successfully. The OS survival model predicted a 50% two-year OS rate with RT doses above 76.47Gy. The OS model validated well against an external cohort and had a high Pearson correlation coefficient of 0.79. Dose escalation may be possible in a subgroup of patients but needs further investigation in a planning study. These models suggest that patients have better outcomes when their tumours are low volume and at high doses, indicating that frequent surveillance and use of SABR for re-irradiation is a strategy which may improve outcomes.

7 Re-irradiation planning

7.1 Introduction

Historically, re-irradiation was planned with photons, bespoke dose constraints and fixed fields. The dose to the cord was prioritised and the dose to other OARs was kept low as possible. This was due to the relatively robust pre-clinical and clinical data on re-irradiation of the spinal cord, and the relatively sparse data on re-irradiation tolerance for other organs. For example, in the prospective phase I/II re-irradiation study using 3D conformal radiotherapy by Wu *et al.*, the only constraint was the spinal cord dose at retreatment (limited to 25Gy) and the V20Gy dose was minimised¹²⁰.

Radiotherapy technology has advanced significantly over the last 20 years. Simulation has moved from 2D X-rays to CT simulation, with 4D-CT scans now commonplace. Radiotherapy planning techniques have become more conformal, from 3D-CRT to IMRT and SABR. The modality of re-irradiation was mainly photons, but now may include carbon ion or protons. Treatment delivery with cone beam computed tomography (CBCT) ensures that the radiation treatment is more likely to be accurately delivered.

Radiotherapy planning has become more advanced with the use of inverse planning, and new technologies such as multi-criteria optimisation (MCO). MCO is a planning algorithm that attempts to find the optimum compromise between competing dose objectives, e.g. low dose to OARs and high dose to PTV⁹³. It aims to solve the issue of several iterations of treatment plans where the planner does not know the best compromise dose. MCO generates several plans for each OAR constraint thereby allowing the planner to modify the dose to a given OAR, whilst seeing in real-time the effect this has on the other OARs of concern. It has been shown to reduce the time taken to generate suitable plans and produce plans with better OAR dose sparing in NSCLC and other tumour sites^{94,269}.

Photon dose calculations methods have also improved. The gold standard of dose calculation has been the Monte Carlo method, but this method is computationally demanding and time-consuming to be in regular clinical use. The Analytical Anisotropic Algorithm (AAA), which was used in the Beatson until

2018, is a 'type b' algorithm which models electron transport (unlike 'type a' algorithms)²⁷⁰. This was superseded by Acuros XB, which has been shown to better match the dose predictions from the Monte Carlo method than AAA, especially in areas where there are changes in the density of tissue, e.g. lung/bone interfaces²⁷¹.

These advances in technology may help when planning re-irradiation, as there are often multiple competing dose objectives, with a need for highly accurate treatment. The recent development and publication of dose constraints now give radiotherapy planners objectives for OARs^{112,146,160}. However, there remains uncertainty in how to best apply the constraints and technology to generate optimal re-irradiation plans.

There are three main areas of uncertainty in thoracic re-irradiation planning. Firstly, there is no widely available methodology to account for previous delivered dose using image and dose registration techniques. McVicar *et al.* developed and tested an in-house Matlab solution to convert the dose from an initial treatment to EQD2 and use this as a base plan when planning a retreatment²⁷². This gives an anatomical map of dose distribution, rather than a simple Dmax value for an organ (as this value would not describe where the area of high dose is from the initial treatment, which is required for accurate re-irradiation planning). However, this technique is not yet commercially available.

Secondly, there is a dose conversion issue. Radiotherapy is planned using physical dose measured in Gray. The cumulative dose constraints are in EQD2 Gy or BED (as they have to account for the different doses and fractionations between two treatments). There is no standard calculation method to convert remaining dose from EQD2 to physical dose. Most calculations are based on the LQ formulation. Paradis *et al.* used a 'discount' method, where assumed recovery depended on the time between initial radiotherapy and re-irradiation when calculating the dose constraints at their institution, however this is not a robustly proven strategy¹¹². Finally, the optimal radiation planning technique or modality for re-irradiation has yet to be determined. Troost *et al.* compared photons and protons for re-irradiation of NSCLC¹⁴⁶. Highly conformal treatments (VMAT, Cyberknife or Intensity modulated proton therapy) were found to reduce the dose to OARs compared to 3D conventionally planned photons and maintain a

high dose to the target volume. MCO was not assessed in this study. As with any planning study, the location of the tumours was not disclosed and therefore it was difficult to relate the findings to clinical practice.

The aim of this re-irradiation planning exercise is to assess a potential re-irradiation workflow for non-small cell lung cancer. The objectives are to apply the recently published dose constraints to the Beatson cohort of patients (who would have been planned using a cord constraint and attempting to keep other OAR doses as low as possible). The patients who failed the dose constraints will be replanned using the dose registration technique outlined in Chapter 4, and a comparison will be made between VMAT and VMAT+MCO plans, to investigate the utility of MCO in this setting. Different strategies to treat patients who did not meet the dose constraints will be attempted, and the optimal re-plans will be verified and assessed using the models in Chapters 5 and 6 to determine the clinical significance of the replans.

7.2 Methods

7.2.1 Ethics and data collection

The NHS GGC Caldicott Guardian approved the use of patient data for this project. The search strategy, contouring, creating of EQD2 and deformable dose registration was the same as described in Chapters 4.2.2 to 4.2.5. To summarise this, patients who received two or more courses of radical thoracic radiation between 01/01/2014 and 02/11/2020 in the Beatson West of Scotland Cancer Centre were identified by a search of the radiotherapy database.

7.2.2 Identification of patients that passed or failed the cumulative dose constraints

These patient scans (both the initial and re-irradiation) had a complete set of OARs contoured by the researcher (RR) and verified by a consultant clinical oncologist with a specialist interest in thoracic malignancies (SH) for accuracy. A complete set of OARs consisted of lungs, heart, brachial plexus, spinal cord, heart and cardiac substructures, aorta, proximal bronchial tree and oesophagus.

Each primary and re-irradiation plan had the dose recalculated using the same plan parameters but using Acuros XB (as some of the older plans used AAA). The updated plans were exported to an image registration, EQD2 dose converter and dose summation programme (Velocity AI version 3.2, Varian Medical Systems, Palo Alto, California, US). The primary and re-irradiation plans underwent dose conversion from physical dose in Gray to EQD2. The EQD2 dose maps and co-registered images from the primary and re-irradiation plan then underwent deformable image registration (DIR). The total cumulative dose in EQD2 was determined by summation of the two dose maps using the deformable image registration. The region of interest for all deformable registrations were determined as the whole lung, based on the evaluation in Chapter 4.

The published dose constraints used were divided into desirable, moderate and essential. The desirable constraints were the lowest dose constraints, the essential were the highest dose constraints (or in the event that there was no value, then as low as reasonably achievable) and the moderate constraints were values in between the essential and desirable constraints. The dose constraints used in this study are summarised in Table 7.1.

Table 7.1 Dose constraints split into desirable, moderate and essential criteria. ALARA, as low as reasonably achievable, ARS: American Radium Society, Dxcc: maximum dose to an organ at risk to a volume of xcc, EQD2 Gy: equivalent dose in 2-Gray fractions, MLD: mean lung dose, PBrT: proximal bronchial tree, Vx: cumulative volume receiving at least x Gray

Desirable	α/β	Metric	EQD2 Gy	Source of constraint
Spinal cord	2	D0.1cc<	57	ARS
Brachial plexus	2	D0.1cc<	80	Delphi
Skin/Chest wall	2.5	D0.1cc<	116	Paradis
Heart	2.5	D0.1cc<	86.1	Paradis
Lung	3	V20<	30	ARS
Lung	3	MLD<	22	Troost
PBrT	3	D0.1cc<	85.8	Paradis
Oesophagus	3	D0.1cc<	87.5	Paradis
Great vessels	3	D0.1cc<	110	Troost
Moderate			EQD2 Gy	Source of constraint
Spinal cord	2	D0.1cc<	61.6	Paradis
Brachial plexus	2	D0.1cc<	85	Paradis/ARS/Troost
Skin/Chest wall	2.5	D0.1cc<	ALARA	Delphi
Heart	2.5	D0.1cc<	ALARA	Delphi

Lung	3	V20<	40	ARS
Lung	3	MLD<	22	Troost
PBrT	3	D0.1cc<	105	Hunter
Oesophagus	3	D0.1cc<	100	Troost
Great vessels	3	D0.1cc<	116.5	Paradis
Essential			EQD2 Gy	Source of constraint
Spinal cord	2	D0.1cc<	67.5	Hunter
Brachial plexus	2	D0.1cc<	95	Chen et al. 2017
Skin/Chest wall	2.5	D0.1cc<	ALARA	Paradis
Heart	2.5	D0.1cc<	ALARA	Paradis
Lung	3	V20<	ALARA	ARS
Lung	3	MLD<	ALARA	Troost
PBrT	3	D0.1cc<	110	ARS/Troost
Oesophagus	3	D0.1cc<	110	ARS
Great vessels	3	D0.1cc<	120	ARS

The cumulative dose data for each patient was compared to the desirable (i.e., most conservative) cumulative dose constraints. Patients who breached the desirable dose constraints were selected for re-planning.

7.2.3 Re-irradiation re-plan

7.2.3.1 Remaining dose calculation

This planning study assumed that the initial radical radiation course is unalterable. Therefore, the remaining dose that an OAR can receive at re-irradiation was calculated by converting the initial dose into EQD2, subtracting this from the constraint, and then converting this to a physical dose to use as an optimisation objective at re-irradiation planning. No discount for recovery in OAR dose was made. The physical dose takes into account the fractionation scheme of the re-irradiation. This mathematical process is outlined below.

1. Calculate delivered dose from first course of radiation

$$BED_1 = D_1 \cdot \left(1 + \frac{d_1}{\alpha/\beta} \right)$$

Or:

$$EQD2_1 = D_1 \cdot \left(\frac{d_1 + \alpha/\beta}{2 + \alpha/\beta} \right)$$

BED_1 = Biological effective dose for treatment 1

$EQD2_1$ = Equivalent dose in 2-Gray fractions for treatment 1

D_1 = Total dose received by the OAR in treatment 1

d_1 = Dose per fraction received by the OAR in treatment 1

α/β = alpha/beta ratio for the OAR

2. Subtract $EQD2_1$ from selected dose constraint then convert remaining dose into BED (BED_{rem})
3. Convert BED_{rem} into physical dose using the chosen re-irradiation dose and fractionation

$$BED_{rem} = D_2 \cdot \left(1 + \frac{d_2}{\alpha/\beta} \right)$$

D_2 = Total dose received by the OAR in treatment 2

d_2 = Dose per fraction received by the OAR in treatment 2

D_2 can be written as $n_2 \cdot d_2$ where n_2 is the number of fractions planned for re-irradiation

$$BED_{rem} = n_2 \cdot d_2 \cdot \left(1 + \frac{d_2}{\alpha/\beta} \right)$$

This can be re-arranged into:

$$BED_{rem} = n_2 d_2 + \frac{n_2 d_2^2}{\alpha/\beta}$$

This is then re-arranged into a quadratic equation:

$$n_2 d_2^2 + \alpha/\beta(n_2 d_2) - \alpha/\beta(BED_{rem}) = 0$$

d_2 is found by entering the known values (BED_{rem} , n_2 , α/β) and taking the positive solution from this equation

$$x = \frac{-b \pm \sqrt{b^2 - 4ac}}{2a}$$

7.2.3.2 Initial re-planning approach

The initial replanning approach used the same dose and fractionation as delivered but the calculated dose constraints in IMRT optimisation. Once an IMRT plan had been developed, the plan was re-optimised using MCO. In all re-planning, the OARs and PTV were unchanged from the original re-irradiation plan. The first stage of this process took all the patients that failed the desirable dose constraints and re-planned them using IMRT or IMRT+MCO using the same desirable dose constraints. As the original plans pre-dated the cumulative dose constraints and were planned with bespoke clinician determined values, this tested whether the desirable dose constraints were achievable if they had been applied. Re-planning was successful if the doses to all OARs were under the physical dose constraints, the D95% of the PTV was 95%, and in non-SABR plans, the PTV D0.1cc was <107% of the prescription dose.

If the patients were unable to be replanned successfully with the desirable dose constraints, the plans would be re-attempted using the moderate constraints. For moderate cumulative constraints which are ALARA (e.g., chest wall, heart) the desirable constraints were kept in the optimisation algorithm, but had the priority reduced sequentially until the other OARs or PTV objectives were met. If this was unsuccessful, the remaining patients would be re-planned using the essential constraints, using the same principles where OAR constraints became ALARA. This process is summarised in Figure 7.1. The generated ideal plans were checked by two physicists experienced in thoracic radiotherapy.

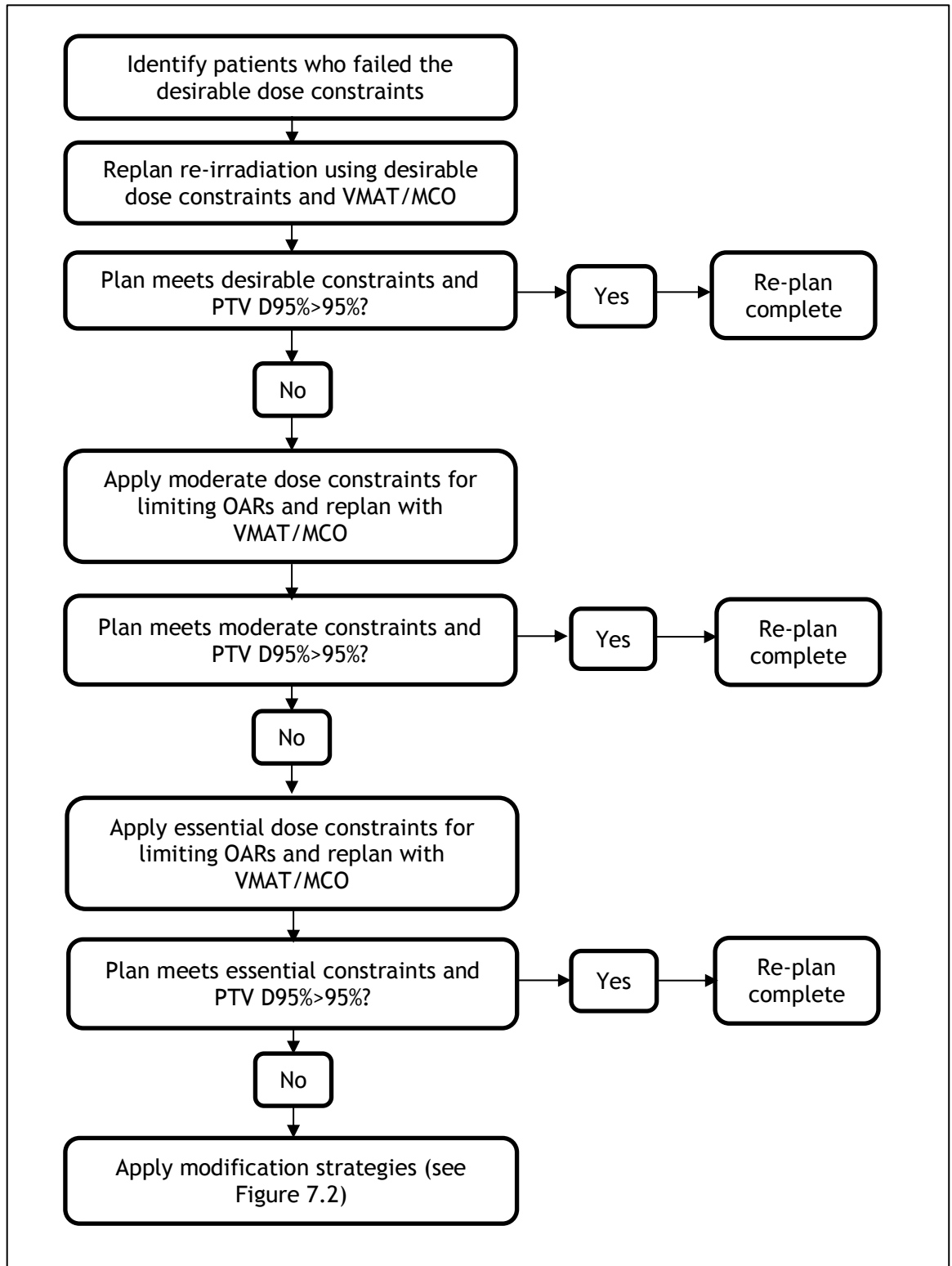


Figure 7.1 Re-irradiation planning process. MCO: multi-criteria optimisation, PTV D95%: dose to 95% of the planning target volume, VMAT: volumetric arc therapy.

7.2.3.3 Replanning approach if failed essential constraints

Where re-irradiation plans were unable to be successfully re-planned to meet the essential constraints, four strategies were employed to deliver a radical dose. The dose and fractionation were changed from the original schedule to a lower dose per fraction e.g., from 55Gy/20fr, to 60Gy/30fr or 54Gy/36fr. If this was not successful, the PTV was altered as per the Delphi recommendations in Chapter 3 (grow CTV by 0.5cm). If this failed, the PTV was cropped from any intersecting OARs. The final method was an adaptive approach, where half the dose was delivered to the planned PTV, then replanned for the remaining dose assuming that the tumour volume had shrunk by 10%. This process is summarised in Figure 7.2.

7.2.4 Cumulative dose verification

Once a re-plan met the criteria for success, this was nominated as the optimal re-irradiation re-plan. The optimal re-plans were then exported to VelocityAI and the dose was converted to EQD2. The replan was then deformably dose registered with each patients' primary radiotherapy plan, and the cumulative EQD2 dose was summed. This cumulative dose volume was then compared against the dose constraints to confirm if the cumulative dose constraints were met.

7.2.5 Outcome risk calculation

The cumulative doses from the re-plans and from the actual cumulative dose for each OAR, were entered into the dose/toxicity models from Chapter 5 (lungs, PBrT, oesophagus, aorta and spinal cord). The predicted 2-year overall survival and local control rates were calculated from the models from Chapter 6. This allowed a risk profile to be created for each patient, comparing the probability of toxicity and efficacy of the delivered dose, and the re-plan. When an OAR model required another variable for prediction other than dose (e.g. the interval with the spinal cord model), the value was taken from each patients' data in the Beatson cohort database.

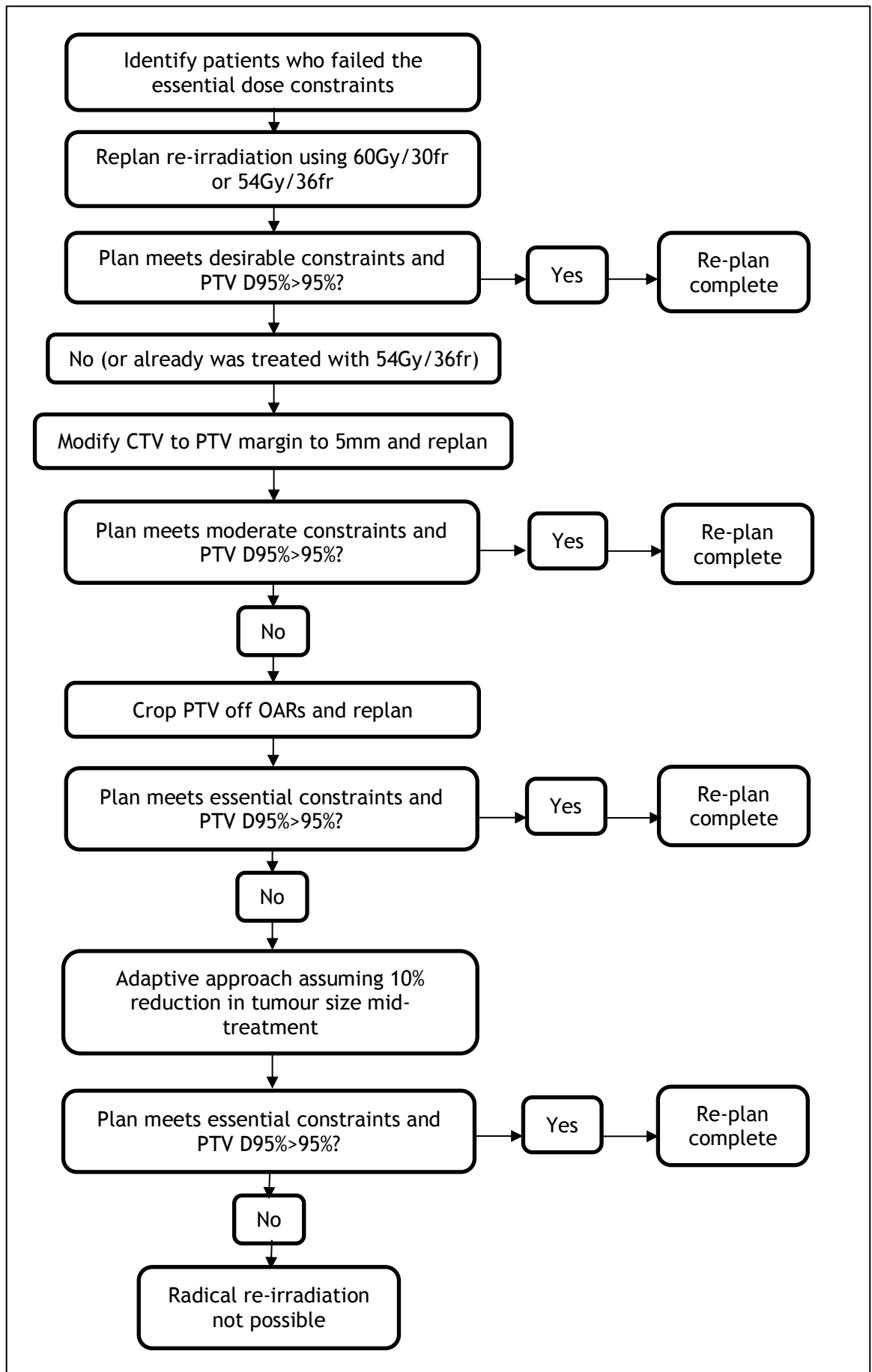


Figure 7.2 Replanning process for plans that failed essential constraints.

CTV: clinical target volume, Fr: fractions, OAR: organ at risk, PTV D95%: dose to 95% of the planning target volume.

7.2.6 Statistical analysis

The mean replanned doses to the OAR and the PTV were compared to the cumulative delivered re-irradiation dose using a paired student's t-test. The dose and risk differences between the delivered dose and the replanned dose were plotted to illustrate the change between the treatments for each patient.

7.3 Results

7.3.1 Desirable dose constraints and cumulative doses delivered in the Beatson cohort

Thirty-nine patients were identified who had radical dose thoracic re-irradiation. Two courses were given to 37 patients, and two patients had three courses of radical radiotherapy. Thirteen patients (33.3%) had local recurrence, as defined as overlapping PTVs on rigid registration. The characteristics of the patients, delivered re-irradiation plans, and the mean doses to each OAR are reported in Chapter 4 (Table 4.1 and 4.4).

The cumulative delivered doses to each OAR for each patient were calculated and compared to the desirable dose constraints detailed in Table 7.1. Eleven plans met the desirable dose constraints, 13 breached the chest wall constraint only, and 15 breached a non-chest wall constraint or more than one constraint (Figure 7.3). The mean PTV overlap was significantly higher in the non-chest wall/ ≥ 2 fails group, compared to the chest wall only fails or no fails (34% against 1.3% and 0.7% respectively, $p < 0.05$). Most of the patients who met the desirable dose constraints had second primary lung cancers (90.9%), whereas 66% of the multiple failure group had local recurrences. Most of the patients in the group that failed the chest wall constraints had SABR re-irradiation (76.9%).

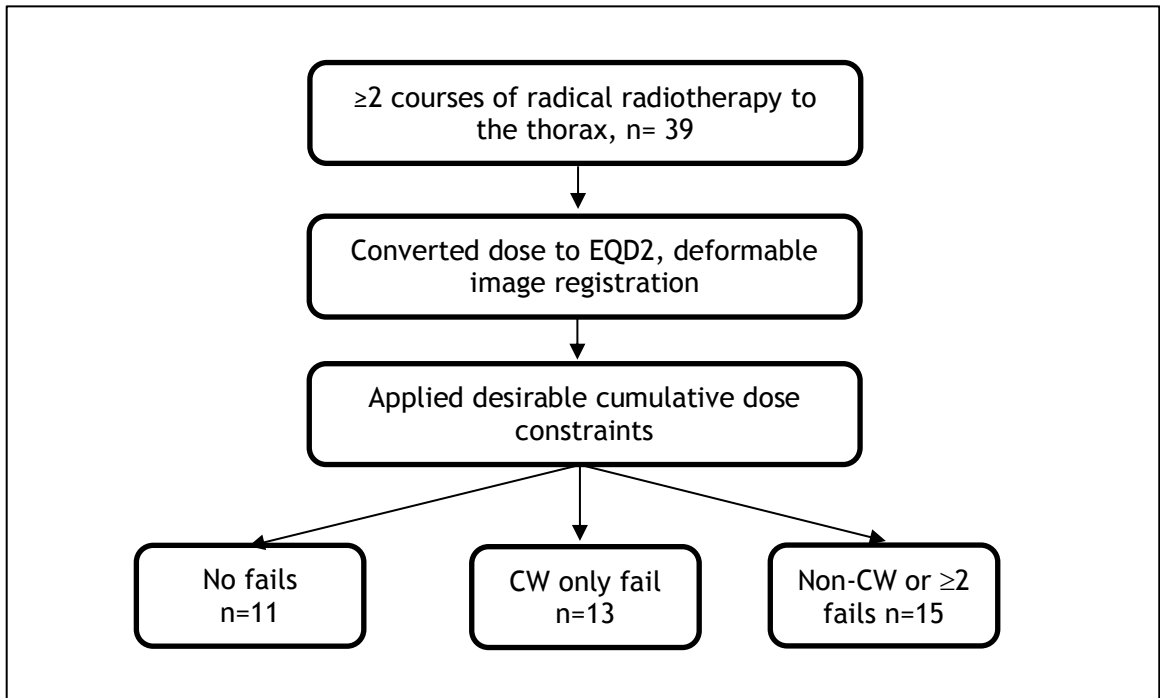


Figure 7.3 Beatson cohort and compliance with desirable dose constraints. CW: chest wall, EQD2: equivalent dose in 2-Gray fractions

The OAR breached the most often was the chest wall (20 plans, 40% of all breaches, Figure 7.4), followed by the proximal bronchial tree (7 plans, 16%) and the heart (6 plans, 12%).

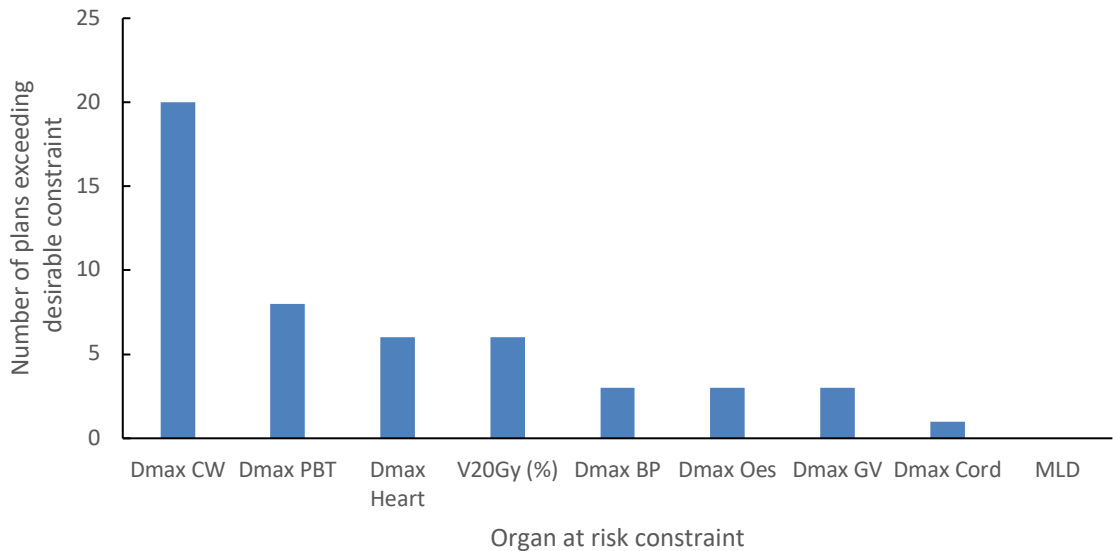


Figure 7.4 Number of breached desirable organ at risk constraints. BP: brachial plexus, CW: chest wall, Dmax: maximum dose, GV: great vessels, PBT: proximal bronchial tree, MLD: mean lung dose, V20Gy: volume of lung receiving at least 20Gy.

The rate of toxicity in those patients where the desirable dose constraint was breached is presented in Table 7.2. For the chest wall constraint and proximal bronchial tree, there was an associated risk of organ specific observed toxicity $\geq 5\%$, suggesting that the desirable constraints in this cohort may have some utility at discriminating patients who may develop toxicity. Interestingly, the cumulative lung constraints (V20 and MLD) did not discriminate for toxicity, with higher rates of organ specific toxicity seen (mostly lung infections) in patients who met the lung constraints.

Table 7.2 Rate of observed toxicity in relation to desirable constraints breached. BP: brachial plexus, CW: chest wall, Dmax: maximum dose, GV: great vessels, PBrT: proximal bronchial tree, MLD: mean lung dose, V20Gy: volume of lung receiving at least 20Gy.

	Number breached	Any \geq Grade 3 tox rate (%)	Organ specific toxicity rate (%)
Dmax CW	20	40	5
	19	31.6	0
Dmax PBrT	8	37.5	12.5
	31	35.5	0
Dmax Heart	6	33.3	0
	33	36.4	0
V20Gy (%)	6	16.7	16.7
	33	39.4	30.3
Dmax BP	3	0	0
	36	38.9	0
Dmax Oes	3	66.7	0
	36	33.3	0
Dmax GV	3	33.3	0
	36	36.1	0
Dmax Cord	1	0	0
	38	36.8	0
MLD	0	0	0
	39	35.8	28.2

7.3.2 Re-planning cohort

7.3.2.1 Replanned with desirable constraints

There were 28 patients who did not meet the retrospectively applied cumulative dose constraints. The 13 patients who had failed only the chest wall constraint were reviewed. Most patients were peripherally located (n=11, 84.6%) and 10

were re-treated with SABR. Two patients had centrally located tumours which were re-treated with CHART. The tumours in the chest wall failure group were all close to the chest wall. As the moderate dose constraints recommend the dose to the chest wall to be as low as reasonably achievable, these 13 plans would have all passed using the moderate constraints. Therefore, these were not replanned, as significant improvements would not be possible due to the tumour location, and that they would have met moderate (and therefore clinically acceptable) dose constraints.

Fifteen re-irradiation plans failed either a dose constraint other than the chest wall or failed two or more constraints. These plans were selected for replanning. The tumour locations, dose and fractionations and overlap of PTV are summarised in Table 7.3. The initial replanning process used the desirable dose constraints and attempted to re-plan the re-irradiation treatments to these retrospectively applied limits. None of the 15 plans were able to be re-planned to meet the desirable criteria (meets dose constraints, PTV D95>95%, PTV Dmax<107% for CFRT plans) with VMAT or with VMAT and MCO. Most of the re-treatments could be planned to meet the cumulative dose constraints (n=13, 86.7%), but none were able to meet the D95>95% target. There was a significantly lower mean dose to the OARs with the VMAT and VMAT+MCO replans for the chest wall, heart, lung V20, proximal bronchial tree, oesophagus and great vessels. There was no statistically significant difference for the cord, brachial plexus or mean lung dose. There was a significantly lower dose to the OARs with VMAT+MCO compared to VMAT alone, except for the brachial plexus dose and the MLD (Table 7.4 and Table 7.5).

Table 7.3 Patient and tumour details for the patients that failed the desirable dose constraints. C: central, LUL/LLL: left upper/lower lobe, P: peripheral, PTV: planning target volume, RUL/RML/RLL: right upper/middle/lower lobe, UC: ultracentral.

Patient number	Age	Sex	Location and prescription dose of first treatment			Location and prescriptions dose of second treatment			Overlap of first PTV and second PTV (%)
1	66.8	M	right hilum	UC	55/20	RLL	P	55/20	9.8
6	65.8	M	right hilum	UC	54/36	Right hilum	UC	55/20	97.5
8	84.6	M	LUL	UC	55/20	LUL	UC	54/36	51.0

11	64.0	F	LLL	P	55/20	RML	C	55/20	34.9
12	63.7	M	LUL	UC	55/20	LUL	UC	54/36	10.6
15	74.8	F	RUL	UC	55/20	RUL	P	55/20	85.1
20	71.2	M	LUL	UC	55/20	LUL	C	55/20	97.4
21	67.2	M	RUL	C	50/5	LUL	C	50/5	0.0
23	80.7	F	LLL	UC	54/36	LLL	UC	55/20	72.9
24	78.0	F	LUL	P	55/20	RML	P	50/5	0.0
25	67.7	M	RLL	UC	55/20	LUL	UC	54/36	0.0
27	71.9	M	LUL	P	55/20	LUL	UC	55/20	9.8
29	79.0	M	LUL	UC	55/20	LUL	UC	55/20	47.8
34	65.7	F	LUL	UC	55/20	RUL	C	54/36	0.0
46	56.9	F	RUL	UC	55/20	LLL	P	54/36	0.0

Table 7.4 Mean delivered and replanned OAR doses. Fifteen patients included. Dxcc: maximum dose to an organ at risk to a volume of xcc, Oes: oesophagus, PBrT: proximal bronchial tree, MCO: multi-criteria optimisation, MLD: mean lung dose, V20Gy: volume of lung receiving at least 20Gy, VMAT: volumetric arc therapy.

	Mean delivered dose	Mean VMAT replan dose	Mean VMAT+MCO replan dose
D0.1cc Cord	15.36	15.10	14.05
D0.1cc brachial plexus	8.97	6.94	6.37
D0.1cc chest wall	51.81	36.48	35.67
D0.1cc Heart	33.69	16.70	15.09
V20-PTV%	9.66	4.91	4.48
MLD	7.13	4.47	4.21
D0.1cc PBrT	40.13	22.60	21.32
D0.1cc Oes	30.40	20.45	18.45
D0.1cc Great vessels	45.33	33.71	32.33

Table 7.5 Differences between delivered and replanned OAR doses. Fifteen patients included. Dxcc: maximum dose to an organ at risk to a volume of xcc, Oes: oesophagus, PBrT: proximal bronchial tree, MCO: multi-criteria optimisation, MLD: mean lung dose, V20Gy: volume of lung receiving at least 20Gy, VMAT: volumetric arc therapy.

	Mean difference between delivered dose and VMAT replan	Paired t-test p-value	Difference between delivered dose and VMAT+MCO replan	Paired t-test p-value	Difference between VMAT and VMAT+MCO replans	Paired t-test p-value
D0.1cc Cord	0.26	0.90	1.31	0.52	1.05	0.01
D0.1cc brachial plexus	2.03	0.14	2.60	0.11	0.57	0.08

D0.1cc chest wall	15.33	0.00	16.13	0.00	0.81	0.03
D0.1cc Heart	16.98	0.00	18.59	0.00	1.61	0.01
V20-PTV%	4.75	0.03	5.18	0.02	0.43	0.00
MLD	2.66	0.08	2.92	0.06	0.26	0.12
D0.1cc PBrT	17.53	0.00	18.81	0.00	1.28	0.03
D0.1cc Oes	9.95	0.02	11.95	0.01	2.00	0.00
D0.1cc Great vessels	11.61	0.01	12.99	0.00	1.38	0.05

The replans using VMAT and VMAT+MCO had significantly lower doses to the PTV D95, D99 and Dmax compared to the delivered dose. The replanned PTVs had a D95 around 41-43% less than the delivered dose (Table 7.6 and Table 7.7).

Table 7.6 Delivered and replanned PTV doses. Dx%: maximum dose to the planning target volume to x% of that volume, Dmax: maximum dose, MCO: multi-criteria optimisation, Pt: Patient, PTV: planning target volume, VMAT: volumetric arc therapy.

Pt	Delivered PTV dose			VMAT replan PTV dose			VMAT+MCO replan PTV dose		
	D95(%)	D99(%)	Dmax	D95(%)	D99(%)	Dmax	D95(%)	D99(%)	Dmax
1	95.5	90.1	111.3	90.8	89.4	105.1	90.1	84.4	110.2
6	81.1	73	109.5	63.1	47.1	106.1	57.9	44.4	105.9
8	96.6	92.2	108.7	39	31.3	65.6	39.8	34.5	65.3
11	95.6	91.7	107.7	35.6	33	82.1	36.6	34.7	89.6
12	96.5	93.5	109.6	73.2	42.6	109.4	70.8	40.9	108.8
15	94.5	90.7	108.6	65.3	53.5	104.3	59.9	52.5	103.3
20	94	89.4	108.0	57.1	42.1	110.6	56.5	42.7	110.3
21	76.1	71.2	125.5	9.2	8.3	21.6	9.3	8.5	21
23	92.3	86.7	108.1	56.3	45.2	95.2	58.5	46.3	100.8
24	88.5	84.9	122.3	39.4	32.4	85.8	36	32.2	81.4
25	93.9	90.7	109.4	12.9	7.7	52.5	12.2	7.4	52.5
27	96.2	93.6	111.5	31.2	17.2	113.2	27.9	16.9	110.1
29	97.9	94	112.5	42.4	36.8	70.9	44.6	36.6	74.4
34	96	90.4	110.6	61.7	39.1	98.4	54	34.4	100.8
46	91.9	87.4	105.5	85.3	70.9	107	82.6	70.7	108.3

Table 7.7 Differences between the delivered and replanned PTV doses. Dx%: maximum dose to the planning target volume to x% of that volume, Dmax: maximum dose, MCO: multi-criteria optimisation, PTV: planning target volume, VMAT: volumetric arc therapy.

Pt	Difference between PTV D95% delivered dose and VMAT replan	Difference between PTV D95% delivered dose and VMAT+MCO replan	Difference between PTV D95%VMAT and VMAT+MCO replans
1	-4.7	-5.4	0.7
6	-18	-23.2	5.2
8	-57.6	-56.8	-0.8
11	-60	-59	-1
12	-23.3	-25.7	2.4
15	-29.2	-34.6	5.4
20	-36.9	-37.5	0.6
21	-66.9	-66.8	-0.1
23	-36	-33.8	-2.2
24	-49.1	-52.5	3.4
25	-81	-81.7	0.7
27	-65	-68.3	3.3
29	-55.5	-53.3	-2.2
34	-34.3	-42	7.7
46	-6.6	-9.3	2.7

This demonstrates that clinically acceptable plans could not be created using the desirable dose constraints despite use of modern planning techniques. VMAT in combination with MCO may have a benefit in reducing doses to the OARs, but not to the extent required to make the re-plans meet the PTV constraints.

7.3.2.2 Replanned with moderate constraints

All 15 patients were replanned using the moderate dose constraints. No replans met the acceptable plan criteria (PTV D95%>95%, all OAR constraints met) when planned with VMAT. However, when MCO was added to the plans, seven plans became acceptable. The moderate dose constraints were met in 14 cases (93.3%). The case where the dose constraints could not be met was a central re-treatment where the dose to the aorta and the PBrT were close to the constraint.

Compared to the delivered dose, the VMAT replans delivered a lower dose to the OARs in general but did not have significantly different mean OAR doses (Table 7.8 and Table 7.9). The exception was the heart dose, which had a significantly

lower dose (33.7% vs 24.8%, p-value 0.01). This analysis did not consider the base of heart dose, high dose to which has been associated with higher mortality rates. Similarly to the VMAT replans, the VMAT+MCO replans had a lower dose to the OARs, meeting statistically significant dose reductions for the heart, PBrT and great vessels. Both VMAT and VMAT+MCO had a non-significantly higher dose to the cord than the mean delivered dose. When VMAT re-plans were compared to the VMAT+MCO re-plans, the latter had significantly lower OAR doses to the cord, PBrT and oesophagus.

Table 7.8 Mean delivered and replanned OAR doses. Fifteen patients included. Dxcc: maximum dose to an organ at risk to a volume of xcc, Oes: oesophagus, PBrT: proximal bronchial tree, MCO: multi-criteria optimisation, MLD: mean lung dose, V20Gy: volume of lung receiving at least 20Gy, VMAT: volumetric arc therapy.

	Mean delivered dose	Mean VMAT replan dose	Mean VMAT+MCO replan dose
D0.1cc Cord	15.36	19.24	17.51
D0.1cc brachial plexus	8.97	7.76	6.88
D0.1cc chest wall	51.81	48.17	49.02
D0.1cc Heart	33.69	24.77	25.98
V20-PTV%	9.66	7.01	6.92
MLD	7.13	5.57	5.20
D0.1cc PBrT	40.13	34.83	33.05
D0.1cc Oes	30.40	27.86	24.55
D0.1cc Great vessels	45.33	38.89	39.67

Table 7.9 Differences between the delivered and replanned OAR doses. Dxcc: maximum dose to an organ at risk to a volume of xcc, Oes: oesophagus, PBrT: proximal bronchial tree, MCO: multi-criteria optimisation, MLD: mean lung dose, V20Gy: volume of lung receiving at least 20Gy, VMAT: volumetric arc therapy.

	Mean difference between delivered dose and VMAT replan	Paired t-test p-value	Difference between delivered dose and VMAT+MCO replan	Paired t-test p-value	Difference between VMAT and VMAT+MCO replans	Paired t-test p-value
D0.1cc Cord	-3.88	0.08	-2.15	0.34	1.73	0.01

D0.1cc brachial plexus	1.21	0.18	2.09	0.12	0.88	0.08
D0.1cc chest wall	3.64	0.07	2.78	0.14	-0.85	0.42
D0.1cc Heart	8.92	0.01	7.70	0.02	-1.22	0.41
V20- PTV%	2.65	0.19	2.74	0.18	0.09	0.57
MLD	1.56	0.30	1.92	0.20	0.37	0.09
D0.1cc PBrT	5.30	0.07	7.07	0.01	1.77	0.04
D0.1cc Oes	2.55	0.44	5.86	0.06	3.31	0.03
D0.1cc Great vessels	6.43	0.08	5.66	0.02	-0.78	0.78

The re-plans with either VMAT or VMAT+MCO had a D95% approximately 8-10% lower than the delivered dose. The mean D95% and D99% values were higher by about 2-4% in the VMAT+MCO group compared with the VMAT group, but was not statistically significant (Table 7.10 and Table 7.11).

Table 7.10 Mean delivered and replanned PTV doses to moderate constraints. Dx%: maximum dose to the planning target volume to x% of that volume, Dmax: maximum dose, MCO: multi-criteria optimisation, PTV: planning target volume, VMAT: volumetric arc therapy.

	Mean delivered dose	Mean VMAT replan dose	Mean VMAT+MCO replan dose
D95% PTV (%)	92.44	82.66	84.64
D99% PTV (%)	87.97	75.58	79.60
Dmax PTV (%)	111.26	107.47	105.69

Table 7.11 Differences between the delivered and replanned PTV doses using moderate constraints. Dx%: maximum dose to the planning target volume to x% of that volume, Dmax: maximum dose, MCO: multi-criteria optimisation, PTV: planning target volume, VMAT: volumetric arc therapy.

	Mean difference between delivered dose and VMAT replan	Paired t-test p-value	Difference between delivered dose and VMAT+MCO replan	Paired t-test p-value	Difference between VMAT and VMAT+MCO replans	Paired t-test p-value
D95% PTV (%)	9.78	0.13	7.80	0.24	-1.98	0.12
D99% PTV (%)	12.39	0.08	8.37	0.23	-4.02	0.06
Dmax PTV (%)	3.79	0.40	5.57	0.16	1.78	0.41

7.3.2.3 Replanned with essential constraints

The eight patients who did not meet either the desirable or moderate constraints were replanned using the essential dose constraints. The VMAT and VMAT+MCO replans all met the essential dose constraints. However, no re-plans met the acceptable PTV criteria of D95>95% and Dmax<107%. Five VMAT+MCO re-plans had D95% >90% but <95%. Six plans had PTV Dmax >107%.

The VMAT and VMAT+MCO plans generally had lower mean doses to the OARs compared to the delivered dose plans (Table 7.12 and Table 7.13). However, the mean cord dose was higher in the replans than in the delivered dose; this difference was only statistically significant for the VMAT replans. The heart, PBrT and great vessels doses were significantly lower in both the VMAT and VMAT+MCO replans. There was no significant difference in VMAT and VMAT+MCO replan doses, except for the cord dose, which was significantly lower with VMAT+MCO.

Table 7.12 Mean delivered and replanned OAR doses. Eight patients included. D_{xxc}: maximum dose to an organ at risk to a volume of xcc, Oes: oesophagus, PBrT: proximal bronchial tree, MCO: multi-criteria optimisation, MLD: mean lung dose, V20: volume of lung receiving at least 20Gy, VMAT: volumetric arc therapy.

	Mean delivered dose	Mean VMAT replan dose	Mean VMAT+MCO replan dose
D0.1cc Cord	19.08	26.97	24.34
D0.1cc brachial plexus	11.26	10.79	9.78
D0.1cc chest wall	48.86	48.42	48.22
D0.1cc Heart	44.01	34.20	36.38
V20-PTV%	13.46	12.30	12.49
MLD	9.53	7.81	7.81
D0.1cc PBrT	53.98	47.51	46.83
D0.1cc Oes	40.15	40.05	38.71
D0.1cc Great vessels	57.58	53.38	53.41

Table 7.13 Differences between the delivered and replanned OAR doses. D_{xxc}: maximum dose to an organ at risk to a volume of xcc, Oes: oesophagus, PBrT: proximal bronchial tree, MCO: multi-criteria optimisation, MLD: mean lung dose, V20: volume of lung receiving at least 20Gy, VMAT: volumetric arc therapy.

	Mean difference between delivered dose and VMAT replan	Paired t-test p-value	Difference between delivered dose and VMAT+MCO replan	Paired t-test p-value	Difference between VMAT and VMAT+MCO replans	Paired t-test p-value
D0.1cc Cord	-7.89	0.01	-5.25	0.08	2.63	0.01
D0.1cc brachial plexus	0.46	0.62	1.48	0.32	1.02	0.20
D0.1cc chest wall	0.44	0.74	0.64	0.60	0.21	0.60
D0.1cc Heart	9.80	0.01	7.63	0.01	-2.17	0.34
V20-PTV%	1.16	0.20	0.98	0.18	-0.19	0.40
MLD	1.71	0.38	1.72	0.34	0.01	0.96
D0.1cc PBrT	6.47	0.02	7.15	0.01	0.68	0.24
D0.1cc Oes	0.09	0.98	1.44	0.65	1.35	0.32
D0.1cc Great vessels	4.19	0.04	4.17	0.03	-0.02	0.95

The VMAT and VMAT+MCO replans had lower PTV D95 values (Table 7.14 and Table 7.15) compared to the delivered plans. The differences were not

statistically significant, but the mean difference in the delivered PTV D95 dose and the VMAT and VMAT+MCO replans were 9.6% and 7% respectively. VMAT+MCO delivered higher mean PTV D95 and PTV D99 (by 2.6% and 6.9% respectively) and were close to statistical significance (p-value 0.07 and 0.05).

Table 7.14 Mean delivered and replanned PTV doses. Dx%: maximum dose to the planning target volume to x% of that volume, Dmax: maximum dose, MCO: multi-criteria optimisation, PTV: planning target volume, VMAT: volumetric arc therapy.

	Mean delivered dose (%)	Mean VMAT replan dose (%)	Mean VMAT+MCO replan dose (%)
D95% PTV	93.74	83.89	86.74
D99% PTV	89.03	70.98	77.89
Dmax PTV	109.52	109.49	109.24

Table 7.15 Differences between the delivered and replanned PTV doses. Dx%: maximum dose to the planning target volume to x% of that volume, Dmax: maximum dose, MCO: multi-criteria optimisation, PTV: planning target volume, VMAT: volumetric arc therapy.

	Mean difference between delivered dose and VMAT replan	Paired t-test p-value	Difference between delivered dose and VMAT+MCO replan	Paired t-test p-value	Difference between VMAT and VMAT+MCO replans	Paired t-test p-value
D95% PTV	9.85	0.10	7.00	0.20	-2.85	0.07
D99% PTV	18.05	0.06	11.14	0.13	-6.91	0.05
Dmax PTV	0.03	0.98	0.28	0.82	0.25	0.85

7.3.3 Unable to meet essential constraints group

Acceptable plans were unable to be made for eight patients using VMAT or VMAT+MCO, despite using the essential (highest cumulative dose constraints). The characteristics of this group are summarised in Table 7.16. These re-plans are either ultracentral retreatments (n=7) or central retreatments (n=1). By contrast, the seven patients that were able to be replanned successfully had relapsed disease that was in a direction away from the mediastinum e.g.,

patient 15 had ultracentral disease at first treatment, but the location of relapse was peripheral to the initial PTV, despite having an 85.1% overlap. Two patients (patients 25 and 34) in the group that were unable to be replanned had no overlap with the original PTV but high levels of dosimetric overlap with the PBrT or great vessels.

These plans were replanned using different strategies to aim to meet dose constraints. The results of this process are summarised in Figure 7.5.

Table 7.16 Characteristics of re-plans unable to meet essential dose constraints. Eight patients included. C: Central, GV: Great vessels, OAR: Organ at risk, Oes: Oesophagus, PBrT: Proximal bronchial tree, PTV: Planning target volume, UC: Ultracentral.

Patient number	Limiting OAR (within 1Gy of constraint)	Location of retreatment	Planned retreatment dose and fractionation	Overlap of first PTV and second PTV (%)
6	PBrT, GV	UC	55/20	97.5
8	PBrT	UC	54/36	51
11	GV, V20	C	55/20	34.9
12	Oes, GV	UC	54/36	10.6
23	PBrT	UC	55/20	72.9
25	PBrT	UC	54/36	0
29	GV	UC	55/20	47.8
34	GV	UC	54/36	0

7.3.3.1 Dose and fractionation change

Three dose/fractionation schemes were tested: 55Gy/20 fractions (EQD2 = 63.3Gy using an α/β of 3), 60Gy/30 fractions (EQD2 = 60Gy), and 54Gy/36 fractions (EQD2 = 48.6Gy). Patients 6, 11, 23 and 29 were suitable for replanning with a prescription dose with a lower EQD2 to normal tissue (as the other patients were already treated with the most conservative fractionation of 54Gy/36fr).

Patients 6 and 23 when planned with 54Gy/36 fractions were able to meet the dose constraints and the PTV targets. The change in dose fractionation to 60/30 or 54/36 did not result in acceptable plans for patients 11 and 29.

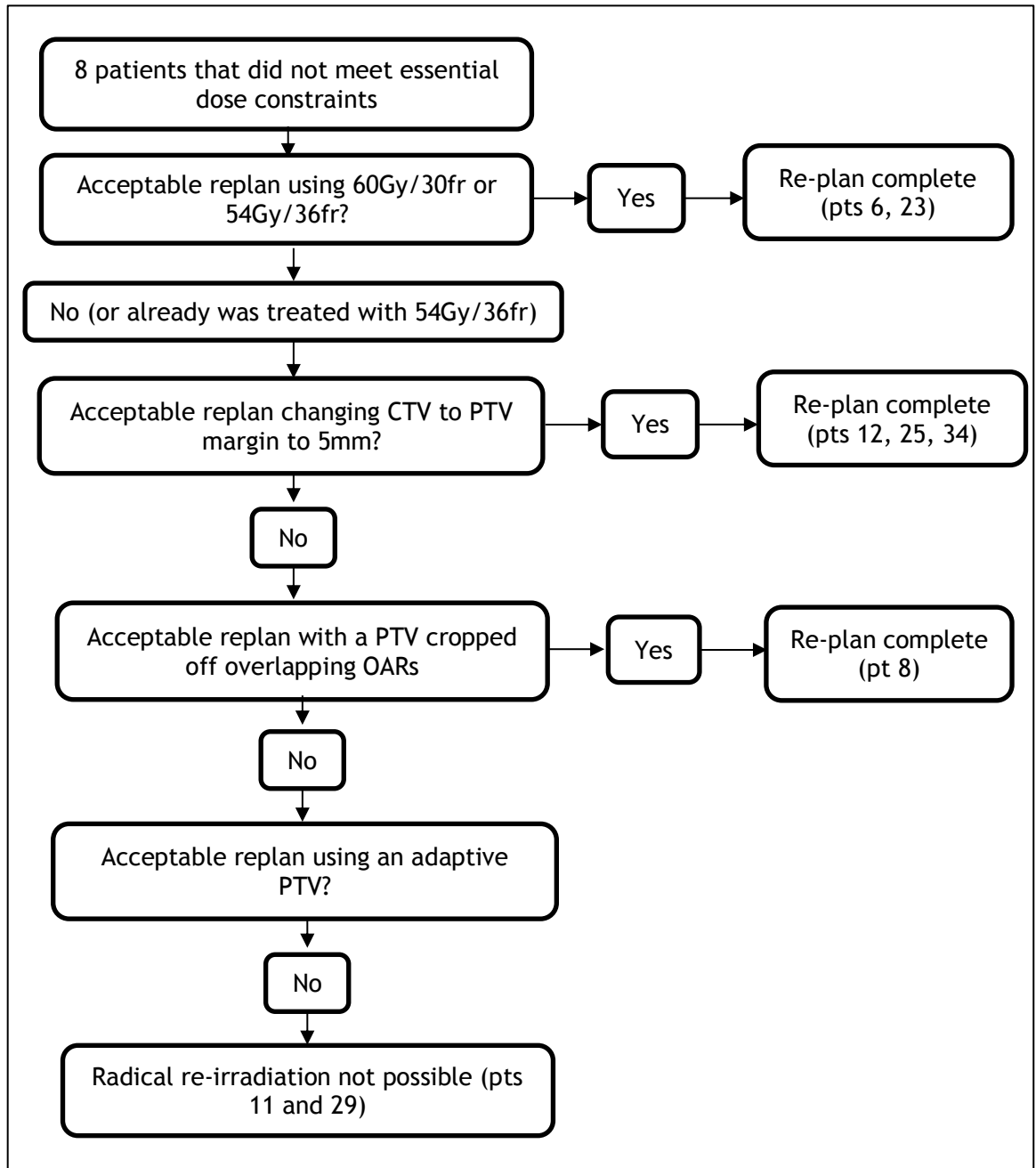


Figure 7.5 Outline of replanning using alternative strategies. CTV: clinical target volume, Fr: fractions, OAR: organ at risk, PTV: planning target volume.

7.3.3.2 Delphi PTV

The PTV growth recommended by the Delphi consensus on re-irradiation suggested a growth from CTV to PTV of 5mm. This is less than the standard growth of 10mm in the Beatson (before 4D-CT and VMAT planning). The retreatment CTVs were re-grown by 5mm isotropically to form Delphi PTVs for the six patients where the change in dose/fractionation did not result in an acceptable plan (patients 8, 11, 12, 25, 29 and 34). The Delphi PTVs were a median of 23.4% smaller (range 7.2 - 44.6%, Table 7.17). Some patients (12 and 25) had a relatively minor reduction in PTV volume suggesting that a smaller expansion than 10mm had been used when forming the original PTV (which had not been documented originally).

Table 7.17 Original and Delphi PTV volumes. CTV: Clinical target volume, PTV: Planning target volume.

Patient number	CTV (cc)	Original PTV (cc)	Delphi PTV (cc)	% reduction
8	86.3	244.1	188.1	22.9
11	41.5	217.5	120.4	44.6
12	199.4	417.4	352.9	15.5
25	182.3	365.9	339.6	7.2
29	82.7	254.6	193.9	23.8
34	95.2	251.1	157.5	37.3

These six patients were replanned using the smaller Delphi PTV, and patients 12, 25 and 34 had re-plans that met the acceptable plan criteria.

7.3.3.3 Cropped PTV

The Delphi consensus process also suggested that the dose to the OARs should be prioritised over the dose to the PTV. This approach was tested on the remaining patients that did not meet dose constraints (patients 8, 11 and 29). These patients had original PTVs that overlapped with OARs (PBrT for patient 8 and great vessels for patients 11 and 29). The original PTVs were cropped to exclude these OARs and the changes in volume are summarised in Table 7.18.

Table 7.18 Original and cropped PTV volumes. CTV: Clinical target volume, PTV: Planning target volume.

Patient number	CTV (cc)	PTV (cc)	Cropped PTV (cc)	% reduction
8	86.3	244.1	233.2	4.5
11	41.5	217.5	194.5	10.6
29	82.7	254.6	223.5	12.2

Patient 8 was replanned using the cropped PTV and met the acceptable plan criteria, but the replans for patients 11 and 29 did not.

7.3.3.4 Adaptive PTV

For the remaining two patients (11 and 29), an exploratory strategy was used where the treatment was split with a mandated replan after half of the prescription dose was delivered. This assumed that the original GTV responded to treatment, and the GTV along its longest plane had shrunk by 1mm. This adaptive GTV was expanded using institutional expansions (GTV to CTV by 5mm, CTV to PTV 5mm circumferentially and 10mm in the superior and inferior directions) to form the adaptive PTV. The second half of the treatment used this smaller adaptive PTV to attempt to reduce dose to the OARs. This process reduced the PTV for the second half of treatment substantially (by 55.5 and 34.6%, Table 7.19).

Table 7.19 Initial and adaptive PTV volumes. GTV: gross tumour volume, PTV: Planning target volume.

Patient number	Initial GTV (cc)	Adaptive GTV (cc)	Initial PTV (cc)	Adaptive PTV (cc)	% reduction
11	11.9	7.1	217.5	96.9	55.5
29	35.6	23.2	254.6	166.4	34.6

Despite the large reductions in volume, the adaptive PTVs for both patients still overlapped with the great vessels. Both replans still did not meet the acceptable plan criteria.

7.3.4 Verification

The OAR dose limits used in the replans were physical doses, calculated using the method outlined in section 7.2.3.1. This accounted for the previous dose delivered in the first treatment and was subtracted from the cumulative dose constraint. As this is a calculation-based process, the final dose needs to be verified anatomically. Therefore, the best retreatment plans of the 15 patients that did not meet the desirable dose constraints were transferred to Velocity, converted into EQD2 and summed with the dose from the initial treatment (also converted into EQD2). This process would confirm if the physical planning process correlated with the cumulative dose delivered, as measured in EQD2 Gy.

The cumulative doses (formed from the initial treatment and the best re-plan) met the expected cumulative dose constraints (moderate or essential depending on the patient) for all OARs except the proximal bronchial tree (Table 7.20). Five of the 15 plans exceeded the planned cumulative dose constraint. This was expected in two patients (11 and 29) as these were known to not have acceptable plans. However, the cumulative physical plans for patients 1, 12 and 27 should have met the planned cumulative dose constraints, as they appeared to have met the physical dose criteria. Patients 1 and 12 exceeded the cumulative dose constraint by approximately 1 Gy EQD2 however patient 27 exceeded the constraint by over 10Gy EQD2 (Table 7.21).

Table 7.20 Summary of verification of cumulative EQD2 doses using the re-plans. GV: great vessels, Oes: oesophagus, PBrT: proximal bronchial tree, MLD: mean lung dose, V20: volume of lung receiving at least 20Gy.

Trial number	Acceptable re-plan and constraints used	Cord	MLD	V20	PBrT	Oes	GV
1	Yes - moderate	Y	Y	Y	N	Y	Y
6	Yes - essential	Y	Y	Y	Y	Y	Y
8	Yes - essential	Y	Y	Y	Y	Y	Y
11	No - essential	Y	Y	Y	N	Y	Y
12	Yes - essential	Y	Y	Y	N	Y	Y
15	Yes - moderate	Y	Y	Y	Y	Y	Y
20	Yes - moderate	Y	Y	Y	Y	Y	Y
21	Yes - moderate	Y	Y	Y	Y	Y	Y
23	Yes - essential	Y	Y	Y	Y	Y	Y
24	Yes - moderate	Y	Y	Y	Y	Y	Y
25	Yes - essential	Y	Y	Y	Y	Y	Y

27	Yes - moderate	Y	Y	Y	N	Y	Y
29	No - essential	Y	Y	Y	N	Y	Y
34	Yes - essential	Y	Y	Y	Y	Y	Y
46	Yes - moderate	Y	Y	Y	Y	Y	Y

For these three patients, the image registration/dose accumulation process was reviewed. Patient 27 was initially treated with a 3-field plan (Figure 7.6). The proximal bronchial tree was not in the high dose area of this treatment, although it was very close. This patient then had the delivered re-irradiation replanned to meet the moderate dose constraints (Figure 7.7). Importantly, there is significant fibrosis and contraction of the left lung field from the first course of radiation. These two plans were subsequently combined using the deformable registration to form the cumulative plan (Figure 7.8). This image shows that the proximal bronchial tree appears to have been pulled into the high dose field where there is overlap between the initial and the re-irradiation treatment. This is likely to represent an error in image registration, as the proximal bronchial tree was not in the high dose area at initial radiotherapy. This error was exacerbated because the PBrT was at the field edge of a three-field plan. Therefore, a small registration error, increased the predicted dose significantly by pulling the PBrT into the field, when previously it was not in it. Similar errors occurred for patients 1 and 12. However, as they both had VMAT plans at initial treatment and at re-irradiation, they did not have areas with such rapid fall off in dose and so the difference was not as marked.

Table 7.21 Proximal bronchial tree cumulative dose from the delivered and replanned treatments that exceeded the dose constraints. EQD2: equivalent dose in 2-Gray fractions.

Patient number	Delivered cumulative EQD2	Replanned EQD2	Difference
1	104.09	106.34	2.25
12	114.31	111.68	-2.63
27	115.67	126.05	10.38

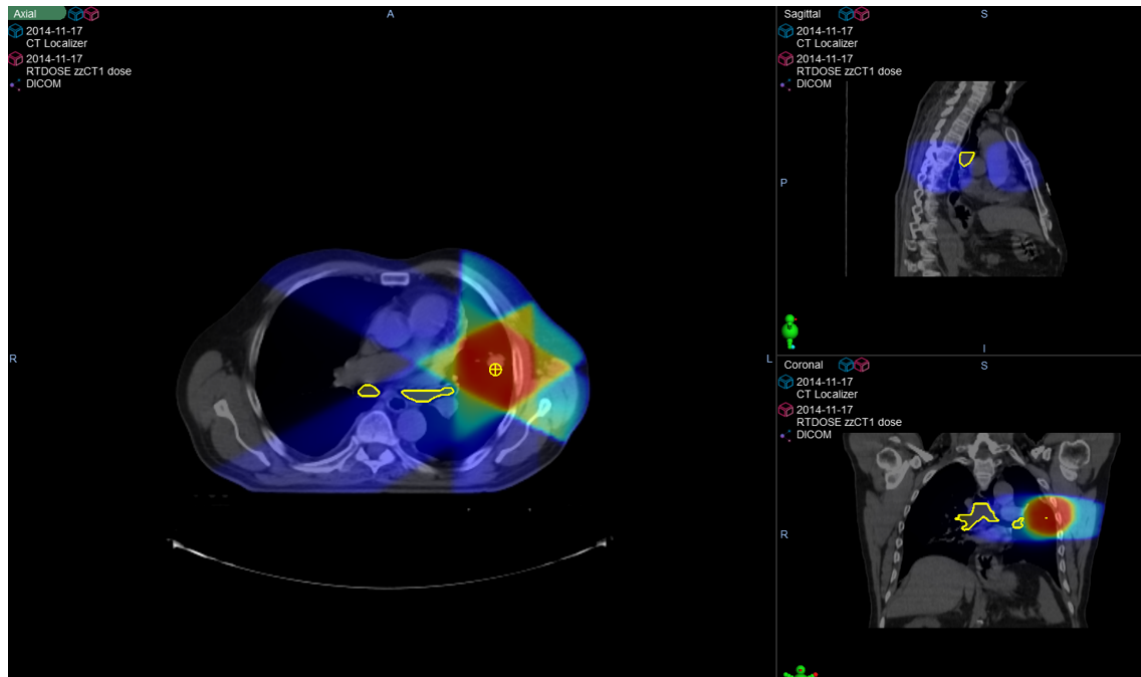


Figure 7.6 Patient 27 initial 3-field radiotherapy plan.

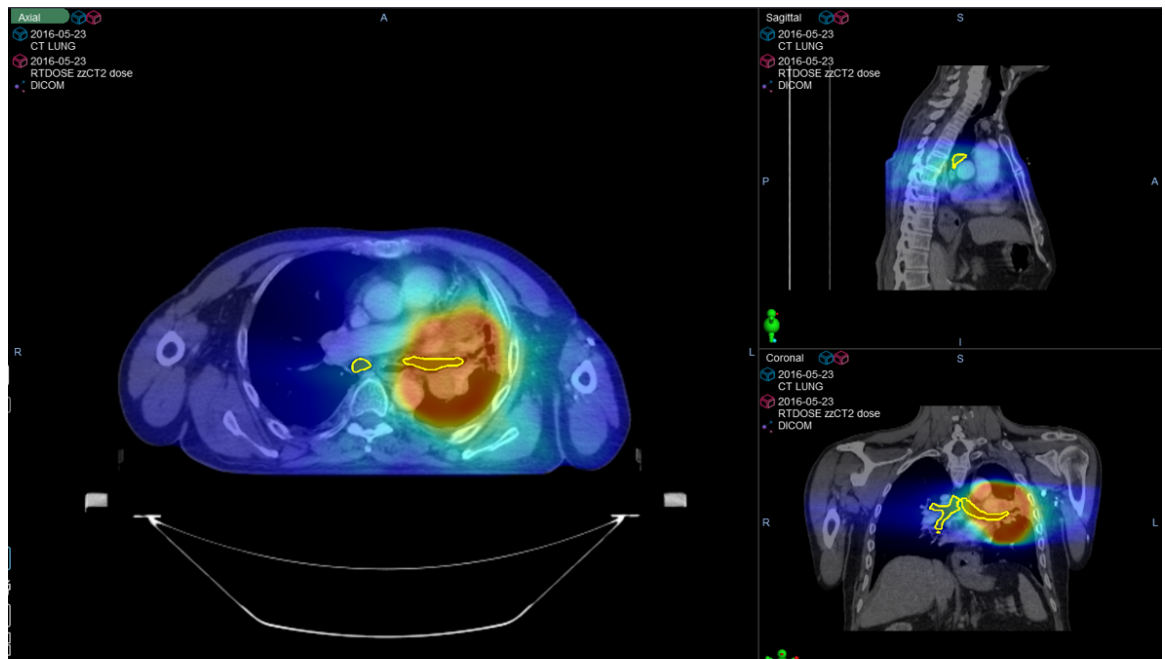


Figure 7.7 Patient 27 re-irradiation re-plan.

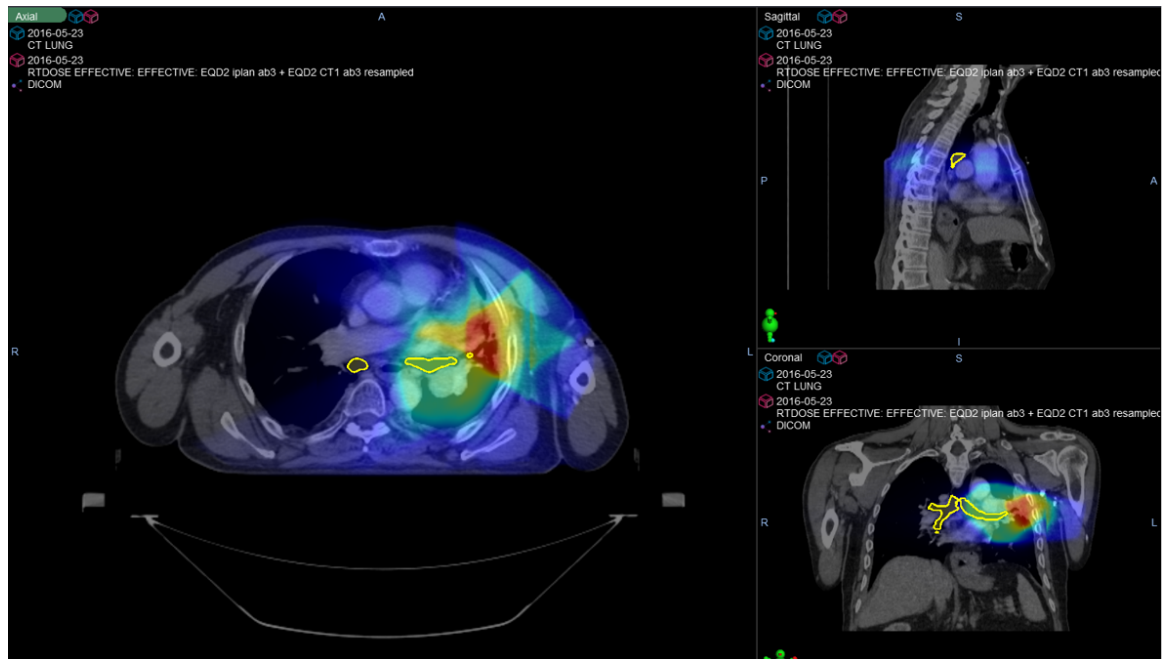


Figure 7.8 Patient 27 cumulative dose plan in EQD2 Gy. EQD2 Gy: equivalent dose in 2-Gray fractions.

7.3.5 Changes in risk compared to delivered dose

The cumulative doses from the 15 replanned courses of re-irradiation were entered into the dose/toxicity models from Chapter 5. The best available re-irradiation plans were combined with the dose from the initial course of radiation. Table 7.22 details the median change of the doses to the cord, lung V20, lung MLD, proximal bronchial tree, oesophagus and aorta. Grouping all the plans together, there was an increase in doses to the lung MLD and V20 which were statistically significant. This indicated that the trade-off from using VMAT+MCO is better avoidance of the serial OARs, at the cost of a small but statistically significant increase in the lung dose. The OAR doses on a per patient basis were analysed to identify individual changes in risk.

Table 7.22 Comparison of delivered and replanned dose to organs at risk. EQD2: equivalent dose in 2-Gray fractions, OAR: organs at risk, PBrT: proximal bronchial tree, MLD: mean lung dose, V20: volume of lung receiving at least 20Gy.

OAR	Median cumulative delivered dose	Median cumulative replan dose	T-test p-value
Cord (EQD2, Gy)	34.9	37.5	0.86
Lung V20 (%)	19.44	20.22	0.05*
Lung MLD (EQD2, Gy)	12.63	13.06	0.02*
PBrT (EQD2, Gy)	104.09	97.47	0.52
Oesophagus (EQD2, Gy)	76.02	76.29	0.22
Aorta (EQD2, Gy)	81.84	79.69	0.15

7.3.5.1 Delivered and replanned cord doses

Figure 7.9 outlines the cumulative dose change for each patient using the delivered dose and the replanned dose to the spinal cord. Five patients had lower doses to the cord and 10 patients had higher doses using the optimal replans. However, as Figure 7.10 demonstrates, despite increased dose, the individual risk of cord toxicity remained below 1%. Patient 20 had a reduction of cord risk from 4% to 0.8% after the replan. The models used the actual interval between initial radiation and re-irradiation as recorded for each patient.

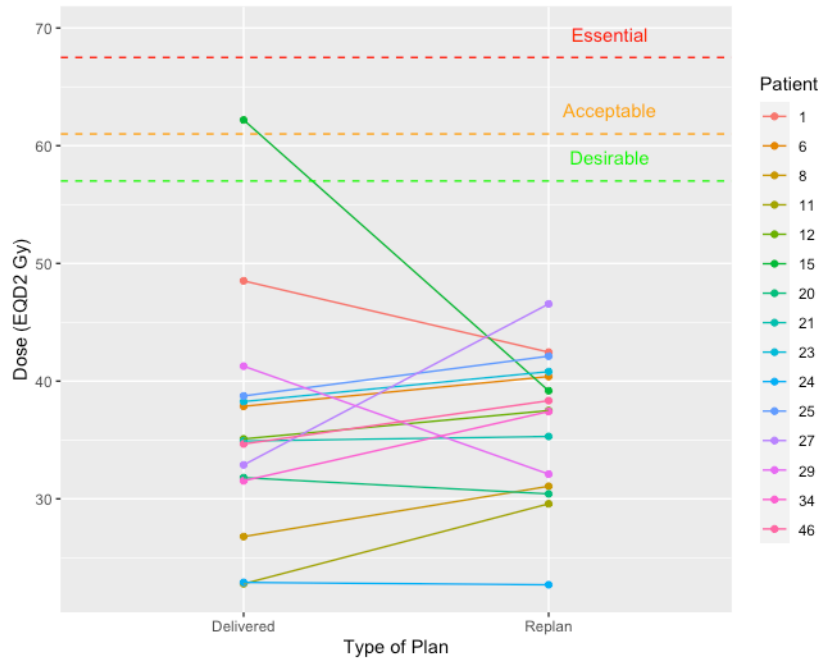


Figure 7.9 Change in cumulative dose to spinal cord between delivered and re-irradiation replan. The green, amber and red lines denote the desirable, acceptable, and essential cumulative dose constraints respectively

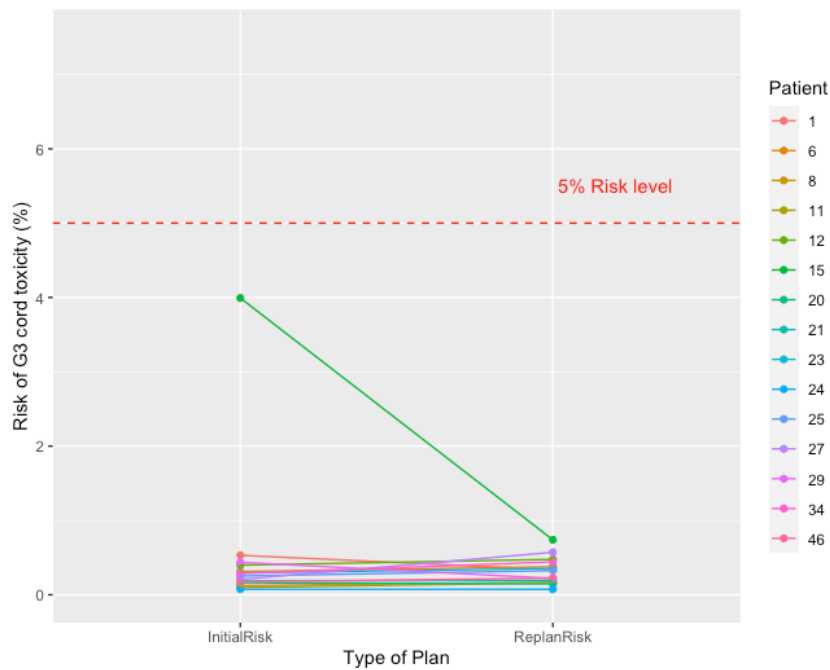


Figure 7.10 Change in cumulative risk to spinal cord between delivered and re-irradiation replans.

7.3.5.2 Delivered and replanned lung V20Gy doses

Figure 7.11 describes the change in lung V20Gy from the delivered dose and the optimal replans. Nine patients have an increase in dose, although only one patient is above the V20<40% constraint. The predicted toxicity rate of patients was above 20% in six patients (patients 11, 15, 25, 29, 34 and 46, Figure 7.12). The patient with the highest risk of grade 3 toxicity at initial treatment had an even higher replan risk (patient 25, risk increased from 77 to 82%). Two other patients (15 and 34) had increased risk of toxicity from the replan (13 to 25% and 35% to 52% respectively). The other 6 patients who had higher V20Gy doses at replan had a small increase in risk, but their risk remained below 7%.

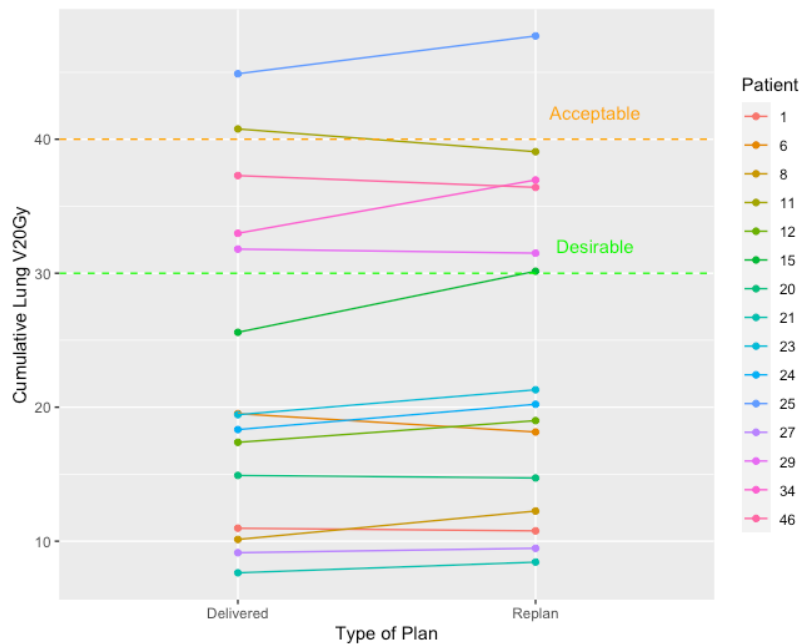


Figure 7.11 Change in cumulative lung V20Gy between delivered and re-irradiation replans. The green and amber lines denote the desirable and acceptable cumulative dose constraints respectively

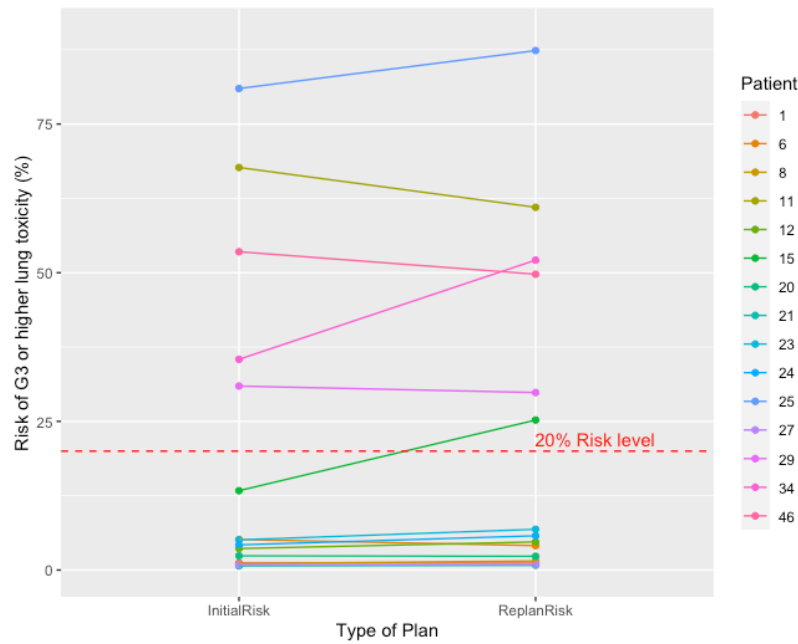


Figure 7.12 Change in cumulative risk for grade 3 lung toxicity between delivered and re-irradiation replans.

7.3.5.3 Delivered and replanned mean lung doses

Figure 7.13 illustrates the changes in cumulative MLD between the delivered treatments and the replanned treatments. The acceptable dose constraint used is 22Gy. Patient 25 exceeded this constraint, with a delivered MLD of 20.8Gy, which increased to 24Gy on the replan. The predicted risk for each treatment is shown in Figure 7.14. Again, Patient 25 has a significant increase in risk of grade 3 toxicity, with the delivered risk of 23% rising to 53.6% with the replan. Patients 15, 29 and 34 had nearly double their delivered risk with the replan, although all three patients had risks less than 15%.

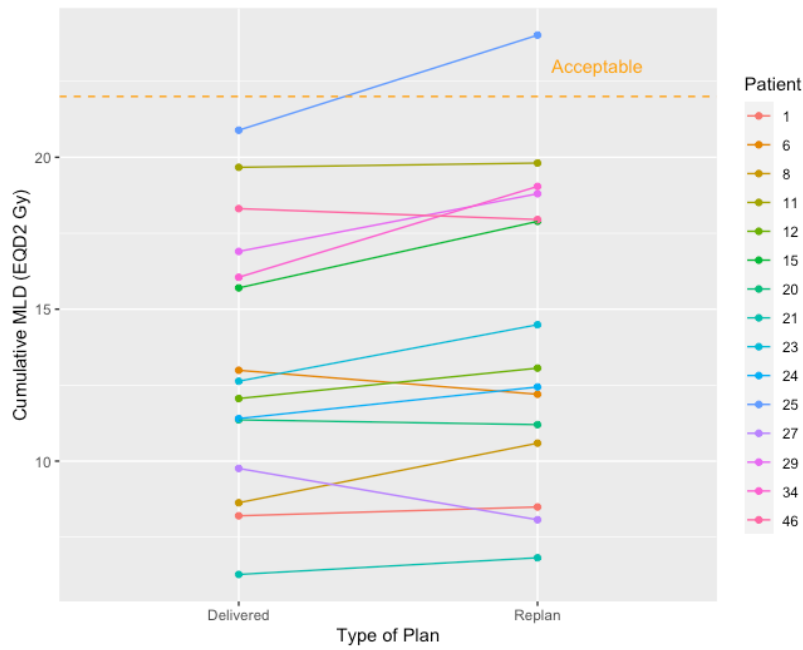


Figure 7.13 Change in cumulative mean lung dose between delivered and re-irradiation replans. The amber lines denote the acceptable cumulative dose constraint.

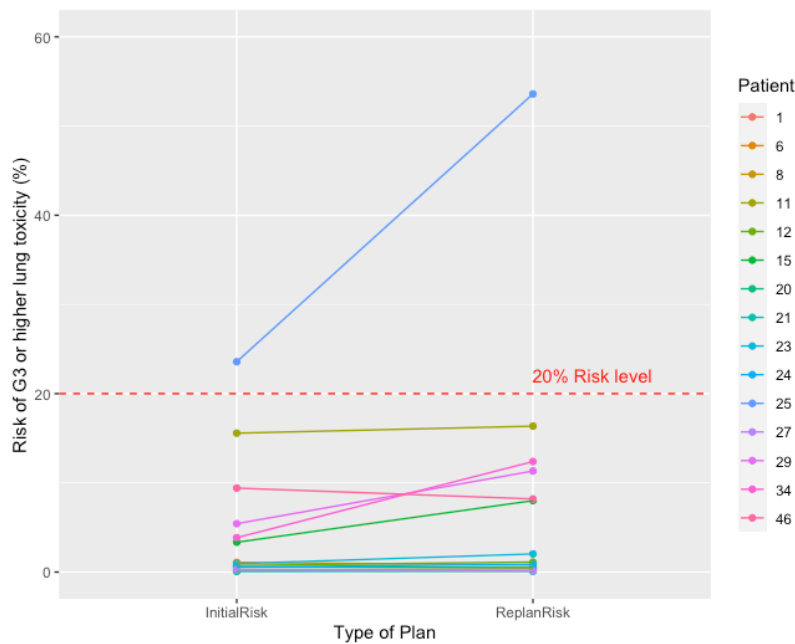


Figure 7.14 Change in cumulative risk for grade 3 lung toxicity between delivered and re-irradiation replans.

7.3.5.4 Delivered and replanned proximal bronchial tree doses

Figure 7.15 demonstrates the change in cumulative dose between the delivered plans and the replans. Five patients (6, 24, 27, 34, 46) had an increased dose to the PBrT, which the other 10 patients had a reduction in dose. Six patients had a

cumulative dose that exceeded the essential dose constraint, and three patients had dose reductions at replan that put the dose below that constraint. Two other patients had reductions that were close to, but not below the constraint. The predicted risk for the delivered and the replanned treatments are shown in Figure 7.16. Interestingly, only three patients exceeded the dose constraints (patients 12, 15, 34). This is likely to be due to the interval for these patients being longer than the median (intervals between treatments for each patient in months 38, 51 and 35 respectively). Although patient 27 had an increased dose to the PBrT at replan, the predicted risk from the replan was still less than 5%.

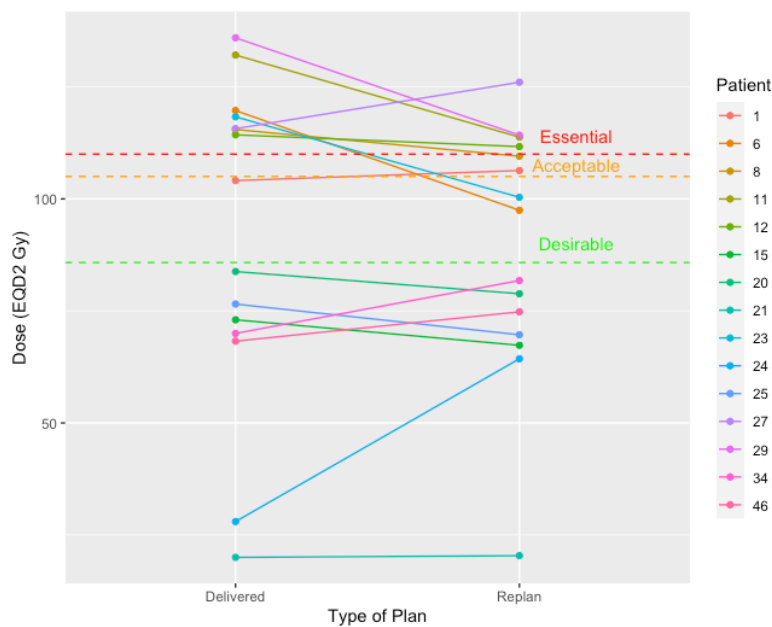


Figure 7.15 Change in cumulative dose to the proximal bronchial tree between delivered and re-irradiation replans. The green, amber and red lines denote the desirable, acceptable, and essential cumulative dose constraints respectively

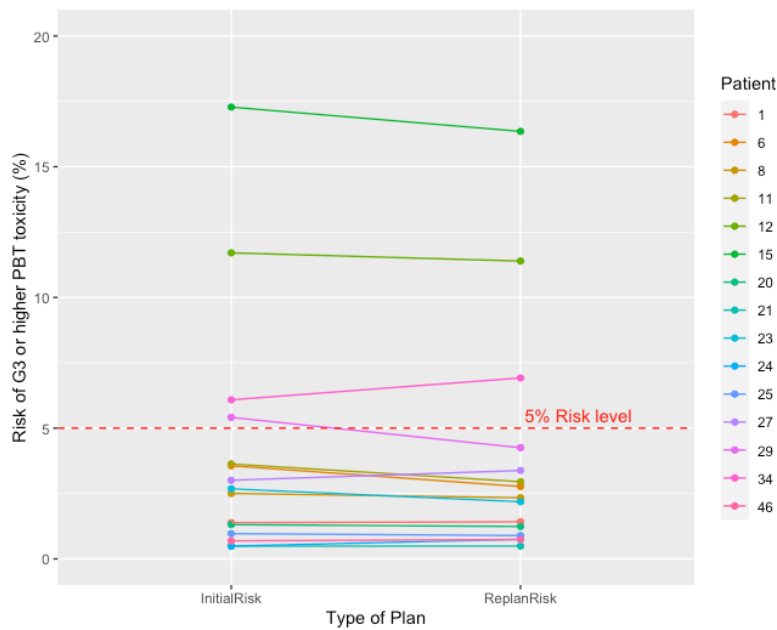


Figure 7.16 Change in cumulative risk for grade 3 proximal bronchial tree toxicity between delivered and re-irradiation replans.

7.3.5.5 Delivered and replanned oesophageal doses

Figure 7.17 and Figure 7.18 show the cumulative doses and predicted risk of grade 3 or higher oesophageal toxicity respectively. The replans all met the acceptable dose constraints except for patient 6, where there was no change in dose or risk. This remained the patient with the highest risk of oesophageal toxicity at replan with a risk of 6.3%. Patients 11 and 23 had a reduction in risk from 13.1 and 7.3% to 3.8% and 3.8% respectively.

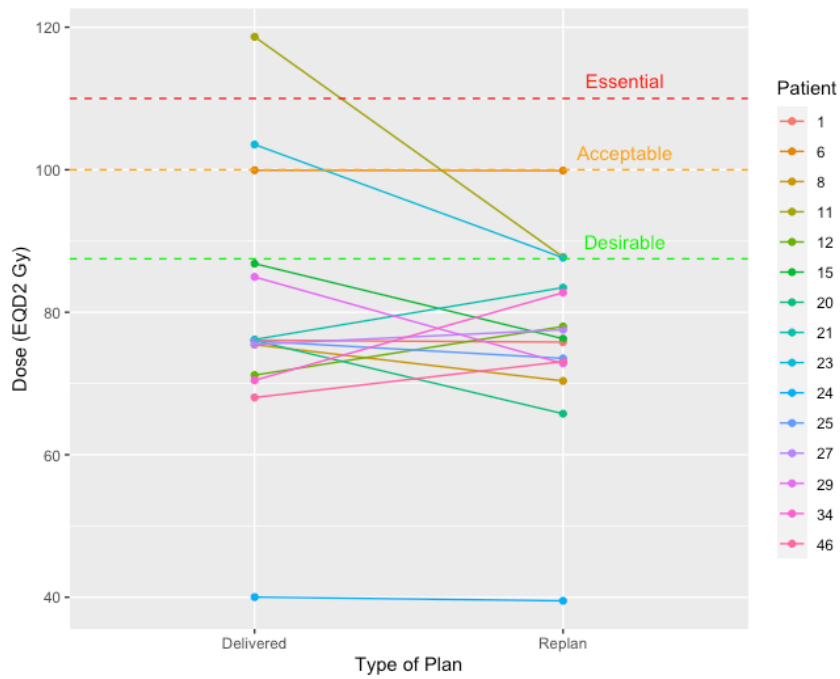


Figure 7.17 Change in cumulative dose to the oesophagus between delivered and re-irradiation replans. The green, amber and red lines denote the desirable, acceptable, and essential cumulative dose constraints respectively

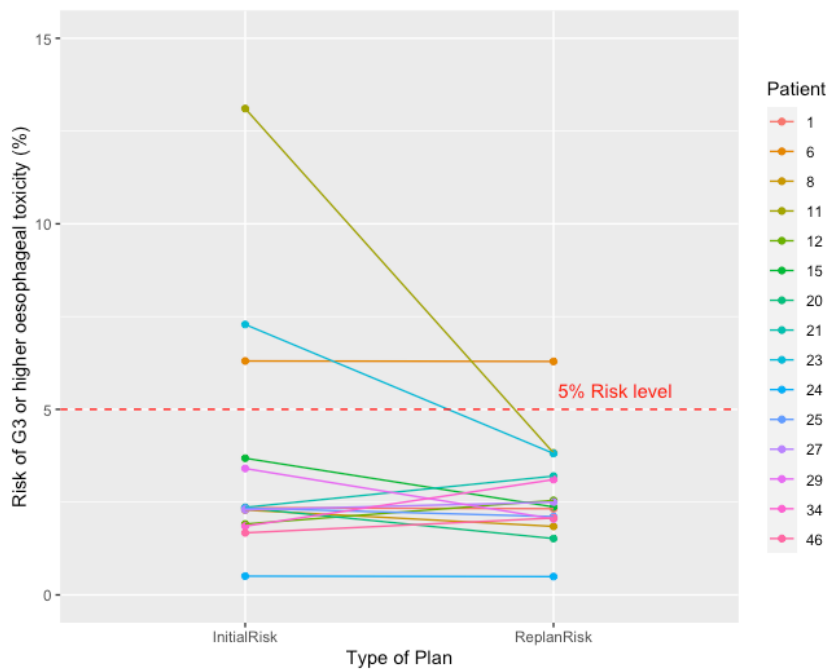


Figure 7.18 Change in cumulative risk for grade 3 oesophageal toxicity between delivered and re-irradiation replans.

7.3.5.6 Delivered and replanned aorta doses

Figure 7.19 and Figure 7.20 show the cumulative dose and predicted risk of grade 3 or above aortic toxicity of the delivered and replanned treatments

respectively. Three patients (11, 23 and 29) had doses exceeding the essential dose constraint and all three were reduced on replanning to below it. For example, patient 29 had the highest delivered dose at 135.4Gy (EQD2) and this was reduced to 115.8Gy by the replan, with a corresponding reduction in risk from 4.2% to 2.6%. All patients had a risk of toxicity less than 5% with both delivered dose and at replans.

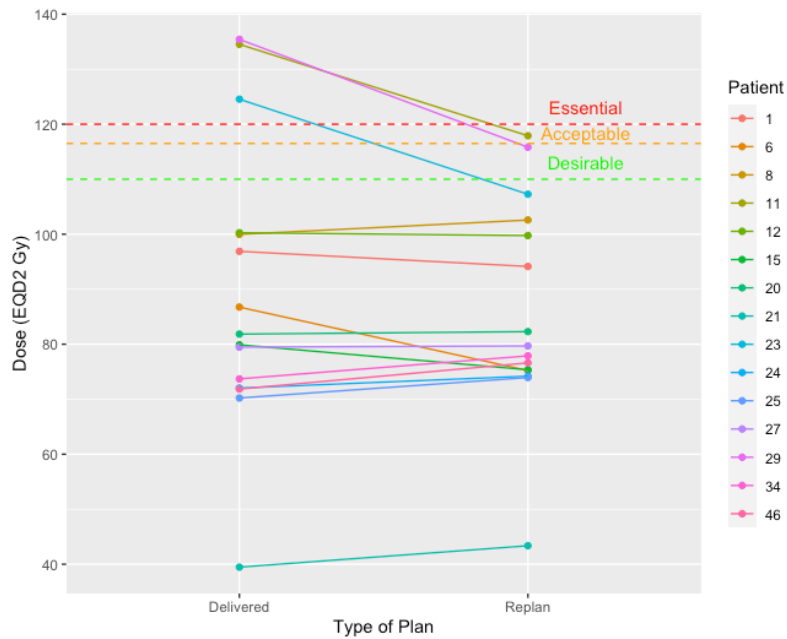


Figure 7.19 Change in cumulative dose to the aorta between delivered and re-irradiation replans. The green, amber and red lines denote the desirable, acceptable, and essential cumulative dose constraints respectively

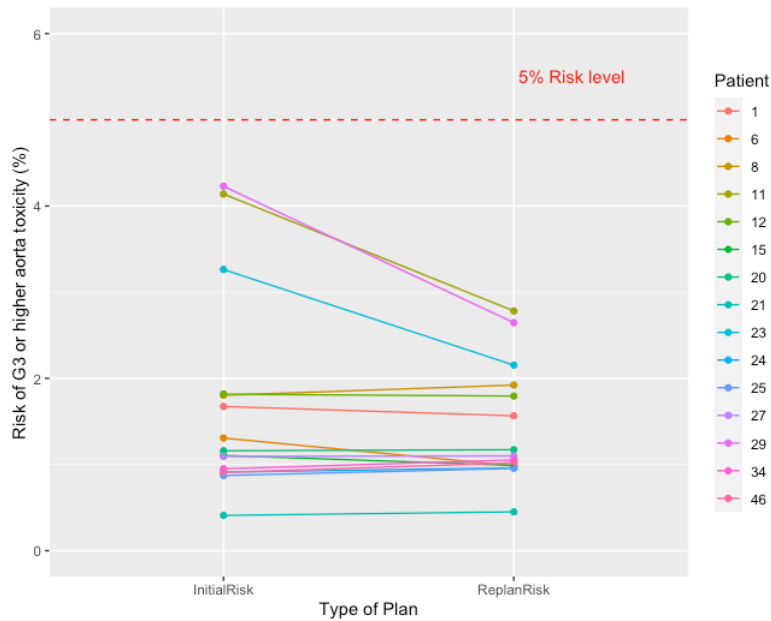


Figure 7.20 Change in cumulative risk for grade 3 or above aortic toxicity between delivered and re-irradiation replans.

7.3.6 Changes in tumour control

In Chapter 6, local control and overall survival models were formulated using data from the literature search. These models were applied to the 10 patients with locally recurrent disease and did not meet the desirable dose constraints initially. The delivered and the re-irradiation PTV doses in EQD2 Gy were used in the modelling. The median delivered PTV Dmax was statistically higher than the replan PTV Dmax (both calculated using EQD2 Gy using $\alpha/\beta = 10$) at 64.10 and 61.84 respectively (t-test p-value <0.01). The 2-year local control rates per patient were predicted from the doses to the PTV from the delivered treatment and the optimal replan (Figure 7.21). The mean 2-year LCRs were 36.1% and 35.0% in the delivered and the replanned treatments (paired t-test, p-value <0.01). For most patients, the local control rate was predicted to be less than the delivered treatment with a median reduction of 0.99% (range -0.14, 3.17%).

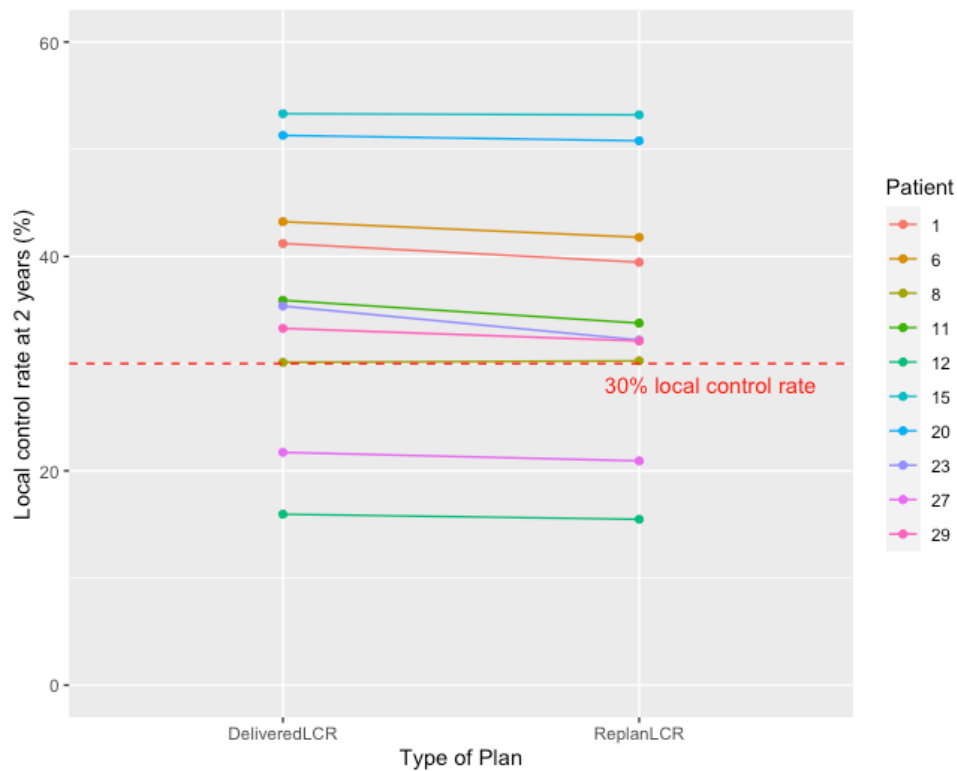


Figure 7.21 Predicted 2-year local control rate between the delivered plans and the re-plans.

The predicted mean 2 year overall survival rate was higher in the delivered dose compared to the replanned group at 39.76% and 37.69% respectively, t-test p-value <0.01, see Figure 7.22. The median reduction in the predicted two year overall survival rate was 2.05% (range -0.26, 5.56).

The lower 2 year local control and overall survival rates in the replans were assessed against the changes in risk to the OARs of each of the 10 patients in this group (Table 7.23). There are some patients where the reduction in dose and predicted efficacy comes with marginal improvements to the risk of toxicity. For example, patient 1 if treated with the replan, would have a 2.9% reduction in the chance of 2 year overall survival, with little improvement in the predicted rate of toxicity in any of the assessed OARs. In contrast, Patient 11 had a 3.7% reduction in the 2 year OS rate, but also had a 9.3% reduction in the risk of a grade 3 or worse oesophageal toxicity. However, both patients 11 and 29 were unable to be safely replanned to meet the dose constraints. Therefore, a more significant reduction in PTV dose (e.g. changing to a high dose palliative regime such as 39Gy in 13 fractions) may make these plans compliant with the dose constraints.

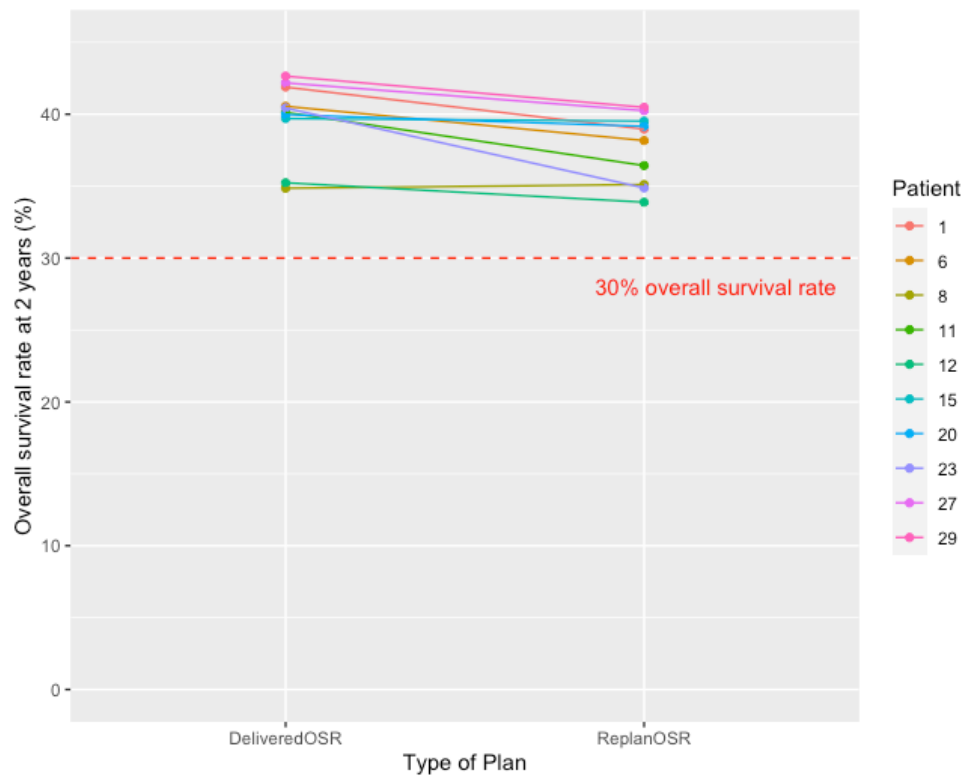


Figure 7.22 Predicted 2-year overall survival rate between the delivered plans and the re-plans.

Table 7.23 Change in predicted efficacy and toxicity between the delivered dose and the replanned treatments. Diff: difference, MLD: mean lung dose, Oes: oesophagus, OS: overall survival, PBrT: proximal bronchial tree, V20Gy: volume of lung receiving at least 20Gy.

Patient	2-yr OS diff	Cord diff (%)	MLD risk (%)	V20 risk diff (%)	PBrT risk diff (%)	Oes risk diff (%)	Aorta risk diff (%)
1	-2.93	-0.19	0.02	-0.04	0.04	-0.03	-0.11
6	-2.38	0.06	-0.31	-1.04	-0.79	-0.01	-0.32
8	0.26	0.05	0.22	0.46	-0.16	-0.44	0.12
11	-3.70	0.06	0.79	-6.69	-0.68	-9.28	-1.36
12	-1.35	0.08	0.38	1.11	-0.31	0.64	-0.02
15	-0.18	-3.25	4.67	11.88	-0.93	-1.31	-0.12
20	-0.81	-0.02	-0.04	-0.08	-0.07	-0.83	0.01
23	-5.56	0.06	1.09	1.78	-0.50	-3.48	-1.11
27	-1.93	0.37	-0.14	0.05	0.37	0.21	0.01
29	-2.17	-0.22	5.91	-1.09	-1.16	-1.36	-1.58

7.4 Discussion

This planning study can be divided into three sections: identification of patients that breached dose constraints and are considered high risk; replanning the re-irradiations to reduce the risk of toxicity using novel techniques and estimation of the clinical benefit of the re-plans using novel models.

7.4.1 Identification of high-risk patients

Fifteen high-risk radical re-irradiation plans from the Beatson cohort were identified. These 15 patients were unable to meet one or more of the desirable cumulative dose constraints. The dose constraints were taken from a range of five published sources, which all used a consensus or expert opinion to suggest a constraint^{112,146,160,161,174}. These sources provided a range of dose constraints, and these were grouped together and divided into the conservative, moderate and aggressive limits. The reason why moderate dose constraints were added rather than simply having two dose categories (optimal (conservative) and critical (most aggressive) constraints) was to allow the heart and chest wall limits to be ALARA, whilst maintaining some limits on the lung dose. These constraints were the first to be relaxed as chest wall toxicity, whilst potentially having a significant effect on patients' quality of life, is unlikely to result in fatal toxicity. Conversely, the data for cumulative heart doses is extremely limited and limiting a possibly radical treatment based on such sparse information is difficult to justify.

The cumulative dose of the initial and re-irradiation used an image registration and dose conversion/summation process. There are significant sources of potential error in this process. Deformable image registration attempts to transform a set of images (in this case, a planning CT scan) to a common coordinate system. This process is dependent on a good initial rigid registration and how the region of interest is set (i.e. is the algorithm asked to deform the whole lung, or a small volume around the PTV)¹⁶³. As the initial treatment and the re-irradiation planning CTs are often years apart, there is often change to the anatomy, typically lung fibrosis resulting in large changes in the anatomy. The patient position is also sometimes different. Patients for three-field conformal radiotherapy were treated with their arms up, whilst for VMAT

treatments, they usually had their arms down by their sides in a beam directional shell. These large differences add significant uncertainty to the image registration.

Another source of error are the algorithms used for dose registration. The Velocity AI algorithm was tested against other DIR software using a deformable phantom. The phantom provided a ground truth to compare the image registrations from each program. The mean error of the VelocityAI algorithm was 1mm, which was the lowest than other comparable programs, and had the lower number of errors $>3\text{mm}$ ²⁷³. Despite this, as shown when investigating the high PBrT doses for one of the patients, in areas where there is a high dose fall-off such as the edge of a field, this small error can yield dramatically different results. In addition, quality assurance and calibration had not been performed on the VelocityAI in use at the Beatson therefore there is no local data to verify that the software performs this well in practice. In addition, with the image registration using treated patients, there is no ground truth to confirm the performance of the image deformation. The assessment of how accurate a registration is performed by the user, rather than a specific calculation. The deformation map is visually assessed to see if the way the algorithm has change the image is biologically feasible. This can be prone to subjective error.

Despite these uncertainties, one of the strengths of this study is the recalculation of every plan using Acuros XB. This ensured that the physical doses for each treatment are consistently calculated and as accurate as possible. Another strength is the use of use of image registration software (Velocity AI) that compares favourably to other programs. This planning study protocolised the setting of the ROI. This reduces a potential variable when performing the image registration, which makes the subsequent dose registration based on the image transformation more reliable. This is consistent with best practice in DIR as suggested in a consensus meeting²⁷⁴.

The patients that did not meet the desirable dose constraints had a higher PTV overlap (34%) and 66% were local recurrences. This is consistent with what would be expected. In situations where there is significant overlap between the initial and re-irradiation PTV (e.g., local recurrence), the same OARs are likely to get a significant dose and therefore are higher risk re-treatments. Conversely, if the

recurrence is away from the mediastinal organs, the risk shifts from high dose to the serial organs (cord, oesophagus) to the lung dose. This is demonstrated by how the patients who could be replanned to the moderate constraints tended to have a recurrence pattern away from the mediastinum.

7.4.2 High risk re-irradiation planning

Of the 15 high-risk re-irradiations, eight of those plans were unable to be successfully replanned and required modifications to the dose/fractionation or PTV. Ultimately two plans were unable to meet even the most aggressive dose constraints. The VMAT+MCO planning technique was superior to VMAT alone when planning re-treatment. This strategy did result in some OARs having higher doses than with the delivered plans, although in most cases, the increased dose did not result in a clinically significant change in risk of toxicity. The verification process checked that the physical doses used in the planning process correlated with the cumulative doses in EQD2. Most plans did meet the cumulative doses as expected although three cases did exceed the expected targets due to suspected registration error.

The re-planning strategy used a calculation taking the Dmax of serial organs at initial radiotherapy, converted into EQD2, and subtracted it from the dose constraint to give the remaining cumulative dose in EQD2. This was then converted from EQD2 to the physical dose that can be used in the re-irradiation planning process. This assumes that the whole OAR was given the highest dose at initial treatment, which is unlikely and over cautious. An alternate approach is where the initial radiotherapy plan is used as a base plan²⁷². The dose that has already been given to the OARs is incorporated in the re-irradiation planning process. This would provide anatomical information as well as dose information. This contrasts with the process used in this chapter, where the previous dose in EQD2 Gy was calculated manually. This identifies the highest dose the OAR received, but crucially not where that dose was delivered. Using a base plan could facilitate higher doses to certain parts of the OAR that received a lower dose at initial radiotherapy but would still meet the overall cumulative dose constraint. Despite being a less accurate process, as most of the patients re-

planned in this planning study had local recurrences, the Dmax from the initial treatment was likely to be in the same radiotherapy field in re-irradiation. Therefore, this approach is still reasonable when re-planning this particular cohort.

This re-irradiation study assumes no recovery for normal tissue and therefore made no corrections for this when calculating the remaining dose that can be delivered. Other planning studies applied a discount for previous dose. For example, Paradis *et al.* assumed a 50% discount for delivered dose after 1 year of treatment for the oesophagus, the spinal cord and the proximal bronchial tree¹¹². Their dose constraints however are lower than used in this planning study, therefore the discount when applied, results in broadly similar constraints. To illustrate this, the Paradis constraint for oesophagus is an EQD2 of 70 and the expert dose constraint is 100Gy EQD2. If an initial dose of 60Gy EQD2 was given hypothetically, after 1 year this would be reduced by 50% to 30Gy EQD, and the maximum re-irradiation dose would be an additional 40Gy EQD2. The total dose, however, would be 100Gy, which is consistent with the constraints used in this study. There is an assumption that normal tissue recovery occurs, although there is a lack of pre-clinical or clinical data to describe the amount and timing of it.

The choice of metric for the serial OARs is also conservative. The Dmax values from the initial radiotherapy could be up to 107% of the prescribed dose if conventional fractionation was used, or much higher with SABR. Using the Dmax values assumes that the volume of highest dose is clinically significant, whereas in practice, the highest dose (or dose hot spot) is often a very small area. An alternative would be to use a metric of D0.1cc which sets a pre-specified volume for the maximum dose and may be more clinically relevant. In contrast, this study did not use PRVs for any of the OARs. This was due to uncertainty of the size of the PRV and whether it would preclude central re-irradiation as many of the OARs in the mediastinum are close to each other. As such, the use of a potentially over cautious metric such as Dmax may be compensated by the absence of PRVs.

The finding that VMAT+MCO is superior to VMAT planning is consistent with another study looking at MCO for primary radiotherapy for NSCLC. Kamran *et al.*

found that MCO had small but significant improvements in a variety of OARs (e.g., MLD was improved by 0.8Gy, oesophagus V60Gy was lower by 1.2%)²⁶⁹. The above data demonstrated a significant improvement in dose sparing especially for the serial OARs at re-irradiation. MCO is well suited to the challenge of re-irradiation as there are often several competing OARs, and the ideal plan is a compromise between these objectives. This is found by generating several plans and allowing the planner to determine the allowable dose to each OAR to find the optimal trade-off.

There are significant cautions when using MCO. There can be some discrepancies between the MCO predicted plan and the clinically deliverable plan. One study which analysed a Raystation (Raysearch Laboratories AB, Stockholm, Sweden) MCO tool found that the clinically deliverable lung plans were had up to 17.2% underdosing of the PTV compared to the predicted MCO plans²⁷⁵. One possible reason for this discrepancy is that the optimal plans depend on very small MLC apertures that are practically undeliverable. The Varian MCO optimiser has a minimum aperture setting that prevents the optimiser planning small MLC areas and therefore increasing the likelihood that an MCO plan is clinically deliverable.

MCO plans also have very steep areas of dose fall off in situations where the optimiser is struggling to meet a dose constraint. This could lead to inadvertent under- or overdoses if the on-treatment verification is not accurate, as a small shift could result in a large change in dose to an OAR. Furthermore, there is a risk that MCO plans deposit dose in low penalty areas especially if there are OARs that are not contoured or included in the optimiser. This can be reduced by voluming the OARs extensively and rigorous plan review.

Finally, MCO can find the optimal trade-off quickly using a resource intensive technique of generating several plans. However, an experienced planner would also be able to predict the necessary planning priorities. Therefore, the apparent improvement in the VMAT+MCO plans may be due to the limited experience of the planner for the VMAT plans. However, all the final plans were reviewed by experienced physicists, suggesting that there is a true beneficial effect of MCO over VMAT alone.

7.4.3 Re-planning failures

Eight patients were unable to be replanned despite using the highest allowed consensus values as constraints. A range of different strategies were used to try to develop a radical treatment in these difficult plans. The option to change the dose/fractionation regime to the lowest radical dose in EQD2 allowed two patients to be replanned. The lowest radical dose in EQD2 is 54Gy in 36 fractions delivered three times a day (CHART regime), with an EQD2 of 48.6Gy EQD2 using an α/β ratio of 10. This is significantly less than the moderately hypofractionated regime of 55Gy in 20 fractions (63.3 Gy EQD2), but the reduced treatment time (12 days compared to 26 days) meant that the treatment did not have to compensate for repopulation after 21 days. CHART is a less suitable re-irradiation regime partially because logistically it is difficult to deliver, with patients generally needing to be admitted for two weeks to complete their treatment. Also, the small fraction sizes may be inferior to a moderately hypofractionated regime if the unknown α/β ratio of recurrent disease is lower than the assumed value of 10.

The reduction in CTV to PTV growth from the standard 10mm to 5mm as suggested in Chapter 4 from the Delphi consensus process led to three acceptable plans. The CTV to PTV margin accounts for the setup error, and internal organ motion. There is no published evidence to suggest that at re-irradiation, either the setup error or organ motion is less than with de novo radiotherapy. Therefore, reducing the margin increases the risk of tumour underdosage. However, there are possible explanations why this expansion could be smaller in the re-irradiation setting. Firstly, patients would have already gone through radiotherapy and may be more relaxed when having treatment. This may result in better reproducibility of setup. Secondly, the initial course of radiotherapy may have caused fibrosis. This may reduce the movement of the tumour through the breathing cycle and minimising the change from organ movement. Thirdly, if the re-irradiation was delivered with daily CBCTs as also suggested in the Delphi consensus, this would increase the accuracy of the treatment. All three explanations lack any data to support them, and further work is required to investigate this.

One patient was successfully replanned by cropping the PTV away from the overlapping OAR, in this case the PBrT. The cropped PTV had D95% of 95%, although a lower D99% of 86.2%. However, the GTV D95% was 96.1 and the D99% was 95%, suggesting that the GTV dose was not compromised. This strategy was based on the Delphi consensus. Again, this increases the risk of tumour underdosage. However, this is a pragmatic planning decision to prioritise meeting the dose constraint (and therefore safety) overachieving high PTV doses. The final strategy for the two remaining patients was the use of an adaptive approach. This was based on a paper that demonstrated that approximately half of patients treated with radiotherapy for NSCLC had some shrinkage of the tumour²⁷⁶. In the adaptive plans made for re-irradiation, the PTV was reduced by approximately 10%, based on the observation from a study in adaptive radiotherapy for NSCLC that the GTV reduced by 1% per day, and the adapted plan for the smaller tumour would start after 10 days of treatment²⁷⁷. However, despite the reduction in PTV size by 34-55%, the overlap with the great vessels remained and the dose constraint could not be met.

The re-irradiation re-plans highlighted that some patients may not meet the cumulative dose constraints. This planning study did not explore reducing the dose from a radical dose to a high dose palliative dose, such as 39Gy in 13 fractions. This fractionation is associated with a modest two-month improvement in overall survival and the lower dose may reduce the risk of toxicity²⁷⁸. An alternate dose strategy would be an isotoxic approach, where the dose to the PTV is escalated until a dose constraint is breached. This process is feasible in de novo radiotherapy for NSCLC although in the re-irradiation setting, given the uncertainty regarding some dose constraints, this could be high risk²⁷⁹.

This re-irradiation study also did not consider the use of protons. Intensity modulated proton therapy, when compared to VMAT, had significantly higher doses to the target volume and lower OAR doses in a 24 patient planning study¹⁴⁶. Protons may reduce normal lung tissue dose due to the rapid dose fall-off beyond the PTV. However, protons may not be able to achieve a reduction in dose to OARs where they are within 1cm of the PTV. This is because of range uncertainty with protons and the need for a safety margin to ensure that the PTV receives a high dose. In the 15 re-planned patients, 14 had OARs abutting or

including the PTV. This cohort therefore may not benefit from protons but would need further investigation. However, peripheral relapses where the field does not need to cover the mediastinal OARs may benefit most from proton therapy.

7.4.4 Dose verification

Dose verification of the re-plans aimed to assess whether the re-irradiation planned in physical dose, matched the cumulative dose as measured in EQD2 Gy. For most patients, the re-plans did adhere to the dose constraints except five patients where the dose to the PBrT was too high. These errors were investigated and highlight the need for visual checking of the deformable dose registration, especially in areas of high dose fall off.

However, the verification process did not model the robustness of the plans. One tool in Varian Eclipse (but not available in Velocity AI) can demonstrate the change in dose with small setup shifts. This would be very important in this study, as the dose gradients caused by the tight constraints and the use of MCO would lead to minor shifts having potentially large dose changes to the OARs or PTV. In addition, the cumulative doses are taken only from the planning scans and so represent an idealised situation. The true delivered dose would need to account for the shifts on CBCT across a course of treatment, which is beyond the scope of this study. Finally, the plan verification did not assess plan deliverability. For example, there is a metric called average leaf pair openings (ALPO) which can suggest if the optimiser has made deliverable plans or has unrealistically small MLC windows. The plans were not independently rechecked using another dose calculation engine or library (e.g., with Radcalc) to confirm that the re-plan dose was consistent.

7.4.5 Risk prediction

The final part of the planning study was to predict the clinical ramifications of the difference in dose from the delivered dose (i.e. the original initial and re-irradiation plans) and the replanned dose (initial and re-planned to the expert dose constraints). The models predicted acceptable risks for the cord, oesophagus and aorta, with certain patients having a significant reduction in risk of grade 3 or above toxicity. The PBrT model predicted three patients had a risk

of $\geq 5\%$ of high grade toxicity. This was more due to the interval between treatments, rather than the modifiable factor of dose, as the interval in the multivariable model had large effect on the prediction. In these serial organs, there was an increase in dose in some plans, although the dose increases generally did not result in a change in predicted toxicity.

The lung models however demonstrated some very high doses and predicted extremely high risk treatments. For the V20Gy prediction, six patients had a risk of grade 3 or worse toxicity greater than 20%. For three patients, the re-plan results in a significant increase in the risk of pneumonitis/fibrosis. The MLD model predictions was marginally better, with only one patient having an increased risk from 23% to 53.6% with the re-plan. These results are due to the use of ALARA as a dose constraint for lung, whilst other OARs had fixed values as constraints. Therefore, the optimiser and MCO would be penalised less for delivering a high lung dose, in preference to ensuring a low dose to the oesophagus or the aorta, and therefore more dose was passed through the lung.

Despite this, only one plan exceeded the cumulative MLD of 22Gy and the V20Gy of 40%. There would be doubts about the safety of this treatment and should also be counted as a re-plan failure. However, the lung toxicity models did not correlate well with the observed toxicity rate in the Beatson data (Chapter 5.3.5.7) and therefore the model predictions may be inaccurate. Predicting lung toxicity is difficult and is likely to be function of several factors (e.g. pre-existing lung disease, cardiac dose).

When predicting the efficacy of re-irradiation, the dose to the tumour was generally lower with the re-plans compared to the delivered dose, as the OARs had been planned to a stricter set of constraints, leading to a small reduction in the predicted rate of 2 year overall survival. This result is possibly because of the planning strategy to prioritise OARs first over the PTV. However, the patients' attitude to risk of re-treatment must also be taken into consideration. Patients may be willing to accept riskier treatment if the chance of survival is higher. Conversely, patients may also be risk averse and wish to minimise side effects as much as possible. Therefore, a bespoke solution is required for every re-irradiation.

7.4.6 Conclusions

This planning study outlines the steps required to safely plan radical dose re-irradiation and highlights the areas of uncertainty and for future development. VMAT+MCO appears to be a superior technique when planning re-irradiation. Where a re-irradiation plan breaches the essential dose constraints, changing the fractionation, reducing the expansion from CTV to PTV to 5mm or cropping the PTV off OARs are reasonable strategies to form a clinically applicable plan. Dose verification using deformable image registration is prone to error, especially in areas of high dose fall off such as the edge of a radiotherapy field. Therefore, registrations should be visually checked for errors.

Patients should be consulted when planning re-irradiation to determine their attitude to risk of toxicity in the context of changes to the efficacy of treatment.

8 Patient perspectives on re-irradiation

8.1 Introduction

Re-irradiation is a non-standard treatment option, used only in selected patients. Evidence for this comes from local data from the Beatson West of Scotland Cancer Centre where 6.7% of the expected number of patients who may be eligible for re-irradiation receive this treatment. Reasons for the low uptake of this treatment may include limited prospective trial data demonstrating efficacy, concerns about safety, unclear planning technique, no clear guidance on surveillance post-radical radiotherapy leading to variable detection of recurrence and patient refusal. A prospective clinical trial would provide important evidence of the safety and efficacy of contemporary radical re-irradiation. In a survey of UK lung oncologists about re-irradiation, 76% of respondents supported further research in this field¹⁵⁰.

The benefits and risks of radical lung re-irradiation have been investigated in previous chapters. From retrospective reviews, radical re-irradiation was associated with a median overall survival of 17.7 months but with significant risks of toxicity (e.g. \geq Grade 3 pneumonitis between 0-21%)¹⁴⁴. The radiobiological modelling in Chapters 5 and 6 quantify the risk of severe toxicity and predict the necessary radiation dose associated with 2 year survival. These models are not validated and would need prospective data from a clinical trial to do so robustly. When considering a clinical trial, it is important to consider the patients perspective. However, the views of patients suffering relapsed disease after previous treatment with radiation have not been studied. There remain several unanswered questions about patients' opinions of re-irradiation that need consideration prior to the design of a clinical trial.

8.1.1 What are patients' perspectives of re-irradiation?

It is critical to involve patients in the design of any prospective study. Initial cancer treatment has enormous physical and psychological burdens. A quarter of all patients who are long-term lung cancer survivors suffering with depressive symptoms or physical limitations after one course of treatment^{280,281}. There are no published data on lung cancer patients' attitudes to re-irradiation, or any

data on potential barriers to re-irradiation clinical trial recruitment. Possible reasons why patients do not want to have re-irradiation could be anxiety and distress from reliving the initial course of radiation, ongoing or resolved side effects, perceived futility, logistical challenges or concern about going through diagnostic procedures again. These issues warrant further investigation before proceeding with a trial.

8.1.2 Relationship of symptoms from initial radiotherapy and willingness for re-treatment

Joseph *et al.*, when reporting a re-irradiation workshop, stated that patients who tolerated initial radiotherapy poorly were unsuitable for re-irradiation²⁸². This refers specifically to clinicians' concerns of causing severe toxicity with re-irradiation and may be a barrier to successful trial recruitment. Early toxicity could be reversible such as oesophagitis or breathlessness, which resolves after a short number of months. This would cause discomfort and may require hospitalization for a short period. Late toxicity, such as lung or oesophageal fibrosis may be permanent and would cause a significant impairment to the patients' quality of life (e.g., needing oxygen at home or not being able to eat solid food). Clinicians would regard severe toxicity from initial radiotherapy as a risk factor for late (and potentially fatal) toxicity from re-irradiation.

The rates of severe toxicity may be lower using the newly published cumulative dose constraints, although this needs validation. There are no prospective published data regarding whether patients who have toxicities are less likely to want further treatment. There is a need to identify if there is a relationship between the severity of patients' symptoms (e.g., breathlessness, fatigue, oesophagitis) during initial treatment and their willingness for re-irradiation. If they are willing to proceed with re-irradiation, investigating what changes they would want to make their second course of radiotherapy more tolerable may help with any future trial.

8.1.3 Alternative treatments

Patients' acceptance of alternative treatments (e.g., systemic treatment or a watch-and-wait strategy) in the locally relapsed setting may also be useful if considering a comparative trial design. It would make trial recruitment too

challenging if the comparator arm of a re-irradiation study had treatments that were not acceptable to patients. Again, no data has been published about patients' choice of treatment in this clinical situation, although there are several studies about patients' acceptance of chemotherapy in the metastatic setting. In a review by Blinmann *et al.* on attitudes to chemotherapy, they conclude that decisions on treatment are complex and difficult to predict from baseline characteristics²⁸³. Extrapolating from this study, accepting that it is a different clinical scenario, it is likely that patients will have individual reasons for choosing one treatment over another. It is unknown whether patients would opt to have radiotherapy again if they had a choice but is a crucial question that needs to be addressed in the early stages of trial design.

8.1.4 Patient perspectives on risk and benefit

The use of therapeutic radiation is a compromise between tumour control and damaging normal tissue. The higher the dose, the better the chance of tumour control, but the higher the risk of severe complications. In primary radiotherapy, clinicians have arbitrarily set a dose limit for normal tissue. For example, in the QUANTEC series of papers, the risk of grade 2 toxicity was set at 20%, and the dose constraints are calibrated to that²²⁶. However, the risk/benefit ratio may well be different in patients with locally relapsed disease. For metastatic chemotherapy, 73 - 78% of patients would accept an increase of the survival rate by 30% at a given time point as a threshold for treatment. However, some (7-45%) would accept an increase by 1%, and some would never accept chemotherapy regardless of the suggested benefit²⁸³. Patients' expectation of the outcomes of radical re-irradiation needs to be investigated in order to shape future clinical trials with regards to target dose, surrounding organ at risk dose and risk of toxicity.

8.1.5 Patient perspectives on surveillance scans

Any future prospective trial in recurrent lung cancer requires timely detection of local relapse. Recent guidelines have suggested surveillance CT scans every 6 months to detect recurrent disease, although the strength of evidence supporting these recommendations are weak¹⁰⁸. Most studies focus on the overall benefits that surveillance has on outcome and very few report on patient's

quality of life, and none focus on the feeling patients have towards surveillance scans. As this is a key element of any study, identifying patients' opinions of frequent CT scan is useful.

8.1.6 Summary

A clinical trial of radical re-irradiation would provide contemporary data on dose constraints and efficacy. The patients' perspectives of re-irradiation are critical in the design of any such study. There are very few studies that assess the patients' views to re-irradiation in terms of willingness to undergo treatment, attitude to risks and benefits, surveillance scans and opinions on alternative treatments. Therefore, a semi-structured qualitative interview study was performed to investigate the patients' perspectives of re-irradiation.

8.2 Aims

8.2.1 Primary objective

- Explore patients' perspectives about having a second course of radiotherapy for recurrent lung cancer

8.2.2 Secondary Objectives

- Identify factors that patients consider when deciding on potential treatments in the setting of locally recurrent lung cancer (including effect of COVID-19 on treatment choice)
- Investigate how patients' acceptance of side effects changes with the different projected outcomes of re-irradiation
- Explore the relationship between the toxicities patients experienced during radiotherapy and their attitudes to a second course of radiotherapy
- Investigate patients' awareness of surveillance imaging after radical treatment and willingness for scans

8.3 Methods

8.3.1 Design

This study is a series of semi-structured qualitative interviews conducted by the researcher over the telephone or via teleconferencing facilities with patients who have completed a course of radical radiotherapy in Glasgow, Scotland.

8.3.2 Ethics approval

This study was given a favourable opinion by the South East Scotland Research Ethics Committee (21/SS/0015) on the 16th April 2021. The study was approved by the NHS GG&C Research and Innovation department on the 24th March 2021. The study opened for recruitment on the 17th April 2021 and closed on the 1st January 2022.

8.3.3 Participants

Patients must meet all the following inclusion criteria to be considered for this study:

- Age 18 years old or above
- Pathological or radiological diagnosis of non-small cell lung cancer
- Undergoing radical radiotherapy to the thorax using the following fractionations (60-66Gy in 30-33 fractions, 55 Gray in 20 fractions, 54 Gray in 36 fractions or any Stereotactic Ablative Body Radiotherapy (SABR) fractionation that delivers a biological effective dose of greater than 100Gy₁₀) as part of their primary lung cancer treatment at time of study enrolment
- Patients receiving concurrent and/or adjuvant systemic therapies are permitted
- Radiotherapy is delivered in the Beatson West of Scotland Cancer Centre

- Signed, written informed consent
- Willing and able to complete study processes

Patients who meet any of the following exclusion criteria will not be enrolled on to the study:

- Not fluent in English

This exclusion criteria are due to the lack of funding for interpreter services.

8.3.4 Recruitment and study process

Patients who are eligible for the study were approached by the direct care team (clinician, nurse specialist or radiographer) in the first two weeks of radiotherapy and given a patient information sheet. They were reviewed one week later. If they wished to participate in the study, they were introduced to the research team and consented. The researcher called the patient 4 weeks after completing radiotherapy and re-checked consent. The recorded telephone interview was conducted 5 weeks after the completion of radiotherapy. The digital recording was saved on to secure NHS systems and transcribed for thematic analysis. This process is summarised in Figure 8.1.

8.3.5 Interview topics

The semi-structured interview had initial questions on the patient's experience of primary radiotherapy and side effects from treatment. This primarily was to identify whether radiotherapy had been a positive or negative event and how their view on treatment was shaped by the toxicities they encountered. The prospect of re-irradiation was explained using the terms "in the hypothetical event of the cancer coming back, one possible treatment is another course of radiation to the chest". Two scenarios were put to the patients, one where re-irradiation controlled the disease for 12 months and another where the disease control was several years.

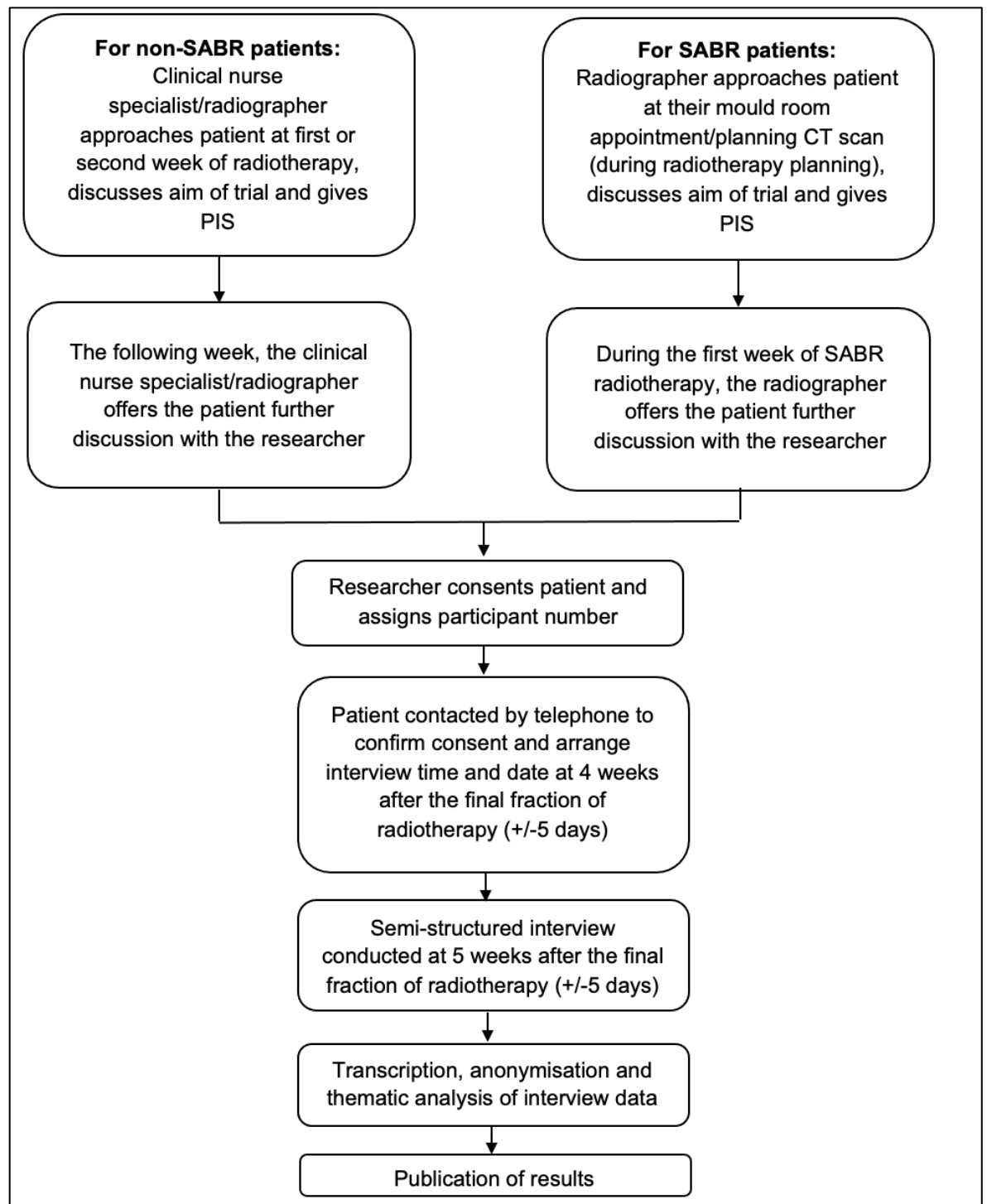


Figure 8.1 Study schema

Participants were asked to consider what their perspectives were on the potential risks of early and late toxicity, and whether their willingness to accept these risks was influenced by the expected outcome of re-irradiation. Alternatives to re-irradiation (e.g., chemotherapy or a watch and wait strategy) were explained to the participants and they were asked to comment on these

options. The final part of the interview invited patients to comment on their perspectives on surveillance CT scanning and to describe the process they go through when deciding about treatments.

8.3.6 Analysis

The recordings were transcribed by the researcher. These were uploaded on to Nvivo (version 12, QSR International Pty Ltd., Doncaster, Australia). The interviews underwent thematic analysis, using the process outlined by Braun and Clarke^{284,285}. Familiarisation with the source data was performed by the researcher conducting the interviews, transcribing the data, and re-reading the transcripts. The initial phase of coding the data was guided by the structure of the interview, with the questions acting as the primary way to group the participants' responses. These were then subsequently coded using an inductive approach to determine common themes within the answers from the participants. This was revisited a third time to regroup some comments that were more pertinent to a particular theme, even if the comment came from a different question group. The transcriptions were re-reviewed to identify any further quotes from the participants that could be included in the same theme.

8.4 Results

8.4.1 Recruitment

Twenty patients were approached to take part in the study. Eight patients agreed to participate in the interviews. The median age was 73.5 and the majority were men. The demographics of the patients are summarised in Table 8.1. No patients treated with CHART participated. The side effects experienced by each patient and demographics are detailed in Table 8.2, with most patients self-assessing the toxicity they experienced as moderate.

Table 8.1 Demographics of trial participants Gy: Gray, fr: fractions, SABR: Stereotactic ablative radiotherapy

Demographic		
Gender (%)	Male	6 (75)
	Female	2 (25)
Median age (range)		73.5 (55-86)
Treatment (%)	SABR	3 (37.5)
	Concurrent chemoradiotherapy	3 (37.5)
	55Gy in 20fr	2 (25)

Table 8.2 Toxicity experienced by participants

Participant number	Age	Gender	Self-assessed severity score	Toxicity experienced
1	62	Male	Moderate	Fatigue, breathless, rash
2	86	Female	Severe	Arm pain
3	55	Male	Moderate	Oesophagitis, breathless, cough, pain
4	74	Male	Moderate	Oesophagitis, fatigue
5	76	Male	Mild	Nil
6	68	Male	Moderate	Breathless, fatigue
7	78	Male	Moderate	Oesophagitis, rash
8	73	Female	Moderate	Fatigue, oesophagitis, cough, rash

Inductive analysis of the transcriptions identified two major themes: fear and control. In each theme, different aspects of the participants responses on re-irradiation have been categorised into sub-themes. These are outlined in Table 8.3.

Table 8.3 Outline of themes and sub-themes

Theme	Main sub-themes	Secondary sub-themes
Fear	Anxiety from first radiotherapy	Fear of unknown new treatment (e.g., chemo)
	Reduced fear as familiar with radiotherapy, familiar with COVID	
Control	Gain of control/agency	Acceptance of re-irradiation
		Insistence on high efficacy
		Surveillance scans
	Loss of control/agency	Loss of control due to side effects/symptoms
		Disease taking control
		Family's advice
	Doctors' advice	

8.4.2 Fear

8.4.2.1 Anxiety from first radiotherapy

Most patients commented on feelings of apprehension or fear when they started radiotherapy treatment. However, as they progressed through treatment, these feelings resolved, as they became more familiar with the process of radiotherapy and as staff explained how the radiotherapy machines worked.

“The first time, it was a wee bit daunting.” [Patient 1, male, age 62]

“It's scary, you know for the patient I think, you're thinking what are they all doing and once it was explained to me, I felt a lot better.” [Patient 2, female, age 86]

Patients had preconceptions of radiotherapy, such as it being painful, and by going through the process of treatment, patients had a much better sense of what treatment involved and it became routine.

“The first two, three, four days especially, ... getting the mask on, that was a wee bit daunting ... at first, not knowing what to expect. And then once I started, I realised that there is no pain with this ... And as I say, you fell into a routine, going to your radiotherapy, you got into a routine.” [Patient 4, male, age 74]

The corollary of already having experienced radiotherapy meant that when considering re-irradiation, patients were better able to understand the process and the side effect profile, and this reduced anxiety about re-treatment. They also had confidence that their body can withstand the side effects of radiotherapy.

“I don't think I would be worried too much the second time round because I've already experienced it so I would know second time around what to be prepared for, what to expect side effect-wise, symptoms-wise you know that's the thing it wouldn't come as such a shock or such a surprise so I wouldn't have any fears.” [Patient 3, male, age 55]

“I would hope that if I got it a second time it wouldn't be any worse. And I know what to expect, and I've handled it no bother, so I think I'll be able to handle it again if it came to it.” [Patient 6, male, age 68]

This lack of fear also applies when considering if they would undergo any cancer treatment during another pandemic. This study was conducted during the coronavirus pandemic and participants had already been treated with the background risk of COVID infection. All participants felt that they would prioritise their cancer care over the risks of the COVID, and this implied that the concerns they had over contracting the virus did not affect their treatment choices.

“No, no I had treatment during this. And I just wanted to get it over and done with, well hopefully over and done with. The virus doesn't come into the equation for me.” [Patient 2, female, age 86]

However, when talking about the uncertainties of treatments they had not experienced before, such as chemotherapy, the participants again describe feelings of anxiety, fear and relied on preconceptions with their answers. Both patient 2 and patient 8 did not have chemotherapy with their initial course of radiotherapy.

“I don't fancy the chemotherapy I really don't. I know so many people who've been on it some successful some not, but they just seem to be sick and ill, and

it's just awful. If possible, I'd rather stay away from that." [Patient 2, female, age 86]

"I'm not having chemotherapy. My hair will fall out for a start, and I've got nice hair." [Patient 8, female, age 73]

Conversely, Patient 3 had already had chemotherapy and his response is more accepting of it.

"I'll just keep going until they say you know we cannot give you anymore treatments. I don't think there's any worse side effects than what I've already had, to be honest" [Patient 3, male, age 55]

This highlights the importance of informing the patients of what to expect with treatment, as it clearly has an influence on their state of mind, and whether they would accept a new treatment.

8.4.3 Control

The second theme identified is that of control, or of having some sort of agency over the disease. This theme is sub-divided into ways of gaining control or losing control.

8.4.3.1 Gain of control

When asked if they would consider radical re-irradiation, all eight patients either agreed or would consider it. This could be interpreted as patients regaining control over recurrent disease, in both the medical sense of preventing cancer progression, but also regaining control over their quality and quantity of life, which cancer could remove from them. This is illustrated by how acceptance of re-irradiation was conditional for some patients (e.g., Patient 2) on factors such as age at relapse, stage of disease at relapse, interval between treatments and general fitness.

"I was hoping that I wouldn't need another dose of radiotherapy - but at the same time, I'd be quite prepared to go and have one if necessary." [Patient 7, male, age 78]

“I think a lot would have to do with how much older I was and also how I felt physically so it's a wee bit difficult to answer ... but I would have no hesitation in doing it again if it was needed to be done....What I'd be worried about was how far gone was it, I mean if it was really maybe 80% wasn't going to help, you know if it was so far gone practically untreatable I don't think I would bother.”
[Patient 2, female, age 86]

“I might do if it was after five years. If it was 3 and a half years, I would think about it long and hard. As I said to you before, it takes five years for your body to heal on the inside.” [Patient 8, female, age 73]

The importance of control was demonstrated in some of the participants responses to the efficacy of re-irradiation they would wish for before agreeing to re-irradiation.

“I'd like the chances to be 99.1%, thank you very much. That's what I want. I want 100% if I've got to go through it. It would be 100% for me... I would want assurances that that it's going to work. Because if it hasn't the first time, why should I go through it again, for it to not work again.” [Patient 8, female, age 73]

This patient justifies accepting a higher chance of success from re-irradiation because she is exposing herself to the side effects of the same treatment again. A different manifestation of control was by having a choice to take, or not take the treatment, regardless of how effective it may be.

“Hypothetically I would quite willingly go along with it if I thought it was going to help me more if there was a possible chance, even if there was a slight chance that it was going to help then I would quite happily do it.” [Patient 3, male, age 55]

This highlights the difference of controlling the disease, as opposed to being in control of one's healthcare decisions. Another way of participants exerting control over their clinical situation is by assessment of tumours by way of surveillance scanning.

All the patients were keen for surveillance scanning. This may be because scanning is the principal method to assess whether the cancer is under control or not, and therefore, if the patient is under control of the disease or vice versa. The actual process of having the scan was not a significant issue, but the anxiety waiting for the results was frequently raised, linking back to the first theme of fear. Patient 6 spoke about the balance between knowing the state of the cancer and the stress of waiting for the results but on balance, preferred to have the scans rather than not.

“I’m looking forward to it [a scan]. Then the doctors would know, and I would know, is there any further treatment needed or does it need to stop.” [Patient 1, male, age 62]

“It’s the unknown, it’s the waiting, that can take its toll on your mind.” [Patient 4, male, age 74]

“At the end of the day, I’d sooner be getting a scan because you think I need it and get proper treatment, whatever the outcome might be. Don’t get me wrong I’m not saying I’m not scared of the outcome.” [Patient 6, male, age 68]

8.4.3.2 Loss of control

Losing control of their situation (either regarding the tumour, or in their general day to day life) was described in some of the answers from the participants. One source of concern was losing function from the side effects of re-irradiation. Several participants spoke of the need to maintain some quality of life, and not lose control over what they can do.

Issues that were important to patients were freedom from breathlessness, independence and effect on family life. Several patients explained that they would refuse treatment should the risk of these complications be high. Conversely, if a short-term admission to hospital was required, that was generally acceptable.

“I’ve heard that some people are more or less confined to the house because they need oxygen all the time. If it was a scenario like that - put it this way if

it was a 50/50 thing that I could end up that way I don't think I'd be willing to take it... to me, living would not be sitting in the house with oxygen.” [Patient 2, female, age 86]

“Interviewer: Would it be fair to say then, even if the radiotherapy was to control the tumour, at the cost of making you lose your independence -

Patient: Then I would refuse it.” [Patient 5, male, age 76]

“What makes my decision, how does it carry on with the family life? That’s the first and foremost thing. How it affects your family.” [Patient 5, male, age 76]

“I don’t know how long I’ve got. I don’t want my last couple of years to be just surviving, if you know what I mean. If I’m going to go through this, I’d want some kind of quality of life. I’m not just keeping myself alive for the sake of keeping myself alive if you know what I mean.” [Patient 6, male, age 68]

“The fact is if it’s going to give me another 4 years, 6 years, 10 years, truthfully I would have no qualms about going for a second dose of radiotherapy to be honest with you... if it means being hospitalised for a short time or whatever, but at the end of the day you come out and you walk away, to my mind it’s worth the risk.” [Patient 4, male, age 74]

One participant expressed the view that being alive takes precedence over the quality of life, and this shows how individualised each patients’ concept of life is and how clinicians when considering radiotherapy should attempt to elucidate this.

“It’ll give you a year. It’s a year of life doctor. It’s a year of time, isn’t it?” [Patient 8, female, age 73]

As a result of this, most patients expressed dissatisfaction with the watch and wait strategy in the hypothetical situation that they had a local relapse. Most patients wanted to be actively treated and felt that delaying treatment until symptomatic would mean that the cancer could progress rapidly.

“I think I would prefer getting the treatment rather than not.” [Patient 1, male, age 62]

“Some people have the aggressive cancers ... so I just think why wait if eventually you're going to have to have [treatment]” [Patient 2, female, age 86]

“Help them immediately, not with watch and wait. The time you watch them and wait and see, the person would be dead.” [Patient 8, female, age 73]

There were two sub-themes also related to loss of control: fatalism about outcomes in lung cancer and allowing family members or doctors to make decisions regarding re-irradiation. A minority of patients had a fatalistic approach to treatment and the outcome from it.

“I'm quite a realist really, as I said. If I'm going to die, I'm going to die. I don't mean to be a doomster, I don't mean it in that way, but I realise I can die ... Whether [treatment will] be any good for me is kind of irrelevant, just to see if it does what you want it to do.” [Patient 6, male, age 68]

“I'm resigned to anything that comes to me. I'm resigned to it. If it comes back, it comes back.” [Patient 8, female, age 73]

Some patients delegated the decision about re-irradiation to either family members or their doctor. Seeking the support of family members seemed to be due to the importance in their life, whereas the doctors' treatment recommendation due to their expertise. Patients clearly had faith in their clinician's opinion and seemed likely to do what was suggested to them.

“I tend to put family first and if they say go ahead then I'll go ahead. Because that is the most important thing in my life, and as I say when this started, they said please do it.” [Patient 3, male, age 55]

“I'm the kind of person that if the doctor says we think that this is the best possible course of action for you then I would agree - I wouldn't disagree if you know what I mean. You are the medical professionals. I would take your advice and go along with that.” [Patient 3, male, age 55]

“If I was told by the doctor that’s what to do, then I would do it. If that’s what I was advised to do, then I’d do what the doctor told me.” [Patient 5, male, age 76]

In one way, this is a pragmatic approach, to allow a person experienced in re-irradiation to decide on whether to proceed with it, but it also could be interpreted as a way of participants opting out of making their own decision. Shared decision making with patients is essential to ensure that the patients’ views are acknowledged and acted upon, rather than simply the clinicians’ opinions, and doctors should ensure that they fully consent the patients when considering re-irradiation.

8.5 Discussion

8.5.1.1 Summary of results

This semi-structured interview study provides the first data on the patient perspective of re-irradiation for lung cancer. The primary aim was to explore patients’ views on re-irradiation. Two themes emerged from thematic analysis: fear and control. These feelings could be associated with all the subsequent responses about re-irradiation. All eight patients would consider radical re-irradiation, but not at any cost. The balance of the chances of success and of severe toxicity, enough to impair patients’ quality of life, are key factors in how patients decide whether to proceed with re-treatment. Other factors are the patients’ age, fitness, stage of disease at relapse and doctors’ recommendation. There was a wide range of opinions on what would constitute an acceptable chance of success - with one patient suggesting a virtual guarantee of tumour control, and others accepting even a slight benefit. Interestingly, some patients felt less fearful of and more confident they could get through treatment because they had experienced it beforehand.

The interviews also provided insights on the secondary outcomes of the study. Patient assessed toxicity severity did not appear to have an impact on acceptance of re-irradiation. When discussing alternative treatments or a watch and wait strategy, most patients preferred active treatment of some sort while chemotherapy was dismissed by half of the patients immediately, and the rest

were more amenable to it. Patients were keen to have follow-up scans to assess the effects of treatment and ongoing disease control although disliked the anxiety of waiting for the results.

8.5.1.2 Implications for practice

This analysis suggests that there are two predominant attitudes to re-irradiation, fear and control. These could be generalisable to any medical treatment. Fear of treatment, which the participants mentioned frequently, is something that can potentially be reduced, by providing patients with detailed information about the treatment that they will receive. This may be informed by staff taking time to go through treatment in the necessary detail, patient leaflets, and past patients sharing their experience or videos shared online. Fear of recurrence was alluded to when discussing surveillance scans, and there is extensive work demonstrating that lung cancer patients are especially prone to this²⁸⁶. Further counselling of patients by the healthcare team and additional support groups may improve patients' understanding and relieve some of their concerns.

The theme of control demonstrated participants wishes to maintain some agency over their health and life. This may be important as they may be disempowered by their diagnosis of cancer. This manifests itself in attempting to take control of the tumour itself, by accepting treatment, or also by controlling the side effects and choosing their quality of life (which may mean to not accept treatment). Shared decision-making in healthcare facilitates discussion of patients' and clinicians' motivations. This analysis supports a detailed consent process for re-irradiation, with clear discussion about the likely efficacy of treatment and the side effects they will experience.

Interviewer bias may have shaped the responses of the participants. The researcher was performing research on re-irradiation leading to a PhD and therefore had a significant interest in this treatment. In addition, the researcher was also a medical doctor. These factors may have subconsciously influenced patients to consider re-irradiation. However, the interview was semi-structured with a clear question structure to limit this bias. The choice of the researcher to perform the interviews was for two reasons. Firstly, the researcher had specific knowledge about radiotherapy and re-irradiation therefore could ask appropriate

questions to enhance the quality of the interviews. Secondly, there was no funding to recruit a specialist interviewer. Ultimately, this is a likely source of bias, but it was attempted to be controlled as much as possible through the study design.

In the dual role of doctor and researcher, there were many learning points that will influence future practice. Fear of the diagnosis and treatment of cancer is prevalent. This study was designed to investigate re-irradiation in the context of a future study and was biased to more practical considerations (e.g., would patients consider this treatment). However, through the repeated analysis of these interviews, the emphasis has shifted from being trial-focused to more patient-centric (in that the themes raised are generalisable to any area of oncological practice). The thematic analysis has been influenced by the researcher's background and it would be interesting to develop themes with a researcher without a medical background, to see if there are different interpretations of the data.

8.5.1.3 Results in the context of a future clinical trial

There are no previous data about patient attitudes to re-irradiation. A related study analysed the attitudes of patients to chemotherapy in the metastatic setting. This demonstrated, as with the current re-irradiation interviews, that each patient would accept a personalised chance of success. Some patients accepted one week of improved survival and another was unwilling to have chemotherapy even if it would lengthen prognosis by 24 months²⁸⁷. However, outcomes from re-irradiation in the locally advanced setting are difficult to predict compared to the chemotherapy in the metastatic setting, where there is negligible chance of survival of several years. Radical re-irradiation delivers long term disease control in a third of patients, but conversely some patients derive little benefit at all. This supports the highly individualised approach suggested in Chapter 4 in the Delphi consensus. The toxicity and tumour control models may also be useful in this context, to allow clinicians to better quantify the likely efficacy and side effects of treatment, and thereby better counsel patients. The practical extension of this is risk-based planning, where the clinician and the patient set target acceptable risks, which are translated using the models into a

planning normal tissue objective. However, the models need to be prospectively verified to have any utility in the clinic.

The views on alternative treatments other than re-irradiation may have an influence on any comparator arm of a study. Patients generally wanted treatment, rather than a watch and wait strategy, but some had robust views about chemotherapy. If a study design randomised between re-irradiation or chemotherapy/observation, patients may be unwilling to proceed if they are randomised to the non-radiotherapy arm and leave the trial. A study design that randomised between radiotherapy and radiotherapy plus a systemic treatment (e.g. immunotherapy) may be more acceptable to patients, because in either arm, they would get some form of active treatment.

The data from the interviews support surveillance scanning. However, surveillance scans have limited evidence of survival benefit. Empirically, treatment of a smaller lesion is likely to have a lower dose to OARs and may be suitable for SABR, which on retrospective evidence, is associated with a better rate of disease control. Therefore, another interesting trial would be devising a prospective surveillance schedule and re-irradiate at the first sign of relapse compared to standard treatment.

8.5.1.4 Limitations and bias

This study has several issues which affect the interpretation of the results. Firstly, only 8 patients were recruited out of 20 patients approached. The target recruitment was between 16 -32 with the intention of achieving data saturation. It is unlikely that all the possible issues that patients have with re-irradiation are discussed in these interviews. Each patient continued to contribute new concepts, and this may also be due to the interviewer developing greater insight into the issues as the number of interviews increased. Guest *et al.*, after analysis of a series of interviews, calculated that approximately 97% of new themes have been found after 12 interviews, and this could be considered the minimum target for this study²⁸⁸.

Conversely, Braun and Clarke argue against the need for numerical targets in data saturation, making the point that there are no set number of themes on any

one topic which the researcher needs to “excavate”. Rather, it is the interpretation of the data by the researcher which generates themes, and the subsequent development of meaning²⁸⁹. In addition, Vasileiou *et al.* highlight that the justification of sample sizes is methodologically difficult in qualitative research. They imply that rather than perform many interviews to achieve data saturation (which is difficult to define), a more applicable concept is data adequacy, which relates to whether the data and the meaning inferred from the sources, is sufficient to answer the relevant questions to the study²⁹⁰. Using data adequacy in this study, several key themes have been elucidated and conclusions can be made in how to shape a clinical trial, therefore the number of interviews may be enough.

This study is affected by selection bias. Twenty patients were approached, which is approximately 10% of the patients who would have had radical radiotherapy during the duration of the study. Twelve of the 20 patients approached declined involvement in the study. This is likely to be due to both bias from the clinical care team and from patients. The clinical care team may have deemed some patients unsuitable for this study. One possible reason is if patients were very anxious already about their treatment, clinicians may have felt that this study would be inappropriate and would not have approached them. The clinical team would likely have been under significant workload pressure and may not have had the time to introduce the study to patients. Additionally, they may have felt concerned about giving patients another task while they were undergoing arduous treatment.

Another type of selection bias is that the patients who agreed to this study were pragmatic and accepted their condition and treatment. This is supported by two observations. Firstly, patients during the interviews seemed accepting of their treatment and the possible results, almost to the point of fatalism. Secondly, anecdotally, when the researcher asked if there was any reason why a patient declined to take part in the study, a common response was that they wanted to forget about their treatment once it was finished. This implies that there is a group of patients who may refuse re-irradiation, possibly due to the stress caused by the initial course of treatment. This category of patients may also be struggling with more severe side-effects compared to the participants in this

study. However, seven of the eight participants did have side effects, with one participant requiring hospitalisation. It is therefore not possible to draw a conclusion that the patients who declined the study had more toxicities. The overall effect of the selection bias is that the patients recruited to the study are more likely to accept re-irradiation.

The inclusion criteria included patients receiving a range of treatments. Some treatments are likely to have more side effects (e.g., 6 weeks of chemo-radiotherapy), less side effects (SABR), or involve admission to hospital (CHART). The type of treatment may have influenced the patients' attitudes to re-irradiation. The low number of patients recruited meant that it was not possible to analyse the patients according to what treatment they received. Nevertheless, the toxicity that patients experienced did not seem to affect whether they would consider re-irradiation. No patients treated with CHART (which involves a two week inpatient stay for thrice-daily radiotherapy) agreed to take part in the study, therefore the results from this study are unrepresentative of this group.

There are also methodological flaws which make extrapolation of results difficult. The main objective of this study was to explore the attitudes to re-irradiation with a view to launching a clinical re-irradiation study. Therefore, the best group to interview would be patients who would be eligible for a proposed study, i.e., with locally relapsed disease after radical radiotherapy. This group was not included because firstly it would be difficult to identify these patients in clinical practice, as surveillance scanning was not protocolised. In addition, it would be potentially distressing to discuss with a patient the option of radical re-irradiation (a non-standard treatment) when they may not be offered this by the treating clinician.

As the ideal target group was unsuitable for interview, patients who had completed a course of radical radiotherapy were targeted. These patients were interviewed after 5 weeks of completion of treatment. This is two months before their routine end of radiotherapy CT scan. The interview timing was selected to avoid the bias introduced by the results of the scan. If it showed a reduction in size of the tumour, this may make patients more accepting of re-irradiation and skew the results of the study. By interviewing patients early, this effect is less.

However, it means that patients would have only experienced early side effects from the radiotherapy. Therefore, it was not possible for patients to comment on late side effects which may take years to manifest. Unless the study follow-up period was at least 2 years, late effects would be under investigated, but such a long follow-up would make this study impractical to conduct. Finally, patients were asked to consider the hypothetical situation of relapse. As it is a hypothetical situation, patients may agree to re-irradiation more frequently, whereas if faced with the reality of the situation, they may make a different choice after more careful consideration. The overall effect of the timing of the interviews could have made patients less likely to consider radiotherapy as they were still experiencing the early side effects of treatment at interview. In addition, the short interval between completing radiotherapy and the interview would reduce the risk of recall bias.

There are several limitations and biases of this study which may have influenced the results, possibly indicating that the patients interviewed may be more likely to consider re-irradiation. Nevertheless, this demonstrates that there is a group of patients who would consider treatment and have given their opinions on how to best shape a future clinical study.

8.6 Conclusion

The main themes that were determined from the interview analysis were fear and control. Clinicians should consider additional ways to prepare patients for treatment and focus on shared decision making when discussing re-irradiation. All patients interviewed would consider re-irradiation for lung cancer, with individualised balances of risks and benefits. Patients are keen for surveillance imaging. Patients would prefer an active treatment strategy over a policy of “watch and wait”. These data will be useful in planning a re-irradiation clinical trial for locally relapsed lung cancer.

9 Final Discussion

The aim of this thesis was to investigate the safety of radical thoracic re-irradiation and patients' attitudes to it with a view to developing a prospective clinical trial. Three issues pertinent to a future study have arisen through the course of this research: the definition of re-irradiation, the rationale for re-treatment and the management of the likely risks.

9.1 Definition of radical thoracic re-irradiation

The definition of re-irradiation is important as it defines the inclusion criteria for any future study and allows standardisation of treatment. The Delphi consensus process explored the uncertainties involved, with the group of lung oncologists unable to agree on a single definition of re-irradiation. The main areas of difference were whether to divide second courses of thoracic radiation by indication (i.e., for local recurrence or second primary lung cancers (SPLC)) or by dose to OARs (i.e., if the dose of a second course exceeds the dose constraint of a single course of radiation).

Definition of re-irradiation by indication requires evidence to suggest that there is a difference between the two groups. The review of the Beatson cohort suggests that there may be a difference in survival, with longer median overall survival with SPLC than local recurrences (35.8 vs 13.8 months respectively, p-value 0.15) although not statistically significant. The SPLC cohort however consisted of a greater proportion of stage I tumours treated with SABR. The difference in stage between SPLC and the local recurrence groups is probably due to easier diagnosis and treatment of a second primary, whereas locally recurrent disease may only become apparent after serial scans, and has no protocolised treatment. Additionally, a previously irradiated cancer is likely to have different biological characteristics than a non-irradiated tumour (see Chapter 9.2.1).

The definition of re-irradiation based on the use of OAR dose has some important benefits but also flaws. It identifies a group of patients who would be at a higher risk of toxicity from re-irradiation. However, it may be over cautious because some OARs (e.g., spinal cord) have well-validated pre-clinical and clinical data

supporting tissue recovery, indicating that exceeding the dose from a single course of treatment may be safe. Conversely, the lung dose constraint is clearly unpredictable based on the modelling in Chapter 5, with toxicity seen at very low doses below what would be accepted dose constraints for a single course of radiation. Additionally, the definition would only be confirmed after a re-irradiation plan had been generated. This process is prone to error, both with image registration (Chapter 4.3.2) and with dose accumulation (Chapter 7.3.4). Therefore, it would be practically difficult to use this definition for inclusion to a trial.

Other groups have suggested definitions. The EORTC/ESTRO group have opened a study entitled ReCare. The goal of this registry is to collect real-world data on the second courses of radiotherapy anywhere in the body^{291,292}. They define re-irradiation as where the “summation of the first and second dose carries a risk of clinically relevant morbidity”. A Delphi consensus study on pelvic re-irradiation had similar issues encountered in the thoracic Delphi process²⁹³. However, this group was able to agree to define SABR re-irradiation in the pelvis as “where there is overlap of previously delivered dose with the new treatment that could result in excess dose to an OAR and/or significant toxicity”. This definition includes overlap, but this group were unable to reach consensus on how much overlap would constitute increased risk. Both these definitions refer to clinician judgement as to whether an OAR dose has a significant likelihood of toxicity that, without validated dose/toxicity models, is hard to predict.

Ultimately, given that either a dose-based or an indication-based approach to a definition is imperfect, the choice of how to phrase the inclusion criteria for a future study depends on what is its primary objective. If it is to determine the safety of re-irradiation, then a dose-based approach may be more useful as used in the ReCare study. If the study is designed to assess the efficacy of re-irradiation in a specific clinical scenario, then an indication-based approach is apt. Both definitions complement each other, and both are areas that the Delphi consensus process identified as where further data is required.

9.2 Rationale for radical re-irradiation

The primary goals of any radical radiotherapy to the lung are twofold: to offer local control of the tumour to prevent development of respiratory symptoms and to provide long term disease control. Re-irradiation for local recurrence is empirically challenging to justify (as opposed to SPLC) as if the tumour has recurred in the same place after a course of radiation, then it could be considered radioresistant. Therefore, a second course of radiotherapy may be futile. However, it is worth reviewing the pre-clinical and clinical data regarding why initial radiotherapy fails, and if a second course of treatment can be clinically beneficial.

9.2.1 The biology of tumour radioresistance

There are several reasons why radiotherapy fails to control tumours. These can be divided into treatment factors (inadequate dose, extended treatment time resulting in repopulation, geographical miss), and biological factors (intrinsic to the tumour). Biological factors can be further subdivided into intrinsic to the tumour and acquired (i.e. changes made after radiation). There are several putative acquired changes in tumour genes and the tumour microenvironment (TME). Pre-clinical *in vitro* studies of NSCLC cell lines after irradiation demonstrate an increase in cancer stem cells and transcription factors associated with epithelial mesenchymal transition^{294,295}. Radiotherapy may also exert a selection pressure for radioresistant clones. Kocakavuk *et al.* demonstrated an increase in DNA small deletions post-radiotherapy which interfere with the DNA damage response (DDR). This was seen across several tumour types including lung cancer. The increased number of small deletions in the surviving cells suggest that this is a marker for cell survival under radiotherapy stress, and therefore further radiotherapy without suppressing this mechanism may be futile²⁹⁶.

Tumour hypoxia is a recognised cause for failure of radiotherapy. The DNA damage caused by ionising radiation is made permanent by oxygen. Hypoxic cells therefore have less DNA damage and are more likely to survive²⁹⁷. Trials targeting hypoxia in NSCLC have been unsuccessful and further research is ongoing²⁹⁸.

In addition, the metabolism of human NSCLC cell lines also has a role in radioresistance. NSCLC cells were irradiated and the surviving cells had increased levels of a redox regulatory protein called Nrf2 related to reactive oxygen species. Inhibition of Nrf2 led to decreased clonogenic survival²⁹⁹.

Beyond the tumour cell itself, there is evidence to suggest that the TME also has some role in survival after radiotherapy. Radiotherapy can affect the vasculature of a tumour making the environment more hypoxic and may affect cancer-associated fibroblasts. Radiotherapy has a mixed response to the immunology of the tumour, causing inflammation and immune stimulation, but also an increase in radioresistant macrophages and T-cells³⁰⁰. The mechanisms underpinning the relationship between radiotherapy and the immune system have recently been elucidated. A pathway called the cGAS-STING (cyclic GMP-AMP synthase-stimulator of interferon genes) detects DNA damage and triggers tumour cells to activate the pro-inflammatory interferon pathway³⁰¹. This can attract other immune cells and trigger immunogenic cell death.

Much of this research has been on *in vitro* cell lines. Data from human biopsies post-radiotherapy are limited. A case study compared the pre-radiotherapy and post-surgery specimens of a patient who had SABR for a small lung cancer, then relapse and then a resection. Next generation sequencing and clonal analysis showed that the mutational repertoire of the tumours was reduced in the post-radiotherapy specimen, leading the authors to conclude that radiotherapy exerts a clonal selection pressure³⁰².

Cancer as an evolutionary process was first considered in the 1970s and has recently become an accepted paradigm to describe the survival of cancer cells^{303,304}. The selection pressure radiotherapy places on tumours has multiple theoretical consequences. A course of radiation may kill radiosensitive sub-clones, leaving radioresistant clones behind to proliferate. However, this cannot be the sole process in irradiated tissues, otherwise every course of radiation would result in radioresistant disease, and local recurrence. There is likely to be another effect of radiation that counterbalances the mutagenic effects of radiation. Radiation can change the tumour micro-environment and therefore move away from favouring one clone, to select for the survival of another clone. These genetic changes are unpredictable and dynamic. Therefore, it may be that

radioresistance is not an immutable genetic characteristic of tumour cells, more a consequence of the tumour microenvironment and the immune response.

At present, there are no methods to determine the radiosensitivity of recurrent disease. In *de novo* disease, a gene expression panel of the tumour can be used to generate a radiosensitivity index (RSI)³⁰⁵. The RSI in combination with the physical dose can be used to derive the genomic adjusted radiation dose (GARD). The GARD is a strong predictor of tumour response, whereas physical dose is not and has been suggested as a method to determine the necessary dose for tumour control²⁵⁹. This method has been criticised as lacking variables (as some of the predicted RSI values are biologically implausible suggesting significant features that are not included in the score calculation) but also under-representing tumour heterogeneity³⁰⁶. However, the development of a tool to determine radiosensitivity would be of great use in re-irradiation, to determine before commencing potentially high risk treatment the dose necessary for tumour control.

Finally, there may be another explanation to suggest that the radiosensitivity of recurrent tumours are similar to the previously treated lesion: tumour re-seeding. Massagué et al. demonstrated in mouse models that circulating tumour cells (CTCs) were able to repopulate the site of origin using breast, colon and melanoma cell lines. They found that metastases preferentially reseeded the tumour site of origin, and that the reseeded tumour had a more aggressive phenotype³⁰⁷. Extrapolating this principle to NSCLC, after radical radiotherapy, there is unlikely to be large metastases providing CTCs to reseed. Therefore, if reseeding occurs, it may be from CTCs shed from the original tumour. This tumour thrived in the tumour micro-environment prior to irradiation, and therefore may preferentially reseed in this area. If this is the case, locally recurrent disease may be radio-naïve reseeded disease from CTCs.

Tumour heterogeneity and associated chromosomal instability is associated with poorer outcomes in the TRACERx study (Tracking Non-Small-Cell Lung Cancer Evolution through Therapy)³⁰⁸. This study analysed the genetic changes of tumours initially taken from patients who had resected disease, and then rebiopsy of the metastatic disease. A companion study, called the SIEVERT study (currently in set-up) aims to determine genetic changes after radiotherapy. This

study has the potential to explore the effect of radiotherapy on the evolution of lung cancer. This clinical study will provide essential information on the biology of tumours after radiotherapy and determine if the changes seen in pre-clinical models are mirrored in clinical practice.

9.2.2 A rationale for why re-irradiation may be effective

Pre-clinical data suggest that the changes in the tumour and in the microenvironment may make further irradiation futile. However, there is clinical evidence to suggest that re-irradiation can be of benefit. Re-irradiation for locally recurrent disease in NSCLC has been shown to have a 2-year survival rate between 11-64% (see Table 1.1). This rate was confirmed in the Beatson cohort, with a 2-year OS rate of 38.5% (Chapter 4). Re-irradiation has also been shown to be effective in other tumour groups.

Re-irradiation in recurrent head and neck cancer has been investigated extensively, as the surgical salvage options are often impossible. There have been several trials of locally recurrent disease that have demonstrated prolonged local control and overall survival post-re-irradiation. In studies with no concurrent chemotherapy, the 2-year OS rate range was 27% to 33%³⁰⁹. In a retrospective study of re-irradiation with systemic treatment, the objective response rate was 75.6% with a 2-year survival of 48.7% (although this study included patients who had salvage surgery as part of their treatment)³¹⁰.

In glioma, hypofractionated re-irradiation in selected patients had a median OS of 8.6 - 12.4 months³¹¹. Pelvic tumours re-irradiated with SABR have a one year local control rate of 51-100%³¹². In addition, breast, lung and sarcoma also have some shown some efficacy of re-irradiation³¹³⁻³¹⁵. Palliative re-irradiation of bone metastases in a randomised trial had a clinical response rate at 2 months between 30-50%³¹⁶.

These studies lack comparative arms where re-irradiation was not given, therefore it is not possible to compare re-irradiation to other treatments or the natural course of the disease in the locally recurrent setting. In addition, a possible source of error is how local recurrence is diagnosed. In some cases, recurrence is made on radiological grounds rather than histological samples. A

study of repeat biopsies after treatment reported that a third of repeat biopsies that had no evidence of malignancy or a second histology (e.g. NSCLC on the initial biopsy and SCLC in the repeat)³¹⁷. Despite these flaws, there appears to be a group of patients who have local control and possibly improvement in OS from re-irradiation.

The tumour control modelling from Chapter 6 demonstrates that 2-year overall survival is associated with higher doses at re-irradiation. The local control model is less convincing, partly due to the smaller sample size and difficulty in diagnosing local recurrence. The predicted dose from the OS model for a 2-year OS rate of 50% is 76.5Gy. This may be skewed due to the use of SABR data in the modelling dataset. However, this indicates that the optimal re-irradiation technique is with SABR, as this dose is easily achievable. SABR affects the tumour in a biologically different way, which may result in better efficacy than fractionated radiotherapy. The data supports this with better efficacy seen in SABR series. However, the efficacy may be subject to confounding as SABR can only be delivered in early-stage tumours (which may have a better prognosis).

Re-irradiation may work due to the inherently stochastic effects of how radiation damages DNA. Given that the most lethal damage to a cell is in the form of dsDNA breaks, repeated radiation may simply be a second attempt at causing these critical lesions, that even previously irradiated cells, despite the acquired radioresistant adaptations, cannot repair.

9.2.3 Re-irradiation compared to alternative treatments

9.2.3.1 Systemic treatment

The evidence base for systemic treatment for isolated local recurrence of NSCLC is limited, with most drugs licensed for metastatic disease.

First line cytotoxic chemotherapy consisting of a platinum doublet has been the standard of care for mutation negative stage IV NSCLC prior to the advent of immunotherapy. Schiller *et al.* compared four different chemotherapy regimes in a large study involving 1203 patients. No chemotherapy regime was superior in efficacy to another. For the whole group, the disease control rate (DCR, the amount of complete or partial responses and stable disease) was 40% and the

median OS was 8 months. The risk of grade 3 toxicity (including haematological toxicity) was 19-28%, grade 4 toxicity was 53-68% and death from treatment was 4-6%¹⁸. In a group of patients mostly with stage IIIB/IV adenocarcinoma, maintenance pemetrexed can also be given, with a longer median OS of 16.9 months, compared to 14 months in the placebo arm when measured from the start of induction therapy³¹⁸. The difference between these two studies may be attributed to better patient selection, with only patients with PS 0-1 allowed into the maintenance pemetrexed trial, and better supportive care.

The combination of platinum doublet chemotherapy and pembrolizumab in the KEYNOTE-189 study improved outcomes compared to chemotherapy alone irrespective of PD-L1 status: the DCR was 84.6% in the experimental arm, and the median OS was 22 months vs 10.7 in the standard arm (HR for death 0.56, 95% CI 0.45 - 0.70). The grade 3-5 toxicity rate was 71.9%^{22,319}. There remains debate whether chemotherapy adds extra efficacy in the PD-L1 \geq 50% patient group, as KEYNOTE-024 demonstrated comparable efficacy of single agent pembrolizumab with a lower toxicity rate (median OS 30 months, grade 3-5 toxicity rate of 31.2%)²³. These studies were for patients with metastatic disease and therefore may not be directly comparable to patients with local relapse.

Benefits of systemic treatments are that they may offer control of micro-metastatic disease, there is the option to modify the dose if the patients develop side effects (which is not possible in re-irradiation, as often the worse toxicity takes weeks to develop) and that most toxicity from systemic treatment resolves after time. However, it generally does not offer long term disease control, with the rare exception of patients who have a durable response from immunotherapy.

9.2.3.2 Salvage surgery

There is a small number of studies that report the outcomes of salvage surgery after radiotherapy. Dickhoff *et al.* analysed 15 patients with locally recurrent stage III NSCLC who underwent salvage surgery at a median of 21 months after completion of radiotherapy. The median OS was 46 months with a morbidity rate of 40% and a mortality rate of 6%³²⁰. A small study reported the outcomes of salvage surgery after SABR. 12 patients underwent resection after isolated local

relapse after SABR. The 5-year OS rate was 58.3%, which may reflect the initial early stage of initial diagnosis, compared to stage III patients³²¹.

There are a series of studies of surgical resection after SABR, with a total of 16 patients reporting few major operative complications (one bronchopleural fistula, and one conversion to open thoracotomy due to adhesions). There was one death at 14 months from recurrent disease, with the other 15 patients alive at time of publication (range of follow-up 2-39 months)³²²⁻³²⁴.

The outcomes from the salvage resections are similar, if not better than, SABR radiotherapy. However, comparisons between these groups are difficult as patients selected for salvage surgery would be fit for major thoracic surgery, whereas patients for re-irradiation may have a greater burden of comorbidities.

9.2.3.3 Practical benefits of re-irradiation

Re-irradiation as a treatment for recurrent disease is an attractive option. At radical doses, it offers the potential of long-term disease control and improvement in local symptoms from the tumour. Patients who are unfit for radical surgery due to comorbidities may be suitable for radical re-irradiation. The treatment can be delivered over two to six weeks, and then the patient will need no further treatment for several months and possibly longer. This may be preferable to systemic treatment, which is delivered approximately every two to six weeks, where the patient may be at risk of ongoing toxicities and need regular hospital visits. Additionally, the grade 5 toxicity rate of re-irradiation is similar to the rate with chemotherapy and with salvage surgery. In health economic terms, the cost of a course of re-irradiation may be less expensive than systemic treatment although this has not been fully explored.

The qualitative research in Chapter 8 has shown that there is a group of patients who would accept re-irradiation, in part because they are familiar with the side effects and the process. In comparison, patients were less keen on systemic therapy or a watch and wait strategy.

In summary, the mechanisms how tumours survive radiotherapy are unclear. Pre-clinical work demonstrates that radiotherapy has wide-ranging effects on clonal

selection, upregulation of certain genes and alterations to the vascular supply and immunogenicity of the TME. Whether these changes reduce the effectiveness of further radiotherapy has not been tested in a pre-clinical environment. Clinically, based on the published studies of re-irradiation, a subset of locally recurrent tumours retain radiosensitivity, respond to re-irradiation, and patients are amenable to second courses of radiation. Further work is required to identify the biological signature to predict those patients who would respond to re-irradiation.

9.3 Prediction and management of the risks of toxicity

Re-irradiation is a high-risk treatment, as shown in the published studies (Table 1.2). In addition, the Beatson cohort as described in Chapter 4 demonstrated a 43.6% rate of grade 3 toxicity with one fatality. Dose/toxicity models have the potential to identify patients at high risk, and this can allow for modification of the treatment to reduce the chance of harm.

9.3.1 Re-irradiation dose/toxicity models

Chapter 5 summarises re-irradiation dose/toxicity models made using logistic regression for the spinal cord, lung, aorta, oesophagus and proximal bronchial tree. Logistic regression performs two functions: it represents the outcome data for the range of the variables that is in the training dataset and; uses the relationship found in those areas to predict the likely outcome where there are no variables in the training dataset. The accuracy of logistic regression, as with any modelling tool, depends on the data available in the areas of most interest.

Due to this, the re-irradiation models must be interpreted with caution. Firstly, there is an unknown amount of either toxic or non-toxic events which have occurred and have not been included in these models. These may not be available due to publication bias, or other factors. However, these may significantly change the predictions. An example of where the selective use of data led to serious consequences was in the analysis of the likelihood of failure of the O-rings in the Space Shuttle Challenger disaster³²⁵. Importantly, the dose constraints derived from the models are similar to the pre-existing expert consensus constraints. It is worth considering whether the modelling results

simply reflect the pre-existing clinician bias and the doses deemed acceptable, rather than an estimation of the true risk.

Secondly, the models are most accurate where data already exists e.g. with the spinal cord model, there are a number of toxic and non-toxic events between 50 - 100Gy, which allows for more accurate prediction in this area of dose. However, in contrast, other models such as the lung V20 models had only 4 patient data above the cumulative dose of V20 > 30%. Therefore, these models are likely to be inaccurate beyond this dose.

Thirdly, re-irradiation toxicity is likely to be multi-factorial. The models in Chapter 5 are simple one or two variable models, because the amount of data available to model is limited. This approach is appropriate for some of the OARs e.g. spinal cord, where the cumulative dose in a serial organ is the main driver of toxicity. However, the lung re-irradiation models were unsuccessful because it is likely that lung toxicity is multifactorial. More complicated models using a range of radiotherapy, clinical and genomic variables may better predict toxicity. For example, an ideal lung toxicity model may include the mean lung dose, the pulmonary function tests, the size and laterality of the tumour, heart dose and some genomic data that suggests normal tissue sensitivity to radiation^{326,327}.

Despite these issues, these models are the most comprehensive datasets for thoracic OARs. Most models (excluding lung) validate with the Beatson cohort and correlate well with the model predicted and observed rates of toxicity. They require further refinement and validation with larger datasets which the ReCare study and analogous re-irradiation databases will hopefully provide^{292,328}.

9.3.2 Risk-based planning

The use of dose/toxicity models in clinical practice is limited mainly due to the use of dose constraints. These are arbitrarily set at a particular toxicity rate that is deemed by the clinician as acceptable. Patients are rarely consulted as to what level of risk they would agree to. However, in re-irradiation, due to the high risk and being a non-standard treatment, this is a consultation that is essential.

The Delphi consensus data and the qualitative research data give insights into the clinicians and the patients attitude to risk respectively. The clinicians' responses are summarised in Table 3.3. To summarise, most clinicians accepted high rates of Grade 1-2 toxicity (between 50-70% for oesophagitis, pneumonitis, and skin erythema), and lower rates of Grade 3-5 toxicity (generally 5% risk). However, the patients interviewed in the qualitative study had a wide range of opinions, with many accepting higher risks of hospitalisation to improve tumour control. Conversely, other patients were risk-averse and wanted to avoid Grade 3 or worse toxicity at all costs. This disparity strongly supports an individualised approach to re-irradiation planning, potentially using the dose/toxicity models to calibrate the dose to OARs to the patients' level of risk.

Radiotherapy planning using individualised dose constraints is possible, using a VMAT or a MCO technique. However, more importantly is whether a patient can truly appreciate what a grade 3 toxicity feels like, sufficient to be adequately informed to consent. In the re-irradiation setting, patients are likely to be better informed, as they may have already experienced toxicity from the initial course of radiotherapy.

In addition, when considering the risk of radiotherapy toxicity, this must be balanced against the risk of non-intervention. For example, haemoptysis after re-irradiation was associated with risk of fatal bleeding of 2.6% in the Beatson cohort. Historical data indicates that the rate of massive haemoptysis in an untreated cohort of 877 patients was 2.7%, although certain patients were at higher risk (tumour close to main bronchus, squamous cell cancers)³²⁹. Therefore, it is appropriate to ensure that the fatal risk from re-irradiation is no greater than the expected risk from non-intervention. The Delphi process suggested cropping the PTV to reduce dose to the OAR where it may exceed the dose constraint, and this was a successful replanning strategy to meet the dose constraints. However, by reducing the dose to the part of the tumour infiltrating the PBrT, this may lead to uncontrolled disease at the exact point which would cause symptoms. In summary, dose/toxicity models require validation with more data, but these could be useful to guide the individualised consent and planning process for re-irradiation.

9.4 Future studies

9.4.1 Studies in progress

Radical re-irradiation for lung cancer is a promising but complicated treatment, and further research is required before it becomes a routine treatment. There are several studies already in progress which are outlined in Table 9.1. There are two large re-irradiation registries in progress: the E²-RADlatE - ReCare project based in Europe and; the clinical registry for oligometastatic disease and re-irradiation (NCT02170181) in North America. They will be large databases, with a projected total of 9000 patients in total which will provide safety and efficacy data. There are some concerns regarding the quality of information recorded. The protocols available do not detail how the cumulative doses will be calculated and unless there is a consistent method, there will be data inaccuracies. This may influence the final conclusions, although with such numbers of data, the overall confidence of the results will likely be robust.

The REDIRECT study (see Table 9.1) promises to deliver reproducible and accurate cumulative doses and toxicity results. However, it plans to recruit only 15 patients per OAR. As it is a prospective study, the doses delivered will depend on the location of relapse and therefore it may struggle to provide data on the dose range of interest, which is the first upward inflection of the sigmoid dose/toxicity curve.

There are two phase I studies in progress in the locally recurrent setting, one using escalating doses of SABR, the other using re-irradiation and nanoparticles. One phase II study investigates hypofractionation in re-irradiation, and the other assesses the safety and efficacy of post-re-irradiation pembrolizumab. These clinical studies are small but may provide promising insights, especially in the use of additional treatments like nanoparticles to overcome radioresistance.

Table 9.1 Re-irradiation studies currently in recruitment Re-irradiation studies currently in recruitment. DIR: deformable image registration, ESTRO: European Society of Therapeutic Radiation Oncology, EORTC: European Organisation for Research and Treatment of Cancer, MTD: maximum tolerated dose, NCT: National clinical trials, NSCLC: non-small cell lung cancer, OAR: organ at risk, Re-RT: re-irradiation, SBRT: stereotactic body radiotherapy

Study title	NCT number	Start date	Finish date	Trial outline
High Dose Re-RT Utilizing Advanced DIR and Individualized OAR Dose Calculations With Organ Specific Toxicity Analysis (REDIRECT)	05301101	March 2022	July 2027	Prospective cohort study using a uniform re-RT process to determine toxicity rates for a given dose for OARs including the spinal cord, brachial plexus, oesophagus and vessels
SBRT Dose Escalation for Re-RT of Inoperable Lung Lesions (STRILL)	04455438	July 2020	Dec 2025	Phase I study designed to escalate the dose of SBRT from 30Gy in 5 fractions to 50Gy in 5 fractions to determine the MTD
Thoracic Re-RT For Locoregionally Recurrent NSCLC	04275687	Feb 2020	Feb 2025	Prospective phase II study to deliver 50-60Gy in 10 fractions to peripheral lesions or 30-40Gy in 6-10 fractions followed by a boost to central tumours
Safety and Efficacy of SBRT in the Re-RT for Ultra-central Thoracic Malignant Tumours	05189054	Jan 2022	April 2027	Prospective cohort study to determine the safety and efficacy of ultracentral re-RT using SBRT
Trial of Consolidation Pembrolizumab After Concurrent Chemotherapy and Proton Re-RT for Thoracic Recurrences of NSCLC	03087760	March 2017	Dec 2026	Single-arm phase II study to assess progression free survival and toxicity of adjuvant pembrolizumab after concurrent chemo and re-RT
NBTXR3 and Radiation Therapy for the Treatment of Inoperable Recurrent Non-small Cell Lung Cancer	04505267	Aug 2020	March 2024	Phase I study to assess the safety of Hafnium Oxide nanoparticles intratumorally and re-RT and determine the MTD
E ² -RADlatE: EORTC-ESTRO RADiotherapy InfrAstrucTure for Europe (E ² -RADlatE) - ReCare	03818503	Jan 2019	April 2024	Prospective registry of patients treated with re-RT collecting toxicity and efficacy data
Clinical Registry for Oligometastatic Disease, Consolidation Therapy, Debulking Prior to Chemotherapy, or Re-RT	02170181	May 2014	Dec 2026	Prospective registry to identify the toxicity and efficacy of re-irradiation

9.4.2 Potential pre-clinical studies

There are several areas that pre-clinical research could guide future trials in humans. This can be divided into two categories: research of the tumour to an initial course of radiation and the recovery dynamics of normal tissue.

The response of tumours to initial radiotherapy, and how this changes the efficacy of a second course of radiation is critical information. The work of Kocakavuk *et al.* and others investigating how tumours survive initial courses of radiotherapy helps trial design in two areas²⁹⁶. This may aid the identification of radioresistant tumours so that patients are not exposed to a futile yet toxic treatment. This research may also show cellular mechanisms that are essential for cell survival, and may reveal druggable targets in conjunction with re-irradiation. The use of pre-clinical re-irradiation models would also be helpful at estimating the α/β ratio of recurrent disease, and this would guide dose/fractionation schedules in the re-irradiation setting.

Other tumour focused work would be an investigation into the clonal selection pressure radiotherapy exerts on tumours. It is clear from the TRACERx studies that lung cancer is an evolutionary system. There is evidence from DNA sequencing that drug treatment drives clonal selection pressure and certain BRAF mutations in lung adenocarcinoma cell lines confer a resistance to ionising radiation³³⁰. The aim of the SIEVERT study (currently in set-up) is to perform genetic sequencing on locally recurrent tumours in humans to investigate if there is a similar effect. The identification of common survival patterns may provide insight into radiosensitisers that can be used with initial radiation, but also make re-irradiation more efficacious.

Pre-clinical models of re-irradiation normal tissue toxicity would also be useful. This could be attempted using a Small Animal Radiotherapy Platform (SARP). While this work would not be able to give true dose/volume constraints, it would provide an idea of the dynamics of recovery, as shown in the spinal cord animal work. The two OARs where there are no studies available are the oesophagus and proximal bronchial tree. This research may be compromised as defining a clinically relevant endpoint (e.g. the equivalent of grade three toxicity oesophagitis in a mouse) would be difficult. This data would be useful to

correlate with the modelling findings suggesting that the longer the interval, the greater the risk of re-irradiation toxicity in the proximal bronchial tree. In addition, there is no information on the nature of cardiac recovery and which substructures are more sensitive to re-irradiation. This would be very difficult for several practical reasons such as reliable dosimetry to the murine heart given its size, and difficulty in measuring cardiac function or pericarditis.

Finally, development of markers of normal tissue radiosensitivity of lung, oesophagus and proximal bronchial tree would be useful to identify patients at high risk of toxicity. A study in 41 patients who had post-mastectomy chest wall radiotherapy, the presence of single nucleotide polymorphisms (SNPs) in five selected genes correlated strongly with skin telangiectasia and fibrosis, with patients without certain SNPs having a radioresistant phenotype³²⁷. Replication of this work in lung tissue could allow the formation of a model to predict toxicity using both genetic features, as well as dose and other clinical variables. At present, the Delphi consensus had a crude measure of whether a patient had grade three toxicity with initial radiotherapy as an indicator of normal tissue radiosensitivity. Preclinical genetic testing may be useful in refining this and may aid treatment selection at initial radiotherapy.

9.4.3 Potential clinical studies

There are several potential options when considering the design of a re-irradiation clinical study, and this is guided by the key question of what is the aim of the study? The key questions for lung re-irradiation are what safe dose constraints are, what is the efficacy of re-irradiation, and how can patients who would benefit from re-irradiation be identified.

9.4.3.1 Safety studies

The traditional method of identifying the maximum tolerated dose of radiotherapy is a phase I dose escalation study. However, re-irradiation does not easily fit this type of trial for several reasons. Firstly, the anatomical location of the tumour will define the doses to the organs at risk (e.g. peripheral tumours will not test the central OARs, but may test the total lung volume). Of the locally recurrent patients in the Beatson cohort, the preliminary feasibility study

about dose escalation showed that 46% would be suitable for some sort of dose escalation, without breaching the pre-existing dose constraints, but this depended on the local relapse being in a peripheral location. Therefore, the number of patients required to test a dose limit may be high for a phase I study, and this may lead to long recruitment times and difficulty funding such research.

Secondly, other variables may affect the likelihood of toxicity, therefore any toxicity seen may not be due to the dose given (e.g., interval between treatments as seen in the proximal bronchial tree model in Chapter 5). The additional values would again increase the numbers required to add statistical validity to the study. Thirdly, the work in this thesis has provided several dose/constraint models which are broadly in alignment with the expert consensus. There are large data registries in process in Europe and North America that will provide additional validation data for these models. Therefore, a phase I study is unlikely to add practice changing data.

9.4.3.2 Efficacy of treatment

The quoted 2-year overall survival rates of re-irradiation are broad (between 11 and 64% with conventionally fractionated radiotherapy), and this reflects the range of disease that has been historically treated from stage I to III. The risks of re-irradiation are higher than initial treatment and therefore, it is important to have robust data on the likely efficacy.

Second primary lung cancers (SPLCs) may have intrinsically different responses to local recurrences. There was some evidence for this from the review of the outcomes from the Beatson cohort, but this may be due to confounding by treatment (as the SPLCs were more likely to be treated with SABR). The diagnosis of SPLCs is also difficult, as some are likely to actually be satellite metastases from a previously treated lung cancer. Biopsy of suspected SPLCs are harder to obtain tissue from as they are often seen on surveillance scans and therefore are smaller. The diagnosis of SPLC as defined in Chapter 1.7.1 is experientially based, and does not have a robust biological basis. However, it should be noted, from the patient perspective, this is largely irrelevant - whether it is a SPLC or a local recurrence, it still requires treatment and generates the same fears and anxieties. One pragmatic study would be to

compare aggressive detection and treatment by using circulating tumour DNA (ctDNA) as an early marker of recurrence, against standard CT surveillance. This would detect early local recurrences and SPLCs and both could be treated with SABR or conventional radiotherapy. This would assess if early retreatment modified the course of the disease. A similar study is already in progress called the Second Primary Lung Cancer Cohort Study (SPORT, NCT04178889), which uses ctDNA to detect recurrence after treatment, but it is out of the trial remit to offer re-irradiation. One possible criticism is that early detection by ctDNA may not aid the use of radiotherapy, as a tumour target needs to be visible on imaging. Therefore, there may not be a difference in the time to treatment between the two groups.

Another study design is to use an isotoxic treatment strategy, where patients with either a SPLC or a local recurrence are treated with SABR or conventionally fractionated radiotherapy, which is dose escalated until an OAR constraint is reached. There would be similar limitations to a phase I MTD study as discussed above, in that possibly only half of the patients recruited would be able to have dose escalation. However, for some patients, it may result in significantly increased dose to the tumour. An additional element to this could be where the patient decides the level of risk they would like to assume, using the dose/toxicity and tumour control models. This would be a novel and patient-centred approach and would personalise treatment in accordance with the results of the qualitative interview in Chapter 8. The models however are not validated, and therefore may under or over-estimate the toxicity rate. This uncertainty could result in significant risk to the patient, especially given radiotherapy toxicity can be permanent.

A randomised study design may be useful in shaping clinical decision making. One such study could compare radical re-irradiation with clinician's choice (e.g., systemic treatment, palliative dose re-irradiation, or a watch and wait strategy). In theory, this study would provide clinicians insight into what treatment they should offer their patients in the locally relapsed setting and would be pragmatic. However, there are some biases inherent in the study design which may prevent a true measure of efficacy. Radical re-irradiation has the possibility of long-term disease control, whereas the treatments in the other arm are

unlikely to achieve this. As patients may be able to have radical re-irradiation off-study, it may result in patients opting out of the study if they are randomised to the non-radical arm. The qualitative research in Chapter 8 suggested that patients were less likely to accept a wait and wait strategy. One solution to this is to reduce the treatment options and randomise between radical re-irradiation and chemo/immunotherapy. This would ensure that all the patients entering the study would be of a good performance status, and the addition of immunotherapy does offer the chance of long-term disease control, at a similar rate to radical re-irradiation.

An alternate study is a phase I study of radical re-irradiation using a novel radiosensitiser. This trial would investigate whether the radioresistance of recurrent disease could be overcome with a drug-radiotherapy combination. This may be the correct approach, but at present, there is insufficient pre-clinical research to help select an effective putative radiosensitiser. It may be that this trial would be better after pre-clinical studies, if a promising druggable pathway is discovered.

Radiotherapy techniques such as FLASH (ultra-high dose rate radiotherapy) or proton treatment could be considered in these possible future studies. Both techniques offer significant normal tissue sparing, which may spare toxicity and facilitate dose escalation to the tumour^{331,332}. The tumour control probability curve from Chapter 6 predicts a 50% 2-year overall survival rate with a dose of re-irradiation of 76.5Gy EQD2, which is likely to exceed the cumulative dose constraints if conventional fractionation is used. This dose is likely to only be reached by using highly conformal techniques like SABR, or more novel approaches such as FLASH or protons.

Underpinning any clinical re-irradiation study will be the need to have a standardised re-irradiation planning process, consistent image registration protocols and robust radiotherapy quality assurance. The planning data in Chapter 7 has demonstrated the superiority of multi-criteria optimisation over standard VMAT at avoiding serial organs, and through the deformable image registration process, has highlighted areas of uncertainty. The calculations to determine the remaining dose present a 'worst case scenario' as it assumed the Dmax for a given OAR falls in the same place over two courses of radiation. The

work by McVicar *et al.* and more recently with Murray *et al.* demonstrate that it is possible to generate a base plan using EQD2s and therefore plan re-irradiation with more anatomical information of where the dose has previously been delivered^{272,333}. These planning modules are not yet widely available but would be useful in a future study.

Patient reported quality of life measures would be essential, as would be an economic analysis of re-irradiation. This would be useful in the comparative study of re-irradiation against chemo/immunotherapy. Re-irradiation would be comparatively inexpensive as the infrastructure and staff are largely already present, compared to the continual drug cost for potentially two years of immunotherapy (as Pembrolizumab is subject to a two-year stopping rule in the UK) and the risk of admission for toxicities. Re-irradiation can be delivered within six weeks and then the patient may not require further treatment, whereas chemo/immunotherapy is an ongoing process every three to six weeks. These aspects of re-irradiation would be important to investigate as they are significant from the patients' experience.

9.4.3.3 Identification of patients likely to benefit from re-irradiation

In the Beatson cohort, most patients (61.5%) with local recurrence who had radical re-irradiation died from progressive cancer. There is a lack of studies to guide selection of patients to benefit from re-irradiation. As seen in the Delphi consensus, there are some clinical indicators such as a long interval between initial treatment and the need for retreatment that may suggest less aggressive disease. However, there is a need for translational research in this group of patients in any future study, to develop insights into this group. A group of UK oncologists interested in re-irradiation have summarised the key areas of pre-clinical development that can be reverse engineered from a clinical study in a recent editorial³³⁴.

In the post-radiotherapy setting, obtaining a biopsy may be difficult due to the fibrosis around the previously irradiated site. The samples may be smaller and non-diagnostic. Surgery is possible, but rarely performed, therefore whole tumour sampling is unlikely to be regularly performed. However, sequencing of ctDNA may offer significant insights into tumour heterogeneity, and the

presence of any mutations. Another non-invasive test could be analysis of the radiomic signature of recurrent tumours or the use of novel PET-tracers to assess for hypoxia or other characteristics. This translational work should be included in any clinical study, as this will provide further insights into how to optimally treat recurrent lung cancer.

There are several different trial designs detailed above. Given funding for radiotherapy trials in the UK is difficult, it is worthwhile to consider the study that is most useful at present. A less expensive option is to perform a large data registry. This will collect data that supports the putative dose constraints and possibly lead to a more standardised system of planning and delivery. However, this approach, because of the wide range of how clinicians approach re-irradiation and the few centres that can perform dose accumulation routinely, will have limited impact due to the relatively low quality data that would be submitted. The most useful study would be a phase II isotoxic re-irradiation study, with a safety run-in period, with translational, health economics and quality of life end points. This would give a protocol on how to deliver re-irradiation in a standardised way, test the dose constraints and collect data robustly. It also provides insights into the radiobiology of recurrent disease, and the patient reported benefits of treatment. This study would then provide a platform for any future randomised control study against a systemic agent.

9.5 Conclusion

This thesis aimed to investigate the safety of radical re-irradiation of non-small cell lung cancer. It has confirmed that patients re-irradiated for local recurrence can have durable responses and created expert consensus on the indications and delivery of this treatment. The relationship between dose and toxicity was quantified with radiobiological models, and a tumour control model provided estimates the likely doses required to achieve long term disease control. These models were used to generate cumulative dose constraints that were applied to a re-irradiation planning study, that demonstrated that most patient could be safely planned to those constraints. The patients' attitude to re-irradiation were obtained through qualitative interviews, revealing that re-irradiation is a treatment that can be considered, and that the acceptable risks of treatment are patient specific. This research, in particular the dose/toxicity models, have

quantified the safety of re-irradiation in a more evidenced based approach than expert consensus and will guide future studies to assess the efficacy of re-irradiation, ultimately to improve outcomes for patients.

List of References

1. Lung cancer statistics. 2017. (Accessed 26/01/2021, at <http://www.cancerresearchuk.org/health-professional/cancer-statistics/statistics-by-cancer-type/lung-cancer/incidence#heading-Two>.)
2. Luengo-Fernandez R, Leal J, Gray A, Sullivan R. Economic burden of cancer across the European Union: a population-based cost analysis. *Lancet Oncol* 2013;14:1165-74.
3. Global Burden of Disease Cancer C, Fitzmaurice C, Allen C, et al. Global, Regional, and National Cancer Incidence, Mortality, Years of Life Lost, Years Lived With Disability, and Disability-Adjusted Life-years for 32 Cancer Groups, 1990 to 2015: A Systematic Analysis for the Global Burden of Disease Study. *JAMA Oncol* 2017;3:524-48.
4. Hart CL, Hole DJ, Gillis CR, Smith GD, Watt GC, Hawthorne VM. Social class differences in lung cancer mortality: risk factor explanations using two Scottish cohort studies. *Int J Epidemiol* 2001;30:268-74.
5. Forrest LF, Adams J, Rubin G, White M. The role of receipt and timeliness of treatment in socioeconomic inequalities in lung cancer survival: population-based, data-linkage study. *Thorax* 2015;70:138-45.
6. Wynder EL. Tobacco as a cause of lung cancer: some reflections. *Am J Epidemiol* 1997;146:687-94.
7. Doll R, Hill AB. The mortality of doctors in relation to their smoking habits; a preliminary report. *Br Med J* 1954;1:1451-5.
8. Doll R, Peto R, Boreham J, Sutherland I. Mortality in relation to smoking: 50 years' observations on male British doctors. *BMJ* 2004;328:1519.
9. Malhotra J, Malvezzi M, Negri E, La Vecchia C, Boffetta P. Risk factors for lung cancer worldwide. *Eur Respir J* 2016;48:889-902.
10. Reck M, Liu SV, Mansfield AS, et al. IMpower133: Updated overall survival (OS) analysis of first-line (1L) atezolizumab (atezo)+ carboplatin+ etoposide in extensive-stage SCLC (ES-SCLC). *Annals of Oncology* 2019;30:v710-v1.
11. Amin M, Edge S, Greene F, Byrd D. *AJCC cancer staging manual*. 8th edition ed. New York: Springer International Publishing; 2017.
12. [NICE] NifHaCE. Lung cancer: diagnosis and management [NICE guideline 122]. 2019.
13. Postmus PE, Kerr KM, Oudkerk M, et al. Early and locally advanced non-small-cell lung cancer (NSCLC): ESMO Clinical Practice Guidelines for diagnosis, treatment and follow-up. *Ann Oncol* 2017;28:iv1-iv21.
14. Pignon JP, Tribodet H, Scagliotti GV, et al. Lung adjuvant cisplatin evaluation: a pooled analysis by the LACE Collaborative Group. *J Clin Oncol* 2008;26:3552-9.
15. Le Pechoux C, Pourel N, Barlesi F, et al. An international randomized trial, comparing post-operative conformal radiotherapy (PORT) to no PORT, in patients with completely resected non-small cell lung cancer (NSCLC) and mediastinal N2 involvement: Primary end-point analysis of LungART (IFCT-0503, UK NCRI, SAKK) NCT00410683. 2020.
16. Evison M, AstraZeneca UKL. The current treatment landscape in the UK for stage III NSCLC. *Br J Cancer* 2020;123:3-9.
17. Planchard D, Popat S, Kerr K, et al. Metastatic non-small cell lung cancer: ESMO Clinical Practice Guidelines for diagnosis, treatment and follow-up. *Annals of Oncology* 2018;29:iv192-iv237.

18. Schiller JH, Harrington D, Belani CP, et al. Comparison of four chemotherapy regimens for advanced non-small-cell lung cancer. *N Engl J Med* 2002;346:92-8.
19. Rosell R, Carcereny E, Gervais R, et al. Erlotinib versus standard chemotherapy as first-line treatment for European patients with advanced EGFR mutation-positive non-small-cell lung cancer (EURTAC): a multicentre, open-label, randomised phase 3 trial. *The Lancet Oncology* 2012;13:239-46.
20. Mok TS, Wu YL, Thongprasert S, et al. Gefitinib or carboplatin-paclitaxel in pulmonary adenocarcinoma. *N Engl J Med* 2009;361:947-57.
21. Solomon BJ, Mok T, Kim DW, et al. First-line crizotinib versus chemotherapy in ALK-positive lung cancer. *N Engl J Med* 2014;371:2167-77.
22. Gandhi L, Rodriguez-Abreu D, Gadgeel S, et al. Pembrolizumab plus Chemotherapy in Metastatic Non-Small-Cell Lung Cancer. *N Engl J Med* 2018;378:2078-92.
23. Reck M, Rodriguez-Abreu D, Robinson AG, et al. Updated Analysis of KEYNOTE-024: Pembrolizumab Versus Platinum-Based Chemotherapy for Advanced Non-Small-Cell Lung Cancer With PD-L1 Tumor Proportion Score of 50% or Greater. *J Clin Oncol* 2019;37:537-46.
24. Vokes EE, Ready N, Felip E, et al. Nivolumab versus docetaxel in previously treated advanced non-small-cell lung cancer (CheckMate 017 and CheckMate 057): 3-year update and outcomes in patients with liver metastases. *Ann Oncol* 2018;29:959-65.
25. Connell PP, Hellman S. Advances in radiotherapy and implications for the next century: a historical perspective. *Cancer Res* 2009;69:383-92.
26. Hasse KE. An anatomical description of the diseases of the organs of circulation and respiration: Sydenham society; 1846.
27. Debaquey M. Carcinoma of the lung and tobacco smoking: a historical perspective. *Ochsner J* 1999;1:106-8.
28. Russell M, Tod M. The Results of Radium and X-ray Therapy in Malignant Disease: Being the Third Statistical Report from the Radium Institute, the Christie Hospital and Holt Radium Institute, Manchester Years 1940 to 1944 Inclusive Assessed at 5 Years and 1934 to 1938 Assessed at 10 Years: Livingstone; 1950.
29. Smart J, Hilton G. Radiotherapy of cancer of the lung; results in a selected group of cases. *Lancet* 1956;270:880-1.
30. Morrison R, Deeley TJ. Inoperable cancer of the bronchus treated by megavoltage x-ray therapy. *Lancet* 1960;2:618-20.
31. Morrison R, Deeley T, Cleland W. The treatment of carcinoma of the bronchus: a clinical trial to compare surgery and supervoltage radiotherapy. *The Lancet* 1963;281:683-4.
32. Perez CA, Stanley K, Grundy G, et al. Impact of irradiation technique and tumor extent in tumor control and survival of patients with unresectable non-oat cell carcinoma of the lung: report by the Radiation Therapy Oncology Group. *Cancer* 1982;50:1091-9.
33. Cox JD, Azarnia N, Byhardt RW, Shin KH, Emami B, Pajak TF. A randomized phase I/II trial of hyperfractionated radiation therapy with total doses of 60.0 Gy to 79.2 Gy: possible survival benefit with greater than or equal to 69.6 Gy in favorable patients with Radiation Therapy Oncology Group stage III non-small-cell lung carcinoma: report of Radiation Therapy Oncology Group 83-11. *J Clin Oncol* 1990;8:1543-55.
34. Saunders M, Dische S, Barrett A, Harvey A, Gibson D, Parmar M. Continuous hyperfractionated accelerated radiotherapy (CHART) versus

- conventional radiotherapy in non-small-cell lung cancer: a randomised multicentre trial. CHART Steering Committee. *Lancet* 1997;350:161-5.
35. Kaster TS, Yaremko B, Palma DA, Rodrigues GB. Radical-intent hypofractionated radiotherapy for locally advanced non-small-cell lung cancer: a systematic review of the literature. *Clin Lung Cancer* 2015;16:71-9.
 36. Graham MV, Pajak TE, Herskovic AM, Emami B, Perez CA. Phase I/II study of treatment of locally advanced (T3/T4) non-oat cell lung cancer with concomitant boost radiotherapy by the Radiation Therapy Oncology Group (RTOG 83-12): long-term results. *Int J Radiat Oncol Biol Phys* 1995;31:819-25.
 37. Fowler J, Chappell RJ. Non-small cell lung tumors repopulate rapidly during radiation therapy. *International Journal of Radiation Oncology*Biolog*Physics* 2000;46:516-7.
 38. Bernier J, Denekamp J, Rojas A, et al. ARCON: accelerated radiotherapy with carbogen and nicotinamide in non small cell lung cancer: a phase I/II study by the EORTC. *Radiother Oncol* 1999;52:149-56.
 39. Prewett SL, Aslam S, Williams MV, Gilligan D. The management of lung cancer: a UK survey of oncologists. *Clin Oncol (R Coll Radiol)* 2012;24:402-9.
 40. Uematsu M, Shioda A, Suda A, et al. Computed tomography-guided frameless stereotactic radiotherapy for stage I non-small cell lung cancer: a 5-year experience. *Int J Radiat Oncol Biol Phys* 2001;51:666-70.
 41. Onishi H, Araki T, Shirato H, et al. Stereotactic hypofractionated high-dose irradiation for stage I nonsmall cell lung carcinoma: clinical outcomes in 245 subjects in a Japanese multiinstitutional study. *Cancer* 2004;101:1623-31.
 42. Timmerman R, Papiez L, McGarry R, et al. Extracranial stereotactic radioablation: results of a phase I study in medically inoperable stage I non-small cell lung cancer. *Chest* 2003;124:1946-55.
 43. Timmerman R, Paulus R, Galvin J, et al. Stereotactic body radiation therapy for inoperable early stage lung cancer. *JAMA* 2010;303:1070-6.
 44. Haasbeek CJ, Lagerwaard FJ, Antonisse ME, Slotman BJ, Senan S. Stage I nonsmall cell lung cancer in patients aged ≥ 75 years: outcomes after stereotactic radiotherapy. *Cancer: Interdisciplinary International Journal of the American Cancer Society* 2010;116:406-14.
 45. Chang JY, Senan S, Paul MA, et al. Stereotactic ablative radiotherapy versus lobectomy for operable stage I non-small-cell lung cancer: a pooled analysis of two randomised trials. *Lancet Oncol* 2015;16:630-7.
 46. Ball D, Mai GT, Vinod S, et al. Stereotactic ablative radiotherapy versus standard radiotherapy in stage 1 non-small-cell lung cancer (TROG 09.02 CHISEL): a phase 3, open-label, randomised controlled trial. *The Lancet Oncology* 2019;20:494-503.
 47. Radiotherapy dose fractionation. 2019. (Accessed 28/09/2021, 2021, at <https://www.rcr.ac.uk/publication/radiotherapy-dose-fractionation-third-edition>.)
 48. Dillman RO, Herndon J, Seagren SL, Eaton WL, Jr., Green MR. Improved survival in stage III non-small-cell lung cancer: seven-year follow-up of cancer and leukemia group B (CALGB) 8433 trial. *J Natl Cancer Inst* 1996;88:1210-5.
 49. Sause WT, Scott C, Taylor S, et al. Radiation Therapy Oncology Group (RTOG) 88-08 and Eastern Cooperative Oncology Group (ECOG) 4588: preliminary results of a phase III trial in regionally advanced, unresectable non-small-cell lung cancer. *J Natl Cancer Inst* 1995;87:198-205.
 50. Sause W, Kolesar P, Taylor SI, et al. Final results of phase III trial in regionally advanced unresectable non-small cell lung cancer: Radiation Therapy

- Oncology Group, Eastern Cooperative Oncology Group, and Southwest Oncology Group. *Chest* 2000;117:358-64.
51. Sause WT, Scott C, Taylor S, et al. Phase II trial of combination chemotherapy and irradiation in non-small-cell lung cancer, Radiation Therapy Oncology Group 88-04. *Am J Clin Oncol* 1992;15:163-7.
 52. Byhardt RW, Scott CB, Ettinger DS, et al. Concurrent hyperfractionated irradiation and chemotherapy for unresectable nonsmall cell lung cancer. Results of Radiation Therapy Oncology Group 90-15. *Cancer* 1995;75:2337-44.
 53. Byhardt RW, Scott C, Sause W, et al. Response, toxicity, failure patterns, and survival in five Radiation Therapy Oncology Group (RTOG) trials of sequential and/or concurrent chemotherapy and radiotherapy for locally advanced non-small-cell carcinoma of the lung. *International Journal of Radiation Oncology* Biology* Physics* 1998;42:469-78.
 54. Furuse K, Fukuoka M, Kawahara M, et al. Phase III study of concurrent versus sequential thoracic radiotherapy in combination with mitomycin, vindesine, and cisplatin in unresectable stage III non-small-cell lung cancer. *Journal of Clinical Oncology* 1999;17:2692-.
 55. Curran Jr WJ, Paulus R, Langer CJ, et al. Sequential vs concurrent chemoradiation for stage III non-small cell lung cancer: randomized phase III trial RTOG 9410. *Journal of the National Cancer Institute* 2011;103:1452-60.
 56. Maguire J, Khan I, McMenemin R, et al. SOCCAR: A randomised phase II trial comparing sequential versus concurrent chemotherapy and radical hypofractionated radiotherapy in patients with inoperable stage III Non-Small Cell Lung Cancer and good performance status. *Eur J Cancer* 2014;50:2939-49.
 57. O'Rourke N, Roque IFM, Farre Bernado N, Macbeth F. Concurrent chemoradiotherapy in non-small cell lung cancer. *Cochrane Database Syst Rev* 2010:CD002140.
 58. Bradley JD, Paulus R, Komaki R, et al. Standard-dose versus high-dose conformal radiotherapy with concurrent and consolidation carboplatin plus paclitaxel with or without cetuximab for patients with stage IIIA or IIIB non-small-cell lung cancer (RTOG 0617): a randomised, two-by-two factorial phase 3 study. *Lancet Oncology* 2015;16:187-99.
 59. Machtay M, Bae K, Movsas B, et al. Higher biologically effective dose of radiotherapy is associated with improved outcomes for locally advanced non-small cell lung carcinoma treated with chemoradiation: an analysis of the Radiation Therapy Oncology Group. *Int J Radiat Oncol Biol Phys* 2012;82:425-34.
 60. Bradley JD, Hu C, Komaki RR, et al. Long-Term Results of NRG Oncology RTOG 0617: Standard- Versus High-Dose Chemoradiotherapy With or Without Cetuximab for Unresectable Stage III Non-Small-Cell Lung Cancer. *Journal of Clinical Oncology* 2020;38:706-+.
 61. Cox JD. Are the results of RTOG 0617 mysterious? *Int J Radiat Oncol Biol Phys* 2012;82:1042-4.
 62. Faivre-Finn C. Dose escalation in lung cancer: have we gone full circle? *The lancet oncology* 2015;16:125-7.
 63. Zhang P, Su DM, Liang M, Fu J. Chemopreventive agents induce programmed death-1-ligand 1 (PD-L1) surface expression in breast cancer cells and promote PD-L1-mediated T cell apoptosis. *Mol Immunol* 2008;45:1470-6.
 64. Dovedi SJ, Adlard AL, Lipowska-Bhalla G, et al. Acquired resistance to fractionated radiotherapy can be overcome by concurrent PD-L1 blockade. *Cancer research* 2014;74:5458-68.

65. Faivre-Finn C, Vicente D, Kurata T, et al. Four-Year Survival With Durvalumab After Chemoradiotherapy in Stage III NSCLC-an Update From the PACIFIC Trial. *J Thorac Oncol* 2021;16:860-7.
66. Antonia SJ, Villegas A, Daniel D, et al. Overall survival with durvalumab after chemoradiotherapy in stage III NSCLC. *New England Journal of Medicine* 2018;379:2342-50.
67. Raben D, Rimner A, Senan S, et al. Patterns of Disease Progression with Durvalumab in Stage III Non-small Cell Lung Cancer (PACIFIC). *International Journal of Radiation Oncology Biology Physics* 2019;105:683-.
68. Mehta M, Scrimger R, Mackie R, Paliwal B, Chappell R, Fowler J. A new approach to dose escalation in non-small-cell lung cancer. *Int J Radiat Oncol Biol Phys* 2001;49:23-33.
69. Munro TR. The relative radiosensitivity of the nucleus and cytoplasm of Chinese hamster fibroblasts. *Radiat Res* 1970;42:451-70.
70. Thames HD, Jr. Early fractionation methods and the origins of the NSD concept. *Acta Oncol* 1988;27:89-103.
71. Thames Jr HD, Withers HR, Peters LJ, Fletcher GH. Changes in early and late radiation responses with altered dose fractionation: implications for dose-survival relationships. *International Journal of Radiation Oncology* Biology* Physics* 1982;8:219-26.
72. Vogelius IR, Bentzen SM. Meta-analysis of the alpha/beta ratio for prostate cancer in the presence of an overall time factor: bad news, good news, or no news? *International Journal of Radiation Oncology* Biology* Physics* 2013;85:89-94.
73. Ray K, Sibson N, Kiltie A. Treatment of breast and prostate cancer by hypofractionated radiotherapy: potential risks and benefits. *Clinical oncology* 2015;27:420-6.
74. Alaswad M, Kleefeld C, Foley M. Optimal tumour control for early-stage non-small-cell lung cancer: A radiobiological modelling perspective. *Phys Med* 2019;66:55-65.
75. Lee P, Loo BW, Jr., Biswas T, et al. Local Control After Stereotactic Body Radiation Therapy for Stage I Non-Small Cell Lung Cancer. *Int J Radiat Oncol Biol Phys* 2021;110:160-71.
76. Landberg T, Chavaudra J, Dobbs J, et al. Report 50. *Journal of the International Commission on Radiation Units and Measurements* 1993;os26:NP-NP.
77. Lyman JT. Complication Probability as Assessed from Dose Volume Histograms. *Radiation Research* 1985;104:S13-S9.
78. Kutcher GJ, Burman C. Calculation of complication probability factors for non-uniform normal tissue irradiation: The effective volume method gerald. *International Journal of Radiation Oncology* Biology* Physics* 1989;16:1623-30.
79. Wu Q, Mohan R, Niemierko A, Schmidt-Ullrich R. Optimization of intensity-modulated radiotherapy plans based on the equivalent uniform dose. *Int J Radiat Oncol Biol Phys* 2002;52:224-35.
80. Niemierko A. Reporting and analyzing dose distributions: a concept of equivalent uniform dose. *Med Phys* 1997;24:103-10.
81. McFarlane MR, Hochstedler KA, Laucis AM, et al. Predictors of Pneumonitis after Conventionally Fractionated Radiotherapy for Locally Advanced Lung Cancer. *Int J Radiat Oncol Biol Phys* 2021.
82. Tucker SL, Li MH, Xu T, et al. Incorporating Single-nucleotide Polymorphisms Into the Lyman Model to Improve Prediction of Radiation

Pneumonitis. *International Journal of Radiation Oncology Biology Physics* 2013;85:251-7.

83. Emami B, Lyman J, Brown A, et al. Tolerance of normal tissue to therapeutic irradiation. *Int J Radiat Oncol Biol Phys* 1991;21:109-22.
84. Bentzen SM, Constine LS, Deasy JO, et al. Quantitative Analyses of Normal Tissue Effects in the Clinic (QUANTEC): an introduction to the scientific issues. *Int J Radiat Oncol Biol Phys* 2010;76:S3-9.
85. Grimm J, Marks LB, Jackson A, Kavanagh BD, Xue J, Yorke E. High Dose per Fraction, Hypofractionated Treatment Effects in the Clinic (HyTEC): An Overview. *Int J Radiat Oncol Biol Phys* 2021;110:1-10.
86. Smith RP, Heron DE, Huq MS, Yue NJ. Modern radiation treatment planning and delivery--from Rontgen to real time. *Hematol Oncol Clin North Am* 2006;20:45-62.
87. Ragazzi G, Cattaneo G, Fiorino C, et al. Use of dose-volume histograms and biophysical models to compare 2D and 3D irradiation techniques for non-small cell lung cancer. *The British journal of radiology* 1999;72:279-88.
88. Ezzell GA, Galvin JM, Low D, et al. Guidance document on delivery, treatment planning, and clinical implementation of IMRT: report of the IMRT Subcommittee of the AAPM Radiation Therapy Committee. *Med Phys* 2003;30:2089-115.
89. Christian JA, Bedford JL, Webb S, Brada M. Comparison of inverse-planned three-dimensional conformal radiotherapy and intensity-modulated radiotherapy for non-small-cell lung cancer. *Int J Radiat Oncol Biol Phys* 2007;67:735-41.
90. Jiang X, Li T, Liu Y, et al. Planning analysis for locally advanced lung cancer: dosimetric and efficiency comparisons between intensity-modulated radiotherapy (IMRT), single-arc/partial-arc volumetric modulated arc therapy (SA/PA-VMAT). *Radiation Oncology* 2011;6:1-7.
91. Bedford JL, Hansen VN, Mcnair HA, et al. Treatment of lung cancer using volumetric modulated arc therapy and image guidance: A case study. *Acta Oncologica* 2008;47:1438-43.
92. Thieke C, Kufer KH, Monz M, et al. A new concept for interactive radiotherapy planning with multicriteria optimization: first clinical evaluation. *Radiother Oncol* 2007;85:292-8.
93. Craft DL, Halabi TF, Shih HA, Bortfeld TR. Approximating convex pareto surfaces in multiobjective radiotherapy planning. *Med Phys* 2006;33:3399-407.
94. Craft DL, Hong TS, Shih HA, Bortfeld TR. Improved planning time and plan quality through multicriteria optimization for intensity-modulated radiotherapy. *International Journal of Radiation Oncology* Biology* Physics* 2012;82:e83-e90.
95. Underberg RW, Lagerwaard FJ, Slotman BJ, Cuijpers JP, Senan S. Benefit of respiration-gated stereotactic radiotherapy for stage I lung cancer: an analysis of 4DCT datasets. *Int J Radiat Oncol Biol Phys* 2005;62:554-60.
96. De Ruyscher D, Nestle U, Jeraj R, Macmanus M. PET scans in radiotherapy planning of lung cancer. *Lung Cancer* 2012;75:141-5.
97. Bainbridge H, Salem A, Tijssen RHN, et al. Magnetic resonance imaging in precision radiation therapy for lung cancer. *Transl Lung Cancer Res* 2017;6:689-707.
98. Jaffray DA, Siewerdsen JH, Wong JW, Martinez AA. Flat-panel cone-beam computed tomography for image-guided radiation therapy. *Int J Radiat Oncol Biol Phys* 2002;53:1337-49.
99. Sonke J-J, Rossi M, Wolthaus J, van Herk M, Damen E, Belderbos J. Frameless stereotactic body radiotherapy for lung cancer using four-dimensional

- cone beam CT guidance. *International Journal of Radiation Oncology* Biology* Physics* 2009;74:567-74.
100. Lu L. Dose calculation algorithms in external beam photon radiation therapy. *International Journal of Cancer Therapy and Oncology* 2014;1.
101. Verhaegen F, Seuntjens J. Monte Carlo modelling of external radiotherapy photon beams. *Phys Med Biol* 2003;48:R107-64.
102. Bush K, Gagne I, Zavgorodni S, Ansbacher W, Beckham W. Dosimetric validation of Acuros® XB with Monte Carlo methods for photon dose calculations. *Medical physics* 2011;38:2208-21.
103. Rana S. Clinical dosimetric impact of Acuros XB and analytical anisotropic algorithm (AAA) on real lung cancer treatment plans. *International Journal of Cancer Therapy and Oncology* 2014;2.
104. Grutters JP, Kessels AG, Pijls-Johannesma M, De Ruyscher D, Joore MA, Lambin P. Comparison of the effectiveness of radiotherapy with photons, protons and carbon-ions for non-small cell lung cancer: a meta-analysis. *Radiother Oncol* 2010;95:32-40.
105. Liao Z, Lee JJ, Komaki R, et al. Bayesian Adaptive Randomization Trial of Passive Scattering Proton Therapy and Intensity-Modulated Photon Radiotherapy for Locally Advanced Non-Small-Cell Lung Cancer. *J Clin Oncol* 2018;36:1813-22.
106. Kong FS. What Happens When Proton Meets Randomization: Is There a Future for Proton Therapy? *J Clin Oncol* 2018;36:1777-9.
107. Offin M, Shaverdian N, Rimner A, et al. Clinical outcomes, local-regional control and the role for metastasis-directed therapies in stage III non-small cell lung cancers treated with chemoradiation and durvalumab. *Radiother Oncol* 2020;149:205-11.
108. Schneider BJ, Ismaila N, Aerts J, et al. Lung cancer surveillance after definitive curative-intent therapy: ASCO guideline. *Journal of Clinical Oncology* 2020;38:753-66.
109. Evison M, Barrett E, Cheng A, et al. Predicting the Risk of Disease Recurrence and Death Following Curative-intent Radiotherapy for Non-small Cell Lung Cancer: The Development and Validation of Two Scoring Systems From a Large Multicentre UK Cohort. *Clin Oncol (R Coll Radiol)* 2021;33:145-54.
110. National Lung Cancer Audit 2018. (Accessed 26/01/2021, at <https://www.rcplondon.ac.uk/projects/outputs/nlca-annual-report-2018>.)
111. Jeremic B, Shibamoto Y, Acimovic L, et al. Second cancers occurring in patients with early stage non-small-cell lung cancer treated with chest radiation therapy alone. *J Clin Oncol* 2001;19:1056-63.
112. Paradis KC, Mayo C, Owen D, et al. The Special Medical Physics Consult Process for Reirradiation Patients. *Adv Radiat Oncol* 2019;4:559-65.
113. Rubins J, Unger M, Colice GL, American College of Chest P. Follow-up and surveillance of the lung cancer patient following curative intent therapy: ACCP evidence-based clinical practice guideline (2nd edition). *Chest* 2007;132:355S-67S.
114. Griffioen GH, Dahele M, de Haan PF, van de Ven PM, Slotman BJ, Senan S. High-dose, conventionally fractionated thoracic reirradiation for lung tumors. *Lung Cancer* 2014;83:356-62.
115. Sandhu L, McWilliam A, Mistry H, et al. Outcomes of re-irradiation & repeat radiotherapy in NSCLC: A propensity matched analysis. *ESTRO*; 2020; Vienna, Austria. p. S153.
116. Viani GA, Arruda CV, De Fendi LI. Effectiveness and Safety of Reirradiation With Stereotactic Ablative Radiotherapy of Lung Cancer After a

First Course of Thoracic Radiation: A Meta-analysis. *Am J Clin Oncol* 2020;43:575-81.

117. Milano MT, Kong FS, Movsas B. Stereotactic body radiotherapy as salvage treatment for recurrence of non-small cell lung cancer after prior surgery or radiotherapy. *Transl Lung Cancer Res* 2019;8:78-87.
118. Murray P, Franks K, Hanna GG. A systematic review of outcomes following stereotactic ablative radiotherapy in the treatment of early-stage primary lung cancer. *Br J Radiol* 2017;90:20160732.
119. Okamoto Y, Murakami M, Yoden E, et al. Reirradiation for locally recurrent lung cancer previously treated with radiation therapy. *Int J Radiat Oncol Biol Phys* 2002;52:390-6.
120. Wu KL, Jiang GL, Qian H, et al. Three-dimensional conformal radiotherapy for locoregionally recurrent lung carcinoma after external beam irradiation: a prospective phase I-II clinical trial. *Int J Radiat Oncol Biol Phys* 2003;57:1345-50.
121. Tada T, Fukuda H, Matsui K, et al. Non-small-cell lung cancer: reirradiation for loco-regional relapse previously treated with radiation therapy. *Int J Clin Oncol* 2005;10:247-50.
122. McAvoy SA, Ciura KT, Rineer JM, et al. Feasibility of proton beam therapy for reirradiation of locoregionally recurrent non-small cell lung cancer. *Radiother Oncol* 2013;109:38-44.
123. Tetar S, Dahele M, Griffioen G, Slotman B, Senan S. High-dose conventional thoracic re-irradiation for lung cancer: updated results. *Lung Cancer* 2015;88:235-6.
124. Sumita K, Harada H, Asakura H, et al. Re-irradiation for locoregionally recurrent tumors of the thorax: a single-institution, retrospective study. *Radiat Oncol* 2016;11:104.
125. Chao HH, Berman AT, Simone CB, 2nd, et al. Multi-Institutional Prospective Study of Reirradiation with Proton Beam Radiotherapy for Locoregionally Recurrent Non-Small Cell Lung Cancer. *J Thorac Oncol* 2017;12:281-92.
126. Ho JC, Nguyen QN, Li H, et al. Reirradiation of thoracic cancers with intensity modulated proton therapy. *Pract Radiat Oncol* 2018;8:58-65.
127. Schlamp I, Rieber J, Adeberg S, et al. Re-irradiation in locally recurrent lung cancer patients. *Strahlenther Onkol* 2019;195:725-33.
128. Yang WC, Hsu FM, Chen YH, et al. Clinical outcomes and toxicity predictors of thoracic re-irradiation for locoregionally recurrent lung cancer. *Clin Transl Radiat Oncol* 2020;22:76-82.
129. Trovo M, Minatel E, Durofil E, et al. Stereotactic body radiation therapy for re-irradiation of persistent or recurrent non-small cell lung cancer. *Int J Radiat Oncol Biol Phys* 2014;88:1114-9.
130. Kilburn JM, Kuremsky JG, Blackstock AW, et al. Thoracic re-irradiation using stereotactic body radiotherapy (SBRT) techniques as first or second course of treatment. *Radiother Oncol* 2014;110:505-10.
131. Patel NR, Lanciano R, Sura K, et al. Stereotactic body radiotherapy for re-irradiation of lung cancer recurrence with lower biological effective doses. *J Radiat Oncol* 2015;4:65-70.
132. Horne ZD, Dohopolski MJ, Clump DA, Burton SA, Heron DE. Thoracic reirradiation with SBRT for residual/recurrent and new primary NSCLC within or immediately adjacent to a prior high-dose radiation field. *Pract Radiat Oncol* 2018;8:e117-e23.

133. Sumodhee S, Bondiau PY, Poudenx M, et al. Long term efficacy and toxicity after stereotactic ablative reirradiation in locally relapsed stage III non-small cell lung cancer. *BMC Cancer* 2019;19:305.
134. Valakh V, Miyamoto C, Micaily B, Chan P, Neicu T, Li S. Repeat stereotactic body radiation therapy for patients with pulmonary malignancies who had previously received SBRT to the same or an adjacent tumor site. *Journal of cancer research and therapeutics* 2013;9:680.
135. Hearn JW, Videtic GM, Djemil T, Stephans KL. Salvage stereotactic body radiation therapy (SBRT) for local failure after primary lung SBRT. *Int J Radiat Oncol Biol Phys* 2014;90:402-6.
136. Kennedy WR, Gabani P, Nikitas J, Robinson CG, Bradley JD, Roach MC. Repeat stereotactic body radiation therapy (SBRT) for salvage of isolated local recurrence after definitive lung SBRT. *Radiother Oncol* 2020;142:230-5.
137. White A, Hornsey S. Time dependent repair of radiation damage in the rat spinal cord after X-rays and neutrons. *Eur J Cancer* 1980;16:957-62.
138. van der Kogel AJ, Sissingh HA, Zoetelief J. Effect of X rays and neutrons on repair and regeneration in the rat spinal cord. *Int J Radiat Oncol Biol Phys* 1982;8:2095-7.
139. Ang KK, Price RE, Stephens LC, et al. The tolerance of primate spinal cord to re-irradiation. *Int J Radiat Oncol Biol Phys* 1993;25:459-64.
140. Ang KK, Jiang GL, Feng Y, Stephens LC, Tucker SL, Price RE. Extent and kinetics of recovery of occult spinal cord injury. *Int J Radiat Oncol Biol Phys* 2001;50:1013-20.
141. Terry NH, Tucker SL, Travis EL. Residual radiation damage in murine lung assessed by pneumonitis. *Int J Radiat Oncol Biol Phys* 1988;14:929-38.
142. Brown JM, Probert JC. Early and late radiation changes following a second course of irradiation. *Radiology* 1975;115:711-6.
143. Wondergem J, van Ravels FJ, Reijnart IW, Strootman EG. Reirradiation tolerance of the rat heart. *Int J Radiat Oncol Biol Phys* 1996;36:811-9.
144. De Ruyscher D, Faivre-Finn C, Le Pechoux C, Peeters S, Belderbos J. High-dose re-irradiation following radical radiotherapy for non-small-cell lung cancer. *Lancet Oncol* 2014;15:e620-e4.
145. Peulen H, Karlsson K, Lindberg K, et al. Toxicity after reirradiation of pulmonary tumours with stereotactic body radiotherapy. *Radiother Oncol* 2011;101:260-6.
146. Troost EGC, Wink KCJ, Roelofs E, et al. Photons or protons for reirradiation in (non-)small cell lung cancer: Results of the multicentric ROCOCO in silico study. *Br J Radiol* 2020;93:20190879.
147. Ren C, Ji T, Liu T, Dang J, Li G. The risk and predictors for severe radiation pneumonitis in lung cancer patients treated with thoracic reirradiation. *Radiat Oncol* 2018;13:69.
148. Badiyan SN, Rutenberg MS, Hoppe BS, et al. Clinical Outcomes of Patients With Recurrent Lung Cancer Reirradiated With Proton Therapy on the Proton Collaborative Group and University of Florida Proton Therapy Institute Prospective Registry Studies. *Pract Radiat Oncol* 2019;9:280-8.
149. Liu H, Zhang X, Vinogradskiy YY, Swisher SG, Komaki R, Chang JY. Predicting radiation pneumonitis after stereotactic ablative radiation therapy in patients previously treated with conventional thoracic radiation therapy. *Int J Radiat Oncol Biol Phys* 2012;84:1017-23.
150. Ghosal N, McAleese J, Hannah G, et al. 151: A UK survey of the practice of re-irradiation of locally relapsed lung cancers after previous thoracic radiotherapy. *Lung Cancer* 2015;87:S54-S55.

151. Loblaw DA, Prestrud AA, Somerfield MR, et al. American Society of Clinical Oncology Clinical Practice Guidelines: formal systematic review-based consensus methodology. *J Clin Oncol* 2012;30:3136-40.
152. Dalkey N, Helmer O. An Experimental Application of the Delphi Method to the Use of Experts. *Management Science* 1963;9:458-67.
153. Barrett D, Heale R. What are Delphi studies? *Evidence-based nursing* 2020;23:68-9.
154. Ludwig B. Predicting the future: Have you considered using the Delphi methodology? *Journal of extension* 1997;35:1-4.
155. Hsu C-C, Sandford BA. The Delphi technique: making sense of consensus. *Practical Assessment, Research, and Evaluation* 2007;12:10.
156. Heiko A. Consensus measurement in Delphi studies: review and implications for future quality assurance. *Technological forecasting and social change* 2012;79:1525-36.
157. Dehing-Oberije C, De Ruyscher D, van Baardwijk A, Yu S, Rao B, Lambin P. The importance of patient characteristics for the prediction of radiation-induced lung toxicity. *Radiother Oncol* 2009;91:421-6.
158. Niezink AGH, de Jong RA, Muijs CT, Langendijk JA, Widder J. Pulmonary Function Changes After Radiotherapy for Lung or Esophageal Cancer: A Systematic Review Focusing on Dose-Volume Parameters. *Oncologist* 2017;22:1257-64.
159. Wong CS, Poon JK, Hill RP. Re-irradiation tolerance in the rat spinal cord: influence of level of initial damage. *Radiother Oncol* 1993;26:132-8.
160. Simone C, Amini A, Chetty I, et al. American Radium Society (ARS) and American College of Radiology (ACR) Appropriate Use Criteria Systematic Review and Guidelines on Reirradiation for Non-small Cell Lung Cancer (NSCLC). *International Journal of Radiation Oncology*Biology*Physics* 2020;108:E48-E9.
161. Hunter B, Crockett C, Faivre-Finn C, Hiley C, Salem A. Re-Irradiation of Recurrent Non-Small Cell Lung Cancer. *Seminars in Radiation Oncology*; 2021: Elsevier. p. 124-32.
162. Brown JM, Carlson DJ, Brenner DJ. The tumor radiobiology of SRS and SBRT: are more than the 5 Rs involved? *Int J Radiat Oncol Biol Phys* 2014;88:254-62.
163. Rigaud B, Simon A, Castelli J, et al. Deformable image registration for radiation therapy: principle, methods, applications and evaluation. *Acta Oncol* 2019;58:1225-37.
164. Mauguen A, Le Pechoux C, Saunders MI, et al. Hyperfractionated or accelerated radiotherapy in lung cancer: an individual patient data meta-analysis. *J Clin Oncol* 2012;30:2788-97.
165. Charlson ME, Pompei P, Ales KL, MacKenzie CR. A new method of classifying prognostic comorbidity in longitudinal studies: development and validation. *J Chronic Dis* 1987;40:373-83.
166. Milo MLH, Offersen BV, Bechmann T, et al. Delineation of whole heart and substructures in thoracic radiation therapy: National guidelines and contouring atlas by the Danish Multidisciplinary Cancer Groups. *Radiother Oncol* 2020;150:121-7.
167. Organs at risk in thoracic radiation therapy. 2021. (Accessed 01/09/2021, 2021, at <https://www.nrgoncology.org/Portals/0/Scientific%20Program/CIRO/Atlases/Lung%20Organs%20at%20Risk.ppt>.)

168. Ricco A, Barlow S, Feng J, et al. Repeat Thoracic Stereotactic Body Radiation Therapy (SBRT) for Nonsmall Cell Lung Cancer: Long-Term Outcomes, Toxicity, and Dosimetric Considerations. *Adv Radiat Oncol* 2020;5:984-93.
169. Kruser TJ, McCabe BP, Mehta MP, et al. Reirradiation for locoregionally recurrent lung cancer: outcomes in small cell and non-small cell lung carcinoma. *Am J Clin Oncol* 2014;37:70-6.
170. Nenoff L, Ribeiro CO, Matter M, et al. Deformable image registration uncertainty for inter-fractional dose accumulation of lung cancer proton therapy. *Radiother Oncol* 2020;147:178-85.
171. Lierova A, Jelicova M, Nemcova M, et al. Cytokines and radiation-induced pulmonary injuries. *J Radiat Res* 2018;59:709-53.
172. Siva S, Lobachevsky P, MacManus MP, et al. Radiotherapy for non-small cell lung cancer induces DNA damage response in both irradiated and out-of-field normal tissues. *Clinical Cancer Research* 2016;22:4817-26.
173. Bezjak A, Paulus R, Gaspar LE, et al. Safety and Efficacy of a Five-Fraction Stereotactic Body Radiotherapy Schedule for Centrally Located Non-Small-Cell Lung Cancer: NRG Oncology/RTOG 0813 Trial. *J Clin Oncol* 2019;37:1316-25.
174. Rulach R, Ball D, Chua KLM, et al. An International Expert Survey on the Indications and Practice of Radical Thoracic Reirradiation for Non-Small Cell Lung Cancer. *Adv Radiat Oncol* 2021;6:100653.
175. Meijneke TR, Petit SF, Wentzler D, Hoogeman M, Nuyttens JJ. Reirradiation and stereotactic radiotherapy for tumors in the lung: dose summation and toxicity. *Radiother Oncol* 2013;107:423-7.
176. Nieder C, Grosu AL, Andratschke NH, Molls M. Update of human spinal cord reirradiation tolerance based on additional data from 38 patients. *Int J Radiat Oncol Biol Phys* 2006;66:1446-9.
177. Sahgal A, Ma L, Weinberg V, et al. Reirradiation human spinal cord tolerance for stereotactic body radiotherapy. *Int J Radiat Oncol Biol Phys* 2012;82:107-16.
178. Feddock J, Cleary R, Arnold S, et al. Risk for fatal pulmonary hemorrhage does not appear to be increased following dose escalation using stereotactic body radiotherapy (SBRT) in locally advanced non-small cell lung cancer (NSCLC). *Journal of Radiosurgery and SBRT* 2013;2:235.
179. Evans JD, Gomez DR, Amini A, et al. Aortic dose constraints when reirradiating thoracic tumors. *Radiother Oncol* 2013;106:327-32.
180. Chen AM, Yoshizaki T, Velez MA, Mikaeilian AG, Hsu S, Cao M. Tolerance of the Brachial Plexus to High-Dose Reirradiation. *Int J Radiat Oncol Biol Phys* 2017;98:83-90.
181. Kirkpatrick JP, van der Kogel AJ, Schultheiss TE. Radiation dose-volume effects in the spinal cord. *Int J Radiat Oncol Biol Phys* 2010;76:S42-9.
182. Schultheiss TE. The radiation dose-response of the human spinal cord. *Int J Radiat Oncol Biol Phys* 2008;71:1455-9.
183. Sahgal A, Chang JH, Ma L, et al. Spinal Cord Dose Tolerance to Stereotactic Body Radiation Therapy. *Int J Radiat Oncol Biol Phys* 2021;110:124-36.
184. Powell S, Cooke J, Parsons C. Radiation-induced brachial plexus injury: follow-up of two different fractionation schedules. *Radiother Oncol* 1990;18:213-20.
185. Gagliardi G, Constine LS, Moiseenko V, et al. Radiation dose-volume effects in the heart. *Int J Radiat Oncol Biol Phys* 2010;76:S77-85.

186. McWilliam A, Kennedy J, Hodgson C, Vasquez Osorio E, Faivre-Finn C, van Herk M. Radiation dose to heart base linked with poorer survival in lung cancer patients. *Eur J Cancer* 2017;85:106-13.
187. Moiseenko V, Marks LB, Grimm J, et al. A Primer on Dose-Response Data Modeling in Radiation Therapy. *Int J Radiat Oncol Biol Phys* 2021;110:11-20.
188. Altman DG, Bland JM. How to obtain the P value from a confidence interval. *Bmj* 2011;343.
189. Ryu S, Gorty S, Kazee AM, et al. 'Full dose' reirradiation of human cervical spinal cord. *Am J Clin Oncol* 2000;23:29-31.
190. Grosu AL, Andratschke N, Nieder C, Molls M. Retreatment of the spinal cord with palliative radiotherapy. *Int J Radiat Oncol Biol Phys* 2002;52:1288-92.
191. Sminia P, Oldenburger F, Slotman BJ, Schneider CJ, Hulshof MC. Re-irradiation of the human spinal cord. *Strahlenther Onkol* 2002;178:453-6.
192. Milker-Zabel S, Zabel A, Thilmann C, Schlegel W, Wannemacher M, Debus J. Clinical results of retreatment of vertebral bone metastases by stereotactic conformal radiotherapy and intensity-modulated radiotherapy. *Int J Radiat Oncol Biol Phys* 2003;55:162-7.
193. Kuo JV, Cabebe E, Al-Ghazi M, Yakoob R, Ramsinghani NS, Sanford R. Intensity-modulated radiation therapy for the spine at the University of California, Irvine. *Medical Dosimetry* 2002;27:137-45.
194. Magrini SM, Biti GP, de Scisciolo G, et al. Neurological damage in patients irradiated twice on the spinal cord: a morphologic and electrophysiological study. *Radiother Oncol* 1990;17:209-18.
195. Bauman GS, Sneed PK, Wara WM, et al. Reirradiation of primary CNS tumors. *Int J Radiat Oncol Biol Phys* 1996;36:433-41.
196. Wong CS, Van Dyk J, Milosevic M, Laperriere NJ. Radiation myelopathy following single courses of radiotherapy and retreatment. *Int J Radiat Oncol Biol Phys* 1994;30:575-81.
197. Jackson MA, Ball DL. Palliative retreatment of locally-recurrent lung cancer after radical radiotherapy. *Medical Journal of Australia* 1987;147:391-4.
198. Wright JL, Lovelock DM, Bilsky MH, Toner S, Zatcky J, Yamada Y. Clinical outcomes after reirradiation of paraspinal tumors. *Am J Clin Oncol* 2006;29:495-502.
199. Rades D, Stalpers LJ, Veninga T, et al. Evaluation of five radiation schedules and prognostic factors for metastatic spinal cord compression. *J Clin Oncol* 2005;23:3366-75.
200. Gwak HS, Yoo HJ, Youn SM, et al. Hypofractionated stereotactic radiation therapy for skull base and upper cervical chordoma and chondrosarcoma: preliminary results. *Stereotact Funct Neurosurg* 2005;83:233-43.
201. Choi CY, Adler JR, Gibbs IC, et al. Stereotactic radiosurgery for treatment of spinal metastases recurring in close proximity to previously irradiated spinal cord. *Int J Radiat Oncol Biol Phys* 2010;78:499-506.
202. Maranzano E, Trippa F, Casale M, Anselmo P, Rossi R. Reirradiation of metastatic spinal cord compression: definitive results of two randomized trials. *Radiother Oncol* 2011;98:234-7.
203. Navarria P, Mancosu P, Alongi F, et al. Vertebral metastases reirradiation with volumetric-modulated arc radiotherapy. *Radiother Oncol* 2012;102:416-20.
204. Chang UK, Cho WI, Kim MS, Cho CK, Lee DH, Rhee CH. Local tumor control after retreatment of spinal metastasis using stereotactic body radiotherapy; comparison with initial treatment group. *Acta Oncol* 2012;51:589-95.

205. Wang Q, Song Y, Zhuang H, et al. Robotic stereotactic irradiation and reirradiation for spinal metastases: safety and efficacy assessment. *Chin Med J (Engl)* 2014;127:232-8.
206. Hashmi A, Guckenberger M, Kersh R, et al. Re-irradiation stereotactic body radiotherapy for spinal metastases: a multi-institutional outcome analysis. *J Neurosurg Spine* 2016;25:646-53.
207. Kawashiro S, Harada H, Katagiri H, et al. Reirradiation of spinal metastases with intensity-modulated radiation therapy: an analysis of 23 patients. *J Radiat Res* 2016;57:150-6.
208. Schröder C, Stiefel I, Tanadini-Lang S, et al. Re-irradiation in the thorax- An analysis of efficacy and safety based on accumulated EQD2 doses. *Radiotherapy and Oncology* 2020;152:56-62.
209. Doi H, Tamari K, Oh RJ, Nieder C. New clinical data on human spinal cord re-irradiation tolerance. *Strahlenther Onkol* 2021;197:463-73.
210. van der Kogel AJ. Dose-volume effects in the spinal cord. *Radiother Oncol* 1993;29:105-9.
211. Pallis CA, Louis S, Morgan RL. Radiation myelopathy. *Brain* 1961;84:460-79.
212. Poltinnikov IM, Fallon K, Xiao Y, Reiff JE, Curran WJ, Jr., Werner-Wasik M. Combination of longitudinal and circumferential three-dimensional esophageal dose distribution predicts acute esophagitis in hypofractionated reirradiation of patients with non-small-cell lung cancer treated in stereotactic body frame. *Int J Radiat Oncol Biol Phys* 2005;62:652-8.
213. Yamaguchi S, Ohguri T, Imada H, et al. Multimodal approaches including three-dimensional conformal re-irradiation for recurrent or persistent esophageal cancer: preliminary results. *J Radiat Res* 2011;52:812-20.
214. Kim YS, Lee CG, Kim KH, et al. Re-irradiation of recurrent esophageal cancer after primary definitive radiotherapy. *Radiat Oncol J* 2012;30:182-8.
215. Katano A, Yamashita H, Nakagawa K. Re-irradiation of locoregional esophageal cancer recurrence following definitive chemoradiotherapy: A report of 6 cases. *Mol Clin Oncol* 2017;7:681-6.
216. Hong L, Huang YX, Zhuang QY, et al. Survival benefit of re-irradiation in esophageal Cancer patients with Locoregional recurrence: a propensity score-matched analysis. *Radiat Oncol* 2018;13:171.
217. Zhou ZG, Zhen CJ, Bai WW, et al. Salvage radiotherapy in patients with local recurrent esophageal cancer after radical radiochemotherapy. *Radiat Oncol* 2015;10:54.
218. Chen Y, Lu Y, Wang Y, et al. Comparison of salvage chemoradiation versus salvage surgery for recurrent esophageal squamous cell carcinoma after definitive radiochemotherapy or radiotherapy alone. *Dis Esophagus* 2014;27:134-40.
219. Owen D, Olivier KR, Song L, et al. Safety and Tolerability of SBRT after High-Dose External Beam Radiation to the Lung. *Front Oncol* 2014;4:376.
220. Binkley MS, Hiniker SM, Chaudhuri A, et al. Dosimetric Factors and Toxicity in Highly Conformal Thoracic Reirradiation. *Int J Radiat Oncol Biol Phys* 2016;94:808-15.
221. Maranzano E, Draghini L, Anselmo P, et al. Lung reirradiation with stereotactic body radiotherapy. *J Radiosurg SBRT* 2016;4:61-8.
222. Hong JH, Kim Y-S, Lee S-W, et al. High-dose thoracic re-irradiation of lung cancer using highly conformal radiotherapy is effective with acceptable toxicity. *Cancer research and treatment: official journal of Korean Cancer Association* 2019;51:1156.

223. Ogawa Y, Shibamoto Y, Hashizume C, et al. Repeat stereotactic body radiotherapy (SBRT) for local recurrence of non-small cell lung cancer and lung metastasis after first SBRT. *Radiat Oncol* 2018;13:136.
224. Herskovic A, Martz K, al-Sarraf M, et al. Combined chemotherapy and radiotherapy compared with radiotherapy alone in patients with cancer of the esophagus. *N Engl J Med* 1992;326:1593-8.
225. Karube M, Yamamoto N, Tsuji H, et al. Carbon-ion re-irradiation for recurrences after initial treatment of stage I non-small cell lung cancer with carbon-ion radiotherapy. *Radiother Oncol* 2017;125:31-5.
226. Marks LB, Bentzen SM, Deasy JO, et al. Radiation dose-volume effects in the lung. *Int J Radiat Oncol Biol Phys* 2010;76:S70-6.
227. Giuranno L, lent J, De Ruyscher D, Vooijs MA. Radiation-Induced Lung Injury (RILI). *Front Oncol* 2019;9:877.
228. Faria SL, Aslani M, Tafazoli FS, Souhami L, Freeman CR. The challenge of scoring radiation-induced lung toxicity. *Clin Oncol (R Coll Radiol)* 2009;21:371-5.
229. Bezjak A, , Paulus R, et al. Primary Study Endpoint Analysis for NRG Oncology/RTOG 0813 Trial of Stereotactic Body Radiation Therapy (SBRT) for Centrally Located Non-Small Cell Lung Cancer (NSCLC). 2016:5-6.
230. Ritter TA, Matuszak M, Chetty IJ, et al. Application of Critical Volume-Dose Constraints for Stereotactic Body Radiation Therapy in NRG Radiation Therapy Trials. *Int J Radiat Oncol Biol Phys* 2017;98:34-6.
231. Siva S, Thomas R, Callahan J, et al. High-resolution pulmonary ventilation and perfusion PET/CT allows for functionally adapted intensity modulated radiotherapy in lung cancer. *Radiother Oncol* 2015;115:157-62.
232. Repka MC, Aghdam N, Kataria SK, et al. Five-fraction SBRT for ultra-central NSCLC in-field recurrences following high-dose conventional radiation. *Radiat Oncol* 2017;12:162.
233. Sood S, Ganju R, Shen X, Napel MT, Wang F. Ultra-central Thoracic Re-irradiation Using 10-fraction Stereotactic Body Radiotherapy for Recurrent Non-small-cell Lung Cancer Tumors: Preliminary Toxicity and Efficacy Outcomes. *Clin Lung Cancer* 2021;22:e301-e12.
234. Trombetta MG, Colonias A, Makishi D, et al. Tolerance of the aorta using intraoperative iodine-125 interstitial brachytherapy in cancer of the lung. *Brachytherapy* 2008;7:50-4.
235. Stoltzfus JC. Logistic regression: a brief primer. *Acad Emerg Med* 2011;18:1099-104.
236. Yamazaki H, Ogita M, Kodani N, et al. Frequency, outcome and prognostic factors of carotid blowout syndrome after hypofractionated re-irradiation of head and neck cancer using CyberKnife: a multi-institutional study. *Radiother Oncol* 2013;107:305-9.
237. Benedict SH, Yenice KM, Followill D, et al. Stereotactic body radiation therapy: the report of AAPM Task Group 101. *Medical physics* 2010;37:4078-101.
238. Moiseenko V, Zhao J, Milano MT, et al. Organs at risk considerations for thoracic stereotactic body radiation therapy: what is safe for lung parenchyma? *International Journal of Radiation Oncology* Biology* Physics* 2021;110:172-87.
239. Diez P, Hanna G, Aitken K, et al. UK 2022 consensus on normal tissue dose-volume constraints for oligometastatic, primary lung and hepatocellular carcinoma stereotactic ablative radiotherapy. *Clinical Oncology* 2022;34:288-300.
240. Hanna G, Murray L, Patel R, et al. UK consensus on normal tissue dose constraints for stereotactic radiotherapy. *Clinical Oncology* 2018;30:5-14.

241. Palma DA, Olson R, Harrow S, et al. Stereotactic Ablative Radiotherapy for the Comprehensive Treatment of Oligometastatic Cancers: Long-Term Results of the SABR-COMET Phase II Randomized Trial. *J Clin Oncol* 2020;38:2830-8.
242. Hurkmans CW, Cuijpers JP, Lagerwaard FJ, et al. Recommendations for implementing stereotactic radiotherapy in peripheral stage IA non-small cell lung cancer: report from the Quality Assurance Working Party of the randomised phase III ROSEL study. *Radiation Oncology* 2009;4:1-14.
243. Adebahr S, Collette S, Shash E, et al. LungTech, an EORTC Phase II trial of stereotactic body radiotherapy for centrally located lung tumours: a clinical perspective. *The British journal of radiology* 2015;88:20150036.
244. King G, Zeng L. Logistic regression in rare events data. *Political analysis* 2001;9:137-63.
245. Senti S, Griffioen GH, van Sornsens de Koste JR, Slotman BJ, Senan S. Comparing rigid and deformable dose registration for high dose thoracic re-irradiation. *Radiother Oncol* 2013;106:323-6.
246. Jain V, Berman AT. Radiation Pneumonitis: Old Problem, New Tricks. *Cancers (Basel)* 2018;10:222.
247. Gillette E, Hoopes P, Ensley B. The response of canine oesophagus to changes in dose per fraction. *The British Journal of Cancer Supplement* 1986;7:37.
248. Dubray B, Henry-Amar M, Meerwaldt JH, et al. Radiation-induced lung damage after thoracic irradiation for Hodgkin's disease: the role of fractionation. *Radiother Oncol* 1995;36:211-7.
249. Kirkpatrick JP, Meyer JJ, Marks LB. The linear-quadratic model is inappropriate to model high dose per fraction effects in radiosurgery. *Semin Radiat Oncol* 2008;18:240-3.
250. Brenner DJ. The linear-quadratic model is an appropriate methodology for determining isoeffective doses at large doses per fraction. *Semin Radiat Oncol* 2008;18:234-9.
251. Fuks Z, Kolesnick R. Engaging the vascular component of the tumor response. *Cancer Cell* 2005;8:89-91.
252. Li S, Shen L. Radiobiology of stereotactic ablative radiotherapy (SABR): perspectives of clinical oncologists. *J Cancer* 2020;11:5056-68.
253. Kim DN, Medin PM, Timmerman RD. Emphasis on repair, not just avoidance of injury, facilitates prudent stereotactic ablative radiotherapy. *Seminars in radiation oncology* 2017;27:378-92.
254. Lyman JT. Complication probability as assessed from dose-volume histograms. *Radiation Research* 1985;104:S13-S9.
255. Marks LB, Yorke ED, Jackson A, et al. Use of normal tissue complication probability models in the clinic. *International Journal of Radiation Oncology* Biology* Physics* 2010;76:S10-S9.
256. Huh GJ, Jang SS, Park SY, et al. Three-dimensional conformal reirradiation for locoregionally recurrent lung cancer previously treated with radiation therapy. *Thorac Cancer* 2014;5:281-8.
257. Kelly P, Balter PA, Rebuena N, et al. Stereotactic body radiation therapy for patients with lung cancer previously treated with thoracic radiation. *Int J Radiat Oncol Biol Phys* 2010;78:1387-93.
258. McAvoy S, Ciura K, Wei C, et al. Definitive reirradiation for locoregionally recurrent non-small cell lung cancer with proton beam therapy or intensity modulated radiation therapy: predictors of high-grade toxicity and survival outcomes. *Int J Radiat Oncol Biol Phys* 2014;90:819-27.

259. Scott JG, Sedor G, Ellsworth P, et al. Pan-cancer prediction of radiotherapy benefit using genomic-adjusted radiation dose (GARD): a cohort-based pooled analysis. *The Lancet Oncology* 2021.
260. Stuschke M, Pottgen C. Altered fractionation schemes in radiotherapy. *Front Radiat Ther Oncol* 2010;42:150-6.
261. Santiago A, Barczyk S, Jelen U, Engenhart-Cabillic R, Wittig A. Challenges in radiobiological modeling: can we decide between LQ and LQ-L models based on reviewed clinical NSCLC treatment outcome data? *Radiation Oncology* 2016;11:1-13.
262. Guyot P, Ades AE, Ouwens MJ, Welton NJ. Enhanced secondary analysis of survival data: reconstructing the data from published Kaplan-Meier survival curves. *BMC Med Res Methodol* 2012;12:9.
263. Potters L, Kavanagh B, Galvin JM, et al. American Society for Therapeutic Radiology and Oncology (ASTRO) and American College of Radiology (ACR) practice guideline for the performance of stereotactic body radiation therapy. *Int J Radiat Oncol Biol Phys* 2010;76:326-32.
264. Stereotactic Ablative Body Radiation Therapy (SABR): A Resource. 2019. (Accessed 06/09/2022, 2022, at <https://www.sabr.org.uk/wp-content/uploads/2019/04/SABRconsortium-guidelines-2019-v6.1.0.pdf>.)
265. Ester EC, Jones DA, Vernon MR, et al. Lung reirradiation with stereotactic body radiotherapy (SBRT). *J Radiosurg SBRT* 2013;2:325-31.
266. Ceylan C, Hamaci A, Ayata H, et al. Re-Irradiation of Locoregional NSCLC Recurrence Using Robotic Stereotactic Body Radiotherapy. *Oncol Res Treat* 2017;40:207-14.
267. Caivano D, Valeriani M, De Matteis S, et al. Re-irradiation in lung disease by SBRT: a retrospective, single institutional study. *Radiat Oncol* 2018;13:87.
268. Hayashi K, Yamamoto N, Karube M, et al. Feasibility of carbon-ion radiotherapy for re-irradiation of locoregionally recurrent, metastatic, or secondary lung tumors. *Cancer Sci* 2018;109:1562-9.
269. Kamran SC, Mueller BS, Paetzold P, et al. Multi-criteria optimization achieves superior normal tissue sparing in a planning study of intensity-modulated radiation therapy for RTOG 1308-eligible non-small cell lung cancer patients. *Radiother Oncol* 2016;118:515-20.
270. Fogliata A, Vanetti E, Albers D, et al. On the dosimetric behaviour of photon dose calculation algorithms in the presence of simple geometric heterogeneities: comparison with Monte Carlo calculations. *Phys Med Biol* 2007;52:1363-85.
271. Fogliata A, Nicolini G, Clivio A, Vanetti E, Cozzi L. Dosimetric evaluation of Acuros XB Advanced Dose Calculation algorithm in heterogeneous media. *Radiat Oncol* 2011;6:82.
272. McVicar N, Thomas S, Liu M, Carolan H, Bergman A. Re-irradiation volumetric modulated arc therapy optimization based on cumulative biologically effective dose objectives. *J Appl Clin Med Phys* 2018;19:341-5.
273. Kirby N, Chuang C, Ueda U, Pouliot J. The need for application-based adaptation of deformable image registration. *Med Phys* 2013;40:011702.
274. Barber J, Yuen J, Jameson M, et al. Deforming to Best Practice: Key considerations for deformable image registration in radiotherapy. *J Med Radiat Sci* 2020;67:318-32.
275. Kyroudi A, Petersson K, Ghandour S, et al. Discrepancies between selected Pareto optimal plans and final deliverable plans in radiotherapy multi-criteria optimization. *Radiotherapy and Oncology* 2016;120:346-8.

276. Jiang C, Han S, Chen W, et al. A retrospective study of shrinking field radiation therapy during chemoradiotherapy in stage III non-small cell lung cancer. *Oncotarget* 2018;9:12443-51.
277. Guckenberger M, Wilbert J, Richter A, Baier K, Flentje M. Potential of adaptive radiotherapy to escalate the radiation dose in combined radiochemotherapy for locally advanced non-small cell lung cancer. *Int J Radiat Oncol Biol Phys* 2011;79:901-8.
278. Macbeth FR, Bolger JJ, Hopwood P, et al. Randomized trial of palliative two-fraction versus more intensive 13-fraction radiotherapy for patients with inoperable non-small cell lung cancer and good performance status. Medical Research Council Lung Cancer Working Party. *Clin Oncol (R Coll Radiol)* 1996;8:167-75.
279. Haslett K, Bayman N, Franks K, et al. Isotoxic Intensity Modulated Radiation Therapy in Stage III Non-Small Cell Lung Cancer: A Feasibility Study. *Int J Radiat Oncol Biol Phys* 2021;109:1341-8.
280. Sugimura H, Yang P. Long-term survivorship in lung cancer: a review. *Chest* 2006;129:1088-97.
281. Stein KD, Syrjala KL, Andrykowski MA. Physical and psychological long-term and late effects of cancer. *Cancer* 2008;112:2577-92.
282. Joseph K, Tai P, Wu J, Barnes E, Levin W. Workshop report: A practical approach and general principles of re-irradiation for in-field cancer recurrence. *Clin Oncol (R Coll Radiol)* 2010;22:885-9.
283. Blinman P, Alam M, Duric V, McLachlan SA, Stockler MR. Patients' preferences for chemotherapy in non-small-cell lung cancer: a systematic review. *Lung Cancer* 2010;69:141-7.
284. Braun V, Clarke V. Using thematic analysis in psychology. *Qualitative research in psychology* 2006;3:77-101.
285. Kiger ME, Varpio L. Thematic analysis of qualitative data: AMEE Guide No. 131. *Med Teach* 2020;42:846-54.
286. Simard S, Savard J, Ivers H. Fear of cancer recurrence: specific profiles and nature of intrusive thoughts. *J Cancer Surviv* 2010;4:361-71.
287. Silvestri G, Pritchard R, Welch HG. Preferences for chemotherapy in patients with advanced non-small cell lung cancer: descriptive study based on scripted interviews. *BMJ* 1998;317:771-5.
288. Guest G, Bunce A, Johnson L. How many interviews are enough? An experiment with data saturation and variability. *Field methods* 2006;18:59-82.
289. Braun V, Clarke V. To saturate or not to saturate? Questioning data saturation as a useful concept for thematic analysis and sample-size rationales. *Qualitative research in sport, exercise and health* 2021;13:201-16.
290. Vasileiou K, Barnett J, Thorpe S, Young T. Characterising and justifying sample size sufficiency in interview-based studies: systematic analysis of qualitative health research over a 15-year period. *BMC Med Res Methodol* 2018;18:148.
291. Re-care definition. 2023. (Accessed 18th April, 2023, 2023, at <https://project.eortc.org/e2-radiate/cohorts/>.)
292. Andratschke N, Willmann J, Appelt AL, et al. European Society for Radiotherapy and Oncology and European Organisation for Research and Treatment of Cancer consensus on re-irradiation: definition, reporting, and clinical decision making. *Lancet Oncol* 2022;23:e469-e78.
293. Slevin F, Aitken K, Alongi F, et al. An international Delphi consensus for pelvic stereotactic ablative radiotherapy re-irradiation. *Radiother Oncol* 2021;164:104-14.

294. Gomez-Casal R, Bhattacharya C, Ganesh N, et al. Non-small cell lung cancer cells survived ionizing radiation treatment display cancer stem cell and epithelial-mesenchymal transition phenotypes. *Mol Cancer* 2013;12:94.
295. Moncharmont C, Levy A, Guy JB, et al. Radiation-enhanced cell migration/invasion process: a review. *Crit Rev Oncol Hematol* 2014;92:133-42.
296. Kocakavuk E, Anderson KJ, Varn FS, et al. Radiotherapy is associated with a deletion signature that contributes to poor outcomes in patients with cancer. *Nature genetics* 2021:1-9.
297. Brown JM, Wilson WR. Exploiting tumour hypoxia in cancer treatment. *Nat Rev Cancer* 2004;4:437-47.
298. Salem A, Asselin MC, Reymen B, et al. Targeting Hypoxia to Improve Non-Small Cell Lung Cancer Outcome. *J Natl Cancer Inst* 2018;110:14-30.
299. Singh B, Patwardhan RS, Jayakumar S, Sharma D, Sandur SK. Oxidative stress associated metabolic adaptations regulate radioresistance in human lung cancer cells. *J Photochem Photobiol B* 2020;213:112080.
300. Barker HE, Paget JT, Khan AA, Harrington KJ. The tumour microenvironment after radiotherapy: mechanisms of resistance and recurrence. *Nat Rev Cancer* 2015;15:409-25.
301. McLaughlin M, Patin EC, Pedersen M, et al. Inflammatory microenvironment remodelling by tumour cells after radiotherapy. *Nat Rev Cancer* 2020;20:203-17.
302. Nakagomi T, Goto T, Hirotsu Y, et al. Elucidation of radiation-resistant clones by a serial study of intratumor heterogeneity before and after stereotactic radiotherapy in lung cancer. *J Thorac Dis* 2017;9:E598-E604.
303. Greaves M, Maley CC. Clonal evolution in cancer. *Nature* 2012;481:306-13.
304. Nowell PC. The Clonal Evolution of Tumor Cell Populations: Acquired genetic lability permits stepwise selection of variant sublines and underlies tumor progression. *Science* 1976;194:23-8.
305. Eschrich SA, Pramana J, Zhang H, et al. A gene expression model of intrinsic tumor radiosensitivity: prediction of response and prognosis after chemoradiation. *Int J Radiat Oncol Biol Phys* 2009;75:489-96.
306. Grimes DR. Limitations of the radiosensitivity index as a direct prognostic marker. *The Lancet Oncology* 2022;23:1352-3.
307. Kim MY, Oskarsson T, Acharyya S, et al. Tumor self-seeding by circulating cancer cells. *Cell* 2009;139:1315-26.
308. Jamal-Hanjani M, Wilson GA, McGranahan N, et al. Tracking the Evolution of Non-Small-Cell Lung Cancer. *N Engl J Med* 2017;376:2109-21.
309. Svajdova M, Dubinsky P, Kazda T. Radical external beam re-irradiation in the treatment of recurrent head and neck cancer: Critical review. *Head Neck* 2021;43:354-66.
310. Biagioli MC, Harvey M, Roman E, et al. Intensity-modulated radiotherapy with concurrent chemotherapy for previously irradiated, recurrent head and neck cancer. *Int J Radiat Oncol Biol Phys* 2007;69:1067-73.
311. Minniti G, Niyazi M, Alongi F, Navarria P, Belka C. Current status and recent advances in reirradiation of glioblastoma. *Radiat Oncol* 2021;16:36.
312. Murray LJ, Lilley J, Hawkins MA, Henry AM, Dickinson P, Sebag-Montefiore D. Pelvic re-irradiation using stereotactic ablative radiotherapy (SABR): A systematic review. *Radiother Oncol* 2017;125:213-22.
313. Graham JD, Robinson MH, Harmer CL. Re-irradiation of soft-tissue sarcoma. *Br J Radiol* 1992;65:157-61.

314. Janssen S, Rades D, Meyer A, et al. Local recurrence of breast cancer: conventionally fractionated partial external beam re-irradiation with curative intention. *Strahlenther Onkol* 2018;194:806-14.
315. Rulach R, Hanna GG, Franks K, McAleese J, Harrow S. Re-irradiation for Locally Recurrent Lung Cancer: Evidence, Risks and Benefits. *Clin Oncol (R Coll Radiol)* 2018;30:101-9.
316. Chow E, van der Linden YM, Roos D, et al. Single versus multiple fractions of repeat radiation for painful bone metastases: a randomised, controlled, non-inferiority trial. *Lancet Oncol* 2014;15:164-71.
317. O'Rourke N, Roberts F, Othman A. Lung Cancer Patients Who'Relapse'After Primary Treatment May Have Different Pathology or No Malignancy. *Journal of Thoracic Oncology*; 2015. p. S461-S.
318. Paz-Ares LG, de Marinis F, Dediu M, et al. PARAMOUNT: Final overall survival results of the phase III study of maintenance pemetrexed versus placebo immediately after induction treatment with pemetrexed plus cisplatin for advanced nonsquamous non-small-cell lung cancer. *J Clin Oncol* 2013;31:2895-902.
319. Gadgeel S, Rodriguez-Abreu D, Speranza G, et al. Updated Analysis From KEYNOTE-189: Pembrolizumab or Placebo Plus Pemetrexed and Platinum for Previously Untreated Metastatic Nonsquamous Non-Small-Cell Lung Cancer. *J Clin Oncol* 2020;38:1505-17.
320. Dickhoff C, Dahele M, Paul MA, et al. Salvage surgery for locoregional recurrence or persistent tumor after high dose chemoradiotherapy for locally advanced non-small cell lung cancer. *Lung Cancer* 2016;94:108-13.
321. Hamaji M, Chen F, Matsuo Y, Ueki N, Hiraoka M, Date H. Treatment and Prognosis of Isolated Local Relapse after Stereotactic Body Radiotherapy for Clinical Stage I Non-Small-Cell Lung Cancer: Importance of Salvage Surgery. *J Thorac Oncol* 2015;10:1616-24.
322. Allibhai Z, Cho BC, Taremi M, et al. Surgical salvage following stereotactic body radiotherapy for early-stage NSCLC. *Eur Respir J* 2012;39:1039-42.
323. Chen F, Matsuo Y, Yoshizawa A, et al. Salvage lung resection for non-small cell lung cancer after stereotactic body radiotherapy in initially operable patients. *J Thorac Oncol* 2010;5:1999-2002.
324. Neri S, Takahashi Y, Terashi T, et al. Surgical treatment of local recurrence after stereotactic body radiotherapy for primary and metastatic lung cancers. *J Thorac Oncol* 2010;5:2003-7.
325. Dixon R. The Challenger Space Shuttle Disaster: A Case Study in the Analysis of Binary Data Using Scatter Diagrams and Logit Regression. *Australian Economic Review* 2021;54:294-305.
326. McWilliam A, Vasquez Osorio E, Faivre-Finn C, van Herk M. Influence of tumour laterality on patient survival in non-small cell lung cancer after radiotherapy. *Radiother Oncol* 2019;137:71-6.
327. Andreassen CN, Alsner J, Overgaard M, Overgaard J. Prediction of normal tissue radiosensitivity from polymorphisms in candidate genes. *Radiother Oncol* 2003;69:127-35.
328. Muirhead R, Dean C, Diez P, Williams M, McDonald F. Launch of the UK SABR Consortium Pelvic Stereotactic Ablative Radiotherapy Re-irradiation Guidelines and National Audit. *Clin Oncol (R Coll Radiol)* 2023;35:29-32.
329. Miller RR, McGregor DH. Hemorrhage from carcinoma of the lung. *Cancer* 1980;46:200-5.
330. Gopal P, Sarihan EI, Chie EK, et al. Clonal selection confers distinct evolutionary trajectories in BRAF-driven cancers. *Nat Commun* 2019;10:5143.

331. Lin B, Gao F, Yang Y, et al. FLASH Radiotherapy: History and Future. *Front Oncol* 2021;11:644400.
332. Zhang X, Li Y, Pan X, et al. Intensity-modulated proton therapy reduces the dose to normal tissue compared with intensity-modulated radiation therapy or passive scattering proton therapy and enables individualized radical radiotherapy for extensive stage IIIB non-small-cell lung cancer: a virtual clinical study. *Int J Radiat Oncol Biol Phys* 2010;77:357-66.
333. Murray L, Thompson C, Pagett C, et al. Treatment plan optimisation for reirradiation. *Radiother Oncol* 2023;182:109545.
334. Murray LJ, Appelt AL, Ajithkumar T, et al. Re-irradiation: From Cell Lines to Patients, Filling the (Science) Gap in the Market. *Clin Oncol (R Coll Radiol)* 2023;35:318-22.